

Lecture Notes in Networks and Systems 1

Salim Chikhi · Abdelmalek Amine  
Allaoua Chaoui  
Mohamed Khireddine Krolladi  
Djamel Eddine Saidouni *Editors*

# Modelling and Implementation of Complex Systems

Proceedings of the 4th International  
Symposium, MISC 2016, May 7–8, 2016,  
Constantine, Algeria

 Springer

# Lecture Notes in Networks and Systems

Volume 1

## **Series editor**

Janusz Kacprzyk, Polish Academy of Sciences, Warsaw, Poland  
e-mail: [kacprzyk@ibspan.waw.pl](mailto:kacprzyk@ibspan.waw.pl)

The series “Lecture Notes in Networks and Systems” publishes the latest developments in Networks and Systems—quickly, informally and with high quality. Original research reported in proceedings and post-proceedings represents the core of LNNS.

Volumes published in LNNS embrace all aspects and subfields of, as well as new challenges in, Networks and Systems.

The series contains proceedings and edited volumes in systems and networks, spanning the areas of Cyber-Physical Systems, Autonomous Systems, Sensor Networks, Control Systems, Energy Systems, Automotive Systems, Biological Systems, Vehicular Networking and Connected Vehicles, Aerospace Systems, Automation, Manufacturing, Smart Grids, Nonlinear Systems, Power Systems, Robotics, Social Systems, Economic Systems and other. Of particular value to both the contributors and the readership are the short publication timeframe and the world-wide distribution and exposure which enable both a wide and rapid dissemination of research output.

The series covers the theory, applications, and perspectives on the state of the art and future developments relevant to systems and networks, decision making, control, complex processes and related areas, as embedded in the fields of interdisciplinary and applied sciences, engineering, computer science, physics, economics, social, and life sciences, as well as the paradigms and methodologies behind them.

### **Advisory Board**

Fernando Gomide, Department of Computer Engineering and Automation – DCA, School of Electrical and Computer Engineering – FEEC, University of Campinas – UNICAMP, São Paulo, Brazil

e-mail: gomide@dca.fee.unicamp.br

Okyay Kaynak, Department of Electrical and Electronic Engineering, Bogazici University, Istanbul, Turkey

e-mail: okyay.kaynak@boun.edu.tr

Derong Liu, Department of Electrical and Computer Engineering, University of Illinois at Chicago, Chicago, USA and

Institute of Automation, Chinese Academy of Sciences, Beijing, China

e-mail: derong@uic.edu

Witold Pedrycz, Department of Electrical and Computer Engineering, University of Alberta, Alberta, Canada and

Systems Research Institute, Polish Academy of Sciences, Warsaw, Poland

e-mail: wpedrycz@ualberta.ca

Marios M. Polycarpou, KIOS Research Center for Intelligent Systems and Networks, Department of Electrical and Computer Engineering, University of Cyprus, Nicosia, Cyprus

e-mail: mpolycar@ucy.ac.cy

Imre J. Rudas, Óbuda University, Budapest Hungary

e-mail: rudas@uni-obuda.hu

JunWang Department of Computer Science City University of Hong Kong  
Kowloon Hong Kong

e-mail: jwang.cs@cityu.edu.hk

More information about this series at <http://www.springer.com/series/15179>

Salim Chikhi · Abdelmalek Amine  
Allaoua Chaoui · Mohamed Khireddine Kholladi  
Djamel Eddine Saidouni  
Editors

# Modelling and Implementation of Complex Systems

Proceedings of the 4th International  
Symposium, MISC 2016, May 7–8, 2016,  
Constantine, Algeria



*Editors*

Salim Chikhi  
Faculty of New Information and  
Communication Technologies  
University of Constantine 2  
Constantine  
Algeria

Abdelmalek Amine  
GeCoDe Laboratory  
Faculty of Technology  
University of Saida  
Saida  
Algeria

Allaoua Chaoui  
Faculty of New Information and  
Communication Technologies  
University of Constantine 2  
Constantine  
Algeria

Mohamed Khireddine Kholladi  
Faculty of Science and Technology,  
Department of Mathematics and  
Computer Science  
University of El Oued  
El Oued  
Algeria

Djamel Eddine Saidouni  
Faculty of New Information and  
Communication Technologies  
University of Constantine 2  
Constantine  
Algeria

ISSN 2367-3370

ISSN 2367-3389 (electronic)

Lecture Notes in Networks and Systems

ISBN 978-3-319-33409-7

ISBN 978-3-319-33410-3 (eBook)

DOI 10.1007/978-3-319-33410-3

Library of Congress Control Number: 2016937376

© Springer International Publishing Switzerland 2016

This work is subject to copyright. All rights are reserved by the Publisher, whether the whole or part of the material is concerned, specifically the rights of translation, reprinting, reuse of illustrations, recitation, broadcasting, reproduction on microfilms or in any other physical way, and transmission or information storage and retrieval, electronic adaptation, computer software, or by similar or dissimilar methodology now known or hereafter developed.

The use of general descriptive names, registered names, trademarks, service marks, etc. in this publication does not imply, even in the absence of a specific statement, that such names are exempt from the relevant protective laws and regulations and therefore free for general use.

The publisher, the authors and the editors are safe to assume that the advice and information in this book are believed to be true and accurate at the date of publication. Neither the publisher nor the authors or the editors give a warranty, express or implied, with respect to the material contained herein or for any errors or omissions that may have been made.

Printed on acid-free paper

This Springer imprint is published by Springer Nature

The registered company is Springer International Publishing AG Switzerland

# Preface

This volume contains research papers accepted and presented at the 4th International Symposium on Modelling and Implementation of Complex Systems (MISC 2016), held on 7–8 May 2016 in Constantine, Algeria. As the previous editions (MISC 2010, MISC 2012, and MISC 2014), this symposium is intended as a tradition offering open forum and meeting space for researchers working in the field of complex systems science.

This year, the MISC symposium received 175 submissions from 12 countries: Algeria, Canada, Ireland, France, Luxembourg, Morocco, Oman, Portugal, Tunisia, Saudi Arabia, UK and USA. In a rigorous reviewing process, the Program Committee selected 25 papers, which represents an acceptance rate of 15 %. However, we have not received the camera-ready copies of two papers. So, the proceedings include 23 papers. The PC included 115 researchers and 31 additional reviewers from 14 countries.

The accepted papers were organized into sessions as follows: Networking and Cloud Computing, Software Engineering and Formal Methods, Intelligent and Information Systems, and Algorithms and Complexity.

This volume includes also the abstracts of the keynote talks presented by Mérouane Debbah, Professor at CentraleSupélec, France; Rafael Capilla, Associate Professor at Rey Juan Carlos University, Madrid, Spain; and Mathieu Roche, Research Scientist at CIRAD, Montpellier, France.

We thank Dr. Nabil Belala for managing EasyChair system for MISC 2016 from submissions to proceedings elaboration.

We are grateful to the Program Committee and Organizing Committee members for their contribution in the success of the symposium.

Finally, we thank the authors who submitted papers to the conference.

Constantine, Algeria  
March 2016

Salim Chikhi  
Abdelmalek Amine

# Organization

The 4th International Symposium on Modelling and Implementation of Complex Systems (MISC 2016) was organized by University of Constantine 2—Abdelhamid Mehri and took place in Constantine, Algeria (7–8 May 2016).

## Honorary Chairs

Mohamed Elhadi Latreche, University of Constantine 2, Algeria  
Zaidi Sahnoun, University of Constantine 2, Algeria

## General Chairs

Salim Chikhi, University of Constantine 2, Algeria  
Abdelmalek Amine, University of Saïda, Algeria

## Steering Committee

Allaoua Chaoui, University of Constantine 2, Algeria  
Salim Chikhi, University of Constantine 2, Algeria  
M Khireddine Krolladi, University of El Oued, Algeria  
Djamel Eddine Saïdouni, University of Constantine 2, Algeria

## Organizing Committee Chairs

Mourad Bouzenada, University of Constantine 2, Algeria  
Chaker Mezioud, University of Constantine 2, Algeria

## **Organizing Committee**

Saïd Labeled, University of Constantine 2, Algeria  
Raida Elmansouri, University of Constantine 2, Algeria  
Ilhem Kitouni, University of Constantine 2, Algeria  
Redouane Nouara, University of Constantine 2, Algeria  
Fayal Bachtarzi, University of Constantine 2, Algeria  
Ahmed Chaouki Chaouche, University of Constantine 2, Algeria  
Sofiane Chemaa, University of Constantine 2, Algeria  
Kamel Houari, University of Constantine 2, Algeria

## **Publication Chairs**

Ahmad Taher Azar, Benha University, Egypt  
Nabil Belala, University of Constantine 2, Algeria  
Hacène Belhadeff, University of Constantine 2, Algeria  
Amer Draâ, University of Constantine 2, Algeria  
Abdesselem Layeb, University of Constantine 2, Algeria

## **Publicity and Sponsor Chairs**

Abdelkrim Bouramoul, University of Constantine 2, Algeria  
Mohamed Gharzouli, University of Constantine 2, Algeria

## **Program Committee Chairs**

Allaoua Chaoui, University of Constantine 2, Algeria  
Djamel Eddine Saïdouni, University of Constantine 2, Algeria

## **Program Committee**

Sihem Abbassen, University of Constantine 2, Algeria  
Abdelkrim Abdelli, USTHB, Algeria  
Nabil Absi, Ecole des Mines de Saint-Etienne, France  
Abdelkader Adla, University of Oran 1, Algeria  
Othmane Ait Mohamed, Concordia University, Canada  
Abdelmalek Amine, University of Saida, Algeria  
Abdelkrim Amirat, University of Souk Ahras, Algeria

Baghdad Atmani, University of Oran 1, Algeria  
M. Chaouki Babahenini, University of Biskra, Algeria  
Abdelmalik Bachir, University of Biskra, Algeria  
Amar Balla, Ecole Supérieure d'Informatique (ESI), Algeria  
Kamel Barkaoui, Cedric-Cnam, Paris, France  
M. Chaouki Batouche, University of Constantine 2, Algeria  
Faiza Belala, University of Constantine 2, Algeria  
Nabil Belala, University of Constantine 2, Algeria  
Ghalem Belalem, University of Oran 1, Algeria  
Hacène Belhadeif, University of Constantine 2, Algeria  
Fouzia Benchikha, University of Constantine 2, Algeria  
Djamel Benmerzoug, University of Constantine 2, Algeria  
Mohamed Benmohammed, University of Constantine 2, Algeria  
Djamal Bennouar, University of Blida, Algeria  
Hammadi Bennoui, University of Biskra, Algeria  
Azeddine Bilami, University of Batna, Algeria  
Salim Bitam, University of Biskra, Algeria  
Karim Bouamrane, University of Oran 1, Algeria  
Djalel Eddine Boubiche, University of Batna, Algeria  
Samia Boucherkha, University of Constantine 2, Algeria  
Rachid Boudour, University of Annaba, Algeria  
Mahmoud Boufaïda, University of Constantine 2, Algeria  
Zizette Boufaïda, University of Constantine 2, Algeria  
Zineddine Bouras, EPST, Annaba, Algeria  
Elbey Bourennane, University of Bourgogne, France  
Mourad Bouzenada, University of Constantine 2, Algeria  
Rachid Chalal, Ecole Supérieure d'Informatique (ESI), Algeria  
Allaoua Chaoui, University of Constantine 2, Algeria  
Foudil Cherif, University of Biskra, Algeria  
Mohamed Amine Chikh, University of Tlemcen, Algeria  
Salim Chikhi, University of Constantine 2, Algeria  
Abdellah Chouarfia, USTO, Oran, Algeria  
Pierre de Saqui-Sannes, ISAE, Toulouse, France  
Méroüane Debbah, CentraleSupélec, France  
Lynda Dib, University of Annaba, Algeria  
Noureddine Djedi, University of Biskra, Algeria  
Karim Djemame, University of Leeds, UK  
Mahieddine Djoudi, University of Poitiers, France  
Amer Draâ, University of Constantine 2, Algeria  
Khalil Drira, LAAS-CNRS, Toulouse, France  
Amel El Fallah, LIP6, University of Pierre and Marie Curie, France  
Zakaria Elberichi, University of Sidi Belabbes, Algeria  
Sami Faiz, ISAMM, Tunisia  
Nadir Farah, University of Annaba, Algeria  
Kamel Mohamed Faraoun, University of Sidi Belabbes

Djamel Fekki, University of Sfax, Tunisia  
Djamel Gaceb, University of Boumerdes, Algeria  
M. Mohcen Gammoudi, ISAMM, Tunisia  
Salim Ghanemi, University of Annaba, Algeria  
Mohamed Gharzouli, University of Constantine 2, Algeria  
Nacira Ghoulmi, University of Annaba, Algeria  
Said Ghouli, Philadelphia University, Jordan  
Djamila Hamdadou, University of Oran, Algeria  
Youcef Hammal, USTHB, Algeria  
Reda Mohamed Hamou, University of Saida, Algeria  
Sofiane Hamrioui, Université de Haute-Alsace, Mulhouse, France  
Jean-Michel Ilić, LIP6, Université Pierre et Marie Curie, France  
Laid Kahloul, University of Biskra, Algeria  
Okba Kazar, University of Biskra, Algeria  
Elhillali Kerkouche, University of Jijel, Algeria  
Tarek Khadir, University of Annaba, Algeria  
Hamamache Kheddouci, University of Lyon 1, France  
Mohamed Fayçal Khelfi, University of Oran 1, Algeria  
M. Khireddine Kholliadi, University of El Oued, Algeria  
Kamel Khoualdi, King Abdulaziz University, KSA  
Mohamed Tahar Kimour, University of Annaba, Algeria  
Nour-Eddine Lachachi, University of Oran 1, Algeria  
Yacine Lafifi, University of Guelma, Algeria  
Slimane Larabi, USTHB, Algeria  
Mohamed Tayeb Laskri, University of Annaba, Algeria  
Abdesselem Layeb, University of Constantine 2, Algeria  
Ali Lemouari, University of Jijel, Algeria  
Latifa Mahdaoui, USTHB, Algeria  
Mimoun Malki, University of Sidi Belabbes, Algeria  
Smaine Mazouzi, University of Skikda, Algeria  
Kamel Eddine Melkemi, University of Biskra, Algeria  
El Kamel Merah, University of Khenchela, Algeria  
Salah Merniz, University of Constantine 2, Algeria  
Hayet-Farida Merouani, University of Annaba, Algeria  
Souham Meshoul, University of Constantine 2, Algeria  
Djamel Meslati, University of Annaba, Algeria  
Belhadri Messabih, USTO, Oran, Algeria  
Chaker Mezioud, University of Constantine 2, Algeria  
Abdelouaheb Moussaoui, University of Sétif 1, Algeria  
Ramdane Mâamri, University of Constantine 2, Algeria  
Smail Niar, University of Valenciennes, France  
Salima Oudfel, University of Constantine 2, Algeria  
Mathieu Roche, CIRAD, Montpellier, France  
Paolo Rosso, Technical University of Valencia, Spain  
Zaidi Sahnoun, University of Constantine 2, Algeria

Djamel Eddine Saïdouni, University of Constantine 2, Algeria  
Larbi Sekhri, University of Oran, Algeria  
Djamel Seriai, University of Montpellier 2, France  
Hamid Seridi, University of Guelma, Algeria  
Hassina Seridi, University of Annaba, Algeria  
Yahya Slimani, ISAMM, Tunisia  
Noria Taghezout, University of Oran 1, Algeria  
Hichem Talbi, AEK University, Constantine, Algeria  
Souad Taleb Zouggar, University of Oran 1, Algeria  
Said Talhi, University of Batna, Algeria  
Thouraya Tebbibel, Ecole Supérieure d'Informatique (ESI), Algeria  
Sadek Labib Terissa, University of Biskra, Algeria  
Chouki Tibermacine, University of Montpellier 2, France  
Salah Toumi, University of Annaba, Algeria  
Belabbas Yagoubi, University of Oran 1, Algeria  
Nacer Eddine Zarour, University of Constantine 2, Algeria  
Tewfik Ziadi, Université Pierre et Marie Curie, Paris, France  
Abdelmadjid Zidani, University of Batna, Algeria

## **Co-editors**

Abdelmalek Amine, University of Saïda, Algeria  
Allaoua Chaoui, University of Constantine 2, Algeria  
Salim Chikhi, University of Constantine 2, Algeria  
M. Khireddine Krolladi, University of El Oued, Algeria  
Djamel Eddine Saïdouni, University of Constantine 2, Algeria

## **Additional Reviewers**

Abdaoui, Amine  
Abdelhamid, Djeflal  
Arfi, Farid  
Benaliouche, Houda  
Bendaoud, Zakaria  
Bennama, Miloud  
Bensalem, Imene  
Berkane, Mohamed  
Bouanaka, Mohamed Ali  
Bouchareb, Nassima  
Brahimi, Said  
Cagnina, Leticia  
Chaouche, Ahmed Chaouki

Cherfia, Taha Abdelmoutaleb  
Chettibi, Saloua  
El Habib Daho, Mostafa  
Gassara, Amal  
Gómez Adrián, Jon Ander  
Hamidouche, Kenza  
Hammal, Youcef  
Hernández Farias, Delia Irazú  
Kef, Mâamar  
Kerdoudi, Mohamed Lamine  
Labeled, Saïd  
Lila, Meziani  
Mokhtar, Taffar  
Mustapha Kamel, Abdi  
Seridi, Hassina  
Settouti, Nesma  
Tibermacine, Okba  
Yachba, Khadidja



# Contents

## Part I Algorithms and Complexity

<b>A Review on Different Image Encryption Approaches</b> . . . . .	3
Amina Souyah and Kamel Mohamed Faraoun	
<b>Palmprint Image Quality Measurement Algorithm</b> . . . . .	19
Fares Guerrache and Hamid Haddadou	
<b>Bioinspired Inference System for Medical Image Segmentation</b> . . . . .	31
Hakima Zouaoui and Abdelouahab Moussaoui	
<b>Realization of Gymnastic Movements on the Bar by Humanoid Robot Using a New Selfish Gene Algorithm</b> . . . . .	49
Lyes Tighzert and Boubekeur Mendil	
<b>Reduction of Solution Space in the Automotive Safety Integrity Levels Allocation Problem</b> . . . . .	67
Youcef Gheraibia, Khaoula Djafri and Habiba Krimou	
<b>A Novel Bio Inspired Algorithm Based on Echolocation Mechanism of Bats for Seismic Hazards Detection</b> . . . . .	77
Mohamed Elhadi Rahmani, Abdelmalek Amine, Reda Mohamed Hamou, Amine Rahmani, Hanane Menad, Hadj Ahmed Bouarara and Mohamed Amine Boudia	
<b>Enhanced Chemical Reaction Optimization for Multi-objective Traveling Salesman Problem</b> . . . . .	91
Samira Bouzoubia, Abdesslem Layeb and Salim Chikhi	
<b>Adaptive Cuckoo Search Algorithm for the Bin Packing Problem</b> . . . .	107
Zakaria Zendaoui and Abdesslem Layeb	

## Part II Intelligent and Information Systems

<b>Greedy Mean Squared Residue for Texture Images Retrieval . . . . .</b>	123
Salah Bougueroua and Bachir Boucheham	
<b>Clustering to Enhance Case-Based Reasoning . . . . .</b>	137
Abdelhak Mansoul and Baghdad Atmani	
<b>Improving the Method of Wrist Localization Local Minimum-Based for Hand Detection . . . . .</b>	153
Sofiane Medjram, Mohamed Chaouki Babahenini, Mohamed Ben Ali Yamina and Abdelmalik Taleb-Ahmed	
<b>Parkinson's Disease Recognition by Speech Acoustic Parameters Classification . . . . .</b>	165
D. Meghraoui, B. Boudraa, T. Merazi-Meksen and M. Boudraa	

## Part III Networking and Cloud Computing

<b>The Finger-Knuckle-Print Recognition Using the Kernel Principal Components Analysis and the Support Vector Machines . . . . .</b>	177
S. Khellat-Kihel, R. Abrishambaf, J. Cabral, J.L. Monteiro and M. Benyettou	
<b>An Intelligent Management of Lighting in an Ambient Environment with a Multi-agent System . . . . .</b>	187
Aouatef Chaib, Boussebough Imen and Chaoui Allaoua	
<b>A Proposal for Shared VMs Management in IaaS Clouds . . . . .</b>	201
Sid Ahmed Makhoulf and Belabbas Yagoubi	
<b>Cloud Simulation Model Based on Large Numbers Law for Evaluating Fault Tolerance Approaches . . . . .</b>	217
Oussama Hannache and Mohamed Batouche	
<b>Towards an Inter-organizational Collaboration Network Characterization . . . . .</b>	233
Kahina Semar-Bitah and Kamel Boukhalifa	
<b>Asymmetric End-to-End Security for Human-to-Thing Communications in the Internet of Things . . . . .</b>	249
Somia Sahraoui and Azeddine Bilami	
<b>Mobile User Location Tracking with Unreliable Data . . . . .</b>	261
Samia Zouaoui and Abdelmalik Bachir	

**Part IV Software Engineering and Formal Methods**

**Two Stages Feature Selection Based on Filter Ranking Methods and SVMRFE on Medical Applications . . . . .** 281  
Hayet Djellali, Nacira Ghoualmi Zine and Nabiha Azizi

**A Formal Approach for Maintainability and Availability Assessment Using Probabilistic Model Checking . . . . .** 295  
Abdelhakim Baouya, Djamel Bennouar, Othmane Ait Mohamed and Samir Ouchani

**A Locally Sequential Globally Asynchronous Net from Maximality-Based Labelled Transition System . . . . .** 311  
Adel Benamira and Djamel-Eddine Saidouni

**A Pairwise Approach for Model Merging . . . . .** 327  
Mohammed Boubakir and Allaoua Chaoui

**Author Index . . . . .** 341

**Part I**  
**Algorithms and Complexity**

# A Review on Different Image Encryption Approaches

Amina Souyah and Kamel Mohamed Faraoun

**Abstract** The design of image encryption schemes that make a good compromise between sufficient level of security and execution time is one of the main directions of research, due to their ever-increasing use in real-time Internet image encryption and transmission applications. For such task, a variety of mathematical and biological strategies are investigated in the literature as chaos theory, cellular automata and DNA computing. The intend of this paper is to present a complete study of some recent and prevalent proposed works in the literature, this study covers the analysis of each work by giving its advantages and limitations in terms of security level and execution time. We believe that our study within this contribution will help in the design of new secure crypto-systems for image encryption.

**Keywords** Cryptography · DNA computing · Chaotic maps · Cellular automata · Known/chosen plain-text attacks

## 1 Introduction

Nowadays, and with the over-increasing growth in demand of transmission, storage, distribution and processing of multimedia data such as digital images over open networks, lead to the need of their protection from unauthorized access that comes quite essential especially in case of including confidential information that can be related to military, medical or even personal interest. Cryptography as the art of science that is more recently considered as a branch of both computer science and mathematics [1], can be utilized as a useful scientific approach to provide image's security, confidentiality and integrity via the research of designing an efficient image encryption scheme that can make a good compromise between satisfactory level of security and

---

A. Souyah (✉) · K.M. Faraoun  
Computer Science Department, Djilalli Liabes University, Sidi Bel Abbes, Algeria  
e-mail: souyah.udl@gmail.com

K.M. Faraoun  
e-mail: kamel\_mh@yahoo.fr

execution time, these purposes can't be accomplished with the direct use of traditional encryption algorithms [2] such as DES [3], IDEA [4], AES [5] that mark their unsuitability for encrypting digital images [6] due to their intrinsic features like bulk data capacity, large data size, high redundancy and strong correlation of adjacent pixels in addition to the large computational time. In this paper, a complete study of some recent and prevalent proposed schemes in the literature are presented in detail, this study puts a focus on analyzing each work by giving its advantages and limitations in terms of security level and execution time. The rest of the paper is organized as follows: different strategies used in image encryption schemes are given as Sect. 2. Description of different approaches as the main objective of this contribution is presented in detail in Sect. 3. A comparative study based on the commonly used types of attacks are performed for all the reviewed approaches as Sect. 4. A conclusion is given in Sect. 5.

## 2 Different Strategies Used in Image Encryption Schemes

Several strategies are investigated in the literature to respond to the challenging issue of designing an image cryptosystem that makes a good compromise between sufficient level of security and execution time among which:

Chaos theory that is a mathematical model and a sort of discrete dynamical system, its inherent features of dependency to initial conditions, control parameters and ergodicity have their counterparts of confusion and diffusion as good cryptographic properties [7] that should be satisfied in the design of chaotic image encryption schemes. This similarity in properties traces an interesting relationship between chaos and cryptography. It was Fridrich [8] who designed the classical permutation-diffusion architecture of chaos based image encryption scheme in which it composes mainly of two stages: the first one is the permutation stage and it consists of relocating the images pixels using two dimensional chaotic map, the second one is the diffusion stage and it consists of changing sequentially these permuted pixels using any discretized or continuous chaotic map. Figure 1 shows a detailed description of the Fridrich's classical architecture.

Cellular automata (CAs) are mathematical, physical and biological models and another kind of discrete dynamical systems where time and space are discrete. Their use in cryptography as a base to design image cryptosystems refers firstly to the works of Steven Wolfram [9] in which cellular automata represent models of complex systems [10].

More recently, the attractive properties of DNA computing such as parallelism, huge storage and information density [11] trace its use in the field of cryptography for designing image cryptosystems. Its hybridation with chaos theory is a top and promising area of research that took and still does the attention of several researchers for investigating in this way.

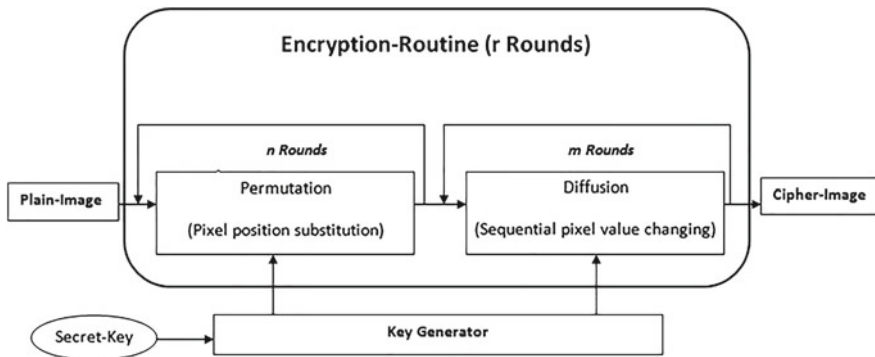


Fig. 1 The block diagram of the proposed scheme

### 3 Description of Different Approaches

**Image encryption scheme proposed by Tiegang Gao and Zengqiang in 2008 [12] (A new image encryption algorithm based on hyper-chaos)**, the proposed approach is based on the use of total shuffling matrix, logistic chaotic map, hyper-chaotic system and confusion-diffusion architecture. In the confusion stage, the plain-image is considered as two-dimensional arrays and both image's rows and columns permutation are applied using two generated chaotic sequences of one dimensional (1D) logistic chaotic map in order to de-correlate the relationship between adjacent pixels. In the diffusion stage, a hyper-chaos and XOR operation are performed to obtain the final ciphered-image.

#### 3.1 Advantages

1. The superiority of using hyper-chaos system as a base to design crypto-systems for image encryption.
2. A tiny modification in the secret key leads to a totally different ciphered image i.e., sensitivity to secret key.
3. A large key space which leads to the immunity of the crypto-system against brute force attacks.

#### 3.2 Limitations

1. The use of logistic map in the confusion stage weakens more the scheme in which sure kind of maps is clarified in [13] to not be selected as a base of chaotic crypto-systems.

2. The low sensitivity to plain-image's small modifications.
3. The generated chaotic sequences that are used in both confusion and diffusion stages are unchangeable whatever the used plain-image, this failing makes the crypto-system vulnerable to known/chosen plain-text attacks.

Moreover, by exploiting the low sensitivity to plain image's tiny modifications and the non-changeable generated key-streams in both confusion/diffusion, the proposed scheme [12] is cryptanalyzed in [14] in which three couples of plain-images/ciphered images are sufficient to break totally the cryptosystem by chosen plain-text attack (CPA) and chosen cipher-text attacks (CCA) and the authors suggested to modify only the diffusion phase by making the generated key-streams plain-image related. More recently in [15], the improvement of the cryptosystem in [14] is analyzed in which it was found that even after the improvement [14], the cryptosystem still suffer from the low plain-image change and the non-resistance to known/chosen plain-text attacks, the authors [15] enhanced the security of the cryptosystem by making both confusion/diffusion plain-image related, so experimented results and simulations clarified that the cryptosystem becomes more sensitive to plain-image change and CPA secure.

**Image encryption scheme proposed by Zhi-liang, Wei Zhang, Kwok-wo Wong and Hai Yu in 2011 [16] (A chaos-based symmetric image encryption scheme using a bit-level permutation)**, the proposed approach is based on Arnold cat map, logistic chaotic map, permutation at a bit level and confusion-diffusion architecture. In the confusion stage, each plain-image's pixel is divided into its composed 8 bits, the positions of these bits are relocated using the generated chaotic sequences of cat map. According to the found results of that the higher 4 bits of each pixel (i.e., 8th, 7th, 6th and 5th) hold how about 94.125 % of the whole image's information and the lower 4 bits (i.e., 4th, 3rd, 2nd and 1st) hold less than 6 %, two different approaches are proposed to shuffle these two groups (i.e., the first is 4 higher bits a and the second is 4 lower bits). At first, an independent permutation is performed for each bit of the first group using generated sequences of cat map with different coefficients. Then, the second group is considered as a whole in permutation to decrease the runtime. The notable effect of this permutation is not only the location of each pixel is changed but also its value as well making the possibility of achieving confusion and diffusion possible in this stage. In the diffusion stage, the classical Fridrich's diffusion is adopted (i.e., the encryption of pixels is performed sequentially at a pixel level) using generated sequences of logistic chaotic map.

### 3.3 Advantages

1. Large key space (i.e., the resistance to brute force attacks is verified).
2. The permutation phase is performed at a bit level leading to achieve both confusion and diffusion in this phase to further enhance the diffusion effect of the crypto-system.



3. A good NPCR, UACI, information entropy, correlation of adjacent pixels values are found which reflect the resistance to statistical and differential attacks.
4. High sensitivity to secret key is verified.
5. The use of higher-dimensional chaotic map (i.e., 2D cat map) that can overcome the drawbacks of one-dimensional (1D) chaotic maps.

### 3.4 Limitations

1. The chaotic key-streams in both confusion and diffusion have no dependency with the characteristics of plain-image which leads to the failing of non-resistance to known/chosen plain-text attacks (i.e., the scheme is not CPA secure).
2. The use of logistic map in the diffusion stage weakens more the scheme in which sure kind of maps is clarified in [13] to not be selected as a base of chaotic crypto-systems.
3. The algorithm takes more execution time due to the use of higher dimensional chaotic maps besides to some required number of rounds.

The security of the crypto-system is analyzed in detail in [17], so besides to the aforementioned limitations especially that of the generated chaotic sequences in both confusion and diffusion stages are unchanged whatever the used plain-image that is considered quite sufficient to break the crypto-system under chosen plain-text attack, another flaws are shown as: the first pixel (0, 0) remains unchanged during all the permutation phase, the connectivity between pixels exists only in the same groups, the fixed value of the parameter  $\alpha = 4$  increases the insecurity of the crypto-system and even the use of logistic chaotic map is unsuitable as a base to design crypto-systems due to its limitations [13]. An improved scheme is proposed in [17] to overcome the limitations of the original work [16] in which the following considerations are taken into account: (1) The encryption procedure is introduced as the first stage after a bit-level permutation is applied using Arnold cat map. (2) Incorporation of the characteristics of the plain-image at the permutation stage. (3) Flipping the sub-images that are obtained from the groups of bits is used as a solution to make the first pixel changeable and as a last improvement. (4) In order to the parameter  $\alpha$  will be changed, it is set to the value of the final parameter of the secret keys.

**Image encryption scheme proposed by Yue Wu, Gelan Yang, Huixia Jin and Joseph P. Noonan in 2012 [18] (Image encryption using the two-dimensional logistic chaotic map)**, the proposed approach is based on a new spatiotemporal chaotic system, nonlinear chaotic map (NCA) and permutation-diffusion architecture. As a primary step, the plain-image is converted to a one dimensional (1D) array of pixels in which a bitwise XOR operation is applied between pixels in order to obtain the diffused image. In the confusion stage, the sum of plain-image's pixels is calculated and the results is converted to [0, 1] range and used as initial condition to generated key-stream of NCA map as a solution to make the generated sequences changeable and plain-image related, a pixel permutation between the diffuse image

and the generated key-stream is performed to obtain the shuffled image. In the diffusion stage, the generated spatiotemporal chaotic sequence is used to diffuse the shuffled image using bitwise XOR operation.

### 3.5 Advantages

1. Large key space (i.e., the resistance to brute force attacks is verified).
2. The generated key-stream in the permutation phase is plain-image's related (i.e., changeable with any change applied to plain-image).
3. A good NPCR (Number of Pixel Change Rate), UACI (Unified Average Changing Intensity), information entropy, correlation of adjacent pixels values are found which reflect the resistance to statistical and differential attacks.
4. High sensitivity to secret key.

### 3.6 Limitations

1. The generated key-stream at the diffusion phase is independent from the processed plain-image i.e., the proposed scheme is not CPA secure.

This failing is exploited in [19] to break the security of the cryptosystem under chosen plain-text attack and it was noticed that a total breaking is possible however under a large number of plain-image/ciphered image pairs. So, the generated key-streams in both the permutation and diffusion modules should have a dependency to plain-image characteristics to avoid the commonly used attacks to break cryptosystems i.e., known/chosen plain-text attacks [15].

**Image encryption scheme proposed by Omid Mirzaei, Mahdi Yaghoobi and Hassan Irani in 2012 [20] (A new Image encryption method: parallel sub-image encryption with hyper chaos)**, the proposed approach is based on chaotic systems, a total shuffling, parallel enciphering and confusion-diffusion architecture. As a primary step, the original image is subdivided into 4 equal sub-images in which the position of each sub-image is scrambled using 4 generated chaotic numbers of logistic chaotic map. In the confusion stage, both row/column permuting is carried out using two generated sequences of logistic chaotic map to obtain the shuffled-image. In the diffusion stage, both Lorenz and Chen's systems are used to generate 15 groups used in encryption, each pixel of the shuffled-image that is subdivided into four equal blocks (sub-images) is enciphered using the matching pixel value of the plain-image, the value of other block and the values of corresponding chosen group. The generated chaotic sequences that are used in both confusion/diffusion stages are key-related.

### 3.7 Advantages

1. Large key space (i.e., the resistance to brute force attacks is verified).
2. A good NPCR, UACI, information entropy, correlation of adjacent pixels values are found which reflect the resistance to statistical and differential attacks.
3. High sensitivity to secret key is verified.
4. The encryption is performed in parallel.

### 3.8 Limitations

1. The permutation phase is performed at a pixel level that leads to just relocating the position of the pixel without changing its value (i.e., there is no diffusion effect) [16].
2. The chaotic key-streams in both confusion and diffusion have no dependency with the characteristics of plain-image which leads to the failing of non-resistance to known/chosen plain-text attacks (i.e., the scheme is not CPA secure).

**Image encryption scheme proposed by Chun-Yan Song, Yu-Long Qiao and Xing-Zhou Zhang in 2013 [21]** (An image encryption scheme based on new spatiotemporal chaos), the proposed approach is based on two-dimensional logistic map and permutation-diffusion architecture under some number of rounds. In the permutation stage, the plain-image is considered as a matrix i.e., 2D array of  $M$  rows and  $N$  columns, using the 2D logistic map two chaotic sequences are generated of  $M \times N$  length and after they are reshaped to form two matrices in order to perform row/column shuffling based on these generated matrices to obtain the permuted image. In the diffusion stage, the permuted image is divided into  $S \times S$  blocks, where  $S$  is the length of the block of pixels determined by plain-image's format ( $4 \times 4$  for grayscale/RGB images and  $32 \times 32$  for binary ones), after each block is encrypted

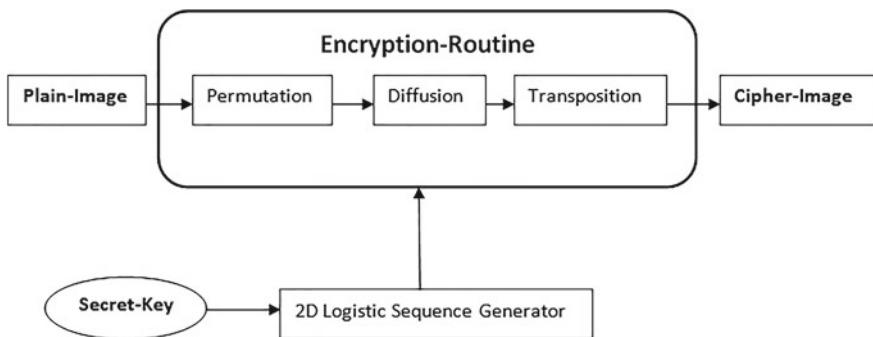


Fig. 2 The block diagram of the proposed scheme

with the generated sequences of 2D logistic map. A transposition step is added which refers to shift each diffused image's pixel using a reference image generated using 2D logistic map from the previous step as a final operation to obtain the ciphered image. Figure 2 shows a detailed description of the proposed scheme.

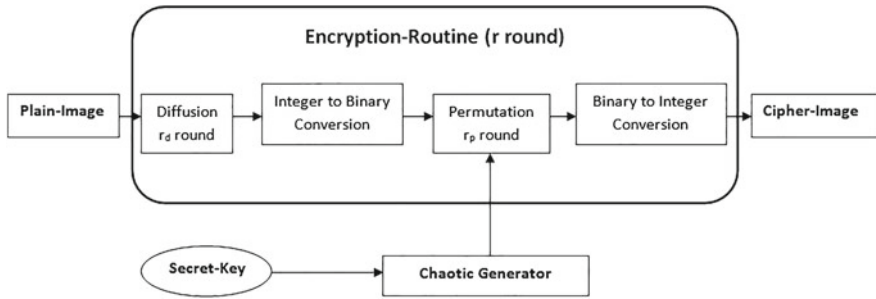
### 3.9 Advantages

1. Large key space (i.e., the resistance to brute force attacks is verified).
2. A good NPCR, UACI, information entropy, correlation of adjacent pixels values are found which reflect the resistance to statistical and differential attacks.
3. High sensitivity to secret key is verified.
4. The use of higher-dimensional chaotic map (i.e., 2D logistic map) that can overcome the drawbacks of one-dimensional (1D) chaotic maps.

### 3.10 Limitations

1. Sufficient level of security is obtained under some number of rounds.
2. The algorithm takes more execution time due to the use of higher dimensional chaotic maps besides to some required number of rounds.
3. The generated key-streams have no dependence with respect to the characteristics of the plain-image that may lead to the non-resistance to known/chosen plain-text attacks.

**Image encryption scheme proposed by Safwan El Assad and Mousa Farajallah in 2015 [22] (A new chaos-based image encryption system)**, the proposed scheme is based on a modified version of 2D cat map, permutation at a bit level and confusion-diffusion architecture. The proposed crypto-system belongs to the category of block ciphers with CBC mode. In the diffusion stage, the plain-image is divided into blocks of 32 bytes and the process is based on binary matrix of size  $32 \times 32$  and XOR bitwise operation, the process is performed under  $rd$  number of rounds in which a local diffusion is achieved. In the confusion stage, a conversion from integer to binary type is performed as the first step and then a bit permutation is carried out using a modified version of 2D cat map that are more powerful than the usual used one, at a bit level not only the position of the bits are modified but also the values of pixels are changed that reflect the achievement of both confusion and diffusion at the permutation layer, the process is performed under  $rp$  number of rounds after that a conversion type from binary to integer is handled to pass to the next round in which the crypto-system is repeated for  $r$  rounds. The used generator for producing the needed chaotic key-streams for the crypto-system is based on the one proposed in [23]. Figure 3 shows the block diagram of the proposed scheme.



**Fig. 3** The block diagram of the proposed scheme

### 3.11 Advantages

1. Large key space (i.e., the resistance to brute force attacks is verified).
2. A good NPCR, UACI, correlation of adjacent pixels values are found which reflect the resistance to statistical and differential attacks.
3. High sensitivity to secret key is verified.
4. The use of higher-dimensional chaotic map (i.e., a modified 2D cat map) that can overcome the drawbacks of one-dimensional (1D) chaotic maps.
5. A permutation is performed at a bit level which leads to not only the bits position is changed but also the corresponding pixel value is did (i.e., attaining both confusion-diffusion in the permutation stage).

### 3.12 Limitations

1. Sufficient level of security is obtained under some number of rounds.
2. The algorithm takes more execution time due to the use of higher dimensional chaotic maps besides to some required number of rounds and the membership to the block cipher category.
3. The crypto-system is performed under a CBC mode (a sequential mode) i.e., any error that affects the transmitted image at a bit level leads to the alteration of the remaining bits after that one (i.e., the transmission of the error).

**Image encryption scheme proposed by Zhongyun Hua and Yicong Zhou in 2016 [24] (Image encryption using 2D logistic-adjusted-Sine map)**, the proposed scheme (LAS-IES) is based on two-dimensional logistic-adjusted-Sine map (2D-LASM), mechanism of inserting random values to plain-image and confusion-diffusion architecture under two encryption rounds. The proposed 2D chaotic map (i.e., 2D-LASM) is characterized by its large chaotic range, unpredictability and a good ergodicity comparing it with several existing chaotic maps, this chaotic map is

used as a base to construct the LAS-IES scheme. The generated chaotic sequences that are used in the scheme are key-related however the mechanism of inserting random values that is applied firstly to the plain-image makes the scheme performing a randomized encryption (RE) i.e., in each time the operation of encryption is executed with the same plain-image and that of the used secret keys, the algorithm is able to produce a new ciphered image that leads to its resistance to both known/chosen plain-image attacks. In the confusion stage, plain-images pixels are shuffled at a bit level to further achieve both confusion and diffusion in the permutation phase. In the diffusion stage, a sequential mode of encrypting pixels is adopted (i.e., for enciphering a new pixel, the previous one is utilized) with the generated chaotic matrix from 2D-LASM. The crypto-system is performed under two rounds of confusion-diffusion.

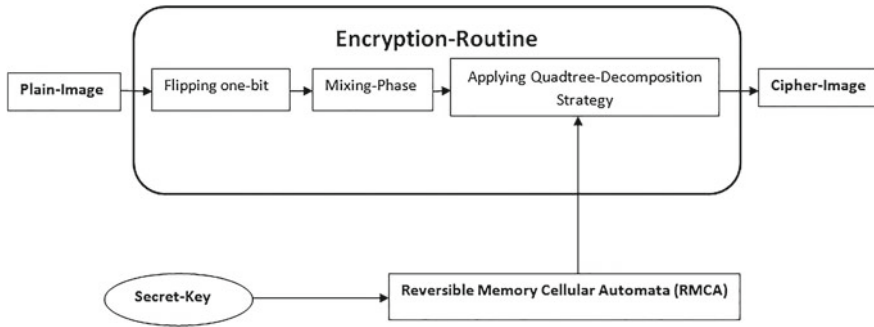
### 3.13 Advantages

1. Large key space (i.e., the resistance to brute force attacks is verified).
2. A good NPCR, UACI, correlation of adjacent pixels values are found which reflect the resistance to statistical and differential attacks.
3. High sensitivity to secret key is verified.
4. The mechanism of random inserting values to the plain-image gives the proposed scheme the ability to resist both known/chosen plain-text attacks (i.e., CPA secure).
5. The scheme performs a random-like enciphering (i.e., a randomized encryption (RE)).
6. The use of new 2D chaotic map with excellent chaotic behavior in comparison with several existing chaotic maps in the literature.
7. A permutation is performed at a bit level which leads to not only the bits position is changed but also the corresponding pixel value is did (i.e., attaining both confusion-diffusion in the permutation stage).

### 3.14 Limitations

1. The 2D chaotic maps are slower than 1D chaotic maps in the use as bases for designing crypto-systems.
2. The scheme is not CCA secure (i.e., the integrity of the image is not verified).

**Image encryption scheme proposed by Amina Souyah and Kamel Mohamed Faraoun in 2015 [25] (Fast and efficient randomized encryption scheme for digital images based on Quadtree decomposition and reversible memory cellular automata)**, the approach is based on the use of one dimensional (1D) reversible memory cellular automata (RMCA) in cooperation with quadtree decomposition



**Fig. 4** The block diagram of the proposed scheme

mechanism (QTD). In the first step, a mixing procedure is adopted to the plain-image for de-correlating the relationship between neighboring pixels and accomplishing a satisfactory level of security using just one encryption round. In the second step, a QTD procedure is employed to the mixed-image in which it is divided consecutively into 4 equal sub-images, these sub-images constitute the four initial configurations of the 4th order RMCA, the encryption/decryption rules (i.e., sub-keys) are obtained from the used secret key by using an efficient key-generation mechanism, the procedure of division and employing RMCA is carried out until reaching  $4 \times 4$  block size, in that case a XOR operation is performed with the last generated rule to obtain the final ciphered image. Figure 4 shows the block diagram of the proposed scheme.

### 3.15 Advantages

1. Large key space (i.e., the resistance to brute force attacks is verified).
2. Good NPCR, UACI, information entropy (global and local), correlation of adjacent pixels values are obtained that reflect the resistance to statistical and differential attacks.
3. High sensitivity to secret key.
4. A good execution time in which just one encryption round is performed.
5. The scheme performs a randomized encryption (RE) (i.e., every time the algorithm is run with the same used plain-image/set of secret keys, it can produce a totally new ciphered image), this property makes the scheme CPA secure (i.e., resistance to known/chosen plain-text attacks).

### 3.16 Limitations

1. The scheme is not CCA secure (i.e., the integrity of the image is not verified).
2. The scheme cant handle the encryption of non-square images.

**Image encryption scheme proposed by Atieh Bakhshandeh and Ziba Eslami 2013 [26] (An authenticated image encryption scheme based on chaotic maps and memory cellular automata)**, the approach is based on the use of both chaos with memory cellular automata (MCA) under permutation-diffusion architecture. In the permutation stage, a piecewise linear chaotic map is adopted to permute the pixels of the plain-image at the pixel level, the generated chaotic sequences are key-related. In the diffusion stage, both logistic chaotic map and one dimensional (1D) linear MCA are employed in which the permuted image is divided into blocks of equal sizes. For every block, its hash value is computed to handle the authentication purpose (i.e., verify the integrity of the original image) after it is enciphered using both 1D LMCA and logistic chaotic map to obtain the ciphred image, it should be mentioned that the generated chaotic sequences in this phase are both key/plain-image related.

### 3.17 Advantages

1. Large key space (i.e., the resistance to brute force attacks is verified).
2. Good NPCR, UACI, information entropy, correlation of adjacent pixels values are obtained that reflect the resistance to statistical and differential attacks.
3. High sensitivity to secret key.
4. Good execution time.
5. The scheme performs authentication (i.e., it is CCA secure).

### 3.18 Limitations

1. The generated key-stream in the permutation has no relation with the characteristics of the plain-image.

This failing is exploited in [27] to break the security of the cryptosystem under chosen plain-text attack and it was noticed that a total breaking using brute force attacks is possible besides to the low sensitivity to plain-image that is experimented and lead to the non-resistance to differential attacks. So, the generated key-streams in both the permutation and diffusion modules should have a dependency to plain-image characteristics to avoid the commonly used attacks to break cryptosystems i.e., known/chosen plain-text attacks [15], in addition to that some suggested improvements are illustrated and experimented in [27] to enhance the sensitivity to plain-image and withstand all the aforementioned attacks.

**Image encryption scheme proposed by Qiang Zhang, Ling Guo and Xiapeng Wei in 2013 [28] (A novel image fusion encryption algorithm based on DNA sequence operation and hyper-chaotic system)**, the approach is based on DNA sequence and Chens hyper-chaotic map. As a first step, the plain-image is encoded



to DNA sequence matrix and the key-matrix that is generated using any random sequence generator is encoded as well. As a second step, the plain-image DNA matrix is scrambled using hyper-chaotic map, the generated chaotic sequences are key-related. As the third step, the scrambled-image is Xored with the key-matrix using DNA XOR operation to obtain the fusion image which is decoded to the corresponding ciphered image. Another image encryption scheme is proposed in [29] by the first and the third previous authors, it is considered as an extension of their previous work [28] in which the main idea around the work [29] is to rather than enciphering one image, two images are enciphered in common. The procedure of encryption is as follows: (1) the two plain-images are encoded using DNA encoding rules, (2) the scrambling mechanism using the generated chaotic sequences of Chen's hyper-chaotic map is applied to each image separately in the confusion stage, (3) DNA subsequence/addition operations are carried out for each permuted-image using the generated chaotic sequences of both Chen's and Lorenz chaotic systems in the diffusion stage, (4) the decoding operation is handled for each image using DNA decoding rules to obtain the final two ciphered-images.

### 3.19 Advantages

1. Large key space (i.e., the resistance to brute force attacks is verified) [28, 29].
2. Good information entropy, correlation of adjacent pixels values are obtained that reflect the resistance to statistical attacks [28, 29].

### 3.20 Limitations

1. The generated chaotic sequences have no relation with the characteristics of the plain-image [28, 29].
2. The image preserves its statistical information due to the use of a single chosen rule during the DNA encoding process [30] in both [28, 29].

This failing is exploited in [31] to break the security of the cryptosystem [28] under chosen plain-text attack in which  $4mn/2 + 1$  (where  $m$  and  $n$  are the height and the width of the image respectively) chosen plain-images are needed, it was noted that even the generated key-matrix should be changed for every encryption process besides to the generated key-streams. In [32], the security of the scheme [28] is analyzed again in which it was found that it can be broken with less than  $\lceil \log_2(4mn)/2 \rceil + 1$  chosen plain-images. More recently, another re-evaluation for the same scheme is studied [33] in which it was shown that the proposed scheme is similar to confusion-only scheme without any diffusion, this later makes its security very vulnerable as indicated in [34] in addition to the generated chaotic sequences that are just key-related (i.e., without taking the characteristics of the plain-image

**Table 1** Comparative results of the commonly used types of attacks

Approach's reference	Resistance to exhaustive key search	CPA secure	CCA secure	Resistance to differential/statistical attacks
[12]	Yes	No	No	No
[16]	Yes	No	No	Yes
[18]	Yes	No	No	Yes
[20]	Yes	No	No	Yes
[21]	Yes	No	No	Yes
[22]	Yes	Yes	No	Yes
[24]	Yes	Yes	No	Yes
[25]	Yes	Yes	No	Yes
[26]	Yes	No	Yes	No
[28, 29]	Yes	No	No	Yes

into account) which leads to its broken by chosen plain-text attack. The same failing is repeated again in the new scheme [29], the generated chaotic sequences for both confusion and diffusion stages are unchangeable in which no dependency to the plain-image characteristics is taken into account, this weakening is exploited in [35] to break the crypto-system using some pairs of chosen plain-texts and their corresponding cipher-texts under chosen plain-text attack.

## 4 Comparison of Different Approaches

A comparative study in terms of the commonly used types of attacks such as: exhaustive key search, known-plaintext attack (CPA secure), chosen-ciphertext attack (CCA secure) and differential/statistical attacks as applied on all the above reviewed approaches. Table 1 shows the comparative results of such attacks of all the reviewed approaches.

## 5 Conclusion

Several image encryption schemes are proposed in the literature based on different strategies such as chaos theory, cellular automata, DNA computing and their hybridization however great amount of them suffer from some security failings that lead to their broken either by brute force attacks in case of small key-space, or differential attacks in case of low diffusion effect that lead to low NPCR and UACI values, or generated chaotic key-streams that are key-related i.e., that they are unchangeable in each encryption process, this later is the commonly used failing even in the design

of new chaotic schemes that conducts to the non-resistance to both known/chosen plain-text attacks, as a solution to overcome this limitation several crypt-analyzers notice to introduce the characteristics of the plain-image in the generation of the chaotic key-streams in order to make them changeable in each time the algorithm is executed even with the same set of keys. In this paper, a complete study of some proposed works in the literature are presented and analyzed in detail in which their advantages and limitations in terms of security level and execution time are well clarified.

## References

1. Acharya, B., Patra, S.K., Panda, G.: Image encryption by novel cryptosystem using matrix transformation. In: ICETET'08. First International Conference on Emerging Trends in Engineering and Technology, pp. 77–81. IEEE (2008)
2. Norouzi, B., Seyedzadeh, S.M., Mirzakuchaki, S., Mosavi, M.R.: A novel image encryption based on row-column, masking and main diffusion processes with hyper chaos. *Multimed. Tools Appl.* **74**(3), 781–811 (2015)
3. Howard, R.: Data encryption standard. *Inf. Age* **9**(4), 204–210 (1987)
4. Lai, X., Massey, J.L.: A proposal for a new block encryption standard. In: *Advances in Cryptology EUROCRYPT90*, pp. 389–404. Springer (1990)
5. Kak, A., Mayes, K.: *Aes: The Advanced Encryption Standard*. Lecture Notes on Computer and Network Security. Purdue University (2013)
6. El Assad, S., Farajallah, M., Vladeanu, C.: Chaos-based block ciphers: an overview. In: 2014 10th International Conference on Communications (COMM), pp. 1–4. IEEE (2014)
7. Pellicer-Lostao, C., Lopez-Ruiz, R.: Notions of chaotic cryptography: sketch of a chaos based cryptosystem (2012). [arXiv:1203.4134](https://arxiv.org/abs/1203.4134)
8. Fridrich, J.: Symmetric ciphers based on two-dimensional chaotic maps. *Int. J. Bifurc. Chaos* **8**(06), 1259–1284 (1998)
9. Wolfram, S.: *Cryptography with cellular automata*. In: *Advances in Cryptology CRYPTO85 Proceedings*, pp. 429–432. Springer (1985)
10. Sarkar, P.: A brief history of cellular automata. *ACM Comput. Surv. (CSUR)* **32**(1), 80–107 (2000)
11. Watada, J., et al.: Dna computing and its applications. In: *ISDA'08. Eighth International Conference on Intelligent Systems Design and Applications*, vol. 2, pp. 288–294. IEEE (2008)
12. Gao, T., Chen, Z.: A new image encryption algorithm based on hyper-chaos. *Phys. Lett. A* **372**(4), 394–400 (2008)
13. Arroyo, D., Rhouma, R., Alvarez, G., Fernandez, V., Belghith, S.: On the skew tent map as base of a new image chaos-based encryption scheme. In: *Second Workshop on Mathematical Cryptology*, pp. 113–117 (2008)
14. Rhouma, R., Belghith, S.: Cryptanalysis of a new image encryption algorithm based on hyper-chaos. *Phys. Lett. A* **372**(38), 5973–5978 (2008)
15. Jeng, F.-G., Huang, W.-L., Chen, T.-H.: Cryptanalysis and improvement of two hyper-chaos-based image encryption schemes. *Signal Process.: Image Commun.* **34**, 45–51 (2015)
16. Zhu, Z., Zhang, W., Wong, K., Hai, Y.: A chaos-based symmetric image encryption scheme using a bit-level permutation. *Inf. Sci.* **181**(6), 1171–1186 (2011)
17. Zhang, Y.-Q., Wang, X.-Y.: Analysis and improvement of a chaos-based symmetric image encryption scheme using a bit-level permutation. *Nonlinear Dyn.* **77**(3), 687–698 (2014)
18. Song, C.-Y., Qiao, Y.-L., Zhang, X.-Z.: An image encryption scheme based on new spatiotemporal chaos. *Optik-Int. J. Light Electr. Optics* **124**(18), 3329–3334 (2013)

19. Rabei, B., Hermassi, H., Abd El-Latif, A.A., Rhouma, R., Belghith, S.: Breaking an image encryption scheme based on a spatiotemporal chaotic system. *Signal Process.: Image Commun.* **39**, 151–158 (2015)
20. Mirzaei, O., Yaghoobi, M., Irani, H.: A new image encryption method: parallel sub-image encryption with hyper chaos. *Nonlinear Dyn.* **67**(1), 557–566 (2012)
21. Wu, Y., Yang, G., Jin, H., Noonan, J.P.: Image encryption using the two-dimensional logistic chaotic map. *J. Electr. Imaging* **21**(1), 013014-1 (2012)
22. El Assad, S., Farajallah, M.: A new chaos-based image encryption system. *Signal Process.: Image Commun.* (2015)
23. El Assad, S., Noura, H.: Generator of chaotic sequences and corresponding generating system (2014)(. US Patent 8,781,116
24. Hua, Z., Zhou, Y.: Image encryption using 2d logistic-adjusted-sine map. *Inf. Sci.* (2016)
25. Souyah, A., Faraoun, K.M.: Fast and efficient randomized encryption scheme for digital images based on quadtree decomposition and reversible memory cellular automata. *Nonlinear Dyn.* 1–18 (2015)
26. Bakhshandeh, A., Eslami, Z.: An authenticated image encryption scheme based on chaotic maps and memory cellular automata. *Optics Lasers Eng.* **51**(6), 665–673 (2013)
27. Kabirirad, S., Hajiabadi, H.: Cryptanalysis of an authenticated image encryption scheme based on chaotic maps and memory cellular automata. *IACR Cryptol. ePrint Arch.* **2015**, 326 (2015)
28. Zhang, Q., Guo, L., Wei, X.: A novel image fusion encryption algorithm based on dna sequence operation and hyper-chaotic system. *Optik-Int. J. Light Electr. Optics* **124**(18), 3596–3600 (2013)
29. Zhang, Q., Wei, X.: A novel couple images encryption algorithm based on dna subsequence operation and chaotic system. *Optik-Int. J. Light Electr. Optics* **124**(23), 6276–6281 (2013)
30. Liao, X., Kulsoom, A., Ullah, S., et al.: A modified (dual) fusion technique for image encryption using sha-256 hash and multiple chaotic maps. *Multimed. Tools Appl.* 1–26 (2015)
31. Zhang, Y., Wen, W., Moting, S., Li, M.: Cryptanalyzing a novel image fusion encryption algorithm based on dna sequence operation and hyper-chaotic system. *Optik-Int. J. Light Electr. Optics* **125**(4), 1562–1564 (2014)
32. Xie, T., Liu, Y., Tang, J.: Breaking a novel image fusion encryption algorithm based on dna sequence operation and hyper-chaotic system. *Optik-Int. J. Light Electr. Optics* **125**(24), 7166–7169 (2014)
33. Zhang, Y.: Cryptanalysis of a novel image fusion encryption algorithm based on dna sequence operation and hyper-chaotic system. *Optik-Int. J. Light Electr. Optics* **126**(2), 223–229 (2015)
34. Li, S., Li, C., Chen, G., Bourbakis, N.G., Lo, K.-T.: A general quantitative cryptanalysis of permutation-only multimedia ciphers against plaintext attacks. *Signal Process.: Image Commun.* **23**(3), 212–223 (2008)
35. Zeng, L., Liu, R.R.: Cryptanalyzing a novel couple images encryption algorithm based on dna subsequence operation and chaotic system. *Optik-Int. J. Light Electr. Optics* **126**(24), 5022–5025 (2015)

# Palmprint Image Quality Measurement Algorithm

Fares Guerrache and Hamid Haddadou

**Abstract** Biometric systems proposed in the literature have reached a correct performance level when the acquired samples are of good quality. However, the performances fall when these samples are of poor quality. In order to face up to this problem, integration of modules for measuring sample quality in the process of biometric recognition is necessary. In this paper, we propose a new approach for measuring palmprint image quality in terms of illumination, and integrate it in the biometric system to reject the palmprint of poor illumination and to make new session of acquisition. The proposed approach has been evaluated on PolyU Palmprint database. The achieved results are very encouraging.

**Keywords** Biometric • Palmprint • Image quality • Quality measurement • Quality evaluation • Quality assessment

## 1 Introduction

The automatic personal identification is an important service for the physical and logical resources security in many areas such as access control to buildings, border control and e-commerce. Traditionally, there are two categories of automatic personal identification: knowledge-based, such as a password and a PIN, and token-based such as a physical key and an ID card. However, these methods have some limitations. In the knowledge-based approach, the “knowledge” can be guessed or forgotten. In the

---

F. Guerrache (✉)

STIC Doctoral School, High National School of Computer Science (ESI),  
BP 68 M Oued Smar, 16309 El Harrach, Algiers, Algeria  
e-mail: f\_guerrache@esi.dz

H. Haddadou (✉)

LCSI Laboratory, High National School of Computer Science (ESI),  
BP 68 M Oued Smar, 16309 El Harrach, Algiers, Algeria  
e-mail: h\_haddadou@esi.dz

token-based approach, the “token” can be easily stolen or lost. As a result, biometric personal identification is a best alternative. Biometrics is an automatic technique for recognizing humans based on physiological characteristics such as fingerprint, palmprint, face, iris pattern and retina, or behavior characteristics such as voice, signature and gait [1]. Unlike the token and the knowledge of the traditional identification approaches, biometric characteristics cannot be lost, stolen, or easily forged, they are also considered to be persistent and unique.

Palmprint recognition is one of the most important newly developing biometric technologies. Palmprint recognition uses the person’s palm as a biometric for identifying or verifying person’s identity. Palmprint personal authentication employs two types of images: high resolution and low resolution images [2]. A wide variety of features can be extracted at different image resolutions. In low resolution images features such as principal lines, wrinkles and textures can be extracted with less than 100 dpi (dots per inch) [3]. However, features like minutiae points, ridges and singular points can be obtained from high resolution images with at least 400 dpi [3]. In general, high resolution images are suitable for forensic applications such as criminal detection, while low resolution images essential for civil and commercial applications such as access control. Initially palmprint research focused on high-resolution images but now almost all research is on low resolution images for civil and commercial applications [4–6]. Palmprint recognition approaches are categorized mainly based on structural features, statistical features or the hybrid of these two types of features [7].

All biometric systems stages (enrolment, identification and verification), based on physiological characteristics, need a step of image acquisition. The biometric image acquired from this step may undergo a number of distortions such as poor illumination on a face, cuts on a fingerprint and reflections in an iris. This may significantly decrease the performances of the biometric systems. In order to face up to this problem, researchers have recently defined the concept of the biometric image quality measurement. It is useful in different settings (enrolment, identification and verification) as well as in different processing phases (pre-processing, matching and decision) of a biometric system [8]. The image quality measurement constitutes a full-fledged module in biometric processes and follows the image acquisition module. The image quality measurement module takes a biometric image  $I$  as input, and returns a value  $Q$  called quality score. The quality score can be used to generate feedback on image acquisition, to guard the enrollment process, to estimate the failure-to-enroll rate (FTE), to improve the matching performance, to enhance the classification performance and to evaluate the sensor state [7, 9–11].

During the past decades, several approaches have been proposed for the biometric image quality measurement and the most of them are addressed to evaluate the image quality of fingerprint [12–16], face [17–20] and iris [21–23]. However, few researchers attempted to measure the quality of low-resolution palmprint image owing to the complex nature of its features. To the best of our knowledge, only Prasad et al. [11] have proposed an approach for measuring the low-resolution palmprint image quality in terms of illumination. This approach divides the palmprint image into non-overlapped square blocks and computed a local quality score

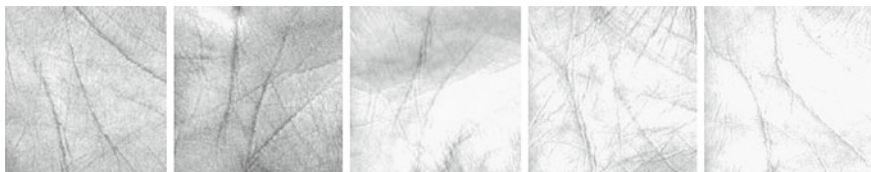
for each block using the root mean square contrast. Based on this local score and a threshold  $K_{th}$ , each non-overlapping block is classified either as good or bad. The global quality score is then computed based on the number of good and bad blocks in the palmpoint. To apply this global quality score in the palmpoint recognition system, this work propose to fusion it with the score match for the recognition performance enhancement. The analysis of experimental results of this work shows that the proposed fusion improves the recognition performance only when the palmpoint image is of good and intermediate illumination. However, when the palmpoint is of poor illumination, the performance remains the same that without fusion.

To deal with this problem, we propose in this paper a new low resolution palmpoint quality measurement approach and we apply it in the palmpoint recognition system to reject the image of poor illumination and generate feedback on image acquisition.

The rest of the paper is organized as follows. Section 2 presents the quality measure (illumination) proposed in our approach. We indicate the details of the proposed palmpoint image algorithm in Sect. 3. Section 4 describes the application of our quality measurement image algorithm in the palmpoint recognition system. Section 5 provides the experimental results of our work. We conclude this work in Sect. 6.

## 2 Proposed Quality Measure

The acquisition process of the low resolution palmpoint image begins generally with the palm lighting using light source of biometric capture. The non-frontal exposure of the palm to the capture light source, its overexposure or underexposure to the light source and the imperfect lighting conditions of the room acquisition can cause bright spots and/or dark spots in captured palmpoint image as shown in Fig. 1. This incorrect illumination affects greatly the palmpoint biometric features, and thus severely degrades the performance of a recognition system. Preprocessing methods are among the most extended and easiest to use of all methods proposed to deal with illumination problems. However, its complete elimination or correction using these preprocessing methods is a complicated and difficult task. This is why we propose the illumination as a quality measure in our new approach for measuring low resolution palmpoint image quality.



**Fig. 1** Palmpoints of different illumination quality from PloyU Palmpoint Database [25]

### 3 Proposed Palmprint Image Quality Measurement Algorithm

The main aim of our work is to propose a new palmprint image quality measurement algorithm that allows determining if the palmprint image is acquired under good illumination conditions or not. Our quality measurement algorithm is based on the assessment of the palmprint image area correctly illuminated by the exclusion of the very bright spots and the very dark spots. To deal the palmprint illumination problem, we adopt here a local approach that takes the palmprint region of interest as input, and returns a scalar value which represents its quality. The following sections present the four main steps of our palmprint image quality measurement algorithm:

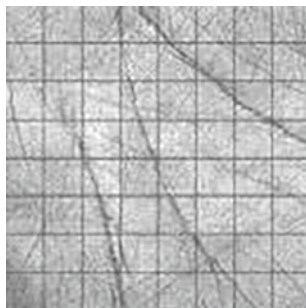
#### 3.1 Palmprint Region of Interest Dividing

In the first step of our algorithm, the  $128 \times 128$  pixel ROI (Region Of interest) of gray level palmprint image is divided into  $N$  non-overlapped square blocks of  $8 \times 8$  pixel everyone as shown in Fig. 2.

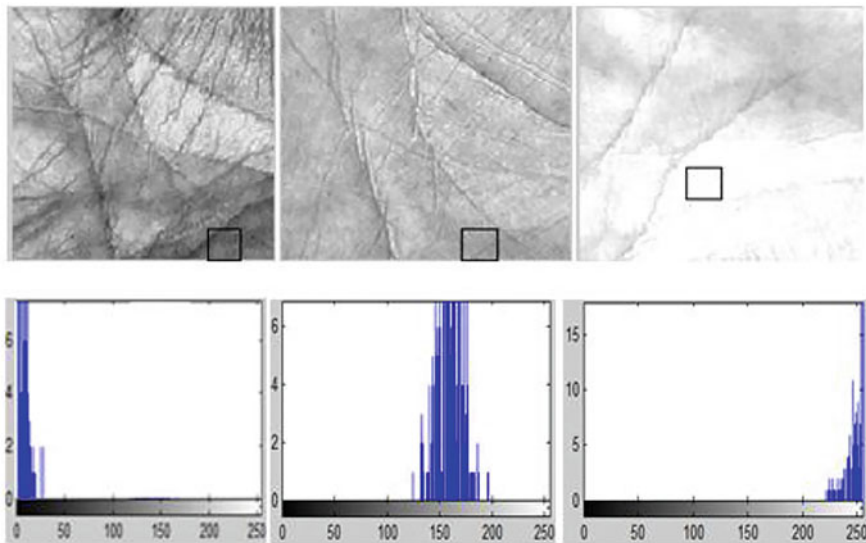
#### 3.2 Reference Bloc Determining

According to Zhang et al. [24], the structural information of images (high-frequency components) is invariant to illumination. Since the principal lines of low resolution palmprint are biometric structural information, we can therefore justify the existence of at least one good quality illumination block located above these lines, even if the palmprint image is of poor illumination. Based on this heuristics, we choose among the  $N$  blocks of the ROI the one that has the best illumination and to designate it as reference block ( $B_R$ ). This choice is based on the gray level histograms of the palmprint image blocks. As shown in Fig. 3, the distribution of the

**Fig. 2** Palmprint image dividing







**Fig. 3** Gray level distribution of different quality blocs

gray level values of a block of a normal illumination is concentrated generally in the middle of the histogram, while the distribution of the gray level values of a block of very dark or very bright illumination is concentrated respectively in the lower or higher end of the histogram [10]. To determine the concentration of the gray level distribution of the histogram  $h_B$  of each block, we compute its center of mass  $mc(h_B)$  as follow:

$$mc(h_B) = \left( \sum_{i=0}^{255} i \cdot h_B(i) \right) / \left( \sum_{i=0}^{255} h_B(i) \right) \tag{1}$$

where  $i$  and  $h_B(i)$  are the gray level and the value of histogram at this level respectively.

After having computed the centers of mass of the histograms of  $N$  blocks, we select the one that has the closest center of mass of the value 127.5 as a reference bloc  $B_R$ .

### 3.3 Local Quality Score Computing

Once the reference block  $B_R$  is located on the ROI of palmprint image, we proceed in this step to calculate the degree of similarity between each block of the ROI

(called test bloc  $B_T$ ) and the reference block  $B_R$ . This degree of similarity is called local quality score  $LQS$ . To compute the  $LQS$ , we propose to calculate the similarity between the gray level histogram  $h_T$  of the test block and the gray level histogram of the reference block  $h_R$  using the following formula:

$$LQS = d(h_T, h_R) = \sum_{i=0}^{255} \min[h_T(i), h_R(i)] \quad (2)$$

where  $h_T(i)$  and  $h_R(i)$  are the values of the test and reference block histograms at the gray level  $i$ .

The  $LQS$  takes its value in the interval  $[0, L]$  where  $L = \sum_{i=0}^{255} h_R(i)$ , 0 means a poor quality block, while  $L$  means good quality block.

However, since we are interested in values in the interval  $[0, 1]$ , we compute the normalized local score quality  $NLQS$  using the following function:

$$NLQS = \frac{SQL}{L} \quad (3)$$

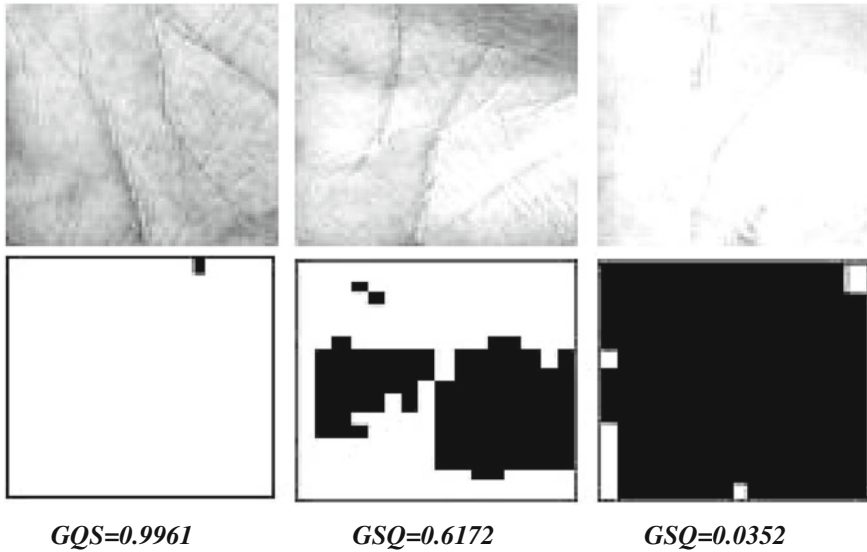
where  $L = \sum_{i=0}^{255} h_R(i)$ , 0 means poor quality block and 1 means good quality block.

### 3.4 Global Quality Score Computing

In order to compute the global quality score  $GQS$  of the whole palmprint image, we propose to mark each block of the ROI palmprint image either as good or poor based on its normalized local sore quality  $NLQS$  and a threshold  $\alpha$  experimentally determined. In fact, the blocks that have the normalized local quality score greater than or equal the threshold  $\alpha$  ( $NLQS \geq \alpha$ ) are marked as good, while those having the normalized local quality score less than the threshold  $\alpha$  ( $NLQS < \alpha$ ) are marked as poor. Hence, the global quality score  $GQS$  is computed by the percentage of blocks marked as good as follows (see Fig. 4):

$$GQS = \frac{N_B}{N} \quad (4)$$

with  $N_B$  and  $N$  are the number of good blocks and the overall blocks number respectively.

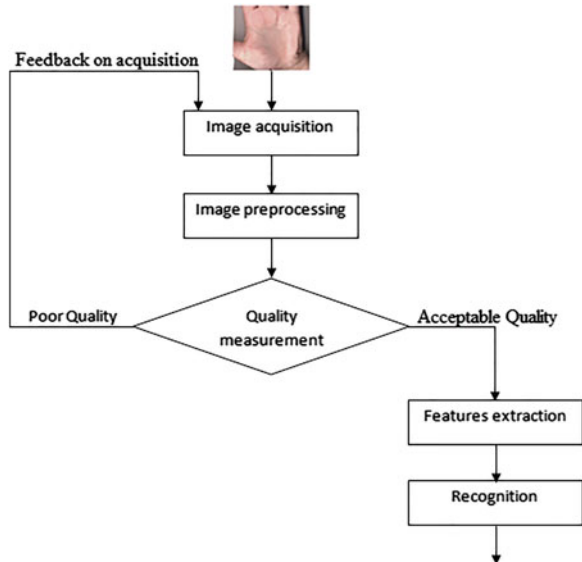


**Fig. 4** The global score quality computation (Blocks with *white color* indicate higher quality and Blocks with *black color* indicate poor quality)

### 4 Application in Palmprint Recognition

In our work, we propose to apply the proposed quality measurement algorithm in palmprint system recognition (enrolment, identification and verification) in order to generate feedback on image acquisition as shown in the framework of Fig. 5. In

**Fig. 5** Framework using our palmprint image quality measurement algorithm



fact, once palmprint images are preprocessed and their quality is evaluated, only images with acceptable quality are received for recognition; others (images with Poor Quality) are discarded and reacquired. To determine the quality of a given palmprint image  $I$ , we propose to divide it into two classes:  $C_1$  for Acceptable Quality and  $C_2$  for Poor Quality. Then, the palmprint image  $I$  is assigned to its class using its global quality score computed by the proposed palmprint quality measurement algorithm and a threshold  $\beta$  experimentally determined, as follow:

$$I \in \begin{cases} C_1 & \text{if } \text{GQS} \geq \beta \\ C_2 & \text{otherwise} \end{cases} \quad (5)$$

## 5 Experimental Results

The presented palmprint image quality measurement approach has been tested on the Hong Kong Polytechnic University (PolyU) palmprint database [25] using MATLAB 7.14.0 (R2012a). The PolyU database has 7752 gray scale low-resolution (75 dpi) palmprint images corresponding to 386 classes. Each class has 18 to 20 images taken in two sessions. The PolyU database palmprint images are captured using CCD-based camera under different illumination conditions. The palmprint images of the first session are acquired under good and intermediate illumination, while those of the second session are acquired under poor illumination. This makes PolyU palmprint as a good choice to test our palmprint image quality measurement approach. We have carried out two experiments in our work. The first is performed to determine the thresholds  $\alpha$  and  $\beta$  of our proposed quality measurement approach. The second experiment aims to validate and directly test the performance of our approach.

### 5.1 Experiment for Determining the Thresholds $\alpha$ and $\beta$

To determine the optimum values of the thresholds  $\alpha$  and  $\beta$ , we have selected randomly a set of 100 poor quality palmprint images of different classes from the images of the second session of PolyU palmprint database. Then, we have evaluated the quality illumination of this image set using our quality measurement approach at different values of  $\alpha$  and  $\beta$ . We have registered for each pair of values ( $\alpha$ ,  $\beta$ ) the number of images judged of poor quality by our approach compared to those randomly selected (see Table 1). The results of this experiment show that the number of the poor quality palmprint images obtained by our approach reaches the number of the poor quality images randomly selected where the values of the thresholds  $\alpha$  and  $\beta$  are respectively 0.3 and 0.6. Thus, the optimum values of the thresholds  $\alpha$  and  $\beta$  are respectively 0.3 and 0.6.

**Table 1** Experiment results for determining the thresholds  $\alpha$  and  $\beta$

$\alpha$	B	Number of poor quality images obtained/randomly set
$\alpha = 0.2$	$\beta = 0.2$	23
	$\beta = 0.3$	42
	$\beta = 0.4$	58
	$\beta = 0.5$	68
	$\beta = 0.6$	70
	$\beta = 0.7$	82
	$\beta = 0.8$	96
$\alpha = 0.3$	$\beta = 0.2$	63
	$\beta = 0.3$	69
	$\beta = 0.4$	72
	$\beta = 0.5$	89
	$\beta = 0.6$	100
	$\beta = 0.7$	100
	$\beta = 0.8$	100
$\alpha = 0.4$	$\beta = 0.2$	100
	$\beta = 0.3$	100
	$\beta = 0.4$	100
	$\beta = 0.5$	100
	$\beta = 0.6$	100
	$\beta = 0.7$	100
	$\beta = 0.8$	100
$\alpha = 0.5$	$\beta = 0.2$	100
	$\beta = 0.3$	100
	$\beta = 0.4$	100
	$\beta = 0.5$	100
	$\beta = 0.6$	100
	$\beta = 0.7$	100
	$\beta = 0.8$	100
$\alpha = 0.6$	$\beta = 0.2$	100
	$\beta = 0.3$	100
	$\beta = 0.4$	100
	$\beta = 0.5$	100
	$\beta = 0.6$	100
	$\beta = 0.7$	100
	$\beta = 0.8$	100

### 5.2 Experiment to Validate and to Test the Performance

In order to validate our image quality measurement approach and to determine its accuracy to assign a given palmprint image at its real quality class: acceptable

**Table 2** Experiment results for testing the performance

Classified quality	Assigned quality	
	Acceptable	Poor
Acceptable	100	5
Poor	0	95
Accuracy	100 %	95 %

(Good and Intermediate) or poor, we have exploited the separating of the image quality in terms of illumination viewed in the database PolyU where the images of acceptable (good and intermediate) are acquired in the first session and those of poor quality are acquired in the second session. In fact, we have selected randomly two sets of 100 palmprint images of different classes from PolyU palmprint database. The first set (SET 1) contains palmprint images of the first session of PolyU (palmprint of acceptable quality); while the second set (SET 2) contains palmprint images of the second session of PolyU (palmprint of poor quality). Then, we have applied our palmprint image quality measurement algorithm on the two sets (SET 1 and SET 2) to determine the number of palmprint images correctly assigned at its real quality classes compared to the quality classification viewed in the database PolyU. Comparing results are shown in Table 2. This results show that our palmprint image quality measurement approach has a very high level accuracy.

## 6 Conclusions

This paper proposes a new approach for measuring low-resolution palmprint image quality in terms of illumination. It is a local-based method that divides the region of interest of the palmprint image into non-overlapped square blocks. A local quality score is then computed for each bloc using the center of mass of the gray level histogram and the best bloc of image. The global score is computed from the local scores. This approach is integrated in the palmprint recognition system to reject the image of poor illumination and generate feedback on image acquisition. The acceptable palmprint images are received for recognition. The experimental results on PolyU palmprint database confirm the effectiveness of our approach and its usefulness in the low-resolution palmprint recognition system.

## References

1. Gorodnichy, D.O.: Evolution and evaluation of biometric systems. In: Proceedings of the IEEE Symposium on Computational Intelligence in Security and Defense Applications (CISDA 2009), Ottawa, pp. 1–8 (2009)
2. Dewangan, D.P., Pandey, A.: A survey on security in palmprint recognition. *Int. J. Adv. Res. Comput. Eng. Tech.* **1**, 347–351 (2012)

3. Zhang, D., Kong, W.K., You, J., Wong, M.: On-line palmprint identification. *IEEE Trans. Pattern Anal. Mach. Intell.* **25**, 1041–1050 (2003)
4. Verma, S., Mishra, P.: A survey paper on palm prints based biometric authentication system. *Int. J. Electric. Electron. Eng.* **1**, 20–27 (2012)
5. Kozik, R., Choras, M.: Combined Shape and Texture Information for Palmprint Biometrics. *J. Inform. Assur. Secur.* **5**, 058–063 (2010)
6. Kong, A., Zhang, D., Kamel, M.: A survey of palmprint recognition. *Pattern Recog.* Elsevier **42**, 1408–1418 (2009)
7. Zheng, Y., Shi, G.S., Wang, Q.R., Zhang, L.: Palmprint Image Quality Measures in Minutiae-based Recognition. China, pp. 140–143 (2007)
8. De Marsico, M., Nappi, M., Riccio, D.: Measuring Measures for Face Sample Quality. *MiFor'11*, Scottsdale Arizona USA, pp. 7–12 (2011)
9. Hsu, R.L.V., Shah, J., Martin, B.: Quality assessment of facial images. In: *IEEE Biometrics Symposium*, pp. 1–6 (2006)
10. Gao, X., Li, S.Z., Liu, R., Zhang, P.: Standardization of face image sample quality. In: *Proceedings of the International Conference on Advances in Biometrics (ICB'07)*, pp. 242–251 (2007)
11. Prasad, S.M., Govindan, V.K., Sathidevi, P.S.: Image quality augmented intramodal palmprint authentication. *IET Image Process* **6**, 668–676 (2012)
12. Awasthi, A., Venkataramani, K., Nandini, A.: Image quality quantification for fingerprints using quality-impairment assessment. In: *IEEE Workshop on Applications of Computer Vision (WACV)*, pp. 296–302 (2013)
13. An, F.J., Cheng, X.P.: Approach for Estimating the Quality of Fingerprint Image Based on the Character of Ridge and Valley Lines. *IEEE*, pp. 113–116 (2012)
14. Tao, X., Yangy, X., Zang, Y., Jia, ., Tian, J.: A novel measure of fingerprint image quality using principal component analysis (PCA). In: *5th International Conference on Biometrics Compendium*, IEEE, pp. 170–175 (2012)
15. Zheng, L., Bo, F., Zhi, H.: A novel method for the fingerprint image quality evaluation. In: *International Conference on Computational Intelligence and Software Engineering CiSE*, pp. 1–4 (2009)
16. Liu, L., Tan, T., Zhan, Y.: Based on SVM automatic measures of fingerprint image quality. In: *IEEE Pacific-Asia Workshop on Computational Intelligence and Industrial Application*, pp. 575–578 (2008)
17. Abaza, A., Harrison, M.A., Bourlai, T.: Quality metrics for practical face recognition. In: *21st International Conference on Pattern Recognition ICPR*, Tsukuba Japan, pp. 3103–3107 (2012)
18. Chen, X.H., Li, C.Z.: Image quality assessment model based on features and applications in face recognition. In: *IEEE International Conference on Signal Processing, Communications and Computing (ICSPCC)*, pp. 1–4 (2011)
19. Rizo-Rodriguez, D., Mendez-Vazquez, H., Garcia-Reyes, E.: An Illumination Quality Measure for Face Recognition. In: *International Conference on Pattern Recognition*, pp. 1477–1480 (2010)
20. Zhou, X., Bhanu, B.: Evaluating the quality of super-resolved images for face recognition. In: *Computer Vision and Pattern Recognition Workshops*, pp. 1–8 (2008)
21. Kalka, N.D., Zuo, J., Schmid, N.A., Cukic, B.: Estimating and Fusing Quality Factors for Iris Biometric Images. *IEEE Trans. Syst. Man Cybern. Part A: Syst. Humans* **40**, 509–524 (2010)
22. Chen, Y., Dasset, S.C., Jain, A.K.: Localized Iris Image Quality Using 2-D Wavelets. *ICB*, pp. 1–7 (2006)
23. Ketchantang, W., Derrode, S., Martin, L., Bourennane, S.: Estimating Video pupil tracking based for iris identification, pp. 1–8. *Anvers Belgique, ACIVS* (2005)
24. Zhang, T., Fang, B., Yuan, Y., Tang, Y., Shang, Z., Li, D., Lang, F.: Multiscale facial structure representation for face recognition under varying illumination. *Pattern Recog.* **42**, 251–258 (2009)
25. PolyU Palmprint Database. [http://www4.comp.polyu.edu.hk/~biometrics/index\\_db.htm](http://www4.comp.polyu.edu.hk/~biometrics/index_db.htm)

# Bioinspired Inference System for Medical Image Segmentation

Hakima Zouaoui and Abdelouahab Moussaoui

**Abstract** In the present article, we propose a new approach for the segmentation of the MRI images of the Multiple Sclerosis which is an autoimmune inflammatory disease affecting the central nervous system. Clinical tracers are used nowadays for the diagnosis and the Inter-observer and intra-observer therapeutic assessment. However, those tracers are subjective and subject to a huge variability. The Magnetic Resonance Imaging (MRI) allows the visualization of the brain and it is widely used in the diagnosis and the follow-up of the patients suffering from MS. Aiming to automate a long and tedious process for the clinician, we propose the automatic segmentation of the MS lesions. Our algorithm of segmentation is composed of three stages: segmentation of the brain into regions using the algorithm FCM (Fuzzy C-Means) in order to obtain the characterization of the different healthy tissues (White matter, grey matter and cerebrospinal fluid (CSF)), the elimination of the atypical data (outliers) of the white matter by the optimization algorithm PSOBC (Particle Swarm Optimization-Based image Clustering), finally, the use of a Mamdani-type fuzzy model to extract the MS lesions among all the absurd data.

**Keywords** Multiple sclerosis · Magnetic resonance imaging · Segmentation · Fuzzy C-Means · Particle swarm optimization · Mamdani

## 1 Introduction

Multiple sclerosis (MS) is a chronic inflammatory demyelinating disease of the central nervous system. Magnetic resonance imaging (MRI) detects lesions in MS patients with high sensitivity but low specificity, and is used for diagnosis,

---

H. Zouaoui (✉) · A. Moussaoui  
Computer Science Department, Ferhat Abbas University, Ain Taya, Algeria  
e-mail: Hak-soraya@yahoo.fr

A. Moussaoui  
e-mail: Moussaoui.abdel@gmail.com



prognosis and as a surrogate marker in MS trials [1, 2]. In this article, we are interested in the brain MRI analysis within the context of following up the patients suffering from Multiple Sclerosis (MS).

The segmentation of various tissues and structures in medical images in a robust and efficient manner is of crucial significance in many applications, such as the identification of brain pathologies in Magnetic Resonance (MR) images [3]. The Magnetic Resonance Imaging (MRI) has widely contributed in the establishment of new knowledge about the Multiple sclerosis that allowed the clinicians to significantly improve effective therapeutic approaches. The Magnetic Resonance Imaging (MRI) is one of the complementary examinations in this disease's diagnosis approach. It plays also a key role in the patient's state follow-up and the quantification of a response after having taken medicines. So, the automatic extraction of quantifiers for the Multiple Sclerosis has many potential applications, in the clinical as well as pharmaceutical fields. On the other hand, reading those images is difficult due to the variability in size, contrast and lesions' localization.

The appearance of new lesions or the raising of ancient patches detected by MRI constitutes one of the acknowledged criteria for definitive diagnosis. If the MRI provides essential information on the appearance of lesions of the white substance (Multiple sclerosis), the evolution of the lesions and their consequences on the clinical state of the patient remain weakly correlated. This observation has underlined the concept of "the clinico-radiological paradox" [4]. Besides, the paradigm of a disease primarily inflammatory is contested at present by the hypothesis of a neurodegenerative pathogen which is reinforced by the observation, that the bouts do not influence the progression of an irreversible handicap. In fact, some recent histological works [5] have clearly shown that, besides focal inflammatory and demyelinating lesions disseminated in the white substance, there is a spread and progressive attack of the whole CNS, in both of the white substance of normal appearance and the grey substance, expressed in microscopic manner by the axonal loss and the tissue atrophy.

In this paper, we focus our studies on Brain MR imaging of the brain and we propose an automatic method of segmentation to detect the lesions of MS. Our algorithm of segmentation is composed of three stages: segmentation of the brain into regions using the algorithm FCM (Fuzzy C-Means) in order to obtain the characterization of the different healthy tissues (White matter, grey matter and cerebrospinal fluid (CSF)). In the second stage, we eliminate the atypical data of the white matter by the Optimization algorithm PSOBC (Particle Swarm Optimization-Based image Clustering). Finally in the third stage, a decision is made to use of a Mamdani-type fuzzy model composed of a group of fuzzy rules "if... then" to extract the MS lesions among all the absurd data.

We present in the second section the related work. We will present the steps of the automatic method of segmentation of the proposed approach to detect the lesions of MS in the third section. The fourth section will present the results obtained on the MRI images. Finally, we will finish by a conclusion and future work in the fifth section.

## 2 Related Work

A variety of approaches to MS lesion segmentation have been proposed in the literature. Generally speaking, they can be classified into two groups: outlier-based and class-based methods.

In outlier-based methods [6–10], MS lesions are treated and detected as the outliers to the normal brain tissue distribution, which is usually modelled with a Finite Gaussian Mixture (FGM) of CSF, GM and WM classes. Van Leemput et al. [6] pioneered this approach. Under their framework, MR field inhomogeneities, parameters of the Gaussian distribution and membership are computed iteratively, with the contextual information being incorporated using a Markov random field. Observed intensity values whose Mahalanobis-distances exceed a predefined threshold are marked as lesions. The thresholds are empirically set in this work. Bricq et al. [11] applied neighborhood information during the inference process using a Hidden Markov Chain model and outliers were extracted using the Trimmed Likelihood Estimator (TLE) [12]. This approach was evaluated on real data including MS lesions using T1 and FLAIR MR images.

Class-based methods [13–18] model the lesions as an independent class to be extracted. In [14], a combination of intensity-based k-nearest neighbor classification (k-NN) and a template-driven segmentation (TDS+) was designed to segment different types of brain tissue. Lesions are modeled as one of the expected tissue types, and the class parameters are obtained through an operator supervised voxel sampling on two randomly selected scans. Since the manual training step is highly data-dependent, it is expected to be conducted for each study or data set. A similar approach was proposed in [7]. The segmentation method determines for each voxel in the image the probability of being part of MS-lesion tissue, and the classification is conducted also based on K-NN algorithm. Voxel intensities and spatial information are integrated as discriminative features, and voxels are classified based on their proximity to the pre-classified samples in the feature space. It should be noted that manual or semiautomatic training is normally a required step in k-NN based methods, and the value of k (number of classes) has to be determined in advance, either interactively [14] or empirically [7].

One should note that in the class-based approaches [7, 14–16, 18], a training procedure, to either calibrate the classifier parameters or to choose the tissue class representatives, is normally required. In order to obtain desired segmentation results, the testing data sets are also expected to be highly similar to the training sets, ideally from the same group. Outlier-based models [6–10] relax the training requirement, but they usually subsume a thresholding step. Those thresholds, critical for segmentation performance and system reproducibility, usually require certain prior to be set up precisely, which are often difficult to be determined.

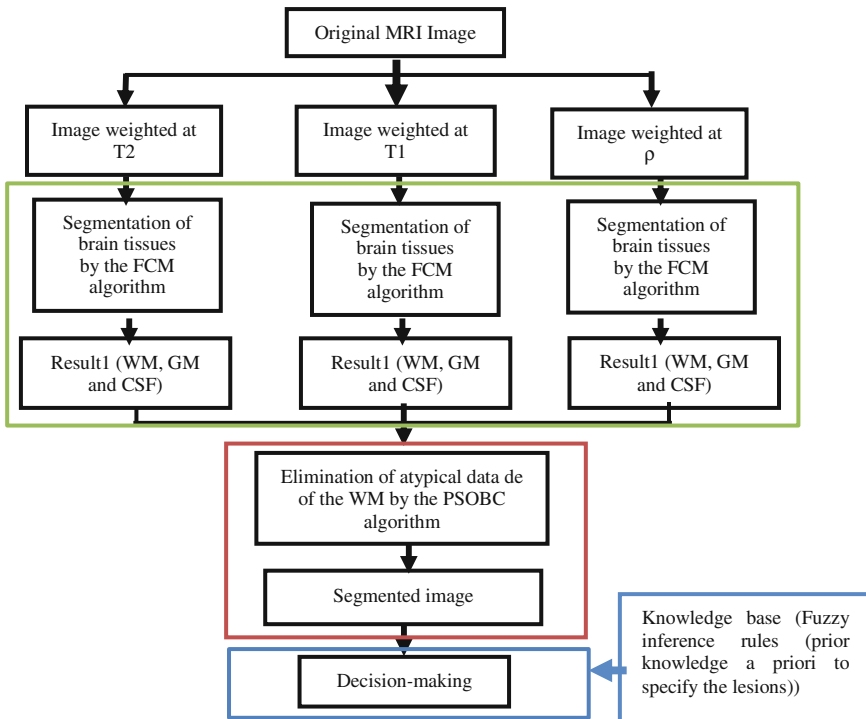
Image segmentation is the process of partitioning a digital image into non-overlapped homogeneous regions with respect to some characteristics, such as gray value, motion, texture, etc. Image segmentation is used in various applications like medical imaging, locating objects in satellite images, face recognition, traffic

control systems, and machine vision, etc. [19]. Several techniques for image segmentation have been proposed [20]. They can be classified into region based approaches [21, 22] and edge detection based approaches [23]. In the present work, we are focused on the region based approach using fuzzy clustering algorithm (soft clustering), instead of hard clustering strategies. In the latter, each data point is assigned to only one cluster, while in soft clustering each data point belongs to all clusters with different degrees of membership, thus taking a better account for poor contrast, overlapping regions, noises, and intensity inhomogeneities [24].

### 3 Proposed Approach

In classical methods, each voxel of the brain is assigned to one of four following classes: WM, GM, CSF, or MS lesions [10]. The Fig. 1 shows the processing sequence proposed for the segmentation of MS lesions. The images are noisy, the inhomogeneities are corrected and all images are registered in the same space. So, our segmentation algorithm can be decomposed into three main steps:

1. Segmentation of brain tissues into three classes (WM, GM, CSF)
2. Segmentation of the white matter to extract the atypical data
3. Decision-making



**Fig. 1** General architecture of the steps of the automatic segmentation of MS lesions

### 3.1 Segmentation of the Brain Tissues

The segmentation of the brain tissues into different compartments (white matter (WM), gray matter (SG) and cerebrospinal fluid (CSF)) is a key step in our study. The outcome of this segmentation serves as the basis for implementing lesion-handling based strategies.

The first question we faced in order to achieve this task is whether a supervised or a non-supervised algorithm will be employed for this purpose.

The use of a supervised algorithm requires a learning database for each class and each patient, which restricts applicability of no such labelled data is fully available as reported in [25]. Given the context of our study, we have chosen a non-supervised based approach.

#### Fuzzy c-means algorithm

*Motivation grounds.* Motivated by its reported success in various fields, i.e., agricultural engineering, astronomy, chemistry, geology, image analysis, medical diagnosis [26, 27], its reduced complexity, easy implementation, especially for large data but also its blurring (integration degree of membership) [28], we advocate in this paper the use of fuzzy c-means (FCM) approach for clustering, which consisted in our case in separating the three classes (white matter (WM), gray matter (SG) and cerebrospinal fluid (CSF)). On the other hand, the FCM algorithm has been widely used for segmentation brain images, regardless of the modality and the type of acquisition (mono or multimodal) and many studies have been performed including imaging magnetic resonance [24, 29, 30].

*Formulating of FCM algorithm.* FCM is a fuzzy clustering method based on the minimization of a quadratic criterion where clusters are represented by their respective centers [31]. More specifically, for a set of data patterns  $X = \{x_1, x_2, \dots, x_N\}$  the fuzzy c-means clustering algorithm allows us to partition the data space, by calculating the centers of classes ( $c_i$ ) and the membership matrix ( $U$ ), by minimizing an objective function  $J$  with respect to these centers and membership degrees

$$J = \sum_{i=1}^C \sum_{j=1}^N (u_{ij})^m d^2(x_j, c_i) \quad (1)$$

Under constraints:

$$\forall j \in [1, N]: \sum_{i=1}^C u_{ij} = 1 \quad \forall i \in [1, C], \forall j \in [1, N]: u_{ij} \in [0, 1] \quad (2)$$

where

$U = [u_{ij}]_{C \times N}$  is the membership function matrix,

$d(x_j, c_i)$  is the metric which calculates the distance between the element  $x_j$  and the center of cluster  $c_i$ ,

$C$  is the number of clusters,

$N$  is the number of data,  
 $m$  is the degree of fuzziness ( $m > 1$ ).

The problem of minimizing the objective function (1) under the constraints (2) is solved by converting the problem to an unconstrained one using the Lagrange multiplier. Both centers of classes and membership degrees cannot be found directly at the same time, so an alternating procedure is used. Firstly, the prototype of classes are fixed arbitrary to find the membership degrees, secondly, the membership degrees are fixed to find the centers corrected. These two steps are alternatively repeated until convergence is attained.

The fuzzy c-means clustering algorithm proceeds according to Algorithm 1.

---

### Algorithm 1

---

**Require:** Set values for the number of clusters  $C$ , the degree of fuzziness  $m > 1$  and the error  $\varepsilon$ .

1: Initialize randomly the centers of clusters  $c_i^{(0)}$ .

2.  $k \leftarrow 1$

3. **repeat**

4. Calculate the membership matrix  $U^{(k)}$  using the centers  $C_i^{(k-1)}$ :

$$u_{ij}^{(k)} \leftarrow \left[ \sum_{l=1}^C \left( \frac{d(x_j, c_l^{(k-1)})}{d(x_j, c_j^{(k-1)})} \right)^{\frac{2}{m-1}} \right]^{-1}$$

5. Update the centers  $c_i^{(k)}$  using  $U^{(k)}$ :  $c_i^{(k)} \leftarrow \frac{\sum_{j=1}^N (u_{ij}^{(k)})^m x_j}{\sum_{j=1}^N (u_{ij}^{(k)})^m}$

6.  $k \leftarrow k+1$

7. **until**  $\|C_i^{(k)} - C_i^{(k+1)}\| \leq \varepsilon$

8. **Return**  $c_i$  the centers of clusters and the membership degrees  $u_{ij}$

---

In image segmentation,  $x_i$  can represent the gray value of the  $i$ th pixel,  $N$  is the number of pixels of the image,  $C$  is the number of the regions (clusters),  $d^2(x_i, c_j)$  is the Euclidean distance between the pixel  $x_i$  and the center  $c_j$  and  $u_{ij}$  is the membership degree of pixel  $x_i$  in the  $j$ th cluster.

### 3.2 Segmentation of the White Matter

Although it is not always correlated with the clinical disability as shown in other studies [32, 33], the load lesional constitutes the primary indicator of inflammatory phenomena. However, the infringement predominantly inflammatory present in the WM is probably in relationship with the mechanisms of degeneration and achievement, axonal. As well, the measurement of the load lesional informs us about the degree of achievement of the WM in the course of the disease.

**Particle swarm optimization algorithm.** The next stage in our methodology is the segmentation of the Multiple Sclerosis lesions. although the segmentation of the multiple sclerosis lesions provides an excellent contrast for the different tissues of the brain parenchyma (white matter, grey matter, CSF). The lesions of the multiple sclerosis are not always well contrasted and their segmentation has become more difficult due to the partial volume with the surrounding tissues. In order to elaborate a segmentation system which accommodates our large variety of images, we consider the segmentation as an optimization problem. The latter makes use of *particle swarm optimization (PSO) based algorithm*. This is motivated by: its simplicity and proven efficiency in similar other segmentation tasks as reported in [34]. Besides, its rapid convergence and ability to deal with high dimension dataset, which enable to fly around the solution space effectively, have been pointed out in [35, 36].

More formally, particle swarm optimization (PSO) is a population-based stochastic optimization algorithm proposed for the first time by Kennedy and Eberhart [37], inspired by bird flocking and fish schooling. The problem is tackled by considering a population (particles), where each particle is a potential solution to the problem. Initial positions and velocities of the particles are chosen randomly. In the commonly used standard PSO, each particle's position is updated at each iteration step according to its own personal best position and the best solution of the swarm. The evolution of the swarm is governed by the following equations:

$$V^{(k+1)} = w.V^{(k)} + c_1.rand_1.(Pbest^{(k)} - X^{(k)}) + c_2.rand_2.(Gbest^{(k)} - X^{(k)}) \quad (3)$$

$$X^{(k+1)} = X^{(k)} + V^{(k+1)} \quad (4)$$

where

$X$  is the position of the particle,

$V$  is the velocity of the particle,

$W$  is the inertia weight,

$Pbest$  is the best position of the particle,

$Gbest$  is the global best position of the swarm,

$rand_1, rand_2$  are random values between 0 and 1,

$c_1, c_2$  are positive constants which determine the impact of the personal best solution and the global best solution on the search process, respectively,

$k$  is the iteration number.

**PSO-Based Image Clustering.** In the context of clustering, a single particle represents the  $C$  cluster centroid vectors. That is, each particle  $x_i$  is constructed as follows:

$$X_i = (x_{i1}, \dots, x_{ij}, \dots, x_{iC}) \quad (5)$$

where  $x_{ij}$  refers to the  $j$ -th cluster centroid vector of the  $i$ -th particle in cluster  $C_{ij}$ . Therefore, a swarm represents a number of candidate clustering's for the current data vectors. The fitness of particles is easily measured as the quantization error,

$$J_e = \frac{\sum_{j=1}^C \left[ \sum_{\forall x_i \in C_j} d(x_i, c_j) \right] / N_j}{C} \quad (6)$$

where

$$d(x_i, c_j) = \sqrt{\sum_{k=1}^{N_d} (x_{ik} - c_{jk})^2} \quad (7)$$

And

- $N_d$  denotes the input dimension, i.e. the number of parameters of each data vector
- $N$  denotes the number of WM image pixels
- $C$  denotes the number of cluster centroids (as provided by the user)
- $x_i$  denotes the coordinates of pixel  $i$
- $c_j$  denote the means of cluster  $j$ .
- $N_j$  is the number of pixels in  $C_j$

The PSO based image clustering algorithm is summarized below

---

### Algorithm 2

---

1. Initialize each particle to contain  $C$  randomly selected cluster means.
  2. For  $t = 1$  to  $t_{\max}$  do
    - (a) For each particle  $i$  do
      - (b) For each pixel  $x_i$ 
        - calculate  $d(x_i, c_{ij})$  to all cluster centroids using equation (7)
        - assign  $x_i$  to cluster  $C_{ij}$  where
 
$$d(x_i, c_{ij}) = \min_{\forall k=1, \dots, C} \{d(x_i, c_{ik})\}$$
        - calculate the fitness using equation (6).
      - (c) Update the global best and local best positions
      - (d) Update the cluster centroids using equations (3) and (4).
- 

where  $t_{\max}$  is the maximum number of iterations.

### 3.3 Decision-Making

The last step consists in the decision-making concerning the belonging of a voxel of the white matter to a class of the MS disease. The MS lesions appear in hypo and hyper-signal in comparison to the WM according to the MRI methods. The weighted images in T2 and PD underline the myelin component in the lesions characterized by the edemas with hyper-intense appearance in comparison to the white matter. Furthermore, the method T1 underlines the irreversible destruction of the tissues with the appearance in the white matter of persistent “black holes” (Hypo-signal) [38]. For this purpose, we propose the use of the Mamdani’s fuzzy inference process. This fuzzy model is composed of:

*Fuzzification stage* (Fig. 2). The system has two inputs, the weighting contrast of MRI and the type of the voxels’ signal. And a signal of output which diagnose the Multiple Sclerosis disease.

The steps of *fuzzification* consist in setting the belonging functions, the steps of which are:

- 1 To set the *linguistic variables*
- 2 To set the fuzzy quantifiers (Number of the *linguistic values*);
- 3 To assign a digital signification to each fuzzy quantifier: *belonging function*

For the fuzzification of the contrast, we choose three fuzzy intervals and belonging functions of the Gaussian types. Figure 3 shows the fuzzy repartition of contrast input variable.

For the fuzzification of signal’s type, we choose two fuzzy intervals and belonging functions of Gaussian types. Figure 4 shows the fuzzy repartition of the input variable of signal’s type.

For the output variable, we choose three fuzzy intervals and Gaussian membership functions, which define predicates: *low, normal and high* of the MS disease in comparison to the white matter. Figure 5 shows the fuzzy repartition of the output variable of the decision of the MS disease.

*Fuzzy rule base.* In the view of intuitive interpretation of the input variables, some fuzzy rules can be set up manually, for instance:

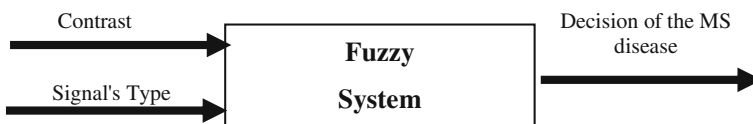


Fig. 2 Diagram of fuzzy system of the MS disease



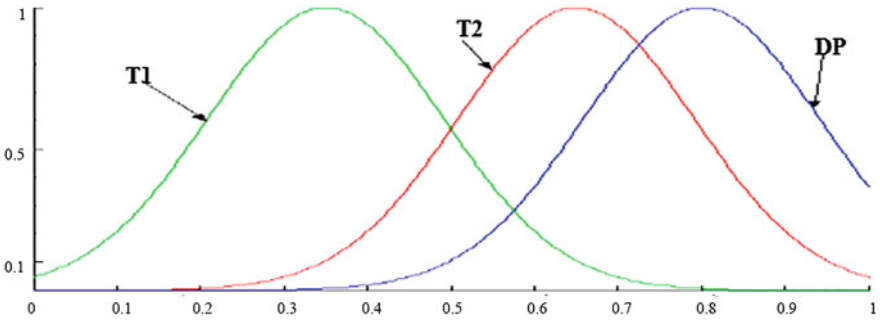


Fig. 3 Fuzzy repartition of contrast input variable

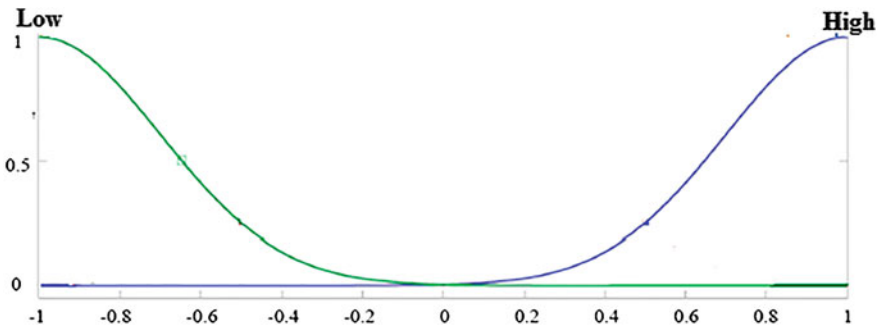


Fig. 4 Fuzzy repartition of input variable of signal's type

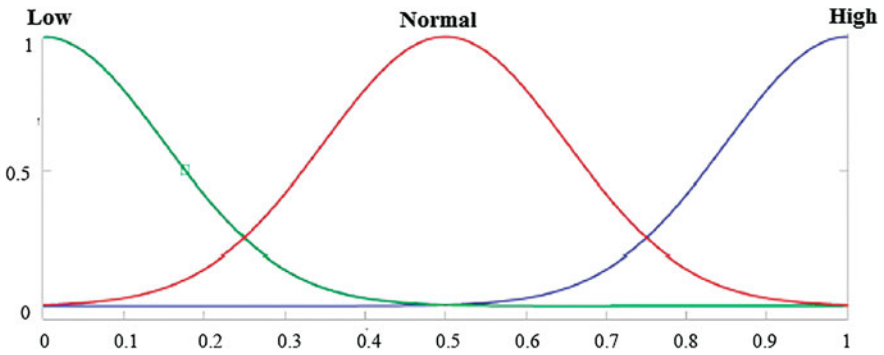


Fig. 5 Fuzzy repartition of the output variable giving the decision of the MS disease

**Table 1** Fuzzy rule base

Signal/Sequence	T1	T2	PD
High	Low/Normal	High	High
Low	Low	High	High
High after injection of gadolinium	Normal	High	High

Here are ten examples of the rules' base represented in a linguistic form:

1. **If** [(the contrast weighted at T1) and (the zones are of high intensity)] **then** (the MS is low).
2. **If** [(the contrast weighted at T1) and (the zones are of high intensity)] **then** (the MS is normal in comparison to the white matter).
3. **If** [(the contrast weighted at T2) and (the zones are of high intensity)] **then** (the MS is high).
4. **If** [(the contrast weighted at PD) and (the zones are of high intensity)] **then** (the MS is high).
5. **If** [(the contrast weighted at T1) and (the zones are of low intensity)] **then** (the MS is low).
6. **If** [(the contrast weighted at T2) and (the zones are of low intensity)] **then** (the MS is high).
7. **If** [(the contrast weighted at PD) and (the zones are of low intensity)] **then** (the MS is high).
8. **If** [(the contrast weighted at T1) and (the zones are of high intensity after injection of gadolinium)] **then** (the MS is normal in comparison to the WM).
9. **If** [(the contrast weighted at T2) and (the zones are of high intensity after injection of gadolinium)] **then** (the MS is high).
10. **If** [(the contrast weighted at PD) and (the zones are of high intensity after injection of gadolinium)] **Then** (the MS is high).

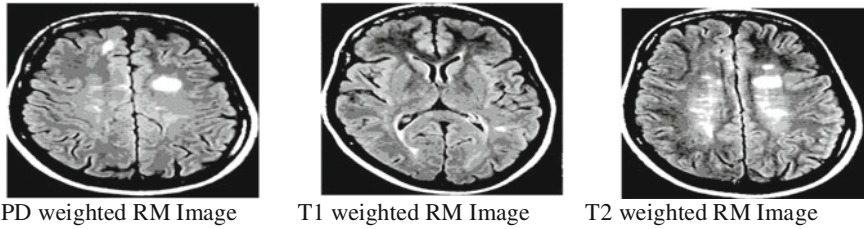
Table 1 summarizes the set of exhibited fuzzy rules.

The selected inference method is Mamdani's method. Consequently, the operator is realized by the calculation of the minimum, whiles the operator OR is realized by the calculation of the maximum.

The *defuzzification* step is done using the method of calculating the center of attraction.

## 4 Results and Discussion

To validate the developed method, we relied on the BrainWeb database (<http://www.bic.mni.mcgill.ca/brainweb/>). This database was chosen as it is frequently used in the literature and thus allows providing an easier comparison with alternative methods proposed in literature.



**Fig. 6** Original Images

The actual images on which we worked were acquired as part of the collaboration between LSI laboratory (Laboratory Intelligent Systems: image and signal team) Ferhat Abbas University of Setif and LAMIH UMR CNRS 8201 (Laboratory of Industrial and Human Automation control, Mechanical engineering and Computer Science) University of Valenciennes Cedex 9 France (Figs. 5 and 6).

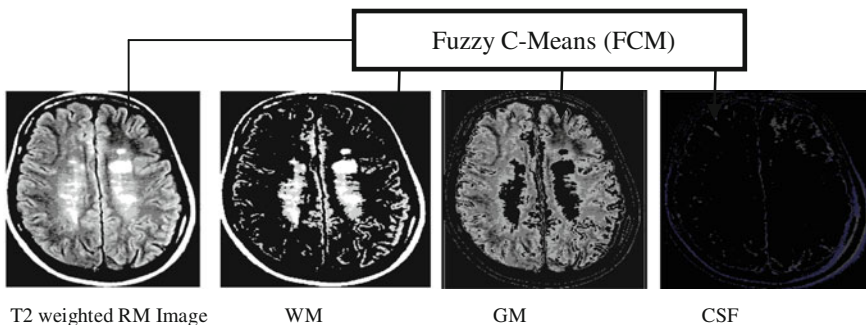
#### 4.1 Analysis of the Results

It concerns the images weighted at T1, T2 and Proton density (Pd) for different old patients (Pixel size = 1 mm, matrix size  $512 \times 512$ ). The images are in the form of DICOM (*Digital Imaging and Communications in Medicine*). The selection of the proposed noise on site BrainWeb is between 0 and 9 % and that of the heterogeneity of the setting values between 0 and 40 %. The brain segmentation was successfully applied on some real images, the results are shown in the following figures

##### Step 1: segmentation of tissues (WM, GM and CSF)

The Fig. 7 show the segmentation by the FCM algorithm for the T2 weighted image in order to obtain a characterization of the different healthy tissues (White matter, Grey matter and cerebrospinal fluid)

To compare the performance of these images, we compute different coefficients reflecting how well two segmented volumes match. We used different performance measures:



**Fig. 7** Image T2 segmented by FCM

**Table 2** Comparison of segmentation results

	T1		T2		PD	
	<i>SI</i>	<i>ovrl</i>	<i>SI</i>	<i>ovrl</i>	<i>SI</i>	<i>ovrl</i>
WM	0.93	0.90	0.96	0.93	0.83	0.76
GM	0.86	0.83	0.95	0.92	0.80	0.70
CSF	0.83	0.67	0.94	0.90	0.78	0.58

$$Overlap \quad (ovrl) = \frac{TP}{TP + FN + FP} \tag{8}$$

$$Similarity \quad (SI) = \frac{2 \cdot TP}{2 \cdot TP + FN + FP} \tag{9}$$

where TP and FP stand for true positive and false positive, which were defined as the number of voxels correctly and incorrectly classified as brain tissue by the automated algorithm. TN and FN stand for true negative and false negative, which were defined as the number of voxels correctly and incorrectly classified as non-brain tissue by the automated algorithm. The comparative results are presented in Table 2 below:

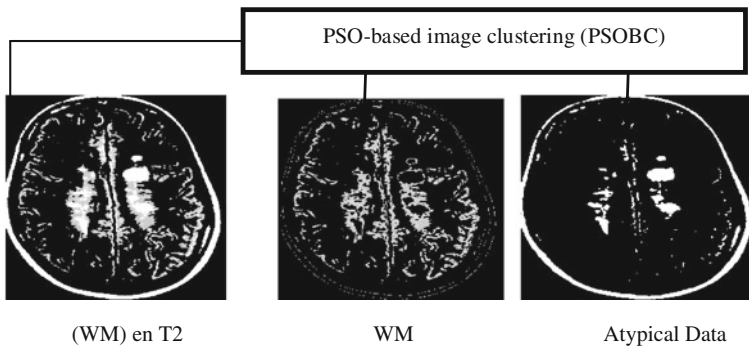
The results in Table 2 show a considerable improvement for all tissues using T2 than T1 and PD.

**Step 2: segmentation of the white matter by PSOBC**

The use of PSOBC allows us to eliminate the atypical data of the white matter for each image (T1, T2, PD) as exhibited in Fig. 8 for image T2.

Table 3 summarizes the segmentation outcome by PSOBC

The results obtained by PSOBC are very satisfactory and well confirm the validity of the algorithm, its ease of implementation gives it a substantial advantage. We have made an improvement in optimizing the white matter and atypical data (Table 4).



**Fig. 8** WM of the image T2 segmented by PSOBC

**Table 3** Comparative results

	T1		T2		PD	
	<i>SI</i>	<i>ovrl</i>	<i>SI</i>	<i>ovrl</i>	<i>SI</i>	<i>ovrl</i>
Atypical Data	0.92	0.93	0.97	0.94	0.95	0.93
WM	0.90	0.87	0.96	0.93	0.91	0.81

**Table 4** Result of the defuzzification of the atypical data of the different sequences

	T1	T2	PD
MS lesions	MS is normal	SEP is high	SEP is normal

### Step 3: Decision-making

However, in complex structure, we can not make a final decision because of the blur. For this, the selected inference method is Mamdani's method. Consequently, the operator is realized by the calculation of the minimum, while the operator OR is realized by the calculation of the maximum.

The following table presents the results of defuzzification:

The decision-making depends always on the expertise, the patient suffers from the multiple sclerosis and the MS lesions are detected in all the sequences by a normal or a high characterization.

## 4.2 Experimental Results

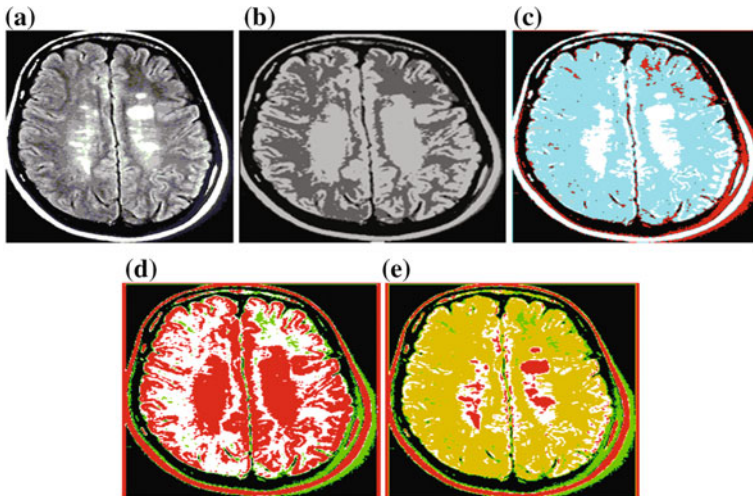
The Fig. 9 shows the results obtained after segmentation of the images (a) weighted T2 on axial plane. The images (b), (c), (d) and (e) are the results of segmentation realized by the expert, FCM, PSOBC and the approach successively proposed.

The results of each stage of the segmentation are presented on a sectional level (Fig. 6) in which the localization allows distinguishing three separated classes of the tissue:

- GM (Pallidum, Putamen, caudate nucleus, thalamus and cortex)
- WM (brain parenchyma).
- CSF (subarachnoid space, lateral ventricles and V3).

The interpretation of our results is done by an expert (hospital center of Ain Naadja Algiers) on simulated and real images. By analyzing the images of the Fig. 9, the expert has established the following statement:

- **Image (b):** The interpretation of the classes is totally improved in relation to (FCM, PSOBC), we notice the distinction between the 03 classes of the brain and the class of the pathology SEP.
- **Image (c):** The class CSF does not conform to the class of the original image. The lack of information about the small grooves (image (a)) and the poor



**Fig. 9** Pathological image (a) and its segmentation gotten by (b) segmentation by the expert; c FCM; d PSOBC and e Proposed approaches

discrimination CSF/GM make that the segmented CSF class does not well represent the fluid distribution. The distributions of the WM and GM get closer to those given by the original image. The detection of the pathology is indicated according to the expert but the details are not well expressed.

- **Image (d):** PSOBC is unsuitable in this segmentation in relation to the image (o).
- **Image (e):** the proposed approach brings a great performance to the segmentation for the three classes and especially for the fourth one which is the pathology that specifies well the size and the details about this later.

We compare the T2 weighted RM Images between the segmentation by the segmentation realized by the expert, FCM and PSOBC for a given time of acquisition and the segmentation by the proposed approach.

The results of the Table 5 and the Fig. 10 underline the advantages of the proposed approach in comparison to the segmentation by FCM and PSOBC for all tissues CSF, WM, GM and MS lesions.

**Table 5** Comparison of the results gotten by different algorithms

	GM (%)	CSF (%)	WM (%)	Lesions (%)
Segmentation by the expert	93	69	95	97
FCM	71	55,9	79.6	74
PSOBC	80,2	64	85	68
Proposed approach	88,7	66	90,5	95,8

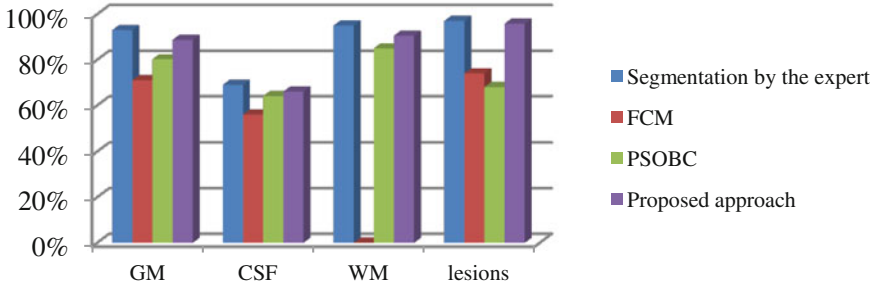


Fig. 10 Performance measures of the results gotten by different algorithms

## 5 Conclusion

In this article, we have proposed a new automatic approach of segmentation of the MS lesions' images. Two reasons explain their difficulties:

1. The first is that there is a very wide variety of abnormal tissues which are different in their size, shape, position and composition.
2. The second reason is that the datum issued from the MRI acquisition is sensitive to the noise background noise and to the sampling collection.

We have firstly split up the process of automatic segmentation of the MS lesions into three fundamental stages:

Firstly, we segmented the brain into regions by using the algorithm FCM (Fuzzy C-Means) in order to obtain the characterization of the different healthy tissues (White matter, Grey matter and cerebrospinal fluid (CSF)). Secondly, we eliminated of the atypical data of the white matter by the optimization algorithm PSOBC (Particle Swarm Optimization -Based image Clustering). Finally, in the framework of our application on the MS disease, we used a Mamdani-type fuzzy model to make decision of the MS disease. We presented the results of our work consisting in the use of an algorithm for the segmentation if medical images in order to improve the quality of the MS lesions' detection. The good quality of our solutions depends on the fact that:

- It is a method totally automatic due to the modeling of the *prior* knowledge of the neuroradiology experts. the fuzzy theory is important for modeling the human knowledge using the mathematical functions and to solve the effect of the partial volume of the MRI.
- It satisfies the application's constraints due to the automaticity and the different final results which may be provided by the fuzzy 3D reconstruction.
- Its performance is better than the performance of the supervised method.
- It is a system based on fuzzy and optimization theory
- It is efficient on 2 types of tissues at least.

## References

1. Miller, D.H.: Biomarkers and surrogate outcomes in neurodegenerative disease: lessons from multiple sclerosis. *NeuroRX*, **1**(2), 284–294 (2004)
2. Daniel, G.-L., Sylvain, P., Douglas, A., Louis, C., Christian, B.: Trimmed-likelihood estimation for focal lesions and tissue segmentation in multisequence MRI for multiple sclerosis. In: *IEEE Transactions on Medical Imaging*, Institute of Electrical and Electronics Engineers (IEEE) (2011)
3. Jason, E.H., Brian, N., Sunanda, M.: An information theoretic approach via IJM to segmenting MR images with MS lesions. In: *IEEE 27th International Symposium on Computer-Based Medical Systems* (2014)
4. Barkhof, F.: The clinico-radiological paradox in multiple sclerosis revisited. *Current Opinion in Neurology*, vol. 15, pp. 239–245. **3**, (2002)
5. Lucchinetti, C.F., Parisi, J., Bruck, W.: The pathology of multiple sclerosis. *Neurol. Clinics* **23**, 77–105 (2005)
6. Van Leemput, K., Maes, F., Vandermeulen, D., Colchester, D., Suetens, P.: Automated segmentation of multiple sclerosis lesions by model outlier detection. *IEEE TMI* **20**(8), 677–689 (2001)
7. Anbeek, P., Vinchen, K.L., van Osch, M.J.P., Bisschops, R.H.C., van der Grond, J.: Probabilistic segmentation of white matter lesions in MR imaging. *NeuroImage* **21**, 1037–1044 (2004)
8. Souplet, J.C., Lebrun, C., Anyche, N., Malandain, G.: An Automatic Segmentation of T2-FLAIR Multiple Sclerosis Lesions. *3D Segmentation in the Clinic: A Grand Challenge II: MS lesion segmentation* (2008)
9. Dugas-Phocion, G., Gonzalez, M.A., Lebrun, C., Chanalet, S., Bensa, C., Malandain, G., Ayache, N.: Hierarchical Segmentation of Multiple Sclerosis Lesions Multi-Sequence MRI. *ISBI'08*
10. Garcia-Lorenzo, D., Prima, S., Morrissey, S.P., Barillot, C.: A Robust Expectation-Maximization Algorithm for Multiple Sclerosis Lesion Segmentation. *Segmentation in the Clinic: A Grand Challenge II: lesion segmentation* (2008)
11. Bricq, S., Collet, Ch., Armspach, JP.: Markovian segmentation of 3D brain MRI to detect multiple sclerosis lesions. In: *IEEE international conference on image processing, ICIP'2008*, pp. 733–736 (2008)
12. Neykov, N., Neytchev, P.: A robust alternative of the of the Maximum Likelihood Estimator. *COMPSTAT—Short Communications*. Dubrovnik, Yugoslavia, pp. 99–100 (1990)
13. Prastawa, M., Guido G.: Automatic MS Lesion Segmentation by Outlier Detection and Information Theoretic Region Partitioning. *3D Segmentation in the Clinic: A Grand Challenge II: MS lesion segmentation* (2008)
14. Wu, Y., Warfield, S.K., Tan, I.L., Wessl III, W.M., Meier, D.S., Van Schijndel, R.A., Barkhof, F., Guttman, C.: Automated segmentation of multiple sclerosis lesion subtype with multichannel MRI. *NeuroImage* **32**, 1025–1215 (2006)
15. Tu, Z., Narr, K., Dinov, I., Dollar, P., Thompson, P., Toga, A.: Brain anatomical structure parsing by hybrid discriminative/generative models. *IEEE TMI* (2008)
16. Morra, J. Tu, Z., Toga, A., Thompson, P.: Automatic Segmentation of MS Lesions Using a Contextual Model for the MICCAI Grand Challenge. *3D Segmentation in the Clinic: A Grand Challenge II: MS lesion segmentation* (2008)
17. Anbeek, P., Vinchen K.L., Viergever, M.A.: Antomated MS-Lesion Segmentation by K-Nearest Neighbor Classification. *3D Segmentation in the Clinic: A Grand Challenge II: MS lesion segmentation* (2008)
18. Bazin, P.L., Pham, D.L.: Statistical and topological atlas based brain image segmentation. *MICCAI* (2007)
19. Christ, M., Parvathi, R.M.S.: Magnetic resonance brain image segmentation, *intern. J. VLSI Design Commun. Syst.* **3**, 121–133 (2012)



20. Dey, V., Zhang, Y., Zhong, M.: A review on image segmentation techniques with remote sensing perspective. In: Wagner, W., Szekely, B. (eds.) ISPRS TC VII Symposium-100 Years ISPRS, vol. XXXVII, pp. 31–42, Vienna, Austria (2011)
21. Ciesielski, K.C., Udupa, J.K.: Region-based segmentation: fuzzy connectedness graph cut and related algorithms. In: Deserno, T.M. (ed.), Biomedical Image Processing, Biological and Medical Physics, Biomedical Engineering. Springer, Berlin, Heidelberg, pp. 251–278 (2011)
22. Nakib, A., Oulhadj, H., Siarry, P.: A thresholding method based on two dimensional fractional differentiation. *Image Vis. Comput.* **27**, 1343–1357 (2009)
23. Papari, G., Petkov, N.: Edge and line oriented contour detection. State of the art. *Image Vis. Comput.* **29**, 79–103 (2011)
24. Benaichouche, A.N., Oulhadj, H., Siarry, P.: Improved spatial fuzzy-c-means clustering for image segmentation using PSO initialization, Mahalanobis distance and post-segmentation correction. *Digit. Signal Proc.* **23**, 1390–1400 (2013)
25. Bezdek, J., Hall, L., Clarke, L.: Review of MR image segmentation techniques using pattern recognition. *Med. Phys.* **20**, 1033–1048, 1993
26. Ghosh, S., Kumar, S.: Comparative analysis of K-means and fuzzy C-means algorithms. *Int. J. Adv. Comput. Sci. Appl.* **4**(4) (2013)
27. Tejwant, S., Manish, M.: Performance comparison of fuzzy C means with respect to other clustering algorithm. *Int. J. Adv. Res. Comput. Sci. Softw. Eng.* **4**(5) (2014)
28. Bezdek, J.C.: Fuzzy mathematics in pattern classification. Ph.D dissertation, Cornell University, Ithaca, NY, 1973
29. Zouaoui, H., Moussaoui, A.: Clustering par Fusion Floue de Données Appliqué à la Segmentation d'Images IRM Cérébrales. CIIA, vol. 547 von CEUR Workshop Proceedings, CEUR-WS.org (2009)
30. Premalatha, K., Natarajan, A.M.: A New approach for data clustering based on PSO with local search. *Comput. Inform. Sci.* **1**(4) (2008)
31. Clark, M., Hall, L., Goldgof, D., Clark, L., Velthuizen R., and Silbiger, M.: MRI segmentation using fuzzy clustering techniques. *IEEE Eng. Med. Biol.* 730–742 (1994)
32. Filippi, M, et al.: Correlations between changes in disability and T2 weighted brain MRI activity in multiple sclerosis. A follow-up study. 2, *Neurology*, **45**, 255–260 (1995)
33. Barkhof, F.: MRI in multiple sclerosis: correlation with expanded disability status scale (EDSS). *Multiple Sclerosis* **5**, 283–286 (1999)
34. El Dor, A., Lepagnet, J., Nakib, A., Siarry, P.: PSO-2S optimization algorithm for brain MRI segmentation. In: Genetic and Evolutionary Computing, pp. 13–22. Springer (2014)
35. Selvi, V., Umarani, Dr. R.: Comparative analysis of ant colony and particle swarm optimization techniques. *Int. J. Comput. Appl.* (0975–8887) **5**(4) (2010)
36. Shi, Y., Eberhart, R.C.: Empirical study of particle swarm optimization, vol. 3, pp. 1945–1950 (1999)
37. Kennedy, J., Eberhart, R.: Particle swarm optimization. In: Proceedings IEEE International Conference on Neural Networks, vol. 4, pp. 1942–1948. Perth, Australia (1995)
38. Ait-Ali, L.S., Prima, S., Edan, G., Barillot, C.: Longitudinal segmentation of MS lesions in multimodal brain MRI. In: 15<sup>ème</sup> Congrès Francophone AFRIF/AFIA de Reconnaissance des Formes et Intelligence Artificielle (RFIA), Tours, France, Janvier (2006)

# Realization of Gymnastic Movements on the Bar by Humanoid Robot Using a New Selfish Gene Algorithm

Lyes Tighzert and Boubekeur Mendil

**Abstract** This paper proposes a new selfish gene algorithm called the Replaces and Never Penalizes Selfish Gene Algorithm (RNPSGA). This new variant of selfish gene algorithm replaces the alleles of the less fit individual by the alleles of the fittest rather than penalizing them. The intensification of the search is then increased. The proposed algorithm is tested under some famous benchmark functions and compared to the standard selfish gene algorithm. We analyze also the quality of convergence, the accuracy, the stability and the processing time of the proposed algorithm. We design by Solidwork a new virtual model of the humanoid robot hanging on the bar. The model is controlled using Simscape/Matlab. The proposed algorithm is then applied to the designed humanoid robot. The objective is to realize the gymnastic movements on the bar. An intelligent LQR controller is proposed to stabilize the swing-up of the robot.

**Keywords** Selfish gene • Computational intelligence • Humanoid • Robots • Gymnastic • Solidworks/Simmechanic • LQR • Optimal control

## 1 Introduction

The evolutionary algorithms are a stochastic search and optimization algorithms inspired from the Darwinian theory of evolution. This kind of computing started in the middle of twentieth century by means of the influence of several works [1, 2]. In the last decades this field have motivated many researchers and scientists who had contributed to its amazing progress. The evolutionary algorithms can be subdivided

---

L. Tighzert (✉) · B. Mendil  
Laboratoire de Technologie Industrielle et de l'Information (LTII),  
Faculté de Technologie, Université de Bejaia, 06000 Bejaia, Algeria  
e-mail: ltighzert@gmail.com

B. Mendil  
e-mail: bmendil@yahoo.fr

into four subfields: evolution strategies [3], evolutionary programming [4], genetic programming [5] and genetic algorithms [6]. As genetic algorithms imitate the process of natural selection of the survival of the fittest, they use a population of individuals that generates offspring by means of crossover and mutation operators. In each generation the algorithm selects the fittest individuals to survive for the next generation. Several variants have been developed and proposed in the literature [7–9]. The basic differences between them is in their representation of chromosomes, their crossover operators, their mutation operators and their selection strategy. In evolutionary algorithms, we are principally interested by the intensification and the diversification of the search process [10]. The crossover operator allows the transfer of genetic information between individuals, hence it helps for the intensification of the search. The mutation adds new information into genotypes and helps the algorithm to explore different regions of search space and to avoid local optimums. The mutations diversify the search process and are indispensable to guaranty the convergence of the algorithm [11]. On 1989, the British biologist Richard Dawkins reformulates the theory of evolution in terms of genes rather than individuals [12]. We call his theory: the selfish gene theory. Dawkins suggests that evolution of spaces is based on genes. The body that have the biological spaces is created by genes to assure their duplication (their own survival).

En 1998 Corno et al. developed a new genetic algorithm based on the theory of Richard Dawkins. The algorithm is called the Selfish Gene Algorithm (SGA) [13]. This algorithm is focalized on genes and uses a pool of genes called the virtual population rather than a population of individuals. As this algorithm is central for our study we give a formal precise definition. Its pseudo code is shown in Fig. 1.

In SGA, the alleles compete for loci. It has each one a probability of selection that measures the chances that has an allele to be selected to form one of the individuals used in the tournament selection. The algorithm uses tournament selection to compare two individuals between them. The alleles of the winner of the tournament are rewarded by incrementing their selection probabilities. And the alleles of the failed individual are penalized by decreasing their selection probabilities. If one of the individual selected is fitter than the best ever found, it replaces it.

In this paper we propose a novel selfish gene algorithm called the Replaces and Never Penalizes Selfish Gene Algorithm (RNP-SGA). This algorithm does not penalize the alleles. The idea behind this variant is to replace the alleles of the fit less individual by the alleles of the fittest (the winner of the tournament). The rest of this paper is organized as fallow. In the next section we introduce the proposed algorithm. In section three we analyze and compare the RNP-SGA and the SGA in terms of quality of convergence, accuracy, stability and the time consumption. The fourth section is devoted to studying, modeling and controlling of a gymnastic humanoid robot on the bar. We use the proposed algorithm to optimize an LQR controller designed to assure the movement of swing-up on the bar. Section five conclude this paper.

---

**Algorithm1:** Selfish Gene Algorithm
 

---

```

1. VP = uniform initialization of the virtual population
2. P = initialize all probabilities  $p_{ij}$  to  $1/n_i$ 
3. B = select (VP) /* assume the best */
4. Repeat
5. /* tournament */
6. G1 = select-individual ( VP,P) ;
7. G2 = select-individual ( VP,P) ;
8. if (fitness(G1) > fitness(G2)) then
9.   reward-alleles (G1) ;
10.  penalize-alleles (G2) ;
11. /* update best */
12. if (fitness(G1) > fitness(B)) then
13.   B = G1 ;
14. End if
15. Else
16.   reward-alleles (G2) ;
17.   penalize-alleles (G1) ;
18. /* update best */
19. if (fitness(G2 > fitness(B)) then
20.   B = G2 ;
21. End if
22. until termination condition
23. return B

```

---

**Fig. 1** The pseudo code of SGA [13]

## 2 The Replaces and Never Penalize Selfish Gene Algorithm

In this section we introduce the algorithm called the Replace and Never Penalize Selfish Gene Algorithm (RNP-SGA). This algorithm is a variant of selfish gene algorithm. The RNP-SGA uses also the tournament selection but it does not penalize alleles. It rewards the alleles of the winner of the tournament and replaces the alleles of the failed individual by the alleles of the winner. This action of replacing allows a duplication of the genes of the winner in the virtual population. Hence, the intensification of the search process is increased. Actually, the proposed algorithm by rewarding the “good” alleles through increasing their selection probabilities will automatically penalize the “bad” ones; their selection probabilities will be relatively less significant. To assure a good exploration of the search space we increment the mutation probability. The mutation in RNP-SGA occurs randomly and can affect

---

**Algorithm 2: Replaces and never penalizes Selfish Gene Algorithm**


---

```

1. VP = uniform initialization of the virtual population
2. P = initialize all probabilities  $p_{ij}$  to  $1/n_i$ 
3. B = select (VP) /* assume the best */
4. Repeat
5. /* tournament */
6. G1 = select-individual ( VP, P );
7. G2 = select-individual ( VP, P );
8. if (fitness(G1) > fitness(G2)) then
9.     reward-alleles (G1) ;
10. /* replace alleles of G2 by those of G1 in VP */
11. VP(G2)= VP(G1) ;
12. /* update best */
13. if (fitness(G1) > fitness(B)) then
14.     B = G1 ;
15. End if
16. Else
17.     reward-alleles (G2) ;
18. /* replace alleles of G1 by those of G2 in VP */
19. VP(G1)= VP(G2) ;
20. /* update best */
21. if (fitness(G2 > fitness(B)) then
22.     B= G2 ;
23. End if
24. End if
25. /* mutation */
26. VP=mutate(VP)
27. until termination condition
28. return B

```

---

**Fig. 2** The pseudo code of the proposed RNP-SGA

any gene in the virtual population. The pseudo code of the proposed algorithm is shown in Fig. 2.

The proposed algorithm uses a virtual population of genes. Each of them has a probability of selection that measures the chances of the given allele to be selected into the chromosomes of the individuals selected to compete in the tournament. The alleles of the winner (the fitter) are duplicated in the virtual population by overwriting (replacing) those of the failed. This action of overwriting ameliorates the intensification of the search. To avoid duplication of the same genes in the entire virtual population long before finding the optimal solution we increment the probability of mutation.

Generally, in evolutionary computing we are aimed to give a dynamic change to the parameters governing the algorithms [11]. So we propose the decreasing of the probability and step size of mutations to assure good accuracy and quality of convergence. Now we propose benchmarking of the proposed algorithm. The results of the simulation tests are shown in next section.

### 3 Benchmarking of the RNPSGA

#### 3.1 Mathematical Functions

We propose in this section the benchmarking of the proposed algorithm under some famous benchmark functions. We choose from literature [8, 9] a set of seven functions. The Table 1 gives the mathematical form of the used benchmark functions. The value of the optimal of all those functions is zero and its position is on the origin of the D dimensions space.

**Table 1** Mathematical form of the test functions

Name and type	Mathematical form	Interval
<b>Uni modal functions</b>		
F1: Sphere function	$\sum_{i=1}^D x_i^2$	[-100,100]
F2: Schwefel’s problem	$\sum_{i=1}^D  x_i ^2 + \prod_{i=1}^D  x_i ^2$	[-100, 100]
F3: Generalized Rosenbrock function	$\sum_{i=1}^{D-1} [100(x_{i+1} - x_i^2)^2 + (x_i - 1)^2]$	[-5.12, 5.12]
<b>Multimodal functions</b>		
F4: Generalized Rastrigin function	$\sum_{i=1}^D [x_i^2 - 10 \cos(2\pi x_i) + 10]$	[-5.12, 5.12]
F5: Generalized Griewank function	$\frac{1}{4000} \sum_{i=1}^D x_i^2 - \prod_{i=1}^D \cos(\frac{x_i}{\sqrt{i}}) + 1$	[-600, 600]
F6: Ackley function	$-20 \exp\left(-0.2 \sqrt{\frac{1}{D} \sum_{i=1}^D x_i^2}\right) - \exp\left(\frac{1}{D} \sum_{i=1}^D \cos(2\pi x_i)\right) + e + 1$	[-32, 32]
<b>Composite functions</b>		
F7: Composite function	Composite function CF2 in [14]	[-5, 5]

### 3.2 Simulation Settings

In order to compare the SGA and the proposed algorithm we give the parameters used in our experiments:

- The maximum number of iteration  $N = 40000$
- Dimension: three case  $D = 10$ ,  $D = 30$  and  $D = 50$
- Dimension of VP is set to  $50 \times D$  (VP is a matrix)
- Normal distribution mutation:  $x = x + \sigma N(0, 1)$
- Probability of mutation  $\mu = 0.01$  for SGA and  $\mu = 0.1$  for RNPSGA
- $segma = 0.5(Max - Min)$
- $segma\_dump\_initial = 1$ ;
- $segma\_dump\_final = 0.992$ ;
- $segma\_dump = \left(\frac{N - K}{N - 1}\right)^2 \times (segma\_dump\_initial - segma\_dump\_final) + segma\_dump\_final$ ;
- Dynamic of the standard deviation:  $segma = segma \times segma\_dump$
- Rewording of genes: additive function  $+0.01$
- Penalizing of the genes: subtractive function  $-0.01$

The algorithms are implemented in Matlab 2014a code source. The computer used for our simulations is Intel® Core™ i5-2350M CPU 2.30 GHz and 8 GB of RAM. The results and the discussion are on the next subsection.

### 3.3 Results and Discussion

We experiment the two described algorithms with the functions listed above. The entire mathematical benchmarks are tested with dimensions 10, 30 and 50. Each function had been tested for 50 independent runs for the different dimensions shown above.

1. Convergence study: the algorithms used for comparison are stochastic. This means that their results differ from one run to another. Hence we need to repeat the same experiment for several times and then we compare the averaged values found. The detailed results are shown in Table 2. The results given in bold style mean that the corresponding algorithm has found a better solution, the averaged value of 50 independent runs, compared to the other. The table give the averaged optimal values found, the standard deviation and the processing time. It indicates also how many times the algorithm is executed for each instance (N). The results given in bold style mean that the corresponding algorithm performs the problem more than the other. We conclude from Table 2 that RNPSGA is batter that SGA. It gives 90.4762 % of good results. The proposed algorithm can be compared to more recent and efficient algorithms to measure objectively its quality (see the results shown in [15–17]).

**Table 2** Average, standard deviation, number of success for each instance (N) and time processing of the best fitness values found by RNP-SGA and SGA

Algorithms		Function D								
		F1			F2			F3		
		10	30	50	10	30	50	10	30	50
RNP-SGA	Avr.	<b>0</b>	<b>0</b>	<b>0.001</b>	<b>0</b>	<b>2.E-6</b>	<b>0.94</b>	<b>10.46</b>	<b>65.41</b>	<b>166.2</b>
	St. d	0	0	0.006	0	7.E-7	1.51	11.81	36.59	64.49
	N	50	50	500	50.0	50.0	50.0	48.0	50.0	50.0
	T	3.54	6.58	9.55	3.642	6.726	9.723	3.847	6.912	9.926
SGA	Avr.	89.7	4350	14355	1.224	24.04	60.38	98.65	4532.	19768
	St. d	91.1	2004.	3301.	0.764	5.726	10.71	61.39	2130.	7089.
	N	0.0	0.0	0.0	0.0	0.0	0.0	2.0	0.0	0.0
	T	3.57	5.91	8.22	3.605	6.071	8.408	3.807	6.232	8.6
Algorithms		Function D								
		F4			F5			F6		
		10	30	50	10	30	50	10	30	50
RNP-SGA	Avr.	<b>6.72</b>	<b>34.16</b>	<b>76.77</b>	<b>0.012</b>	<b>6.E-4</b>	<b>0.023</b>	<b>0.399</b>	19.11	19.50
	St. d	2.49	9.850	14.90	0.015	0.002	0.017	2.794	3.902	2.754
	N	37.0	50.0	50.0	50.0	50.0	50.0	49.0	39.0	50.0
	T	3.63	6.691	9.699	3.954	6.926	9.914	3.865	6.857	9.823
SGA	Avr.	9.24	86.35	212.3	1.700	39.86	137.0	4.825	<b>19.05</b>	<b>17.02</b>
	St. d	3.79	16.69	28.35	0.960	13.42	28.85	1.592	1.607	0.046
	N	13.0	0.0	0.0	0.0	0.0	0.0	1.0	11.0	0.0
	T	3.60	6.091	8.431	3.960	6.278	8.673	3.830	6.181	8.540
Algorithms		Function D								
		F7								
		10	30	50	10	30	50	10	30	50
RNP-SGA	Avr.	<b>108.9</b>			<b>0.040</b>			<b>0.175</b>		
	St. d	28.88			0.279			0.328		
	N	44.0			50.0			50.0		
	T	33.81			39.08			44.92		
SGA	Avr.	154.6			169.7			226.4		
	St. d	32.57			14.84			14.47		
	N	6.0			0.0			0.0		
	T	34.03			38.66			43.77		

- Algorithms' stability: the standard deviation is the most used indicator of stability. It measures the distribution of the results found around the averaged value of 50 independent runs. We conclude through this measure the accuracy of the proposed algorithm.
- Computational time: the time that makes an evolutionary algorithm to generate the solution is an important factor. In real word applications we search for fast algorithms. The evolutionary algorithms are not recommended for online



problems in many applications. Add to this that real applications need high time for an algorithm to generate their solutions. If we compare the time processing of the proposed algorithm and the SGA, we can conclude that there are no difference between them. As SGA had been used in real-world applications, the RNP-SGA can be also used.

## 4 Realisation of Gymnastic Movement on the Bar by Humanoid Robot

In this section we propose the utilization of the RNPSGA to realize the swing-up movement on the bar by a humanoid robot. Firstly we need the dynamic model of the humanoid robot on the bar. Secondly, we derivivate the linear model around the swing-up position. Then the RNPSGA can be applied to compute the matrix  $Q$  and  $R$  for the designing of the optimal LQR controller.

### 4.1 Virtual Model

We present here the virtual model designed using Solidworks 2014. The complete model of the humanoid robot hanging on a high bar is represented in Fig. 3. To control the humanoid robot, we combine between Solidwork and Simscape/Matlab. The model of the designed robot on Simmechanics/Matlab is shown in Fig. 4. Therefore, the exact mechanical properties of the humanoid are copied directly from Solidworks. The details are shown in Table 3.

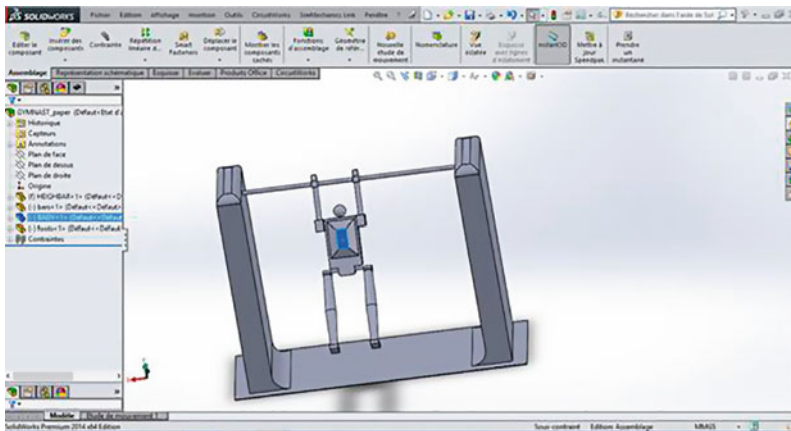
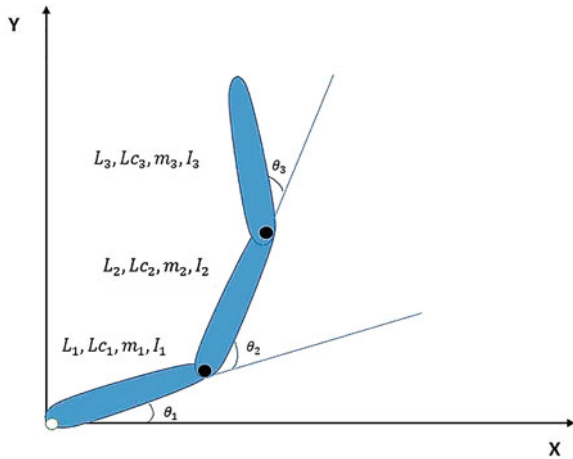


Fig. 3 Virtual model of the humanoid designed with Solidworks

**Fig. 4** The humanoid as a three link underactuated pendulum



**Table 3** Parameters of the humanoid robot

The link	$M$	$I$	$l_c$	$l$
Link 1	8.0076	0.505	0.39874	0.50542
Link 2	31.8146	1.52895	0.23665	0.57
Link 3	21.2453	3.10134	0.48835	0.9767

### 4.2 The Nonlinear Dynamic Model of the Gymnastic Humanoid Robot

The Gymnastic humanoid robot can be seen as being compound of three main links [15, 18]. The first link represents the arms, the second represents the torso and a third represents the legs. The joints of the robot are therefore the hands, the shoulders and the hips. Both shoulders and hips are actuated by two servos in each side. The hands are not actuated indeed, and therefore the system can be approximated by a three link underactuated pendulum. The dynamic behavior of this multi-body robotic system can be derived from the classical Euler-Lagrange equations. The model is represented in Fig. 4.

We precise here the used notations:

- $\theta_i$  is the angle of joint  $i$  in respect to the previous link.
- $m_i$  is the mass of link  $i$ .
- $I_i$  is the inertia of link  $i$ .
- $\tau_i$  is the torque actuated on the active joint  $i$ .
- $L_i$  is the length between joint  $i$  and joint  $i + 1$ .
- $Lc_i$  is the length between joint  $i$  and the center of gravity of the mass  $i$ .

The direct cinematic model of the center of mass of each link is:

$$x_1 = Lc_1 \cos(\theta_1) \quad (1)$$

$$y_1 = Lc_1 \sin(\theta_1) \quad (2)$$

$$x_2 = L_1 \cos(\theta_1) + Lc_2 \cos(\theta_1 + \theta_2) \quad (3)$$

$$y_2 = L_1 \sin(\theta_1) + Lc_2 \sin(\theta_1 + \theta_2) \quad (4)$$

$$x_3 = L_1 \cos(\theta_1) + L_2 \cos(\theta_1 + \theta_2) + Lc_3 \cos(\theta_1 + \theta_2 + \theta_3) \quad (5)$$

$$y_3 = L_1 \sin(\theta_1) + L_2 \sin(\theta_1 + \theta_2) + Lc_3 \sin(\theta_1 + \theta_2 + \theta_3) \quad (6)$$

The Lagrangian of the system is given by:

$$L = \sum_{i=1}^3 (T_i - U_i) \quad (7)$$

where the kinetic energy T and the potential energy U of links are given by:

$$T_1 = \frac{1}{2} [m_1 (\dot{x}_1^2 + \dot{y}_1^2) + I_1 \dot{\theta}_1^2] \quad (8)$$

$$T_2 = \frac{1}{2} [m_2 (\dot{x}_2^2 + \dot{y}_2^2) + I_1 (\dot{\theta}_1 + \dot{\theta}_2)^2] \quad (9)$$

$$T_3 = \frac{1}{2} [m_2 (\dot{x}_3^2 + \dot{y}_3^2) + I_1 (\dot{\theta}_1 + \dot{\theta}_2 + \dot{\theta}_3)^2] \quad (10)$$

$$U_1 = m_1 g y_1 \quad (11)$$

$$U_2 = m_2 g y_2 \quad (12)$$

$$U_3 = m_3 g y_3 \quad (13)$$

The nonlinear model is then derived from Euler-Lagrange equations. We found the model given by Eq. 14

$$\begin{bmatrix} d_{11} & d_{12} & d_{13} \\ d_{21} & d_{22} & d_{23} \\ d_{31} & d_{32} & d_{33} \end{bmatrix} \begin{bmatrix} \ddot{\theta}_1 \\ \ddot{\theta}_2 \\ \ddot{\theta}_3 \end{bmatrix} + \begin{bmatrix} G_1 \\ G_2 \\ G_3 \end{bmatrix} + \begin{bmatrix} C_1 \\ C_2 \\ C_3 \end{bmatrix} = \begin{bmatrix} 0 \\ \tau_1 \\ \tau_2 \end{bmatrix} \quad (14)$$

where the inertial terms are:

$$d_{11} = A_1 + 2m_2L_1Lc_2 \cos(\theta_2) + 2m_3L_1L_2 \cos(\theta_2) + 2m_3L_2Lc_3 \cos(\theta_3) \\ + m_3L_1Lc_3 \cos(\theta_2 + \theta_3)$$

$$d_{12} = A_2 + m_2L_1Lc_2 \cos(\theta_2) + m_3L_1L_2 \cos(\theta_2) + 2m_3L_2Lc_3 \cos(\theta_3) \\ + m_3L_1Lc_3 \cos(\theta_2 + \theta_3)$$

$$d_{13} = A_3 + m_3L_2Lc_3 \cos(\theta_3) + m_3L_1Lc_3 \cos(\theta_2 + \theta_3)$$

$$d_{21} = d_{12}$$

$$d_{22} = A_2 + 2m_3L_2Lc_3 \cos(\theta_3)$$

$$d_{23} = A_3 + m_3L_2Lc_3 \cos(\theta_3)$$

$$d_{31} = d_{13}$$

$$d_{32} = d_{23}$$

$$d_{33} = A_3 + m_3L_2Lc_3 \cos(\theta_3)$$

$$A_1 = m_1Lc_1^2 + m_2L_1^2 + m_2Lc_2^2 + m_3L_1^2 + m_3L_2^2 + m_3Lc_3^2 + I_1 + I_2 + I_3$$

$$A_2 = m_2Lc_2^2 + m_3L_2^2 + m_3Lc_3^2 + I_2 + I_3$$

$$A_3 = m_3Lc_3^2 + I_3$$

The gravitational terms are:

$$G_1 = B_1 \cos(\theta_1) + B_2 \cos(\theta_1 + \theta_2) + B_4 \cos(\theta_1 + \theta_2 + \theta_3)$$

$$G_2 = B_3 \cos(\theta_1 + \theta_2) + B_4 \cos(\theta_1 + \theta_2 + \theta_3)$$

$$G_3 = B_4 \cos(\theta_1 + \theta_2 + \theta_3)$$

$$B_1 = (m_1lc_1 + m_2l_1 + m_3l_1)g$$

$$B_2 = (m_2lc_2 + m_3l_2)g$$

$$B_3 = (m_2lc_2 + m_3l_2)g$$

$$B_4 = m_3lc_3g$$

And the Coriolis:

$$\begin{aligned} C_1 = & F_4(\dot{\theta}_2 + \dot{\theta}_3)(2\dot{\theta}_1 + \dot{\theta}_2 + \dot{\theta}_3)\sin(\theta_2 + \theta_3) \\ & + F_1\dot{\theta}_2(2\dot{\theta}_1 + \dot{\theta}_2)\sin(\theta_2) + F_2\dot{q}_2(2\dot{\theta}_1 + \dot{\theta}_2)\sin(\theta_2) \\ & + F_3\dot{\theta}_3(2\dot{\theta}_1 + 2\dot{\theta}_2 + \dot{\theta}_3)\sin(\theta_3) \end{aligned}$$

$$\begin{aligned} C_2 = & -F_1\dot{\theta}_1^2\sin(\theta_2) - F_2\dot{\theta}_1^2\sin(q_2) + F_3\dot{\theta}_3(2\dot{\theta}_1 + 2\dot{\theta}_2 + \dot{\theta}_3)\sin(\theta_3) \\ & - F_4\dot{q}_1^4\sin(\theta_2 + \theta_3) \end{aligned}$$

$$C_3 = -F_3(\dot{\theta}_1 + \dot{\theta}_2)^2\sin(\theta_3) - F_4\dot{\theta}_1^2\sin(\theta_2 + \theta_3)$$

$$F_1 = -m_2L_1Lc_2, F_2 = -m_3L_1L_2, F_3 = -m_3L_2Lc_3, F_4 = -m_3L_1Lc_3,$$

### 4.3 Linearization of the Model

We are interested by the realization of the gymnastic movement. In the literature we talk about the swing-up control problem [14]. The objective is to realize and to stabilize the humanoid at the vertical unstable equilibrium position. As the model derived from Euler-Lagrange equations is highly nonlinear, we derive here the linearized model around the vertical position.

$$\theta = \left[ \frac{\pi}{2} \quad 0 \quad 0 \right]^T \text{ and } \dot{\theta} = [0 \quad 0 \quad 0]^T$$

The linearized model of the humanoid for the vertical unstable equilibrium is given by the following equations:

$$D\ddot{q} + Gq = T\tau \quad (15)$$

$$\begin{bmatrix} d_{11} & d_{12} & d_{13} \\ d_{21} & d_{22} & d_{23} \\ d_{31} & d_{32} & d_{33} \end{bmatrix} \begin{bmatrix} \ddot{\theta}_1 \\ \ddot{\theta}_2 \\ \ddot{\theta}_3 \end{bmatrix} + \begin{bmatrix} g_{11} & g_{12} & g_{13} \\ g_{21} & d_{22} & g_{23} \\ g_{31} & g_{32} & g_{33} \end{bmatrix} \begin{bmatrix} \theta_1 - \frac{\pi}{2} \\ \theta_2 \\ \theta_3 \end{bmatrix} = \begin{bmatrix} 0 & 0 \\ 1 & 0 \\ 0 & 1 \end{bmatrix} \begin{bmatrix} \tau_1 \\ \tau_2 \end{bmatrix} \quad (16)$$

where:

$$d_{11} = A_1 + 2m_2L_1Lc_2 + 2m_3L_1L_2 + 2m_3L_2Lc_3 + 2m_3L_1Lc_3$$

$$d_{12} = A_2 + m_2L_1Lc_2 + m_3L_1L_2 + 2m_3L_2Lc_3 + m_3L_1Lc_3$$

$$d_{13} = A_3 + m_3L_2Lc_3 + m_3L_1Lc_3$$

$$\begin{aligned}
d_{21} &= d_{12} \\
d_{22} &= A_2 + 2m_3L_2Lc_3 \\
d_{23} &= A_3 + m_3L_2Lc_3 \\
d_{31} &= d_{13} \\
d_{32} &= d_{23} \\
d_{33} &= A_3 + m_3L_2Lc_3 \\
g_{11} &= B_1 + B_2 + B_4 \\
g_{12} &= B_3 + B_4 \\
g_{12} &= B_4 \\
g_{22} &= g_{21} = g_{12} \\
g_{33} &= g_{31} = g_{32} = g_{23} = g_{13}
\end{aligned}$$

#### 4.4 The State Space Model of the Humanoid

The state vector is constituted by the position vector  $\mathbf{q}$  and  $\dot{\mathbf{q}}$ , hence we have:

$$X = [q_1 - \frac{\pi}{2} \quad q_2 \quad q_3 \quad \dot{q}_1 \quad \dot{q}_2 \quad \dot{q}_3]^T \quad (17)$$

The state space model is given by:

$$\dot{x}(t) = Ax(t) + Bu(t) \quad (18)$$

$$y(t) = Cx(t) + Du(t) \quad (19)$$

The matrix A, B, C and D are given by:

$$A = \begin{bmatrix} 0_{n \times n} & I_{n \times n} \\ D^{-1}G & 0_{n \times n} \end{bmatrix}, B = \begin{bmatrix} 0_{n \times m} \\ D^{-1}T \end{bmatrix}, C = I_{n \times n} \text{ and } D = 0$$

The numerical values of the state space matrix A and B are:

$$A = \begin{bmatrix} 0 & 0 & 0 & 1 & 0 & 0 \\ 0 & 0 & 0 & 0 & 1 & 0 \\ 0 & 0 & 0 & 0 & 0 & 1 \\ 18.8797 & -21.4186 & -5.1879 & 0 & 0 & 0 \\ -18.3221 & 46.7787 & 8.3809 & 0 & 0 & 0 \\ -0.2202 & -10.0165 & 6.1066 & 0 & 0 & 0 \end{bmatrix} \quad B = \begin{bmatrix} 0 & 0 \\ 0 & 0 \\ 0 & 0 \\ -0.2169 & 0.0326 \\ 0.4124 & -0.1147 \\ 0.1147 & -0.1410 \end{bmatrix}$$

#### 4.5 Realization of the Gymnastic Movement by the Humanoid Robot

We propose in this subsection the designing of an intelligent optimal controller to stabilize the humanoid robot on the vertical unstable position (swing-up control). Therefore, we design firstly the LQR controller and then we optimize its parameters (the Q and R) by the RNP-SGA algorithm proposed in this paper and we compare the results given by RNPSGA and the results found by SGA. The optimization criterion is derived from the error between the trajectory of the variables  $X$  and the position of the swing up movement. The mathematical formula of this criterion is:

$$J = \sqrt{\int_{t_0}^{t_f} (X(t) - \hat{X})^2} \quad (20)$$

where  $X(t)$  is the trajectory of the state is space and  $\hat{X}$  is the desired position. We note that  $\hat{X} = [\frac{\pi}{2} \ 0 \ 0 \ 0 \ 0 \ 0]^T$ . The matrix Q and R are assumed diagonal. We propose here to compute them using the SGA and the proposed RNPSGA. The Simscape model is shown in Fig. 5. The result are shown in the next subsection.

#### 4.6 Results and Discussion

We present here the results given by the SGA and the RNPSGA. The algorithms search for the diagonal elements of the matrix Q and R that minimize the criterion  $J$ . Once Q and R are known, we calculate the feedback  $K$  that stabilizes the robot on the vertical position. In LQR control, we search for K that minimizes the cost function given by:

$$C = \int \{x' Q x + u' R u + 2^* x' N u\} dt \quad (21)$$

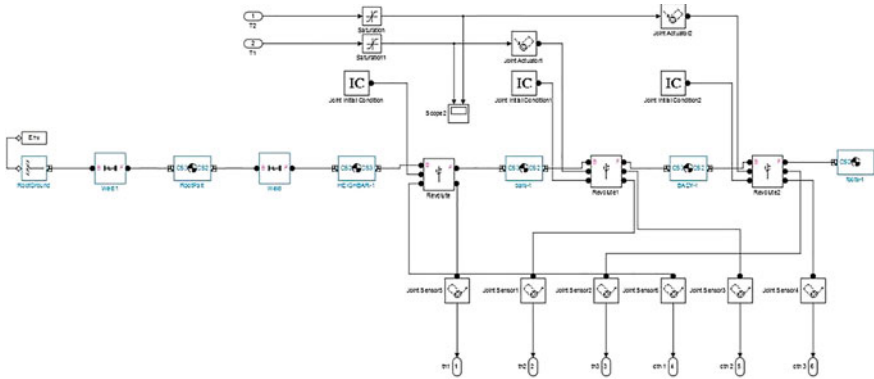


Fig. 5 Simscape model of the gymnastic humanoid robot

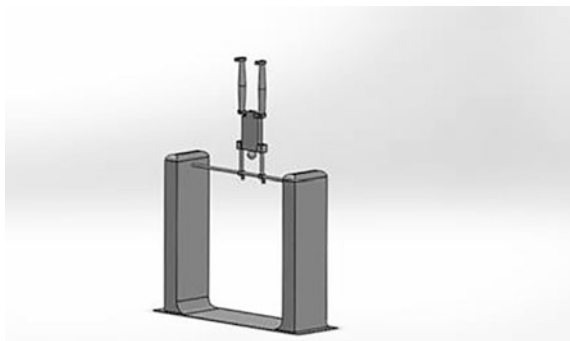
The feedback  $K$  is calculated using the algebraic Riccati equation. The low for the LQR controller is known to be:  $u(t) = -k(t)x$

The results found by SGA and RNP-SGA are summarized in Table 4. The results found by RNPSGA are better than those found by SGA. The Fig. 6 gives the allure of the obtained gymnastic movement in virtual 3D space. The allures of the evolution of optimization process is shown in Fig. 7.

Table 4 The results found by SGA and RNP-SGA

Algorithm	Average of J	Q	R
RNPSGA	0.205	Diag[ 595.85    0.02    2.00E-4 0.013    0.05    972.9751 ]	Diag[1.0E-5 1.0E-5]
SGA	0.431	Diag[ 494    1.0E-5    1.0E-5 1.0E-5    39.175    968.3 ]	Diag[1.0E-5 1.0E-5]

Fig. 6 The swing-up movement obtained





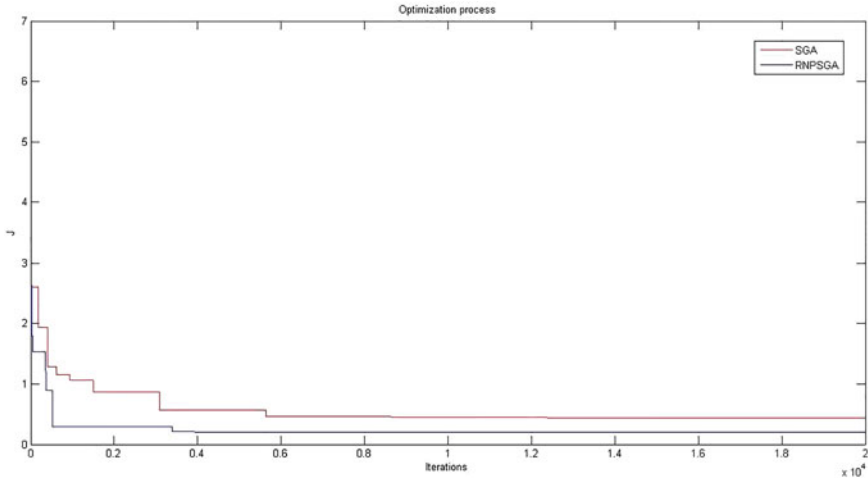


Fig. 7 Optimization process

## 5 Conclusion

This paper purposes a new variant of selfish gene algorithm called the Replaces and Never Penalizes Selfish Gene Algorithm (RNP-SGA). The algorithm uses tournament selection and overwrites the genes of failed individual by the alleles of the winner of the tournament. As the algorithm duplicates the genes of the winners of the tournament in the virtual population, then it allows more intensification. The proposed algorithm is tested firstly for unconstrained optimization problem using unimodal and multimodal benchmark functions. A statistical study shows its high performance compared to standard SGA in terms of quality of convergence, accuracy, stability and processing time. Secondly we test the algorithm on a humanoid robot. The objective is to stabilize the movement of the swing-up control. The model of the humanoid robot is designed using Solidwork specifically to do the movements of the gymnastic on horizontal bar. The results given by RNP-SGA are compared to those found by SGA.

## References

1. Bremermann, H.J.: Optimization through evolution and recombination. In: Yovits, M.C. et al. (eds.) *Self-Organizing Systems*. Spartan, Washington, DC (1962)
2. Box, G.E.P.: Evolutionary operation: a method for increasing industrial productivity. *Appl. Stat.* **VI**(2), 81–101 (1957)
3. Rechenberg, I.: *Cybernetic solution path of an experimental problem*. Royal Aircraft Establishment, Library translation No. 1122, Farnborough
4. Fogel, L.J.: Autonomous automata. *Ind. Res.* **4**, 14–19 (1962)

5. Burgin, G.H.: On playing two-person zero-sum games against nonminimax players. *IEEE Trans. Syst. Sci. Cybern.* **SSC-5**(4), 369–370 (1969)
6. Holland, J.H.: Outline for a logical theory of adaptive systems. *J. Assoc. Comput. Mach.* **3**, 297–314 (1962)
7. Neema, M.N., Maniruzzaman, K.M., Ohgai, A.: New genetic algorithms based approaches to continuous p-median problem. Springer Science (2008)
8. Chow, C.K., Yuen, S.Y.: An evolutionary algorithm that makes decision based on the entire previous search history. *IEEE Trans. Evol. Comput.* **15**(6), 741–768 (2011)
9. Yuen, S.Y., Devr, C.K.C.: A genetic algorithm that adaptively mutates and never revisits. *IEEE Trans. Evol. Comput.* **13**(2), 454–472 (2009)
10. Ghosh, D.: A Diversification Operator for Genetic Algorithms. In: *OPSEARCH*. Springer (2012)
11. Marsili Libelli, S., Alba, P.: Adaptive mutations in genetic algorithms. *Soft Comput.* (2000)
12. Dawkins, R.: *The Selfish Gene*, new edn. Oxford University Press, London (1989)
13. Como, F., Reorda, M.S., Squillero, G.: The selfish gene algorithm: a new evolutionary optimization strategy. In: *ACM Symposium on Applied Computing SAC'98*, Atlanta (1998)
14. Xin, X., Kaneda, Masahiro: Swing-up control for a 3-DOF gymnastic robot with passive first joint: design and analysis. *IEEE Trans. Robot.* **23**(6), 1277–1285 (2007)
15. Liang, J.J., Suganthan, P.N., Deb, K.: Novel composition test functions for numerical global optimization. In: *Swarm Intelligence Symposium, 2005. SIS 2005. Proceedings 2005*, pp. 68–75. IEEE (2005)
16. Chow, C.K., Yuen, S.Y.: An evolutionary algorithm that makes decision based on the entire previous search history. *IEEE Trans. Evol. Comput.* **15**(6), 741–769 (2011)
17. Yuen, S.Y., Chow, C.K.: A non-revisiting simulated annealing algorithm. *Proceedings of IEEE Congress on Evolutionary Computation*, pp. 1886–1892 (2008)
18. Teodoro, P.D.D.: Humanoid robot: development of a simulation environment of an entertainment humanoid robot. Master Thesis, Instituto Superior Técnico (2007)

# Reduction of Solution Space in the Automotive Safety Integrity Levels Allocation Problem

Youcef Gheraibia, Khaoula Djafri and Habiba Krimou

**Abstract** Automotive Safety Integrity Levels (ASILs) are a key concept of ISO 26262, the new automotive functional safety, tasked with ensuring that new automotive systems provide the required safety. This is largely accomplished by allocating safety requirements as ASILs to components that may cause the failure of critical functionalities. Assigning appropriate ASILs to components is a major design issue, and due to the combinatorial nature of the problem, a huge number of solutions is available in the search space. However, searching through this space may become impracticable in large and complex systems and, therefore, research efforts to develop techniques that find optimal ASIL allocations in reasonable time are ongoing. In this paper, we introduce a couple of strategies to reduce the solution space. These strategies have been applied on different cases studies where we demonstrate their efficacy in reducing the solution space.

**Keywords** Solution space reduction · Optimization · ASIL · Safety requirement · ISO 26262

## 1 Introduction

ISO 26262 is an adapted version of the functional safety standard IEC 61508 released in 2011 [1]. It represents a functional safety standard applicable to automotive safety related systems [2]. The standard proposes the concept of Automotive Safety

---

Y. Gheraibia (✉) · K. Djafri · H. Krimou  
Department of Computer Science, University of Souk-Ahras,  
Souk-Ahras, Algeria  
e-mail: youcef.gheraibia@univ-soukahras.dz

K. Djafri  
e-mail: D.Khaoula@univ-soukahras.dz

H. Krimou  
e-mail: H.Krimou@univ-soukahras.dz

Integrity Levels (ASILs) to represent the strictness of safety requirements. ASILs are an adaptation of SILs (Safety Integrity Levels) proposed in IEC1508 [2].

In the course of development of a system, ISO26262 requires an early hazard analysis to identify a set of hazards caused by system malfunctions. Based on analysis of controllability, severity and exposure, an ASIL is assigned to the hazard and a safety goal is defined [2]. Safety goal represent top-level safety requirements that reduce risk to acceptable levels.

ASILs allocated to subsystems and components describe the safety requirement to be met during the development life cycle of the system. Developing a system or component to a certain ASIL implies a certain costs which gets higher as the ASIL increases. In order to reduce the ASIL of an element and make sure that the safety requirements are still met, ASILs can be decomposed over the components that implement the element. The standard proposes an algebra allowing such decomposition.

ASILs are assigned integer values:  $ASIL(QM) = 0$ ,  $ASIL(A) = 1$ ,  $ASIL(B) = 2$ ,  $ASIL(C) = 3$ ,  $ASIL(D) = 4$  [3]. As the ASIL value increases the safety requirement becomes more stringent. The decomposition rules define that when an element is implemented by a number of independent components which must all fail for the element to fail then the ASIL of the element can be decomposed in a way that the sum of the ASILs of components equals the ASIL of the element. For instance, if component C is allocated ASIL(D), and C is implemented with three independent sub-components SC1,SC2,SC3 these can be allocated ASIL(A), ASIL(A) and ASIL(B) respectively. Such decomposition allows reducing the cost required for safety requirements to be met.

For each ASIL there are many possibilities of decomposition, e.g.  $ASIL(C) = ASIL(A) + ASIL(A) + ASIL(A)$  or  $ASIL(C) = ASIL(A) + ASIL(B)$ , or  $ASIL(C) = ASIL(QM) + ASIL(C)$ . For a system with n components, where each component is assigned an ASIL, there are many different ways to meet the system safety requirements, i.e. there is typically a very large number of feasible allocations of requirements to components that defines a space within which one needs to look for a cost-optimal solution. The process of finding an optimal ASIL allocation is an NP-hard problem, which requires the intervention of optimization methods to reach an optimal, economic ASIL allocation in reasonable time.

In this paper we propose a couple of strategies to reduce the dimension of solution space. These strategies reduces the space of solutions which will help algorithms dedicated to solve ASILs allocation to converge to an optimal solution in a faster, more efficient way.

In section two a brief description of ASIL allocation problem is presented, followed with a background study of algorithms used to solve the ASIL allocation problem. Section three describes the proposed strategies to reduce the solution space. Section four provides an experimental study and section five presents conclusions and further work.

## 2 The ASIL Allocation Problem

ASIL allocation can be presented and formulated as the problem of finding the optimal set of ASILs that corresponds to the hazardous events of a system regarding the given constraints while minimizing the overall cost.

$$\min f = \sum_{i=1}^n C(ASIL[i]). \quad (1)$$

Subject to:

$$\left( \sum_{j=1}^{mk} ASIL[j] \right) \geq k_{ASIL} \quad 1 \leq k \leq l \quad (2)$$

$$ASIL_i, k_{ASIL} \in Z \cap ASIL_i, k_{ASIL} \in [0, 4]$$

where:

$n$ : number of the hazardous events.

$l$ : number of ASIL allocation constraints.

$mk$ : number of hazardous events in the  $k$ th ASIL allocation constraint.

$C(ASIL_i)$ : cost of the ASIL allocated to the  $i$ th Hazardous event.

$k_{ASIL}$ : ASIL requirement for the  $k$ th ASIL allocation constraint.

The work presented in [4] proposes a fault propagation logic based algorithm to automatically allocate and decompose SILs using a safety analysis tool called HIP-HOPS (Hierarchically Performed Hazard Origin and Propagation Studies).

In [2] ASILs allocation is defined as a system of linear equations. The idea is to use a set constraints based on fault tree cut-sets as a basis of constructing the equations, and then provide an augmented matrix which has been undergone Gauss Jordan elimination and transform it to the Row Reduced Echelon Form. The solution of the system, grants an exact ASILs allocation to system components, otherwise the algorithm is re-executed after applying some changes to the preferences of the algorithm.

Another exact algorithm is described in [5] where ASIL allocation and decomposition is transformed into an integer linear programming problem, the approach uses a framework equipped with a solver designed to solve integer linear programming problems. An EAST-ADL (Electronic Architecture and Software Technology-Architecture Description language) model is created by the framework to automatically generate fault trees, from which constraints are extracted. Constraints which are represented in the form of cut sets are used by the solver to provide a solution to the ASILs allocation problem.

Exact solvers are dedicated to find exact, i.e. verifiably optimal, solutions but take long time while searching for the solution. As a consequence the urge for solvers that find near optimal or optimal solutions in reasonable time has appeared. These solvers use optimization algorithms which do not exhaustively search the entire solution space but can still grand near-optimal or optimal solutions in reasonable time.

The work presented in [6] uses a Penguins-inspired algorithm to solve ASILs allocation. The idea is to reach an optimal allocation of ASILs by imitating the hunting behaviour of Penguins [7]. The algorithm uses priority classes to assign high priority to failure modes with low cost, in order to reduce the solution space. The process starts with a population of penguins divided into groups of  $n$  penguins. Each penguin generates neighboring solutions regarding its oxygen reserve, for each neighboring solution the algorithm checks for its feasibility and calculates its fitness. If the fitness of the new solution is higher than the current best solution, then the algorithm replaces the current one with the neighboring solution and updates the oxygen reserve of the penguin, then the population of penguins is redistributed according to probabilities. The stopping criterion is reached when cost stops decreasing i.e. the optimal ASIL allocation is found.

A Tabu search algorithm was also used to allocate ASILs in the work presented in [8]. The key idea was to use the Steepest Ascent Mildest Descent (SAMD) method to solve ASIL allocation. The SAMD is a maximization method, so it was inverted to the Steepest Descent Mildest Ascent (SDMA) to suit this particular problem where cost is minimized. This means that in each iteration the algorithm changes the solution by taking the steepest descent until a local minima is reached, then takes the mildest ascent to avoid getting trapped in the local minima. The algorithm stops when the termination criteria is met.

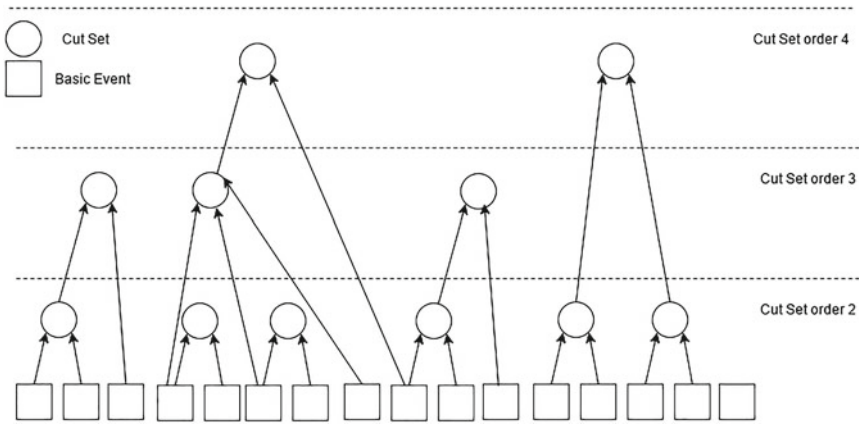
In the work presented in [3] a Genetic Algorithm (GA) was used. The algorithm was equipped with a penalty method to get a handle of constraints. The algorithm starts with generating a population of candidate solutions, then check for their feasibility and penalizes the infeasible candidates. Candidates are selected based on their fitness to undergo mutation and recombination to create new candidate solutions. For each new candidate, the algorithm checks whether its a feasible solution or not, if feasible the new candidate is added to the population and the algorithm proceeds until a stopping criterion is reached.

### **3 The Proposed Strategies for Solution Space Reduction**

Due to the combinatorial nature of the problem, the solution space is typically very large, making the process of finding an optimal allocation even harder. The objective of this work has been to reduce the dimension of solutions space using two strategies, where the solutions space undergoes the first strategy, then the resulting solution spaces goes through the second strategy which grants a considerable reduction in the dimension of solution space.

#### ***3.1 CutSet Based Reduction***

A cut set is a minimal combination of failures of components, which if they occur in conjunction lead to a hazard. Cut sets are determined using Fault Tree Analysis (FTA) of a system architecture [9]. In this strategy cut sets are used for reducing the



**Fig. 1** CutSet based reduction

solution space where cut sets with different orders are formulated as trees. Roots and nodes of the tree are the cut sets while leaves are the basic events (see Fig. 1).

The cut set based strategy provides a considerable reduction in the solution space by imposing constraints to the ASILs values that a basic event may hold regarding the ASIL of the cut sets that include that basic event.

The idea is to restrict the ASIL of each and every basic event in the trees between two values  $\alpha$  and  $\beta$ , where  $\alpha$  and  $\beta$  are deduced from the set of cut sets that the basic event belongs to, which leads to reduce the solution space by limiting the SILs that a basic event may hold.

In theory, if the problem is left unconstrained the ASIL that a basic event may hold is within the range of [0, 1, 2, 3, 4]. All combinations of those values of different events then become candidate solutions. However if the basic event is involved in a set of specific cut sets, then its maximum value cannot exceed the value of the highest ASIL of those specific cut sets. In addition, its minimum value is not unconstrained. If for example the event participates in a cutset of order one, its value cannot be less than the value of this cut set.

As an example, suppose the basic event BE and that BE is involved in the set of cut sets  $M = CS1, CS2, CS3$ . Let us assume that the ASILs of the  $M$  cut sets are 1, 3, 3 respectively. According to the proposed strategy, the ASIL of BE, i.e. ASIL(BE), is restricted between  $\alpha$  and  $\beta$ , where  $\alpha$  is equal to ASIL(QM) = 0 and  $\beta$  is equal to ASIL(C) = 3. This eliminates the ASIL(D) = 4 from the solution space, and by doing so, the solution space is reduced. The second strategy is presented next.

### 3.2 Heuristic Cost Based Reduction

Cost heuristics are functions that determine the cost of associating the ASILs to each component of the system. This cost of fulfilling the requirements by assigning

**Table 1** ASIL cost heuristics

Cost heuristics	QM	A	B	C	D
Linear	0	10	20	30	40
Logarithmic	0	10	100	1000	10000
Experiential-I	0	10	20	40	50
Experiential-II	0	5	30	35	50

ASILs to the hazardous events is represented by the sum of all components ASILs. Cost heuristic are defined in Table 1. The distance between different ASILs cost is the reason why several solutions with the same costs can vary. For instance, as it is shown in Table 1, the linear cost heuristic which is the based model, defines costs for the ASILs where the difference between any ASIL and its successive is equal. From here, if solutions that have the same cost like (ASIL 2, ASIL 2),(ASIL 4) and (ASIL 1, ASIL 3) are considered equivalent, the solution space is reduced. This is not the case where steps between ASILs costs are not equal, the solution space will be larger where solutions with different costs can be found [6]. In order to reduce the solution space, equivalent classes are defined to prioritise which combination of ASILs is the most appropriate for a given set of hazardous events. These classes can provide the same safety but yet, not the same cost. Elements with the classes that give lower cost are given higher priorities, therefore classes and their priorities are computed to deduce the most cost-effective combinations. ASIL preference extraction process is as follows [6].

- **Equivalent classes construction:** Construct all possible combinations of ASILs allocations to fulfill a safety requirement.
  - Class (ASIL S2)** = (ASIL 2); (ASIL 1, ASIL 1)
  - Class (ASIL S3)** = (ASIL 2, ASIL 1); (ASIL 3); (ASIL 1, ASIL 1, ASIL 1)
  - Class (ASIL S4)** = (ASIL 4); (ASIL 2, ASIL 2); (ASIL 3, ASIL 1); (ASIL 2, ASIL 1, ASIL 1); (ASIL 1, ASIL 1, ASIL 1, ASIL 1)
- **Compute cost of elements for each class:** Here the cost of classes' elements is calculated and depends on the cost heuristic used.
  - Class (ASIL S2)** = Cost (ASIL2); 2 x Cost (ASIL1)
  - Class (ASIL S3)** = Cost (ASIL3); Cost (ASIL2) + Cost (ASIL1); 3 x Cost (ASIL1)
  - Class (ASIL S4)** = Cost (ASIL4); 2 x Cost (ASIL2); Cost (ASIL3) + Cost (ASIL1); Cost (ASIL2) + 2 x Cost (ASIL1); 4 x Cost (ASIL1)
- **Priority generation:** In each class, after calculating the elements costs, they will be ordered in ascending order. High priority is assigned to the least cost and vice versa. The following example shows how this works using Experiential-II heuristic function. Let  $F = (5, 30, 35, 50)$  be a cost heuristic allocated to (ASIL 0, ASIL 1, ASIL 2, ASIL 3, ASIL 4) respectively.



The classes of equivalent solutions and the solution cost in each case within a class are:

**Class (ASIL s2)** = Cost (ASIL2); 2 x Cost (ASIL1) = 30, 10

**Class (ASIL s3)** = Cost (ASIL3); Cost (ASIL2) + Cost (ASIL1); 3 x Cost (ASIL1) = 35, 35, 15

**Class (ASILs4)** = Cost (ASIL4); 2 x Cost (ASIL2); Cost (ASIL3) + Cost (ASIL1); Cost (ASIL2) + 2 x Cost (ASIL1); 4 x Cost (ASIL1)

This way, priorities will be assigned to elements according to following process:  
 If (Cost(ASIL1) + Cost(ASIL1)  $\leq$  Cost (ASIL2)) Then ASIL1 **has a higher priority than ASIL2**

Else

ASIL2 has a higher priority than ASIL1

If (Cost (ASIL2) + Cost(ASIL1)  $\leq$  Cost (ASIL3)) Then

ASIL2 **has a higher priority than ASIL3**

Else

ASIL3 has a higher priority than ASIL2

If (Cost(ASIL3) + Cost(ASIL1)  $\leq$  Cost (ASIL4)) Then

ASIL3 **has a higher priority than ASIL4**

Else

ASIL4 **has a higher priority than ASIL3**

High priorities assigned to each ASIL can vary from low that is equal 4 to the high equals 1. For instance, from the given example above, it is extracted that ASIL 1 has the highest priority of 1, and ASIL 4, ASIL 2, ASIL 3, ASIL 4 are given the priorities 2, 3, 4 respectively [6].

## 4 Experimental Study

### 4.1 Hybrid Braking System Description

Hybrid braking systems (HBS) was introduced, studied and detailed in [10]. It is intended to serve the purpose of both normal and anti-lock braking strategies for electrical vehicles of 4 In Wheels Motors (IWMs) i.e. one motor per wheel. HBS is a brake-by-wire system which means that there is no mechanical or hydraulic connection between the braking pedal and the actuators. It is called “hybrid” because it combines the actions of both Electromechanical brakes (EMBs) and In-Wheel Motors (IWMs) [11]. The HBS is composed of a two pedals, one mechanical brake pedal, and one electronic pedal, a bus system, a local control unit, power electronics, the powertrain battery, the auxiliary battery, friction and electric braking solution (Electrohydraulic Braking System, In-Wheel Motor Braking System). The required braking is achieved by joining the efforts of the two braking devices: electric and frictional braking. As the driver’s action on the mechanical pedal is sensed at the electronic one, the later processes the action and acts as a central control unit that

**Table 2** Characteristics of the case studies

Case study	Failure modes	AAC	Max AAC size	Size search space
HBSM1	24	31	2	$5.96 \times 10^{16}$
HBSM2	60	94	2	$8.67 \times 10^{41}$
HBSM3	60	11573	8	$8.67 \times 10^{41}$
NYTT60	185	8218	4	$2.04 \times 10^{219}$

**Table 3** Results of applying reduction strategies

Case study	Initial size search space	Reduced size search space
HBSM1	$5.96 \times 10^{16}$	$2.50 \times 10^{12}$
HBSM2	$8.67 \times 10^{41}$	$2.49 \times 10^{30}$
HBSM3	$8.67 \times 10^{41}$	$8.67 \times 10^{41}$
NYTT60	$2.04 \times 10^{219}$	$2.40 \times 10^{111}$

coordinated the four local wheel controllers. The interconnection of all units is achieved through a communication network composed of buses that allows exchanging information. The characteristics of different HBSs that were used in this paper as case studies are described in Table 2.

## 4.2 Experimentation of Different Strategies

Results presented in Table 3 show that the application of the proposed strategies on the case studies has led to a considerable reduction in the search space, where the initial search space with the original size has undergone cut sets based reduction which reduces the range of SILs that a basic event may hold from  $[0,4]$  to a dynamic interval of  $[\alpha,\beta]$  for each failure mode, the resulting search space goes through the second strategy, that is, cost based reduction which reduces the search spaces by using the concept of equivalent classes and grant low cost classes a high priority, when applied to the HBSM1, HBSM2, NYTT60, results were very promising, the search space of the HBSM1 was reduced from  $5.96 \times 10^{16}$  to  $2.50 \times 10^{12}$ , while the size of the search space of HBSM2 was reduced up to  $2.49 \times 10^{30}$  after it used to be equal to  $8.67 \times 10^{41}$ , then comes the largest case study NYTT60 with an original size of  $2.04 \times 10^{219}$  which has gone through an appreciable reduction up to  $2.40 \times 10^{111}$ . The reduced size search space of HBSM3 remained the same because the all SILs of the cut sets that belong to the HBSM3 was equal to 4, which means that in the cut sets based reduction alpha and beta were equal to 0 and 4 respectively and the range of SILs that a basic event may hold was kept the same as the original, the reason that the second strategy couldnt perform any reduction to the size of search space was due to the absence of equivalent classes in the HBSM3. The resulted space search after

reduction can offer a great deal of help to solvers dedicated to reach an economic, optimal ASILs allocation in a reasonable time.

## 5 Conclusion

Automotive Safety Integrity Levels are classes proposed by the ISO26262 Standard to represent the stringency of safety requirement in the automotive field, to reduce the risk to acceptable level ASILs are decomposed and allocated to different sub-systems and components of the system. ASILs allocation as a combinatorial problem admits a huge number of feasible solutions, which make the process of finding an appropriate allocation a tough task using both exact and optimization solvers. In this paper, we introduced two strategies to reduce the dimension of the solution space of ASILs allocation problem, a cut set based strategy that reduces the solution space regarding the ASIL of each cut set and a cost based strategy that reduces the solution space regarding the cost of ASILs. When applied on HBSM1, HBSM2, HBS3, NYTT60, the proposed strategies have proven their efficiency in reducing the solution space.

**Acknowledgments** I would like to take this opportunity to express my profound gratitude and deep regard to Prof Yiannis Papadopoulos and Dr. David Parker from The University of Hull, for their exemplary guidance, valuable feedback and constant encouragement throughout the duration of the project.

## References

1. Mader, R., Armengaud, E., Leitner, A., Steger, C.: Automatic and optimal allocation of safety integrity levels. In: Reliability and Maintainability Symposium (RAMS), 2012 Proceedings-Annual, pp. 1–6, IEEE (2012)
2. da Silva Azevedo, L., Parker, D., Walker, M., Papadopoulos, Y., Esteves Araujo, R.: Assisted assignment of automotive safety requirements. *Software, IEEE*, vol. 31, no. 1, pp. 62–68 (2014)
3. Parker, D., Walker, M., Azevedo, L.S., Papadopoulos, Y., Araújo, R.E.: Automatic decomposition and allocation of safety integrity levels using a penalty-based genetic algorithm. In: IEA/AIE, pp. 449–459. Springer (2013)
4. Papadopoulos, Y., Walker, M., Reiser, M.-O., Weber, M., Chen, D., Törngren, M., Servat, D., Abele, A., Stappert, F., Lonn, H., et al.: Automatic allocation of safety integrity levels. In: Proceedings of the 1st Workshop on Critical Automotive Applications: Robustness and Safety, pp. 7–10, ACM (2010)
5. Dhoubi, M.S., Perquis, J.-M., Saintis, L., Barreau, M.: Automatic decomposition and allocation of safety integrity level using system of linear equations. *Complex Syst*, pp. 1–5 (2014)
6. Gheraibia, Y., Moussaoui, A., Azevedo, L.S., Parker, D., Papadopoulos, Y., Walker, M.: Can aquatic flightless birds allocate automotive safety requirements? In: 2015 IEEE Seventh International Conference on Intelligent Computing and Information Systems (ICICIS), pp. 1–6, Dec 2015
7. Gheraibia, Y., Moussaoui, A.: Penguins search optimization algorithm (PeSOA). In: Recent Trends in Applied Artificial Intelligence, pp. 222–231. Springer (2013)

8. Azevedo, L.S., Parker, D., Walker, M., Papadopoulos, Y., Araujo, R.E.: Automatic decomposition of safety integrity levels: optimization by tabu search. In: SAFECOMP 2013-Workshop CARS (2nd Workshop on Critical Automotive Applications: Robustness and Safety) of the 32nd International Conference on Computer Safety, Reliability and Security, p. NA (2013)
9. Murashkin, A., Azevedo, L.S., Guo, J., Zulkoski, E., Liang, J.H., Czarnecki, K., Parker, D.: Automated decomposition and allocation of automotive safety integrity levels using exact solvers. *SAE Int. J. Passeng. Cars-Electron. Electr. Syst.* **8**(1), 70–78 (2015)
10. de Castro, R., Araújo, R.E., Freitas, D.: Hybrid ABS with electric motor and friction brakes. In: Proceedings of the 22nd International Symposium Dynamics of Vehicles on Roads and Tracks, pp. 1–7 (2011)
11. Azevedo, L.S., Parker, D., Papadopoulos, Y., Walker, M., Sorokos, I., Araújo, R.E.: Exploring the impact of different cost heuristics in the allocation of safety integrity levels. In: Model-Based Safety and Assessment, pp. 70–81. Springer (2014)

# A Novel Bio Inspired Algorithm Based on Echolocation Mechanism of Bats for Seismic Hazards Detection

Mohamed Elhadi Rahmani, Abdelmalek Amine, Reda Mohamed Hamou, Amine Rahmani, Hanane Menad, Hadj Ahmed Bouarara and Mohamed Amine Boudia

**Abstract** Since the first birth of computers, a lot of works had done in many fields of computer science and inspired generations and generations of researches. Alan Turing pioneered researches by its works in heuristics, and now, hundreds of algorithms and approaches are developed in this field. The last two decades witnessed a very huge movement in field of artificial intelligence. Researchers went far than invention of algorithms based on calculation, they created Bio inspired algorithms which are sort of implementation of natural solutions to solve hard problems so called NP problems. This paper presents a new bio inspired algorithm based in the echolocation behaviour of bats for seismic hazard prediction in coal mines. The implementation of the algorithm includes three fields of studies, data discovery or so called data mining, bio inspired techniques, and seismic hazards predictions.

**Keywords** Seismic hazards detection · Data mining · Meta heuristic · Bio inspired algorithm · Bat echolocation · Machine learning

## 1 Introduction

Mining hazards is a subfield of mining activities connected to the dangers. They are the causes of disasters and accidents, mining hazards plays an important role in shaping industrial safety in coal mines. Similar to an earthquake, detection and prediction of seismic hazards present the hardest issue of natural hazards detection. Seismic activity and seismic hazard in underground coal mines occur in case of specific structure of geological deposit and the way of exploitation of coal. The nature of these hazards is influenced by a large number of factors which causes a complex and insufficiently recognized relationships among them. One example of a situation, with a

---

M.E. Rahmani (✉) · A. Amine · R.M. Hamou · A. Rahmani · H. Menad ·  
H.A. Bouarara · M.A. Boudia  
GeCoDe Laboratory, Department of Computer Science,  
University of Dr. Tahar Moulay, Saida, Algeria  
e-mail: r\_m\_elhadi@yahoo.fr

© Springer International Publishing Switzerland 2016  
S. Chikhi et al. (eds.), *Modelling and Implementation  
of Complex Systems*, Lecture Notes in Networks and Systems 1,  
DOI 10.1007/978-3-319-33410-3\_6

particularly strong intensity, occurs in the Upper Silesian Coal Basin where there are additional conditions connected with: multi-seam structure of deposit, consequences of the long history of exploitation of this area and complex surface infrastructure. In almost all mines of this area there are systems which detect and assess a current degree of seismic hazard [1].

Hazard of high-energy destructive tremor which may result in a rock burst is a particular case of one of the major studies of coal mine geophysical stations work. As a phenomena related with mining seismicity, Rock bursts pose a serious hazard to miners and can destroy long walls and the equipment.

Nature contains a lot of sub-disciplines, a very big number of complex mechanisms that help life keep going on. Understanding these mechanisms is a principal source to inspire different algorithms and solution for problems in technology era. Over the last few decades, it has stimulated many successful algorithms and computational tools for dealing with complex and optimization problems. The real beauty of nature inspired algorithms lies in the fact that it receives its sole inspiration from nature. With their ability to solve hard problems by describing the complex relationships from intrinsically very simple initial conditions and rules with little or no knowledge of the search space Nature is the perfect example for optimization, all kinds of features or phenomenon in nature, always find the optimal strategy to solve different problems. Computer networks, security, robotics, bio medical engineering, control systems, parallel processing, data mining, power systems, production engineering and many more, covering all fields of computer science, bio inspired algorithm presents a mapping of different strategies exist in nature, it come up as a new era in computing encompassing a wide range of researches and applications.

Speaking about bio inspired algorithms, we speak about heuristics because bio inspired algorithms are such heuristics that mimics/imitate the strategy of nature since many biological processes can be thought of as processes of constrained optimization. Heuristics are superior and better than classical methods such as logical, mathematical programming in solving complex optimization problems. Literally, it exist a huge number of bio inspired approaches for solving an impressive array of problems, and that is clear regarding to the number of researches and studies published recently. Bio inspired algorithms are divided to three main types, evolutionary algorithms inspired from the evolution behaviour of animals, swarm intelligence based on the collective life in colonies, ecological approaches inspired from some bio geological phenomenon.

This paper discusses a novel bio inspired algorithm based on the echolocation phenomenon of bats for seismic hazards detection.

The organisation of the paper is as follow, Sect. 2 presents some recent works on seismic hazards prediction. Section 3 we give a summary of [2], which presented a view of literature about bat algorithm. Section 4, we discuss the proposed approach, we gave the artificial model of bats algorithm. Section 5 illustrates a discussion of the obtained results. Finally, Sect. 6 provides a summary and suggestions for further work.

## 2 Related Works for Seismic Hazards Detection

According to [3], advanced seismic and seismoacoustic monitoring systems allow a better understanding rock mass processes, so [4] defined a seismic hazards prediction methods, but these methods required a non-standard measuring apparatus, for this reason they are not used in seismic mining. Kornowski [5] proposed a linear method to predict seismoacoustic energy in a given time horizon. Works on seismic prediction continued with [6] that gave clustering methods to predict the energy of future seismic tremors emitted in a given time horizon based on probabilistic analysis, in which fuzzy numbers and Markov chains were applied. However, the accuracy of all those methods is so far from perfect. Neural Networks also appeared in many studies for prediction of seismic tremors, beginning with [7] in which an application to mining tremor prediction has been tested and methodological conditions have been obtained by treatment of induced seismic activity prediction that was treated as a problem of time series extrapolation of maximum cumulative amplitudes and numbers of seismic events recorded per day, the treatment was done using multilayer perceptron, [8] is another work that presented an approach using neural network for determining an influence of the type and shape of the input data on the efficiency of such a prediction. The considerations are based on a selected example of the seismic activity recorded during long wall mining operations conducted in one of the Polish mines. And also [9] gave a study that demonstrated the potential of the clustering technique in evaluation of the increment of the seismic hazard over a limited area.

All mentioned works reported their methods in form of bi-class problem for prediction of Hazardous and Non-Hazardous seismic, and they are the based works in seismology for prediction of earthquake occurrences [10, 11] in which two of the most known methods in data mining were applied, decision trees and rules induction.

## 3 A View of Literature About Bat Algorithm

### 3.1 *Bat Echolocation Behaviour*

Bats are a special fascinating kind of mammals with their wings and their lifestyle, as we know bats are active only at night and in the dark places. They estimated about 996 species of bats, more than half rely on sounds for navigation while they fly, the use of this trick is to detect obstacles and forage for food. This mechanism is called Echolocation or SONAR (SOund Navigation And Ranging). It gives to a bat the ability to generate signals that bounce off surrounding objects and using a processing of the returning echoes with extraordinary acuity, the bat can determine the direction, the distance and the features of these objects.

The echolocation mechanisms are different and correlated with the hunting strategies of each species; the most of bats use short, frequency-modulated signals to sweep through about an octave. In this strategy, a pulse only lasts a few thousandths of a second (up to about 8–10 ms) in the frequency range of 25–150 kHz. The typical range of frequencies for most bat species are in the region between 25 and 100 kHz, though some species can emit higher frequencies up to 150 kHz. During hunting, the rate of pulse emission can be sped up to about 200 pulses per second when homing on their prey. Studies show the integration time of the bat ear is typically about 300–400  $\mu$ s, which give to the bats a fantastic ability to process the signal. Taking in mind that the speed of sound in air is typically  $v = 340$  m/s, the wavelength  $\lambda$  of the ultrasonic sound bursts with a constant frequency  $f$  is given by  $\lambda = v/f$  [2].

Such echolocation behaviour of bats can be formulated mathematically in such a way that it can be associated with many problems solving objective, for that and based on the original work of [12], we are interested in some features of the echolocation of bats to formulate a mathematical implementation for seismic assessment.

### 3.2 Bat Algorithm

In order to benefit of the amazing power of echolocation of bats in hunting to solve one of the major problems in seismology, we took in consideration three features or so called rules cited by [12] to implement a bat-inspired algorithm as follow:

1. All bats use echolocation to sense distance, and they also know the difference between food/prey and background barriers in some magical way;
2. Bats fly randomly with velocity  $v_i$  at position  $x_i$  with a fixed frequency  $f_{min}$ , varying wavelength  $\lambda$  and loudness  $A_0$  to search for prey. They can automatically adjust the wavelength (or frequency) of their emitted pulses and adjust the rate of pulse emission  $r \in [0, 1]$ , depending on the proximity of their target;
3. Although the loudness can vary in many ways, we assume that the loudness varies from a large (positive)  $A_0$  to a minimum constant value  $A_{min}$ .

## 4 Proposed Approach

As mentioned above, we were interested by the three rules of bat algorithm given by [12] to create a new model for classification of seismic data; Fig. 1 shows the architecture of the global system.

As shown in the diagram, our proposed approach is constructed for 6 steps in which 5 of them represents one iteration. Before beginning the treatment, we have to initialize two parameters, initial loudness  $A_0$  that decrease in each iteration, and learning parameter that is used to adjust the frequency of emitted pulses. In our approach, we considered that one bat is represented by one vector from test set, which



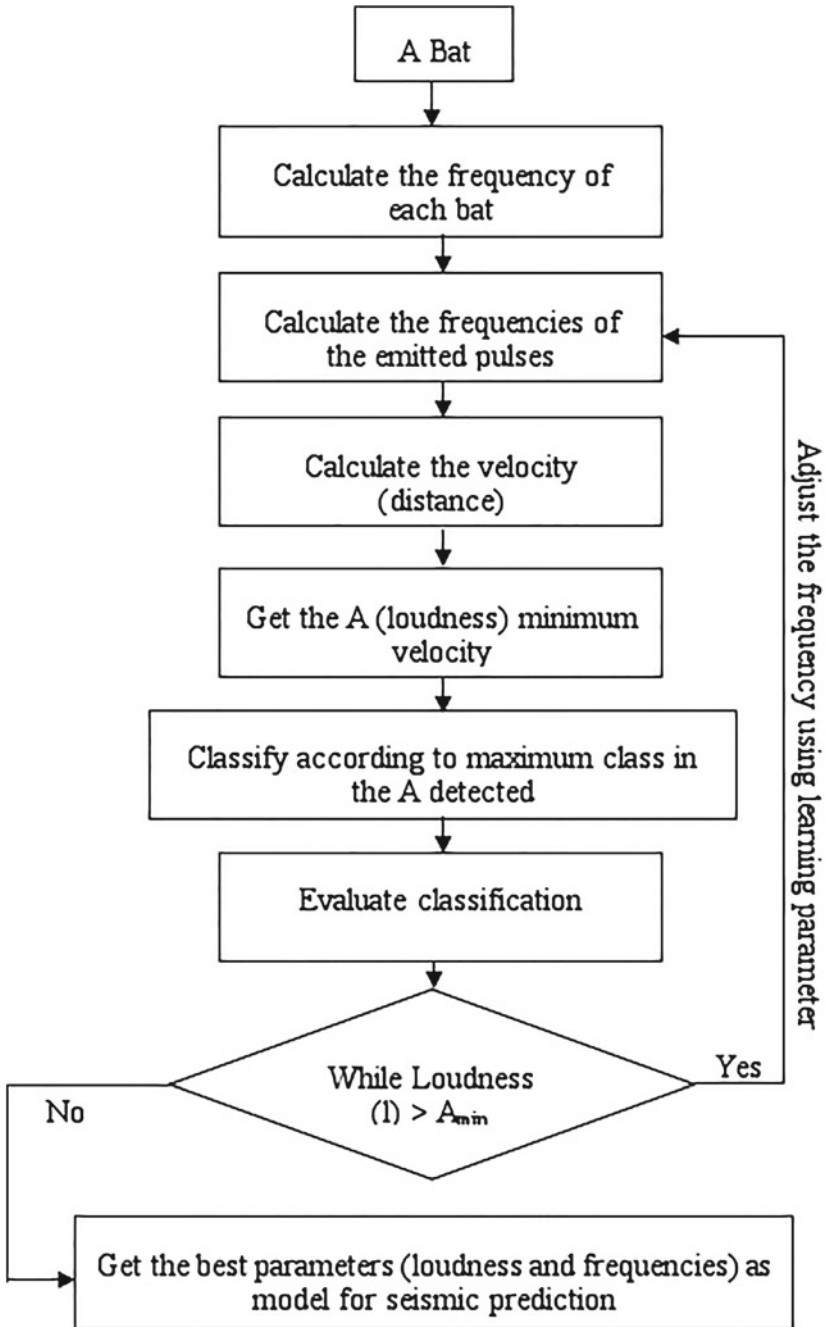


Fig. 1 Architecture of the global system

will look for neighbours to enjoy their class, in other words, this is a distance based approach similar to K-Nearest Neighbours algorithm with additional parameters.

To classify a bat, we first calculated the mean of each vector elements in training set as frequency of a bat ( $f_{bat}$ ) to catch that prey (vector of the training set). After that, the bat calculates the frequency of emitted pulses ( $f_{ep}$ ), which initially presents the average of the bat elements. Using the two frequencies, we calculated the frequency  $f$  based on Doppler Effect of sounds,  $f$  is calculated as follow:

$$f = |f_{bat} - f_{ep}| \quad (1)$$

After getting the frequency, we calculated a velocity as distance between the bat and the prey, in the implementation we tested the Euclidean distance as follow:

$$D(X, Y) = \sum \sqrt{(x_i - y_i)^2} \quad (2)$$

The final step before prediction of seismic hazards, we calculated a similarity between bats and preys using the velocity and the frequency. The similarity is simply the wavelength  $\lambda$  that each bat in real life uses it during hunting to echolocate preys, from that we conclude the formula of classification as follow:

$$\lambda = \frac{v}{f} \quad (3)$$

Prediction of seismic hazards presents the step of classification, in which, from all wavelengths resulted, we selected only  $A_0$  wavelengths, where  $A_0$  is an integer defined in the beginning, in other words, we selected the  $A_0$  most similar vectors from training set to classify the test vector and to use them in the next iteration.  $A_0$  presents the initial loudness. Finally, we took the maximum class appears in all selected vectors, and we associated the bat (test vector) to that class. The whole process mentioned presents one iteration. The stop criterion we tested is the loudness. According to [12], the loudness varies from a large (positive)  $A_0$  to a minimum constant value  $A_{min}$ , so we chose the loudness to stop the algorithm. By passing from iteration to another, the algorithm chooses the incorrectly classified vectors from test set and adjusts their frequencies by multiply it by the learning parameter, and decreases the loudness. The training set of an iteration  $i+1$  will be the chosen vectors from the iteration  $i$ . We chose the initial loudness based on simple heuristic, because we deal here with a Bi-class problem, we gave the initial loudness an impair number, and it decreases by two in each iteration, that is to assure that we have always a majority neighbours that present a class than the those who present the other class.

In the end of each iteration, we evaluated the classification of seismic hazards and we saved the parameters. And in the end of the algorithm, we took the best parameters as a model for seismic prediction, the model is defined by: vectors of the training set, their frequencies and loudness.

## 4.1 Evaluation of Classification

To calculate different metrics used for evaluation of classification, we have to introduce other measures:

1. True Positive (TP): present the average of the vectors that are correctly predicted relevant obtained in each iteration
2. True Negative (TN): present the average of the vectors that are correctly predicted as not relevant obtained in each iteration
3. False Positive (FP): present the average of the vectors that are predicted relevant but they are not relevant obtained in each iteration
4. False Negative (FN): present the average of the vectors that are correctly predicted not relevant but they are relevant obtained in each iteration

Using these four measures, we calculated the most famous measures that are used to evaluate classification algorithms:

1. For classification, the accuracy estimates is the overall number of correct classifications from the 10 iterations, divided by the total number of tuples in the initial data [13].

$$Accuracy = \frac{TP + TN}{TP + FP + TN + FN} \quad (4)$$

2. Precision and recall are the measures used in the information retrieval domain to measure how well an information retrieval system retrieves the relevant elements requested by a user. The measures are defined as follows [14]:

$$Precision = \frac{TP}{TP + FP} \quad (5)$$

$$Recall = \frac{TP}{TP + FN} \quad (6)$$

3. Instead of two measures, they are often combined to provide a single measure of retrieval performance called the F-measure as follows [14]:

$$Fmeasure = \frac{2 * Recall * Precision}{Recall + Precision} \quad (7)$$

4. ROC Curve: ROC Curve (receiver operating characteristic) is a graph in which for a binary classifier, each points is characterized by the FPRate in the x axis and TPRate in the y axis The ROC curve is independent of the P:N ratio and is therefore suitable for comparing classifiers when this ratio may vary [15].

The FPRate and TPRate are calculated as follow:

$$FPRate = \frac{FP}{TN + FP} \quad (8)$$

$$TPRate = \frac{TP}{TP + FN} \quad (9)$$

for precision, recall, fmeasure, FPRate and TPRate are weighted measures calculated two times, first to evaluate the prediction of hazardous states (*hazardous\_measure*) and second to evaluate the prediction of non-hazardous states (*non\_hazardous\_measure*). Then we calculated the finale measures (*final\_measure*) using weights as follow:

$$Final\_measure = \frac{(93.4 * non\_hazardous\_measure) + (6.6 * hazardous\_measure)}{100} \quad (10)$$

The choice of the weights was according to percentage of examples that present a class (93.4 % for *non\_hazardous* states and 6.6 % for *hazardous* states), we chose this method for evaluation because we deal with an unbalanced data which presents a big issue in the domain of classification and prediction, so we tried to evaluate the prediction of the two states, then combine the measures.

## 5 Results and Discussion

After describing the proposed approach, we discuss in this section the results obtained by the approach, before that, we describe the used data set in our experiments.

### 5.1 Used Dataset (*Seismic Bumps Dataset*)

In the data set each row contains a summary statement about seismic activity in the rock mass within one shift (8 h). If decision attribute has the value 1, then in the next shift any seismic bump with energy higher than  $10^4$  J was registered. That task of hazards prediction bases on the relationship between the energy of recorded tremors and seismoacoustic activity with the possibility of rock burst occurrence. Hence, such hazard prognosis is not connected with accurate rock burst prediction. Moreover, with the information about the possibility of hazardous situation occurrence, an appropriate supervision service can reduce a risk of rock burst (e.g. by distressing shooting) or withdraw workers from the threatened area. Good prediction of increased seismic activity is therefore a matter of great practical importance. The presented data set is characterized by unbalanced distribution of positive and negative examples. In the data set there are only 170 positive examples representing class 1.

Attribute of the data set are:

1. seismic: result of shift seismic hazard assessment in the mine working obtained by the seismic method (a—lack of hazard, b—low hazard, c—high hazard, d—danger state);
2. seismoacoustic: result of shift seismic hazard assessment in the mine working obtained by the seismoacoustic method;
3. shift: information about type of a shift (W—coal-getting, N—preparation shift);
4. genenergy: seismic energy recorded within previous shift by the most active geophone (GMax) out of geophones monitoring the long wall;
5. gpuls: a number of pulses recorded within previous shift by GMax;
6. gdenergy: a deviation of energy recorded within previous shift by GMax from average energy recorded during eight previous shifts;
7. gdpuls: a deviation of a number of pulses recorded within previous shift by GMax from average number of pulses recorded during eight previous shifts;
8. ghazard: result of shift seismic hazard assessment in the mine working obtained by the seismoacoustic method based on registration coming from GMax only;
9. nbumps: the number of seismic bumps recorded within previous shift;
10. nbumps2: the number of seismic bumps (in energy range  $[10^2, 10^3]$ ) registered within previous shift;
11. nbumps3: the number of seismic bumps (in energy range  $[10^3, 10^4]$ ) registered within previous shift;
12. nbumps4: the number of seismic bumps (in energy range  $[10^4, 10^5]$ ) registered within previous shift;
13. nbumps5: the number of seismic bumps (in energy range  $[10^5, 10^6]$ ) registered within the last shift;
14. nbumps6: the number of seismic bumps (in energy range  $[10^6, 10^7]$ ) registered within previous shift;
15. nbumps7: the number of seismic bumps (in energy range  $[10^7, 10^8]$ ) registered within previous shift;
16. nbumps89: the number of seismic bumps (in energy range  $[10^8, 10^{10}]$ ) registered within previous shift;
17. energy: total energy of seismic bumps registered within previous shift;
18. maxenergy: the maximum energy of the seismic bumps registered within previous shift;
19. class: the decision attribute—“1” means that high energy seismic bump occurred in the next shift (“hazardous state”), “0” means that no high energy seismic bumps occurred in the next shift (“non-hazardous state”).

## 5.2 The Obtained Results

Taking in mind that seismic dataset is an unbalanced data; we chose a balanced data as training set, in which we took 100 examples that present “hazardous state”, and

100 examples present “non-hazardous state”, and for evaluation we took the rest of data (70 examples presents hazardous state and 2313 presents non-hazardous state).

The obtained results are presented in Table 1 where the first column presents the initial value of loudness the second one presents the accuracy, the third shows the error, the fourth and fifth show the obtained precision and recall respectively, the sixth shows the values of fmeasure, and the last column presents the best loudness in which we got these results for each case.

The results presented in Table 1 are the best results got beginning from initial loudness  $A_0$  down to minimum loudness  $A_{min}$  that equals to 1. As we see in the table, the obtained results are very good results. The interpretation of results is done as follow:

- In terms of Accuracy and Error: Accuracy measures how well the system can predict correctly the state of seismic hazards, in Table 1; we see that the prediction rate is high (from 89.87 to 93.41 %) which proves that our system is very efficient.
- In terms of Precision: the precision gives a value of correctly prediction of the relevant states of seismic hazards among all predicted states. More it converges to 1, more is the system considered as efficient system. In our case, we see that the value of precision converges to 1 (0.87), here we can say that our system proves its efficiency, even if it is not very efficient.
- In terms of Recall: the recall gives a value of correctly prediction of the relevant states of seismic hazards among all states in the initial dataset. Like precision, more it converges to 1, more is the system considered as efficient system. The Bat algorithm shows a high recall (more than 0.9); this means that the proposed approach can predict more than 90 % of relevant states for seismic hazards.
- In terms of Fmeasure: the fmeasure is a metric used to combine the precision and the recall in one metric as an average of the two. More it converge to one, more the system is efficient. The Bat algorithm shows a high fmeasure (about 0.9). In general, our proposed bat echolocation based algorithm proves a high efficiency for prediction of seismic hazards.

**Table 1** The obtained results using our approach according to the initial value of loudness

Loudness	Accuracy (%)	Error (%)	Precision	Recall	Fmeasure	Best loudness
1	89.87	10.13	0.878	0.9	0.887	1
3	93.21	6.79	0.873	0.933	0.902	3
5	93.33	6.67	0.873	0.933	0.902	3
7	93.41	6.59	0.875	0.936	0.905	7
9	93.41	6.59	0.875	0.936	0.905	7
11	93.41	6.59	0.875	0.936	0.905	9

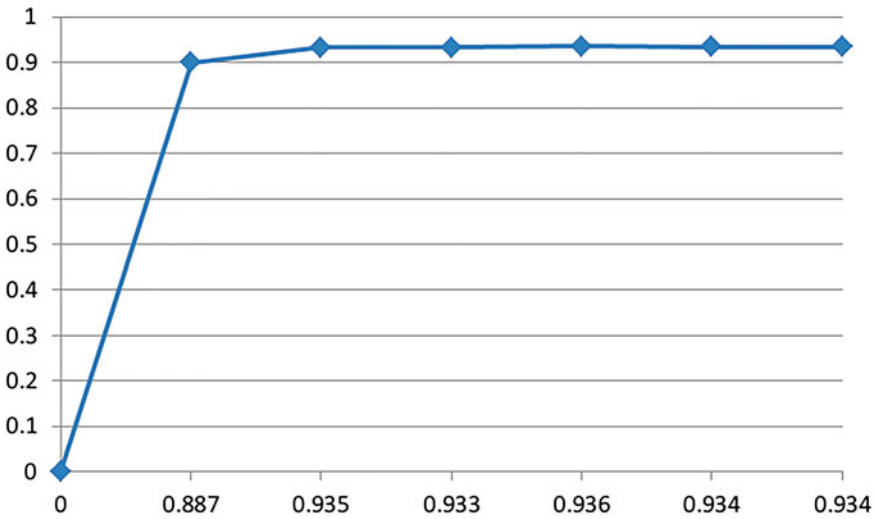


Fig. 2 The ROC curve that shows the influence of initial loudness on the results

- In terms of Initial Loudness: because the initial weights (frequency of a bat is the average of values of its attributes) are the same in all cases whatever is the initial loudness. The changes are summarized in the adjustment of these weights (frequencies). For that, we tested many values of initial loudness to study its influence in the final results. The Table 1 shows that beginning with initial loudness equals to 1 gives the worst results, and then the results increase when we increased the initial loudness until it fixed at the value of 7. To see that clearly, we presented the influence of the initial loudness by the ROC curve.

The roc (Fig. 2) curve shows the effect of the initial loudness on the final results of prediction of seismic hazards. In the curve, the x-axis presents the FPRate, the y-axis presents the TPRate, and each point presents the initial loudness (1, 3, 5, 7, 9 and 11). It is clear here that from loudness equals to 1–7, more it is higher, more we get better results, and that is because of the adjustment of weights, for initial loudness equals to 1, there is only one iteration, so the bat echolocation approach did not adjust the weights, and for loudness from 3 to 7, it was adjusted loudness 1 times, then the approach defined the suitable loudness according to the best results. And then results became stable for loudness higher than 7.

## 6 Conclusion

The paper has presented a novel approach inspired from the echolocation behaviour of bats for prediction of seismic hazards in coal mines. It presents the intersection of

two research domains bio inspired algorithms and machine learning algorithms. The proposed approach is a simple bio inspired algorithm that uses distance calculation based on representative examples from previous experiences in seismic hazards to predict new states.

Our algorithm shows many advantages: easy to understand and easy to implement, although there are parameters defined in the beginning, the algorithm generates the best parameter from experiences which allows using it as model to predict the new states. The main advantage of this approach is its efficiency; it gives very good results in terms of accuracy, precision, and recall.

For future work, we plan to use this approach for other ecological problems like plant leaves classification, land cover clustering, and why not, use it on different areas such as information retrieval. We also plan to combine this approach with other approaches to optimize the results. But the main future work is developing news approaches that deal with unbalanced data of the seismic hazards, because this kind of dataset presents a big issue in the domain of data mining in general.

## References

1. Kabiesz, J.: Effect of the form of data on the quality of mine tremors hazard forecasting using neural networks. *Geotech. Geol. Eng.* **24**(5), 1131–1147 (2006)
2. Yang, X.S., He, X.: Bat algorithm: literature review and applications. *Int. J. Bio-Inspired Comput.* **5**(3), 141–149 (2013)
3. Gale, W.J., Heasley, K.A., Iannacchione, A.T., Swanson, P.L., Hatherly, P., King, A.: Rock damage characterisation from microseismic monitoring. In: *DC Rocks 2001, The 38th US Symposium on Rock Mechanics (USRMS)*. American Rock Mechanics Association (2001)
4. Gibowicz, S.J., Lasocki, S.: Seismicity induced by mining: ten years later. *Adv. Geophys.* **44**, 39–181 (2001)
5. Kornowski, J.: Linear prediction of aggregated seismic and seismoacoustic energy emitted from a mining longwall. *ACTA MONTANA* **129**, 5–14 (2003)
6. Lasocki, S.: Probabilistic analysis of seismic hazard posed by mining induced events. In: *Proceedings of 6th International Symposium on Rockburst in Mines Controlling Seismic Risk*. ACG, Perth, pp. 151–156 (2005)
7. Rudajev, V., Ciz, R.: Estimation of mining tremor occurrence by using neural networks. *Pure Appl. Geophys.* **154**(1), 57–72 (1999)
8. Makwka, J., Kabiesz, J.: Prediction of sites and energy of seismic tremors methods and results. In: *Proceedings of the Conference Mining Natural Hazards*. Ustron (2005)
9. Leniak, A., Isakow, Z.: Spacetime clustering of seismic events and hazard assessment in the Zabrze-Bielszowice coal mine, Poland. *Int. J. Rock Mech. Min. Sci.* **46**(5), 918–928 (2009)
10. Bodri, B.: A neural-network model for earthquake occurrence. *J. Geodyn.* **32**(3), 289–310 (2001)
11. Sikora, M.: Induction and pruning of classification rules for prediction of microseismic hazards in coal mines. *Expert Syst. Appl.* **38**(6), 6748–6758 (2011)
12. Yang, X.S.: A new metaheuristic bat-inspired algorithm. In: *Nature Inspired Cooperative Strategies for Optimization (NICSO 2010)*, pp. 65–74. Springer, Berlin (2010)



13. Han, J., Kamber, M., Pei, J.: Data Mining: Concepts and Techniques (2011)
14. Sammut, C., Webb, G.I. (eds.): Encyclopedia of Machine Learning. Springer (2011)
15. Vuk, M., Curk, T.: ROC curve, lift chart and calibration plot. Metodoloski zvezki **3**(1), 89–108 (2006)

# Enhanced Chemical Reaction Optimization for Multi-objective Traveling Salesman Problem

Samira Bouzoubia, Abdesslem Layeb and Salim Chikhi

**Abstract** The multi-objective traveling salesman problem (MOTSP) is an essential and challenging topic in the domains of engineering and optimization problems. In this paper we propose new variant of multi-objective chemical reaction optimization (MOCRO) called Enhanced MOCRO (EMOCRO) for solving MOTSP. The key idea of the proposed variant is the use of the dominance strategy and chemical reaction concepts. Compared to MOCRO, EMOCRO has a reduced number of parameters and a simplified general scheme. In order to give the quality of the algorithm, several MOTSP instances taken from the TSP library are used. The proposed approach is statistically compared with MOCRO and NSGA2. Results indicate that the EMOCRO outperformed other approaches in most of the test instances.

**Keywords** Chemical reaction optimization · Multi-objective optimization · Bio-inspired algorithm · Multi-objective traveling salesman problem

## 1 Introduction

The multi-objective traveling salesman problem (MOTSP) is widely studied combinatorial optimization problem that belongs to the class of NP-hard problems. The MOTSP has many applications in different engineering and optimization problems. Formally, a MOTSP is formulated as follows.

---

S. Bouzoubia (✉) · A. Layeb · S. Chikhi  
MISC Laboratory, Department of Fundamental Computer Science  
and Its Applications, Constantine 2 Abdelhamid Mehri University,  
25017 Constantine, Algeria  
e-mail: samira.bouzoubia@univ-constantine2.dz

A. Layeb  
e-mail: layeb.univ@gmail.com

S. Chikhi  
e-mail: chikhi@misc-umc.org

Given  $N$  cities and  $p$  costs  $C_{(i,j)}^k (k = 1, \dots, p)$  to travel from city  $i$  to city  $j$ , the MOTSP consists in finding a Hamiltonian cycle of the  $N$  cities that optimizes the following minimization problem [1]:

$$Z_k(p) = \sum_{i=1}^{N-1} (c_{(p(i),p(i+1))}^k + c_{(p(N),p(1))}^k), k = 1, \dots, p. \quad (1)$$

Since the objectives in Eq. 1 usually conflict with each other. Consequently, there is not a single tour that can minimize all the objectives simultaneously. The optimality of a multi-objective optimization problem (MOP) as MOTSP is a set of tradeoff solutions, called Pareto optimal set (PS) in the decision space or Pareto front (PF) in the objective space [2].

Considering the difficulty of the MOTSP, several methods were proposed to solve this problem in the literature. The most popular ones among them include the bio-inspired meta-heuristics as well as non-dominated sorting based genetic algorithm 2 (NSGA2) [3] and Strength Pareto Evolutionary Algorithm 2 [4]. These methods were developed first in the mono-objective and then generalized to tackle the MOP. Examples of the bio-inspired meta-heuristics include, but are not limited to, genetic algorithm [5], simulated annealing [6], and recently chemical reaction optimization (CRO). It imitates the interactions of molecules in chemical reactions to reach the global optimum, is proposed by Lam and Li [7]. This algorithm has many advantages such as its variable population size that allows to the system the ability to adapt to the problems automatically. Moreover, CRO combines the main advantages of Genetic Algorithm and Simulated Annealing. However, the main limitation of CRO is the high number of parameters that influence the effectiveness of the algorithm. However, the real-life problems require the consideration of several criteria simultaneously. That is why, it is necessary to generalize CRO to the multi-objective.

In this work, a multi-objective CRO variant is proposed, called Enhanced Multi-objective Chemical Reaction optimization (EMOCRO). It simplifies the structure of CRO and uses some NSGA2 concepts [3].

Consequently, the rest of this paper is organized as follows. Section 2 describes some MOTSP related works. Section 3 presents the basic scheme of CRO, and some interesting works using this algorithm. Section 4 presents the framework of proposed algorithm. Section 5 contains the adaptation of EMOCRO for MOTSP. Section 6 describes the benchmark problems, the parameter settings, and the metrics used to measure the performance of the proposed algorithm. Moreover, it gives the simulation results, a comparative study. Finally, our conclusions are provided in Sect. 7.

## 2 Related Works

A large number of methods were proposed to solve the MOTSP that can be classified in two categories, exact and approximation techniques. Exact approaches like multi-objective dynamic programming branch and bound [8]. These methods have

been shown to be very successful in achieving the optimal PF. Unfortunately, they require considerable computational efforts. This limitation is the reason why the approximation techniques were developed to tackle the MOPs. Multi-objective meta-heuristics represents interesting subclass of these techniques. Two major classes of meta-heuristics are widely used in the literature: multi-objective local search algorithm and multi-objective population based algorithms.

## ***2.1 Multi-objective Local Search Algorithms***

Several algorithms were applied to deal with MOTSP. Paquete and Stutze [9] have analyzed algorithmic components of stochastic local search algorithms for the multi-objective travelling salesman problem. On the other hand, Hansen [10] applied Tabu Search algorithm based scalarizing functions for a Multi-Objective TSP. Two-phase Pareto local search is developed by Lust and Teghem to solve the bi-objective traveling salesman problem (2PPL) [1]. 2PPL has two steps, the first one generates an initial population composed of a good approximation of the extreme supported efficient solutions. Then in the second step, 2PPL applied a Pareto Local Search method to each solution in the initial population.

Despite the simplicity of these algorithms and their ease of implementation, these methods have a high computational time and give a poor quality PF [11].

## ***2.2 Population Based Multi-objective Algorithms***

A number of works for MOTSP have been proposed. Gao et al. [12] introduced a multi-objective estimation of distribution algorithm based on decomposition which combines the multi-objective evolutionary algorithm based on decomposition [13] with probabilistic model based methods for MOTSP. Later, Ke et al. [14] have proposed a multi-objective evolutionary Algorithm using ant colony and decomposition to solve MOTSP. Experimental study proved that this approach surpasses bi-criterion ant algorithm [15] in all the given instances of MOTSP. Recently, Membrane algorithm is used to solve multi-objective multiple traveling salesman problem in [16]. Moreover, multi-objective chemical reaction optimization (MOCRO) is presented in [11]. MOCRO employs the chemical reaction concepts and the NSGA2 strategies to solve the MOTSP. Two variants in MOCRO are proposed, MOCRO-Dom and MOCRO-WS. The first one used the amount of domination and the second one applied the weighted sum to tackle MOTSP.

Compared to multi-objective local search algorithms, the multi-objective meta-heuristics take a reasonable computation time. Moreover, these methods give a good quality of PF.

### 3 Chemical Reaction Optimization

Chemical reaction optimization (CRO) is a new developed mono-objective meta-heuristic. It mimics the transition from a higher energy state to lower by collisions among the molecule, and the reaction process follows the law of conservation of energy [17]. Each molecule has several attributes that are, Molecular structure  $\omega$ , Potential energy  $PE$ , Kinetic energy  $KE$ , number of hits and some other optional attributes. More precisely,  $\omega$  represents the solution of the problem, the Potential energy is the objective function value.  $KE$  corresponds to the tolerance of a molecule to accept a worse solution than the existing one. This attribute allows to CRO the ability to escape from local optima.

The basic chemical reaction algorithm has four reaction operators, including on-wall ineffective collision, decomposition, inter-molecular ineffective collision and synthesis.

#### 3.1 *On-wall Ineffective Collision*

On-wall ineffective collision is uni-molecular collision. It occurs when a molecule collides with a wall of the container and then bounces away remaining in one single unit. In this collision, CRO only perturbs the existing  $\omega$  to produce  $\omega'$  [7].

#### 3.2 *Decomposition*

Decomposition is uni-molecular operator and allows the system to explore other regions of the search space through the generation of solutions. It represents the situation when a molecule hits a wall and then breaks into several parts [7].

#### 3.3 *Inter-molecular Ineffective Collision*

This inter-molecular operator occurs when two or more molecules collide with each other and then separate. The number of molecules involved in this collision remains unchanged after the collision [7].

#### 3.4 *Synthesis*

Synthesis is the opposite of the decomposition, it refers to the situation when multiple molecules collide with each other and form one new single molecule. This process implies that the search regions are expanded. This inter-molecular operator gives diversification of solutions [7].

Several variants of CRO were proposed to solve a variety of optimization problem. Sun et al. combined Lin-Kernighan local search and CRO to deal with the mono-objective traveling salesman problem [18]. CRO has also been applied for the 0–1 knapsack problem in [19]. Moreover, CRO has been adapted for the multi-objective optimization. Li and Pan have proposed a discrete CRO for solving the flexible job-shop scheduling problems [20]. Recently, a new multi-objective extension of CRO named Multi-objective chemical reaction optimization (MOCRO) was developed to solve the multi-objective traveling salesman in [11]. MOCRO is based on NSGA2 techniques and the elementary reactions of CRO. It combines dominance and crowding distance with the concepts of CRO like conservation energy strategy and collision operators. The general scheme of MOCRO is in Fig. 1.

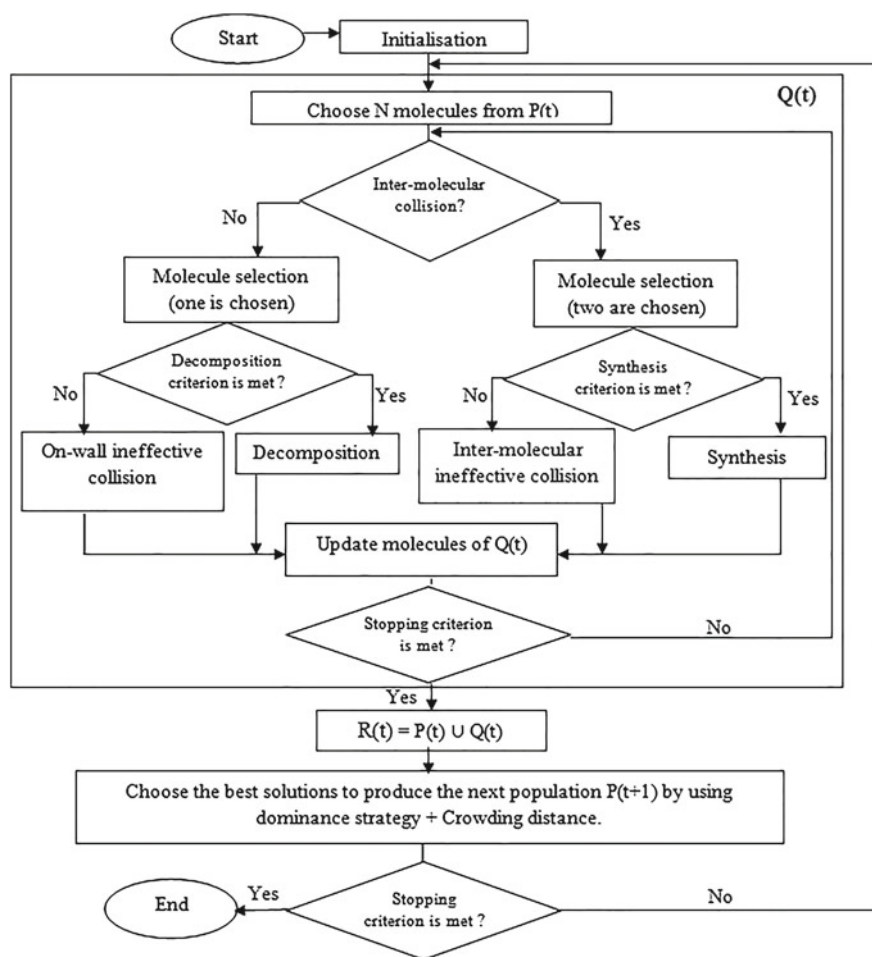


Fig. 1 General scheme of MOCRO

Despite the effectiveness of MOCRO, it has a high number of parameters which reduces its adaptation to the problems. In this paper we propose an enhanced variant of MOCRO to solve MOTSP. EMOCRO has the purpose to reduce the number of parameters and simplify the general scheme of MOCRO.

## 4 Enhanced Multi-objective Chemical Reaction Optimization

Here we introduce the enhanced multi-objective chemical reaction optimization meta-heuristic algorithm EMOCRO, and we describe how it is implemented. As EMOCRO is based on MOCRO, it employs dominance features and characteristics of chemical reaction as well as the chemical operators, the tolerance to accept the worse solutions and energy conservation conditions. In order to tackle several criteria, EMOCRO energy conservation conditions are based on the weighted sum method. In the following part, we present in more detail the scheme of EMOCRO.

### 4.1 EMOCRO Scheme

The step-wise procedure for the implementation of EMOCRO can be summarized as follows.

*Algorithm: EMOCRO*

```

MOP; Stopping criterion; (Input)
Pareto set; (Output)

begin
  Step 1 Initialize the population P(t) of N molecules
    and initialize algorithmic parameters;
  Step 2 If the stopping criterion is satisfied
    then output the Pareto front set;
    else perform Step 3;
  Step 3 Create offspring population Q(t) of size N
  Step 3.1 Select sub-population Q(t) from P(t);
  Step 3.2 Chemical collisions
    For t=1, ..., N
      If (Synthesis condition is met) then
        Perform Synthesis and update M1 and M2
        according to the conservation energy
        condition of synthesis;
      Else
        Perform On-wall ineffective collision,
        update M according to conservation energy
        condition of on-wall ineffective collision;

```

```
End
End
Step 4 Form the combined population  $R(t)$  of size  $2N$  where
       $R(t)=Q(t)+ R(t)$ ;
Step 5 Sort  $R(t)$  according domination strategy;
Step 6 Choose the best solutions to produce the next
      population  $P(t+1)$  by using domination and KE
      of each molecule; Go back to Step 2;
end.
```

In the initialization step, a population  $P(t)$  of  $N$  molecules is randomly created. Each molecule has mainly five attributes: the kinetic energy  $KE$  initialized by the initial kinetic energy (*InitialKE*), the vector of potential energy  $PE$  that corresponding to the  $m$  objective functions values, the molecular structure  $\omega$  that contains a solution to the problem. Moreover, we initialize the algorithmic parameters including: *Popsiz*e, number of neighbors  $T$  and synthesis threshold  $\beta$ .

In the second stage of the algorithm, we construct an offspring population  $Q(t)$  as follows. First, we select  $N$  molecules by using binary tournament selection. Second, we apply chemical reaction to  $Q(t)$ . The molecules can either hit on a wall of the container or collide with each other according to the synthesis condition. If the synthesis criterion is met ( $KE \leq \beta$ ) then the system has two molecules. Therefore, we have an inter-molecular collision, i.e., synthesis. Otherwise, a uni-molecular collision (On-wall ineffective collision) is applied. After each elementary reaction, we check if the energy conservation condition is satisfied and  $Q(t)$  is updated.

In the next step, we combine the two populations  $P(t)$  and  $Q(t)$  in new one  $R(t)$ . The combined population is sorted according dominance technique. In order to form the next population  $P(t+1)$ , we select the  $N$  Non dominated molecules from  $R(t)$ . However, we often have some molecules with the same domination rank. In this case, the kinetic energies of these molecules are used to decide between two non-dominant molecules. When a molecule has too little  $KE$ , it loses potentially its ability to escape from a local minimum [7]. Hence, we prefer those having more ability to escape from a local minimum, i.e., the molecules with the largest  $KE$  values. The process is looped until the stopping criterion is met. At the end of process the algorithm gives the first non-dominated front found in the last generated population. The EMOCRO's scheme is shown in Fig. 2. It has the same general scheme of NSGA2 except the crowding distance step which is replaced by comparison of KE values of the molecules. Thus, the major computational costs are in Step 5. In this step, we have used the same dominance strategy of NSGA2 which takes  $O(MN^2)$  computations, where  $M$  represents the number of objectives and  $N$  the population size [3]. Consequently, the overall computational complexity of EMOCRO is  $O(MN^2)$ , which is governed by the non-dominated sorting part of the algorithm.



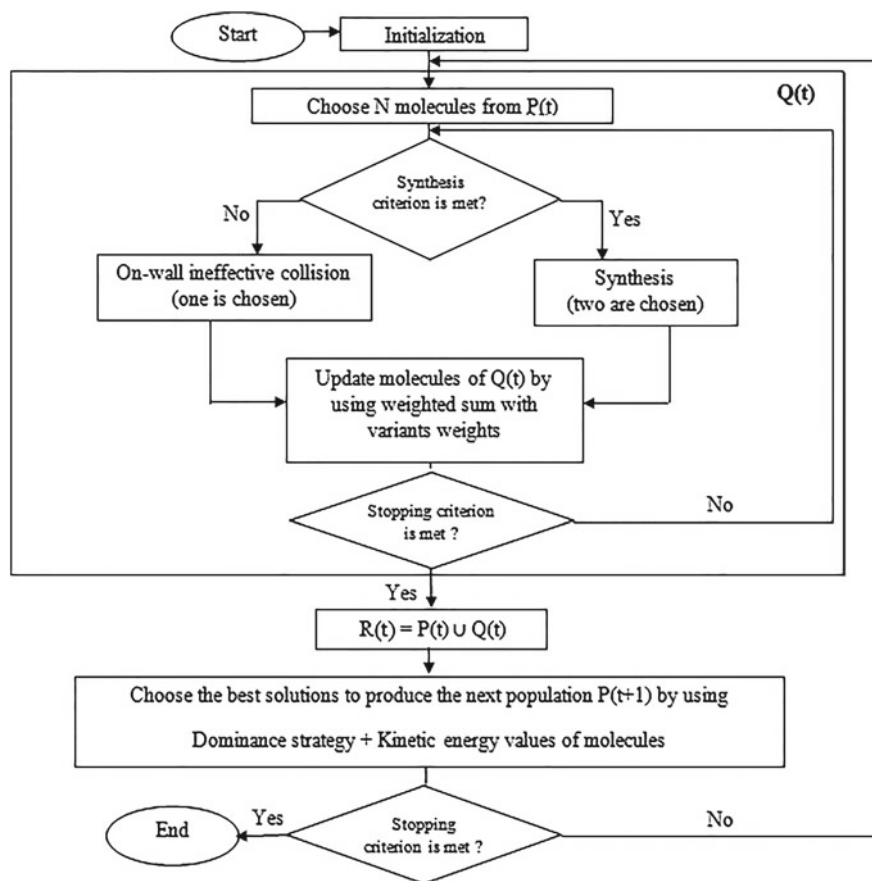


Fig. 2 General scheme of EMOCRO

## 4.2 Diversification/Intensification Preservation

EMOCRO keeps good balance between exploration and exploitation for producing a set of representative solutions. For that, it employs the On-wall ineffective collision operator to tackle the local search. However, it ensures the diversification by applying the synthesis. Moreover, the conservation energy conditions have a tolerance to accept worse solutions than the existing ones that give the system the ability to escape from the local minima. In order to produce the next population  $P(t + 1)$ , EMOCRO uses dominance strategy. When we have to choose between non dominated molecules, EMOCRO prefers molecules with largest  $KE$  values to maintain diversity of population members.

### 4.3 Conservation Energy Conditions

Likewise in MOCRO [11], the energy conservation conditions ensure the selection of the new solutions. In other words, elementary reaction can only take place when the energy conservation condition is satisfied. In the basic mono-objective CRO, the following energy conservation condition is used [7].

$$\sum_{i=1}^k (PE_{\omega_i} + KE_{\omega_i}) \geq \sum_{i=1}^l PE_{\omega'_i} \quad (2)$$

where  $l$  and  $k$  represent the number of molecules involved before and after a particular elementary reaction, and  $\omega$ ,  $\omega'$  are the molecular structures of an existing molecule and the one to be generated from the elementary reaction, respectively. Unfortunately, we cannot apply this formula directly to deal with multiple criteria. Similarly to MOCRO, the energy conservation conditions of EMOCRO are implemented according the aggregation technique. Consequently, the general formula of these conditions in the multi-objective is as follows.

$$\sum_{i=1}^M \sum_{j=1}^k (w_i PE_i(\omega_j) + KE_{\omega_j}) \geq \sum_{i=1}^M \sum_{j=1}^l w_i PE_i(\omega'_j) \quad (3)$$

where  $M$  is the number of objectives. Similarly,  $l$ ,  $k$ ,  $\omega$  and  $\omega'$  represent the same attributes as in condition (2).  $w_i$  represents the weight of the  $i$ th objective function with  $\sum_{i=1}^M w_i = 1$  and  $w_i \neq 0$ . Each molecule has its own weight vector. In the case of bi-objective optimization problem, we generate  $w_i$  by using the following formulas (Eq. 4).

$$(w_1, w_2) = \left( \frac{j}{popsize}, \frac{popsize - j}{popsize} \right) \quad (4)$$

where  $j \in 1, \dots, popsize$  and  $popsize$  is the number of molecules. It is important to notice that EMOCRO uses the weighted sum strategy only in the step of conservation energy conditions which decide if elementary reactions can take place. The rest of process of EMOCRO uses the non-dominance strategy to deal with multiple criteria.

### 4.4 Comparison of the EMOCRO Algorithm and MOCRO

EMOCRO is multi-objective population-based meta-heuristic as well as the MOCRO. The general scheme of the two algorithms is similar. In the case of EMOCRO, we have reduced the number of operators to two, i.e. on-wall ineffective collision and synthesis, instead of four in MOCRO which are on-wall

**Table 1** Comparison of EMOCRO and MOCRO

Characteristics	EMOCRO	MOCRO
Operators	Two operators	Four operators
Conservation energy conditions	Weighted sum with variants weights	Weighted sum with fixed weights
Selection of best solutions	Dominance strategy + KE values	Dominance strategy + crowding distance
Parameters of algorithm	$Popsiz$ , $initialKE$ , $T$ , $\beta$ , $KElossRate$	$Popsiz$ , $molecoll$ , $buffer$ , $\alpha$ , $\beta$ , $KElossRate$ , $initialKE$ , $w_i$ , $T$

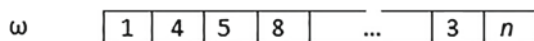
$Popsiz$  = Population size;  $initialKE$  = Initial kinetic energy value;  $T$  = Number of neighborhood;  $\beta$  = Synthesis threshold;  $buffer$  = Initial energy buffer;  $w_i$  = Weight vector;  $\alpha$  = Decomposition threshold;  $molecoll$  = Molecular Collision Rate

ineffective collision, decomposition, intermolecular ineffective collision and synthesis. The weighted sum technique is used in the both algorithms, but in EMOCRO we use variable values of the weight vectors while in MOCRO these values are fixed. Moreover, MOCRO uses crowding distance and dominance to select the next population but EMOCRO uses for that the kinetic energy of each molecule and the dominance technique. Table 1 summarizes the major differences between EMOCRO and MOCRO.

## 5 EMOCRO for MOTSP

To evaluate the performances of the proposed variant, the bi-objective traveling salesman problem is used. This one is known as a hard combinatorial optimization problem, it has two objectives to optimize, i.e., the minimization of two tour lengths. In our study, each molecule  $M_\omega$  represents a feasible solution of MOTSP. The main attributes of  $M_\omega$  include:

- *Molecular structure*  $\omega$  defines a feasible solution of MOTSP. Considering that the number of cities is  $n$ , Fig. 3 represents a possible MOTSP solution; it is permutation of  $n$  cities.
- *Potential energy*  $PE$  represents costs vector of the tour. The length of PE is equal to the number of objectives.
- *Kinetic energy*  $KE$  is the tolerance to accept a worse solution than the existing one.
- *Number of hits* is a record of the total number of collisions that the molecule has taken.
- *Weight vector*  $w_i = (w_1, \dots, w_m)$  where  $w_j \geq 0$  and  $\sum_{j=1}^m w_j = 1$ .

**Fig. 3** Molecular structure scheme

## 5.1 EMOCRO Operators for MOTSP

In EMOCRO, we have used two operators that are the synthesis and on-wall ineffective collision. These operators are similar to those applied in MOCRO [11]. The exploration is enhanced by the synthesis and the intensification is provided by the on-wall ineffective collision operator.

**Synthesis** The synthesis is used to produce a new molecule by combining two molecules. EMOCRO uses the same synthesis operator of MOCRO [11]. To have a new  $\omega'$  from  $\omega_1$  and  $\omega_2$ , we have to generate randomly two points  $[P_1, P_2]$ .  $\omega'$  takes the part between  $[P_1, P_2]$  from  $\omega_1$  and obtain the rest from  $\omega_2$ . At the end of the operation,  $\omega'$  must form a Hamiltonian cycle.

**On-wall ineffective collision** This operator is applied to change the state of the selected molecule. We have to perturb the selected solution  $\omega$  and generate  $\omega'$ . EMOCRO uses the same on-wall ineffective collision operator of MOCRO [11]. For that, we generate randomly  $N$  neighbors of  $\omega$  by swapping the positions of two components in  $\omega$ . Then, we sort the  $N$  neighbors according to the dominance relation,  $\omega'$  is one of the non-dominated neighbors.

## 6 Computational Study and Results

In order to evaluate the performances of our proposed variant, we have compared EMOCRO with multi-objective chemical reaction optimization algorithm, MOCRO [11] and a non-dominated sorting based genetic algorithm, NSGA2 [3] in MOTSP test instances. The MOTSP benchmarks are taken from the TSPLIB [21]. In each MOTSP instance is constructed using the distance of two single TSP tests with the same number of cities. For example, *EuclidAB100* is the combination of the first objective *EuclidA100* and *EuclidB100* as the second objective.

### 6.1 Performance Metrics

In order to evaluate the performance of EMOCRO, the C-metric [22] and D-metric [23] are used in the experiments.

**Set coverage metric (C-metric)** Let  $A$  and  $B$  be two approximations to the PF of a MOP,  $C(A, B)$  is defined as the percentage of the solutions in  $B$  that are dominated by at least one solution in  $A$ , i.e.

$$C(A, B) = \frac{(|\{u \in B \mid \exists v \in A : v \text{ dominates } u\}|)}{|B|} \quad (5)$$

$C(A, B)$  is not necessarily equal to  $1 - C(A, B)$ .  $C(A, B) = 1$  means that all solutions in  $B$  are dominated by some solutions in  $A$ , and  $C(A, B) = 0$  means that no solution in  $B$  is dominated by a solution in  $A$ .

**Distance from representatives in the PF (D-metric)** Let  $P^*$  be a set of uniformly distributed points along the PF. Let  $A$  be an approximation to the PF, the average distance from  $A$  to  $P^*$  is defined as:

$$D(A, P^*) = \frac{\sum_{v \in P^*} d(v, A)}{|P^*|} \quad (6)$$

where  $d(v, A)$  is the minimum Euclidean distance between  $v$  and the points in  $A$ . If  $|P^*|$  is large enough to represent the PF very well,  $D(A, P^*)$  could measure both the diversity and convergence of  $A$ . To have a low  $D(A, P^*)$  value,  $P^*$  must be close to the PF and cannot miss any part of the whole PF. In our experiments, all  $P^*$  are taken from the TSPLIB [21].

## 6.2 Parameters Setting

In our experimental study, EMOCRO, MOCRO and NSGA2 are implemented by Matlab 7.10.0 and executed in the same environment. For all the algorithms, the population size is set to be 80, and the number of generations is 200 for all benchmarks instances. All the algorithms have been independently run for 10 times for each test instance on the same computer (2.5 GHZ, 4.00 GB RAM).

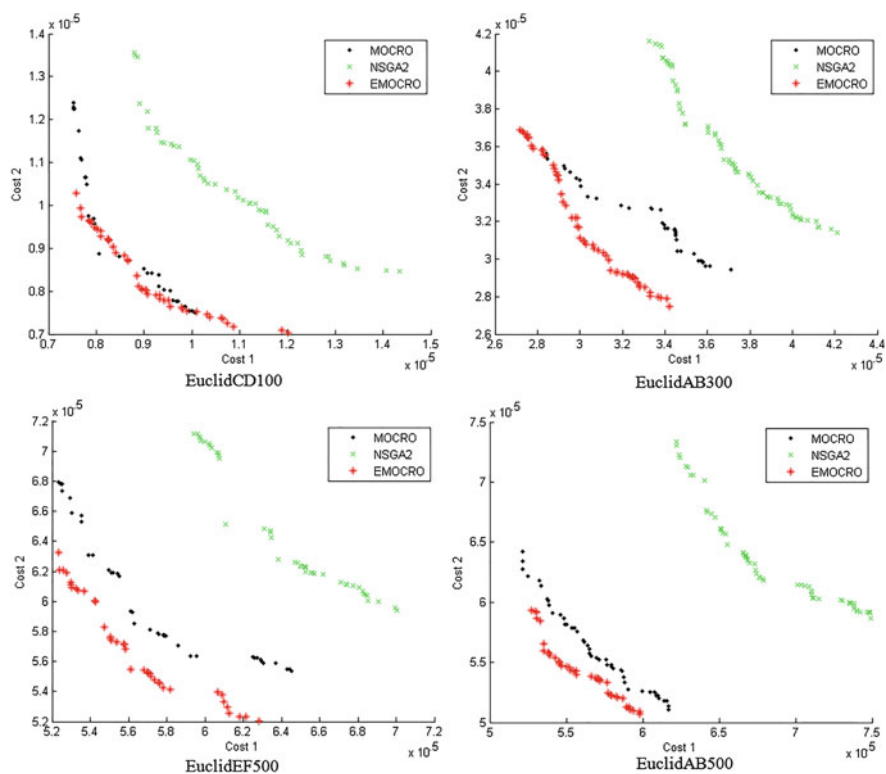
After several trial runs, the parameter values of EMOCRO and MOCRO are set as follows:  $initialKE = 1000$ ,  $KELossRate = 0.2$ , number of neighborhood  $T = 30$ , and Synthesis Threshold  $\beta = 100$ . Moreover, MOCRO has additional parameters that are, Initial energy buffer = 0, Molecular Collision Rate  $MoleColl = 0.47$ ,  $w_i$  which is set to be 0.5, and Decomposition Threshold  $\alpha = 50$ . It should be noted that, the MOCRO and EMOCRO parameter values are problem-dependent. Thus, to have a good performance of these algorithms for a particular problem, the user may perform some parameter tunings to determine a good combination of the parameter values.

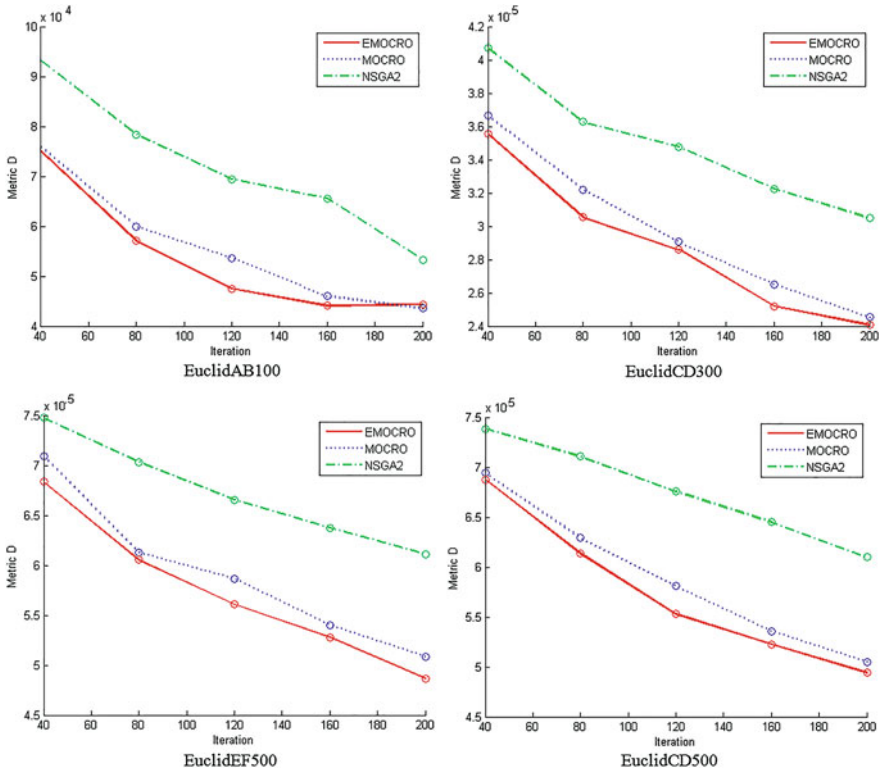
## 6.3 Experimental Studies and Comparisons

In this section, we compare the proposed variant to MOCRO and NSGA2 for nine MOTSP test instances taken from TSPLIB. Table 2 represents the means and standard deviations results of C-metric values of each algorithm for 10 independent runs. It reveals that on the average, 77.03 % and 99.03 % solutions obtained by MOCRO and NSGA2 respectively are dominated by those obtained by EMOCRO. On the contrary, only 14.13 % of final solutions generated by EMOCRO are dominated by

**Table 2** Statistical results (MEAN  $\pm$  STD) of EMOCRO (A), MOCRO (B), and NSGA2 (D) over 10 runs

Instances	C-metric			
	C(A, B)	C(B, A)	C(A, D)	C(D, A)
EuclidAB100	<b>0.542</b> $\pm$ 0.327	0.351 $\pm$ 0.298	<b>0.962</b> $\pm$ 0.072	0 $\pm$ 0
EuclidCD100	<b>0.568</b> $\pm$ 0.326	0.365 $\pm$ 0.398	<b>0.996</b> $\pm$ 0.008	0 $\pm$ 0
EuclidEF100	<b>0.497</b> $\pm$ 0.276	0.416 $\pm$ 0.337	<b>0.955</b> $\pm$ 0.052	0 $\pm$ 0
EuclidAB300	<b>0.859</b> $\pm$ 0.142	0.022 $\pm$ 0.065	<b>1</b> $\pm$ 0	0 $\pm$ 0
EuclidCD300	<b>0.837</b> $\pm$ 0.176	0.014 $\pm$ 0.039	<b>1</b> $\pm$ 0	0 $\pm$ 0
EuclidEF300	<b>0.866</b> $\pm$ 0.135	0.016 $\pm$ 0.031	<b>1</b> $\pm$ 0	0 $\pm$ 0
EuclidAB500	<b>0.956</b> $\pm$ 0.125	0 $\pm$ 0	<b>1</b> $\pm$ 0	0 $\pm$ 0
EuclidCD500	<b>0.841</b> $\pm$ 0.308	0.088 $\pm$ 0.279	<b>1</b> $\pm$ 0	0 $\pm$ 0
EuclidEF500	<b>0.967</b> $\pm$ 0.052	0.003 $\pm$ 0.012	<b>1</b> $\pm$ 0	0 $\pm$ 0

**Fig. 4** The approximations obtained by the three algorithms. The *red* stars are with EMOCRO, the *black* points are with MOCRO, and the *green* crosses are with NSGA2

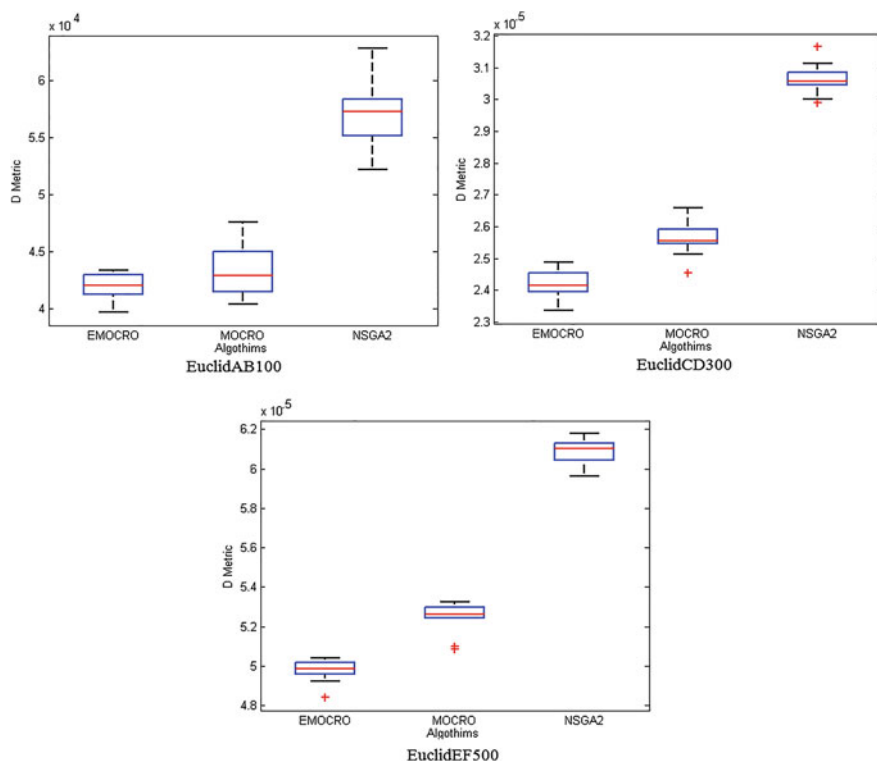


**Fig. 5** D-metric versus number of iteration in the instance with 100, 300 and 500 cities. The red circles are with EMOCRO, the green circles are with NSGA2 and the blue circles are with MOCRO

MOCRO and any solution obtained by EMOCRO is dominated by those obtained by NSGA2. Moreover, we note that the effectiveness of EMOCRO increases comparing to the results obtained by MOCRO and NSGA2 in the large instances test. On other hand, the different Pareto approximations of EMOCRO, MOCRO and NSGA2 are plotted in Fig. 4. It shows that EMOCRO surpasses NSGA2 and MOCRO in all the benchmarks.

Figure 5 represents the D-metric evolution of the algorithms versus the number of iterations. It can be seen from Fig. 5 that our proposed variant outperforms the two comparison algorithms in all the instances in term of D-metric. Moreover, Fig. 6 show the box plots of the values of D-metric obtained by the three algorithms. We can observe that EMOCRO is more close to PF than MOCRO and NSGA2.

Deleting decomposition and intermolecular ineffective collision operators has slight impact on the diversity of the final PF approximation. However, the gain acquired in this modification is the easier adaptation of the algorithm to the problems due to the minimization of the parameters number. Moreover, the elimination of these operators has not degraded the effectiveness of the algorithm according to the statistical results analysis in the experimental study.



**Fig. 6** Comparison of EMOCRO, MOCRO, and NSGA2 in term of D-metric over 10 runs

## 7 Conclusion

In this paper we have proposed a new variant of CRO, named enhanced multi-objective chemical reaction optimization. EMOCRO combines the chemical reaction concepts and dominance strategy. It simplifies the scheme of CRO and reduces considerably the high number of parameters of CRO which gives to the system more ability to be adapted to problems. To validate our proposed variant, we apply EMOCRO to solve MOSTP. The statistical results demonstrate that our proposed approach surpasses NSGA2 and MOCRO in the most of given test in term of C-metric and D-metric. To improve the effectiveness of our approach we will be focused our future work to ameliorate the distribution of the Pareto optimal solution set obtained by EMOCRO algorithm. Moreover, apply it to solve multi-objective dynamic optimization problems.



## References

1. Lust, T., Teghem J.: The multiobjective traveling salesman problem: a survey and new approach. In: *Nature Inspired Computing*. vol. 272, pp. 119–137. Springer, Berlin (2010)
2. Deb, K.: *Multi-objective Optimization Using Evolutionary Algorithms*. John Wiley and Sons Ltd. (2001)
3. Deb, K., Pratap, A., Agarwal, S., Meyarivan, T.: A fast and elitist multi-objective genetic algorithm: NSGA-II. *IEEE Trans. Evol. Comput.* **6**, 182–197 (2002)
4. Zitzler, E., Laumanns, M., Thiele, L.: SPEA2: Improving the Strength Pareto Evolutionary Algorithm. Technical report (2001)
5. Goldberg, D.E.: *Genetic Algorithms in Search, Optimization, and Machine Learning*. Addison-Wesley, Reading, MA, USA (1989)
6. Kirkpatrick, S., Gelatt, C.D., Vecchi, M.P.: Optimization by simulated annealing. *Science* **220**, 671–680 (1983)
7. Lam, A., Li, V.: Chemical-reaction-inspired meta-heuristic for optimization. *IEEE Trans. Evol. Comput.* **14**, 381–399 (2010)
8. Fisher, R., Richter, K.: Solving a multiobjective traveling salesman problem by dynamic programming. *Mathematische operations for schung und statistik, Series Optimization* **13**, 247–252 (1982)
9. Paquete, L., Stutzle, T.: Design and analysis of stochastic local search for the multiobjective traveling salesman problem. *Comput. Oper. Res.* **36**, 2619–2631 (2009)
10. Hansen, M.P.: Use of substitute scalarizing functions to guide a local search based heuristic: the case of moTSP. *J. Heuristics* **6**, 419–431 (2000)
11. Bouzoubia, S., Layeb, A., Chikhi, S.: A multi-objective chemical reaction optimisation algorithm for multi-objective travelling salesman problem. *Int. J. Innovative Comput. Appl.* **6**, 87–101 (2014)
12. Gao, F., Zhou, A., Zhang, G.: An estimation of distribution algorithm based on decomposition for the multi-objective TSP. In: *International Conference on Natural Computation (ICNC 2012)*, pp. 817–821 (2012)
13. Zhang, Q., Li, H.: MOEA/D: a multi-objective evolutionary algorithm based on decomposition. *IEEE Trans. Evol. Comput.* **11**(6), 712–731 (2007)
14. Ke, L., Zhang, Q., Battiti, R.: MOEA/D-ACO: a multiobjective evolutionary algorithm using decomposition and ant colony. *IEEE Trans. Cybern.* **43**(6), 1845–1859 (2013)
15. Iredi, S., Merkle, D., Middendorf, M.: Bi-criterion optimization with multi colony ant algorithms. *Evolutionary Multi-criterion Optimization*, pp. 359–372. Springer (2001)
16. He, J.: Solving the multiobjective multiple traveling salesmen problem using membrane algorithm. *Bio-inspired Computing, Theories and Applications, Communications in Computer and Information Science*, vol. 472, pp. 171–175 (2014)
17. Xu, J., Lam, A.Y.S., Li, V.O.K.: Chemical reaction optimization for the grid scheduling problem. In: *Proceedings of the IEEE ICC*, pp. 1–5 (2010)
18. Sun, J., Wang, Y., Li, J., Gao, K.: Hybrid algorithm based on chemical reaction optimization and lin-kernighan local search for the traveling salesman problem. In: *Seventh International Conference on Natural Computation*, pp. 1518–1521 (2011)
19. Truong, T.K., Li, K., Xua, Y.: Chemical reaction optimization with greedy strategy for the 0–1 knapsack problem. *Appl. Soft Comput.* **13**, 1774–1780 (2013)
20. Li, J.Q., Pan, Q.K.: Chemical reaction optimization for flexible job-shop scheduling problems with maintenance activity. *Appl. Soft Comput.* **12**, 2896–2912 (2012)
21. Reinelt, G.: TSPLIB a traveling salesman problem library. *ORSA J. Comput.* **3**, 376–384 (1991)
22. Zitzler, E.: *Evolutionary algorithms for multi-objective optimization: methods and applications*. Ph.D. thesis, Swiss Federal Institute of Technology, Zurich (1999)
23. Deb, K., Agrawal, S., Pratap, A., Meyarivan, T.: A fast elitist non-dominated sorting genetic algorithms for multi-objective optimization. Technical report, Institute of technology, Kanpur India (2000)

# Adaptive Cuckoo Search Algorithm for the Bin Packing Problem

Zakaria Zendaoui and Abdesslem Layeb

**Abstract** Bin Packing Problem (BPP) is one of the most difficult NP-hard combinatorial optimization problems. For that, an adaptive version of Cuckoo Search (CS) is used to deal with this problem. This algorithm has proved to be effective in solving many optimization problems. The idea of the adaptive CS (ACS) is based on integer permutations based levy flight and a decoding mechanism to obtain discrete solutions. The ranked order value (ROV) rule is the key to any passage from a continuous space to a combinatorial one. The experimental results show that ACS can be superior to some metaheuristics for a number of BPP instances.

**Keywords** Combinatorial optimization · Cuckoo search · First fit algorithm · Bin packing problem

## 1 Introduction

The combinatorial optimization plays very important role in operational research, discrete mathematics and computer science. The objective of this field is to solve several combinatorial optimization problems that are NP-hard because the number of combinations increases exponentially with the size of the problem. Consequently, searching for every possible combination is computationally expansive and not practical. Bin packing problem (BPP) is known to be NP-Hard optimization problem. There are three main variants of BPP: one, two and three dimensional BPP. They have several real applications such as container loading, cutting stock, packaging design and resource allocation, etc. In this paper, we deal with the

---

Z. Zendaoui (✉) · A. Layeb  
MISC Laboratory, Department of Computer Science and Its Applications,  
University of Constantine 2, Constantine, Algeria  
e-mail: zakaria.zendaoui@gmail.com

A. Layeb  
e-mail: Layeb.univ@gmail.com

one-dimensional Bin Packing Problem (BPP-1) [1–3]. As NP-hard optimization problem, not all existing algorithms are able to find the optimum solution within a reasonable time. In fact, several approximate methods have been proposed to solve this problem, which are generally based on heuristics or metaheuristics.

Metaheuristic algorithms are among the efficient optimization tools used for solving hard optimization problems. Metaheuristics present two important advantages which are simplicity and flexibility [4, 5]. In recent years, Most of metaheuristic algorithms are nature inspired, mimicking the successful features of the underlying biological, physical, or sociological systems. Not all algorithms perform equally well, some may obtain better results than others for a given problem, and there is no universally efficient algorithm to deal with all problems. So many challenges remain, especially for solving tough, NP-hard optimization problems [6].

Many heuristics have been used to solve the BPP like the First Fit algorithm (FF), the Best Fit algorithm (BF), etc. [7–9]. Moreover, many kinds of metaheuristics have been used too like genetic algorithms [10], Ant colony [11], etc.

CS is an optimization algorithm developed by Yang and Deb in 2009 [12]. It was inspired by the obligate brood parasitism of some cuckoo species by laying their eggs in the nests of other host birds (of other species). The cuckoo's behavior and the mechanism of Lévy flights [13, 14] have leading to design of an efficient inspired algorithm performing optimization search [15, 16]. In this paper, we present an adaptive CS algorithm, called ACS, by combining CS and decoding mechanism for solving bin packing problem. In the ACS, Ranked-Order-Value (ROV) technique is employed to convert continuous solutions into discrete ones. Results show that ACS obtains better performance than four other meta-heuristic algorithms on the bin packing problem.

This paper is organized as follows: Sect. 2 briefly introduces the CS. Section 3 present briefly the BPP. Section 4 describes the ACS. Section 5 shows the experimental results on a set of benchmarks of BPP-1. Finally, Sect. 6 concludes the paper.

## 2 Cuckoo Search Algorithm

In the standard CS, a cuckoo searches for a new nest via Lévy flights [17], rather than by simple isotropic random walks. Lévy flights essentially provide a random walk while their random steps are drawn from a Lévy distribution for large steps which has an infinite variance with an infinite mean. Here the consecutive jumps/steps of a cuckoo essentially form a random walk process which obeys a power-law step-length distribution with a heavy tail [18]. CS is based on the following three idealized rules [19]:

- Each cuckoo lays one egg at a time, and dumps it in a randomly chosen nest.
- The best nests with high quality of eggs will carry over to the next generations.

- The number of available host nests is fixed, and a host can discover an alien egg with a probability  $p_a \in [0, 1]$ . In this case, the host bird can either get rid of the egg, or simply abandon the nest and build a completely new nest.

In the last rule, the parameter  $p_a$  is named switching probability. A fraction  $p_a$  of the  $n$  host nests are replaced by new nests (with new random solutions at new locations).

The pseudo-code of CS algorithm can be summarized in Algorithm 1 from which can see that the parameter  $p_a$  control the balance between local and global explorative random walks.

The local random walk can be written as

$$x_i^{t+1} = x_i^t + \alpha s \otimes H(p_a - \varepsilon) \otimes (x_j^t - x_k^t) \quad (1)$$

where  $x_j^t$  and  $x_k^t$  are two different solutions selected randomly,  $H(u)$  is a Heaviside function,  $\varepsilon$  is a random number drawn from a uniform distribution, and  $s$  is the step size.

On the other hand, the global random walk is carried out by using Lévy flights

$$x_i^{t+1} = x_i^t + \alpha L(s, \lambda) \quad (2)$$

where

$$L(s, \lambda) = \frac{\lambda \Gamma(\lambda) \sin(\pi\lambda/2)}{\pi} \frac{1}{s^{1+\lambda}}, \quad (s \gg s_0 > 0) \quad (3)$$

here  $\alpha > 0$  is the scaling factor, which should be related to the scales of the problem of interest, and  $L(s, \lambda)$  determines the characteristic scale.

---

#### Algorithm 1 Cuckoo Search via Lévy Flights

---

```

Objective function  $f(x), x = (x_1, \dots, x_d)^T$ 
Generate initial population of  $n$  host nests  $x_i (i = 1, \dots, n)$ 
while ( $t < \text{MaxGeneration}$ ) or (stop criterion) do
  Get a cuckoo (say,  $i$ ) randomly by Lévy flights
  Evaluate its quality/fitness  $F_i$ 
  Choose a nest among  $n$  (say,  $j$ ) randomly
  if ( $F_i > F_j$ ) then
    Replace  $j$  by the new solution
  end if
  A fraction ( $p_a$ ) of worse nests are abandoned
    and new ones/solutions are built/generated
  Keep the best solutions (or nests with quality solutions)
  Rank the solutions and find the current best;
end while

```

---

### 3 The Bin Packing Problem (BPP)

The BPP-1 [8, 20] consists to pack a set of items having different weights into a minimum number of bins which may have also different capacities. Among the most popular heuristics used to solve the bin packing problem, the First Fit algorithm (FF) which places each item into the first bin in which it will fit. The second popular heuristic algorithm is the Best Fit (BF) which puts each element into the filled bin in which it fits. Moreover, the FF and BF heuristics can be improved by applying a specific order of items like in First Fit Decreasing (FFD) and Best Fit Decreasing (BFD), etc. [9, 21].

Formally, the bin packing problem can be stated as follows:

$$\text{Min } z(y) = \sum_{j=1}^n y_j \quad (4)$$

Subject to constraints:

$$\sum_{i=1}^n w_i x_{ij} \leq C_{y_j}, j = 1..n \quad (5)$$

$$\sum_{j=1}^n x_{ij} = 1, i = 1..n \quad (6)$$

where,

$$y_j = \begin{cases} 1, & \text{if bin } j \text{ is used} \\ 0, & \text{otherwise} \end{cases} \quad (7)$$

$$x_{ij} = \begin{cases} 1, & \text{if item } i \text{ is placed in bin } j \\ 0, & \text{otherwise} \end{cases} \quad (8)$$

In the above model, the objective minimizes the total number of bins used to pack all items. We assumed here that all the bins have the same capacity  $C$ . The first constraint guarantees that the weights of items ( $w_i$ ) filled in the bin  $j$  do not exceed the bin capacity. The second constraint ensures that each item is placed only in one bin.

It appears to be impossible to obtain exact solutions in polynomial time. The main reason is that the required computation grows exponentially with the size of the problem. Therefore, it is often required to find near optimal solutions to these problems in reasonable time. Efficient heuristic algorithms offer a good alternative to accomplish this goal. Within this perspective, we are interested in applying a CS to solve this problem.

## 4 Solving the BPP with CS

Now, the cuckoo search adaptation for solving the BPP is presented in detail.

### 4.1 BPP Solution Representation

The CS algorithm was designed for continuous optimization problems, while BPP is a discrete problem. Thus, standard CS cannot be directly adopted for the BPP. So, the most important issue to apply CS for the BPP is to find a suitable relationship between the real number solutions and the item permutations. For this issue, different techniques have been proposed, such as the largest ranked value (LRV) [22], the smallest position value (SPV) [23], the largest order value (LOV) [24], and ranked order value (ROV) [25]. By sorting the position values of a continuous solution in different order, different item permutations are obtained. Figure 1 presents an example of the four rules. It can be seen from Fig. 1 that ROV rule give the closest integer solution to continuous solution.

In this paper, the ROV rule is used [25]. The ROV is a simple method based on random key representation [26] with guarantees feasibility of new solutions without creating additional overhead.

We assume that a cuckoo lays a single egg in one nest, and each nest contains only one egg. This egg is a solution represented by an item permutation, and we use a decoding mechanism that reveals the actual assignment of the items to bins corresponding to this solution. Since the FF and BF methods are easily implemented, we have adapted them in our algorithm as a decoding mechanism.

For the sake of clarity, let's consider an instance of BBP-1. Table 1 contains 6 items to pack, numbered 1 through 6. The capacity of each bin is equal to 8.

To generate a BPP solution from a permutation of the items, we can take the items one by one in the order given by the permutation, and assigning them to the available bin according to the FF or BF method. In the current example, we use FF

Continuous solution	3.29	1.00	4.59	5.00	2.00	5.10
LRV	4	6	3	2	5	1
SPV	2	5	1	3	4	6
LOV	6	4	3	1	5	2
ROV	<b>3</b>	<b>1</b>	<b>4</b>	<b>5</b>	<b>2</b>	<b>6</b>

Fig. 1 An example for the four rules

Table 1 An instance of BBP

Items	1	2	3	4	5	6
$w_i$	2	2	2	3	3	4

Step 1: Permutation of numbers	4	3	1	5	6	2
Step 2: FF method	4    3		1	5    6		2
	bin 1			bin 2		bin 3

Fig. 2 Procedure of generation a random initial solution

method, so the result is a partition of items, with indicates that the item  $i$  is packed in the bin  $j$  as showed in Fig. 2.

### 4.2 Objective Function

The objective function is an important parameter in any optimization algorithm. Indeed, a good objective function helps the search process to find the optimal solution. In the context of the bin packing problem, using the number of bins as objective function can make the algorithm suffer from stagnation because there can be several arrangements which have the same number of bins. Though, this information will be better if it is integrated with other information like the fullness of the bins. That’s why we have used the objective function defined by Falkenauer and Delchambre in [27], which contains both item’s weight and bin capacities information. This objective function is given by the Eq. (9)

$$Maxf = (sum_i / C)^k / nbin \tag{9}$$

where,

$sum_i$  is the sum of all weight items packed in the bin  $i$ ;

$C$  is the capacity of bin;

$nbin$  is the number of used bins;

$k$  is the parameter that defines equilibrium of the filling bins. By increasing  $k$ , we give a higher fitness to solutions that contain a mix of well-filled and less well-filled bins, rather than equally filled bins.

### 4.3 Moving in the Search Space

In this ACS to solve BPP, we have two moves that generate a new solution from an existing solution by changing the order of assigned items. The first move is the local random move (Fig. 3) that is given by the Eq. (1). The second move is the global random move that is carried out by using Lévy flights (Fig. 4) given by the Eq. (2). Both move give real values, so, the smallest value of a solution is firstly picked and assigned a rank value 1. Then, the second smallest position value will be assigned rank value 2. In a similar way, the new solution can be obtained.

Existing solution	4	1	6	5	2	3	
Result of Eq. (1)	3.29	1.00	4.59	5.00	2.00	5.10	
New solution	3	1	4	5	2	6	

Fig. 3 Local random move

Existing solution	4	1	6	5	2	3
Result of Eq. (2)	3.74	5.41	5.63	5.08	2.46	2.98
New solution	3	5	6	4	1	2

Fig. 4 Global random move

Algorithm 2: Adaptive Cuckoo Search

---

```

Objective function  $f(x), x = (x_1, \dots, x_d)^T$ 
Generate initial population of  $n$  host nests  $x_i (i = 1, \dots, n)$ 
while ( $t < \text{MaxGeneration}$ ) do
     $X_i$  = Generate new solution by Lévy flights;
     $P_i$  = Convert  $X_i$  to an item permutation based on ROV rule;
    Replace  $X_i$  by  $P_i$ ;
     $F_i$  = Evaluate  $P_i$ ;
     $P_j$  = Randomly choose solution from population;
    if ( $F_i > F_j$ ) then
        Replace  $P_j$  the new solution  $P_i$ ;
    end if
    A fraction ( $p_a$ ) of worse solutions are abandoned
        and new ones are generated according Eq. 1;
    Convert the new solutions to item permutations;
    Replace the new solutions by the item permutations;
    Evaluate their fitness;
    Rank the solutions and find the current best
end while

```

---

The pseudo-code of ACS algorithm can be seen in Algorithm 2.



## 5 Experimental Results

In order to test our approach and show the performance, The ACS to BPP is implemented and tested on some instances (benchmarks) of BPP-1 taken from the site <http://www.wiwi.uni-jena.de/Entscheidung/bin-pp/>. The benchmark data sets are divided into three classes: easy, medium and hard class instances. We have implemented our approach in Matlab 8.3 under the 32 bits Seven Operating System. Experiments are concluded on a laptop with the configurations of Intel(R) CoreTM 2 Duo 2.00 GHz, and 2 GB of RAM.

The parameters used in the experiments are shown in Table 2. The selected parameters are those values that gave the best results for both the solution quality and the computational time. Table 3 shows that the maximum number of iterations can be set to 200.

The obtained results are summarized in Tables 4, 5 and 6, where the first column is the name of the instance. The column ‘Best Known’ contains the best known results. The column ‘FFD’ contains the results of the first fit decreasing heuristic. The column ‘AS’ contains the results of the Ant System algorithm [28]. The column ‘FCO’ contains the results of the firefly algorithm based ant colony optimization [28]. The column ‘QICS’ contains the results of the quantum cuckoo search algorithm [29], and the column ‘ACS’ contains the results of our approach. Moreover, we have used the Friedman test for comparing statistically the obtained results.

**Table 2** Parameter settings

Parameter	Value	Meaning
$n$	20	Population size
$p_a$	0.2	Portion of bad solutions
$N\_IterTotal$	200	Maximum number of iterations
$\alpha$	0.01	Step size
$Lb$	1	Lower bounds
$Ub$		Number of items

**Table 3** Average of best solutions of 10 runs for HARD0, N4W2B1R0 and N4C1W4\_A

Instance	Best known	Iteration				
		1	2	90	185	500
HARD0	56	59	59	58	58	58
N4W2B1R0	101	107	106	106	105	105
N4C1W4_A	368	368	368	368	368	368

**Table 4** Results of algorithms for the easy class

Instance	Best known	FFD	AS	FCO	QICS	ACS
N1C1W1_A	25	<b>25</b>	<b>25</b>	<b>25</b>	<b>25</b>	<b>25</b>
N1C1W1_D	28	<b>28</b>	<b>28</b>	<b>28</b>	<b>28</b>	<b>28</b>
N1C1W1_G	25	<b>25</b>	<b>25</b>	<b>25</b>	<b>25</b>	<b>25</b>
N1C1W1_B	31	<b>31</b>	<b>31</b>	<b>31</b>	<b>31</b>	<b>31</b>
N1C1W1_E	26	<b>26</b>	<b>26</b>	<b>26</b>	<b>26</b>	<b>26</b>
N1C1W1_F	27	<b>27</b>	<b>27</b>	<b>27</b>	<b>27</b>	<b>27</b>
N1C1W1_I	25	<b>25</b>	<b>25</b>	<b>25</b>	<b>25</b>	<b>25</b>
N2C1W2_P	68	<b>68</b>	<b>68</b>	<b>68</b>	<b>68</b>	<b>68</b>
N2C1W2_N	64	<b>64</b>	<b>64</b>	<b>64</b>	<b>64</b>	<b>64</b>
N2C1W2_O	64	<b>64</b>	<b>64</b>	<b>64</b>	<b>64</b>	<b>64</b>
N2C1W2_R	67	<b>67</b>	<b>67</b>	<b>67</b>	<b>67</b>	<b>67</b>
N4C1W2_T	323	<b>323</b>	<b>323</b>	<b>323</b>	<b>323</b>	<b>323</b>
N4C1W4_C	365	<b>365</b>	<b>365</b>	<b>365</b>	<b>365</b>	<b>365</b>
N4C1W4_A	368	<b>368</b>	<b>368</b>	<b>368</b>	<b>368</b>	<b>368</b>
N4C1W4_D	359	<b>359</b>	<b>359</b>	<b>359</b>	<b>359</b>	<b>359</b>
N4C1W4_B	349	<b>349</b>	<b>349</b>	<b>349</b>	<b>349</b>	<b>349</b>

**Table 5** Results of algorithms for the medium class

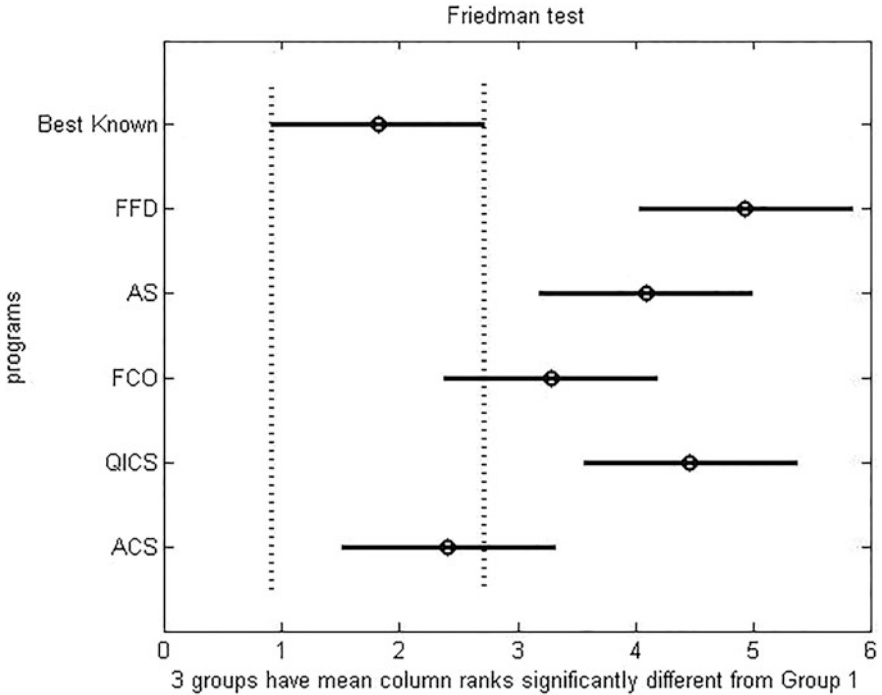
Instance	Best known	FFD	AS	FCO	QICS	ACS
N1W1B2R1	17	18	18	<b>17</b>	<b>17</b>	<b>17</b>
N1W1B1R9	17	19	<b>17</b>	<b>17</b>	18	<b>17</b>
N1W1B1R2	19	20	20	<b>19</b>	20	<b>19</b>
N1W1B2R0	17	18	18	18	18	<b>17</b>
N1W1B2R3	16	17	17	17	17	17
N2W1B1R0	34	37	37	35	36	<b>34</b>
N2W1B1R3	34	38	36	36	37	35
N2W1B1R1	34	37	36	36	37	35
N2W1B1R4	34	37	35	35	37	<b>34</b>
N2W3B3R7	13	<b>13</b>	<b>13</b>	<b>13</b>	<b>13</b>	<b>13</b>
N2W4B1R0	12	<b>12</b>	<b>12</b>	<b>12</b>	<b>12</b>	<b>12</b>
N4W2B1R0	101	109	107	106	109	105
N4W2B1R3	100	109	106	105	108	104
N4W3B3R7	74	<b>74</b>	<b>74</b>	<b>74</b>	<b>74</b>	<b>74</b>
N4W4B1R0	56	58	58	57	58	57
N4W4B1R1	56	58	58	58	58	57

**Table 6** Results of algorithms for the hard class

Instance	Best known	FFD	AS	FCO	QICS	ACS
HARD0	56	59	59	59	59	58
HARD1	57	60	60	59	60	59
HARD2	56	60	60	59	60	59
HARD3	55	59	59	59	59	58
HARD4	57	60	60	60	60	59
HARD5	56	59	59	59	59	58
HARD6	57	60	60	59	59	59
HARD7	55	59	59	58	59	58
HARD8	57	60	60	59	59	59
HARD9	56	60	59	59	59	59

In Table 4, the experimental results of the first series of easy instances are given. From this table we see that the results obtained by FFD, AS, FCO, QICS, and ACS are completely identical to the best know solutions.

In Table 5, the experimental results of the second series of medium instances are given. It can be seen from this table and Fig. 5 that ACS outperforms the other



**Fig. 5** Friedman test for medium instances

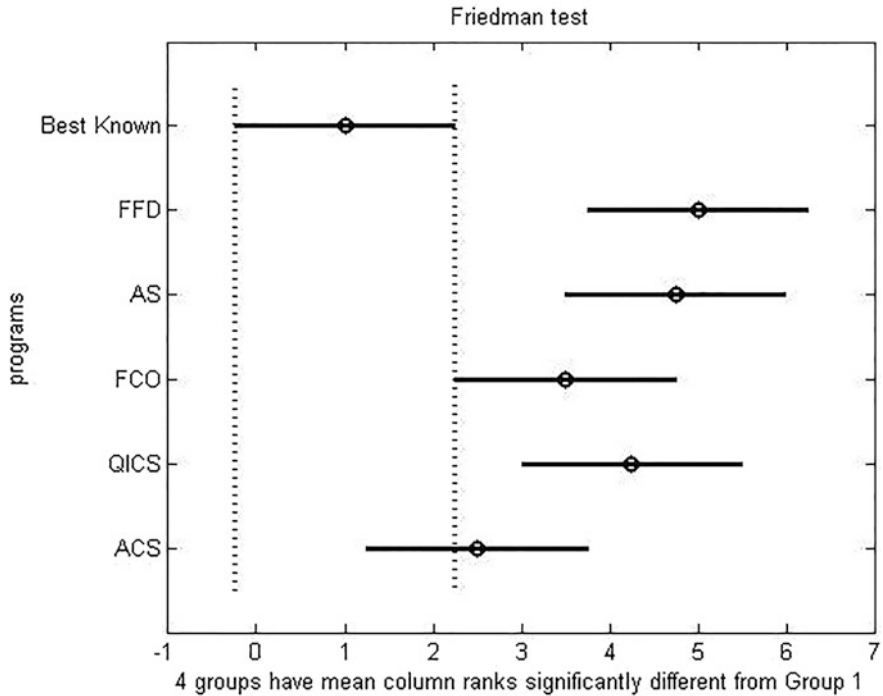
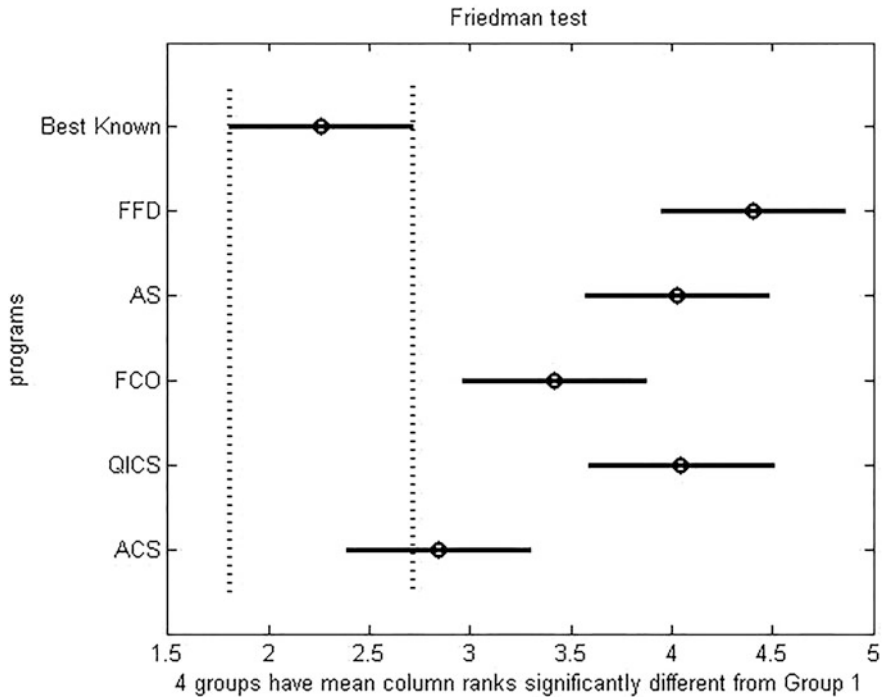


Fig. 6 Friedman test for hard instances

algorithms in solving all the sixteen tested instances. The ACS obtains nine best known solutions while FFD/AS/FCO/QICS only obtains three/four/six/four best known solutions among sixteen instances.

In Table 6, the experimental results of the third series of hard instances are given. It can be seen from this table and Fig. 6 that ACS outperforms the other algorithms in solving all the ten tested instances. The ACS is better, in term of solution quality, than FFD/AS/FCO/QICS in ten/nine/four/seven instances.

As it is well seen from the results presented in Fig. 7 of Friedman test for the three types of instances (Tables 4, 5 and 6), our ACS succeeds in finding the near optimal solutions compared to the other methods.



**Fig. 7** Friedman test for all instances

## 6 Conclusion

In this paper, we have adapted Cuckoo Search algorithm to solve the one-dimensional bin packing problem (BPP-1). In our Adaptive Cuckoo Search (ACS) to BPP, the ROV technique is used to transform continuous solutions into discrete integer permutations. ACS has been implemented and its performance has been tested on three classes benchmark BPP-1 instances. Its performance has been compared with the FFD, AS, FCO and QICS algorithms. The results of the comparison have shown that the ACS outperforms all four methods for solving BPP-1 instances. ACS has few numbers of parameters and thus it is easier to implement and to tune these parameters. Furthermore, further studies can be fruitful when focusing on the improvement of ACS by introducing local search strategy, and the use of parallelism techniques.

## References

1. Martello, S., Toth, P.: Bin-packing problem. In: *Knapsack Problems: Algorithms and Computer Implementations* (8), pp. 221–245. Wiley (1990)
2. Coffman, E.G. Jr., Garey, M.R., Johnson, D.S.: Approximation algorithms for bin packing: a survey. In: Hochbaum, D. (ed.) *Approximation Algorithms for NP-Hard Problems*, pp. 46–93. PWS Publishing, Boston (1996)
3. Fleszar, K., Hindi, K.S.: New heuristics for one-dimensional bin-packing. *Comput. Oper. Res.* **29**(7), 821–839 (2002)
4. Gandomi, A.H., Yang, X.S., Talatahari, S., Alavi, A.H.: *Metaheuristic Applications in Structures and Infrastructures*. Newnes (2013)
5. Yang, X.S.: *Nature-Inspired Metaheuristic Algorithms*. Luniver Press, Bristol (2010)
6. Wolpert, D.H., Macready, W.G.: No free lunch theorems for optimization. *Evolut. Comput. IEEE Trans.* **1**(1), 67–82 (1997)
7. Ivim, A.C.F., Ribeiro, C.C., Glover, F., Aloise, D.J.: A hybrid improvement heuristic for the one-dimensional bin packing problem. *J. Heuristics* **10**, 205–229 (2004)
8. Kao, C.-Y., Lin, F.-T.: A stochastic approach for the one-dimensional bin-packing problems. *Syst. Man Cybern.* **2**, 1545–1551 (1992)
9. Scholl, A., Klein, R., Juergens, C.: Bison: a fast hybrid procedure for exactly solving the one-dimensional bin packing problem. *Comput. Oper. Res.* **24**(7), 627–645 (1997)
10. Falkenauer, E.: A hybrid grouping genetic algorithm for bin packing. *J. Heuristics* **2**, 5–30 (1996)
11. Wang, S., Shi, R., Wang, L., Ge, M.: Study on improved ant colony optimization for bin-packing problem. In: *International Conference on Computer Design and Application* (4), pp. 489–491 (2010)
12. Yang, X.S., Deb, S.: Cuckoo search via lévy flights. In: *World Congress on Nature and Biologically Inspired Computing. NaBIC 2009*, pp. 210–214. IEEE, New York (2009)
13. Payne, R.B., Sorenson, M.D., Klitz, K.: *The Cuckoos*. Oxford University Press (2005)
14. Pavlyukevich, I.: Lévy flights, non-local search and simulated annealing. *J. Comput. Phys.* **226**, 1830–1844 (2007)
15. Tein, L.H., Ramli, R.: Recent advancements of nurse scheduling models and a potential path. In: *Proceedings 6th IMT-GT Conference on Mathematics, Statistics and its Applications (ICMSA 2010)*, pp. 395–409 (2010)
16. Dhivya, M.: Energy efficient computation of data fusion in wireless sensor networks using cuckoo based particle approach (CBPA). *Int. J. Commun. Netw. Syst. Sci.* **4**(4), 249–255 (2011)
17. Shlesinger, M.F., Zaslavsky, G.M., Frisch, U.: Lévy flights and related topics in physics. In: *Levy Flights and Related Topics in Physics*, vol. 450 (1995)
18. Yang, X.S., Deb, S.: Engineering optimisation by cuckoo search. *Int. J. Math. Model. Numer. Optim.* **1**(4), 330–343 (2010)
19. Yang, X.S.: *Nature-Inspired Metaheuristic Algorithms*, pp. 105–107, 2nd edn. Luniver Press (2010)
20. Alvim, A.C., Ribeiro, C.C., Glover, F., Aloise, D.J.: A hybrid improvement heuristic for the one-dimensional bin packing problem. *J. Heuristics* **10**(2), 205–229 (2004)
21. Monaci, M.: Algorithms for packing and scheduling problems. *Q. J. Belg. Fr. Ital. Oper. Res. Soc.* **1**(1), 85–87 (2003)
22. Liang, J., Pan, Q.K., Tiejun, C., Wang, L.: Solving the blocking flow shop scheduling problem by a dynamic multi-swarm particle swarm optimizer. *Int. J. Adv. Manuf. Technol.* **55**(5–8), 755–762 (2011)
23. Tasgetiren, M.F., Liang, Y.C., Sevcli, M., Gencyilmaz, G.: Particle swarm optimization and differential evolution for the single-machine total weighted tardiness problem. *Int. J. Prod. Res.* **44**(22), 4737–4754 (2006)

24. Qian, B., Wang, L., Rong, H., Wang, W.L., Huang, D.X., Wang, X.: A hybrid differential evolution method for permutation flow-shop scheduling. *Int. J. Adv. Manuf. Technol.* **38**(7–8), 757–777 (2008)
25. Liu, B., Wang, L., Qian, B., Jin, Y.H.: Hybrid Particle Swarm Optimization for Stochastic Flow Shop Scheduling with No-wait Constraint. *International Federation of Automatic Control*, Seoul (2008)
26. Bean, J.C.: Genetic algorithms and random keys for sequencing and optimization. *ORSA J. Comput.* **6**, 154–160 (1994)
27. Falkenauer, E., Delchambre, A.: A genetic algorithm for bin packing and line balancing. In: *Proceedings of the IEEE 1992 International Conference on Robotics and Automation*, Nice, France (May 1992)
28. Layeb, A., Benayad, Z.: A novel firefly algorithm based ant colony optimization for solving combinatorial optimization problems. *Int. J. Comput. Sci. Appl.* **11**(2), 19–37 (2014)
29. Layeb, A., Boussalia, S.R.: A novel quantum inspired cuckoo search algorithm for bin packing problem. *Int. J. Inf. Technol. Comput. Sci. (IJITCS)* **4**(5), 58 (2012)

**Part II**  
**Intelligent and Information Systems**



# Greedy Mean Squared Residue for Texture Images Retrieval

Salah Bougueroua and Bachir Boucheham

**Abstract** In this paper, we propose a new algorithm for texture retrieval, using clustering strategy. Indeed, it is largely noticed that in existing CBIR systems and methods, the collection of the images similar to the query is realized on the basis of comparison of the database images to the query solely. Hence, the results might not be globally homogeneous. In this paper, the collection of the images most similar to the query is realized considering the global homogeneity of the whole cluster (result). Knowing that this is of an exponential order problem, we use a greedy solution consisting in growing the cluster corresponding to a query, one image at a time, based on the *Mean Squared residue* measure of Cheng and Church (Proceedings of the Eighth International Conference on Intelligent Systems for Molecular Biology, 2000) [1], originally proposed for the biclustering of gene expression data. At each stage, the new added image to the cluster will be that that preserves most the homogeneity of the current cluster. The texture descriptor used in this work is the uniform-LBP. Experimentations were conducted on two texture image databases, Outex and Brodatz. The proposed algorithm shows an interesting performance compared to the uniform-LBP combined to Euclidean metric.

**Keywords** CBIR · Image retrieval · Biclustering · Mean squared residue · Texture · Similarity measure · Greedy search · Optimization

---

S. Bougueroua (✉) · B. Boucheham  
Department of Computer Science, 20 Août 1955 University of Skikda,  
B.P. 26 Route d'El-Hadaiek, 21000 Skikda, Algeria  
e-mail: s\_bougueroua@yahoo.fr; s.bougueroua@univ-skikda.dz

B. Boucheham  
e-mail: boucheham\_bachir@yahoo.fr; b.boucheham@univ-skikda.dz

## 1 Introduction

Content Based Image Retrieval (CBIR), [1] is an alternative technique which has been proposed in the early 1980s [2] to overcome the disadvantages of the text based retrieval (TBIR). These disadvantages are summarized into two aspects; hardness of the annotation, especially for large databases, and subjectivity of the attributed keywords.

CBIR systems are essentially composed of two steps: *features extraction* from low level visual attributes, and *the retrieval of visually similar images* using one of the similarity measures. The most exploited visual attributes in the literature are Color, Texture and Shape. Specifically, texture is a characteristic that is ubiquitous in objects in general, remote sensing and scenes images particularly. This puts texture as privileged feature that captures attention of researchers in the computer vision fields (classification, retrieval, recognition, etc.).

In the context of image characterization based on texture, the “co-occurrence matrices” of Haralick et al. [3] is one of the earliest methods. This was specifically proposed for texture classification. The Local Binary Pattern (LBP) of Ojala et al. [4, 5] is another technique for texture feature extraction. Although simple, this method is very effective technique. Particularly, the LBP operator has known great success since its apparition in texture retrieval applications. It was also successfully used in face recognition [6], gender and age classification [7]. For example, the combination LBP-GLCM (Gray Level Co-Occurrence Matrix) showed interesting results for tea leaves classification [8]. Due to its success, a significant number of LBP variants were introduced, such as ILBP [9], LTP [10], DLBP [11], block-based LBP [12], EILBP [13], GLIBP [14].

Despite the success of the above mentioned methods in image retrieval by content, these methods show generally difficulties to stay effective in all situations. For this reason, usage of more sophisticated methods has been imposed as a necessity, such as, the combination of different visual attributes, e.g. [15–22].

In image retrieval, the comparison step plays a crucial role. In this context, many measures were proposed in the literatures, such as: *histograms intersection* of Swain and Ballard [23], the *Earth Mover’s Distance* (EMD) [24], and *Comparing Histograms by Clustering* (CHIC) [25]. Other more simple metrics are also widely used, such as the *Euclidean*, *Manhattan* and *Canberra* metrics. Some of the above metrics and other ones are compared by the authors of [26, 27]. Their results show clearly the important role that the distance metrics play.

The present work proposes a contribution in the comparison step of CBIR systems. Unlike the strategy of classical approaches in image retrieval methods by content, that consists in selecting the resulting images matching the query, one at time, but, by ignoring, in each step, the previous selected images; our contribution is based on the assumption that: *the feature vectors of the images which are visually similar have the same variation (co-regulation) over the features*. Following this

assumption, we focused our attention on (Bi)-Clustering techniques. Particularly, the *Mean Squared Residue* (MSR) is a measure introduced by Cheng and Church [1] for the biclustering of gene expressions. To the best of our knowledge, no previous works in the CBIR field have used this measure. Indeed, the proposed algorithm is distinguished by the fact that all images in the current set of selected images contribute in the selection of the next image, at each step.

The remaining of this paper is organized as follows. In the next section, we address briefly materials related to our work; including biclustering and the Mean Squared Residue (MSR). Our proposal is presented in the Sect. 3. The experimentations and obtained results are discussed in the Sects. 4 and 5, respectively. A conclusion and perspectives are expressed in the Sect. 6.

## 2 Materials and Methods

### 2.1 The Biclustering

By contrast to the clustering techniques, which classify the samples over all the features (values), the biclustering techniques aim to cluster simultaneously the rows and the columns. In expression data analysis, the rows correspond to the genes and the columns correspond to the conditions. Accordingly, the biclustering of gene expression data aims to find the subset(s) of genes which they are highly correlated over a subset(s) of conditions.

Formally, let  $A$  be the expression data composed of the set of the genes (rows)  $X$  and the set of conditions (columns)  $Y$ .

The biclustering techniques try to find the bicluster (sub-matrix)  $A_{IJ}$ , where  $I \subseteq X$  and  $J \subseteq Y$  such that the genes in  $I$ , are highly co-regulated over the set of conditions  $J$ .

### 2.2 The Mean Squared Residue (MSR)

Cheng and Church [1] introduced an efficient node-deletion algorithm for the biclustering of the expression data. Their algorithm attempts to find the maximum bicluster with low Mean Squared Residue.

The MSR  $H$  of the bicluster with the set of rows and columns  $I$  and  $J$ , respectively, is calculated as follow:

$$H(I, J) = \frac{1}{|I||J|} \sum_{i \in I, j \in J} (a_{ij} - a_{iI} - a_{jJ} + a_{IJ})^2 \quad (1)$$

where

$$a_{iJ} = \frac{1}{|J|} \sum_{j \in J} a_{ij} \quad (2)$$

$$a_{Ij} = \frac{1}{|I|} \sum_{i \in I} a_{ij} \quad (3)$$

And

$$a_{IJ} = \frac{1}{|I||J|} \sum_{i \in I, j \in J} a_{ij} \quad (4)$$

More information on biclustering techniques can be found in the interesting survey of Madeira and Oliveira [28].

### 3 The Mean Squared Residue for Texture Retrieval

Our proposed method is based on the MSR measure, with adaptation to the CBIR case. The matrix (expression data) is replaced by the index (i.e. database images feature vectors), where the rows correspond to the images and the columns correspond to the features.

Since we are interested by the image retrieval based on texture, we have chosen the LBP method for texture features extraction. Indeed, the LBP operator and its various variants are known for their effectiveness and efficiency. However, the use of the LBP histogram is not the only descriptor allowed in our algorithm and it can be generalized to other descriptors, such as, color histogram.

The LBP histogram of an image is 256-valued (when 8 neighbors are considered). Therefore, for more compactness, we have used the LBP uniform ( $LBP_{P,R}^{u2}$ ) [4], radius (R) equal to 1, and 8 neighbors (i.e. P = 8). This yields 58 uniform patterns (i.e. histogram of 59 bins, one bin for the non uniform pattern). Consequently, if the database is composed of  $M$  images, the matrix will be of  $M \times 59$  values.

The proposed algorithm is composed of two main steps, as follows.

- Step 1 *Initialization*: Let  $I$  be the cluster representing the selected images corresponding to a given query  $Q$ . In this step, the cluster is initiated to *empty*. (The first step in Fig. 1)
- Step 2 *Growing*: in this step,  $I$  is made grow by adding to it selected images from the database, one at a time, so that the currently added image is that that preserves most the overall homogeneity of  $I$ . For this purpose, we used a

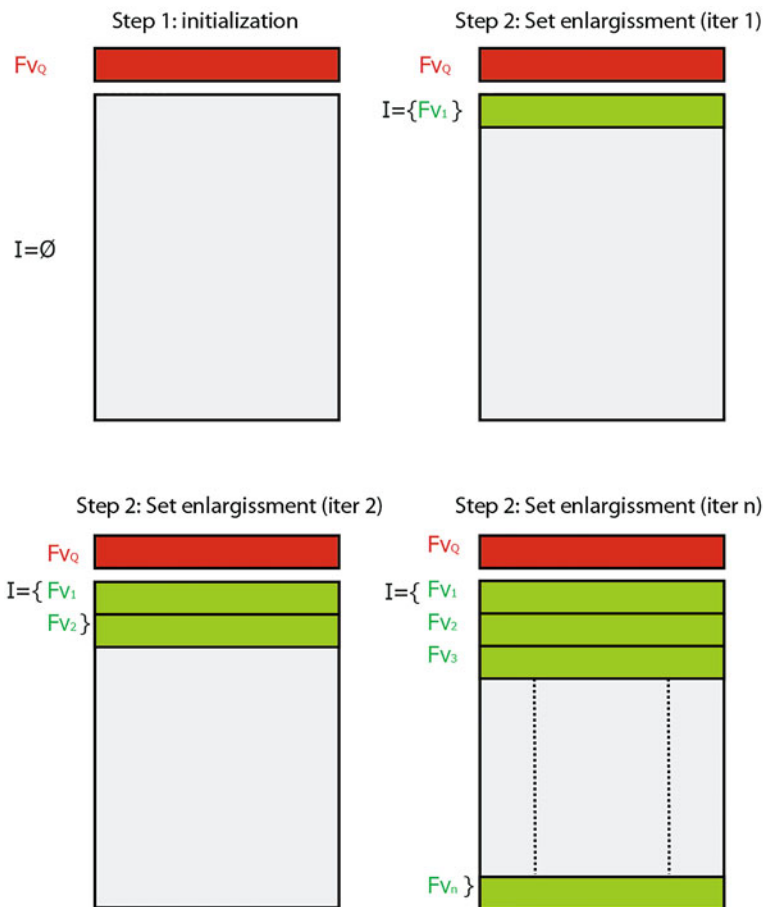


Fig. 1 Steps of growing set  $I$

greedy search, where the image which causes the lowest *cost* is included to the cluster (Eq. 5). By “cost”, we mean the *difference* between the MSR of the cluster *before* and the MSR *after adding* the feature vector of image  $i$  (Eq. 6). This step is repeated until satisfying a stop criterion. The criterion we used is the number of images in the cluster (i.e. the number of cluster rows)

$$\Delta MSR_i(Q, I) = H(Q \cup I, Y) - H(Q \cup I \cup \{i\}, Y) \tag{5}$$

$$\arg \min_i (\Delta MSR_i(Q, I)) \tag{6}$$

A description of the proposed algorithm is given below:

```

Algorithm: texture image retrieval using the MSR;
Input: index:matrix[m,n];
//m the number images in database.
//n the number of patterns
Q:vector; // Query Feature vector
sizeCR:integer; // the maximum number of rows (images) in
//the result cluster I.
Output: the set I of images which are visually most
//similar to the query Q.
Begin
I= $\emptyset$ ;
While (size(I)<sizeCR) do
  begin
    //Search for image i which brings the minimum  $\Delta MSR$ 
    //among the images not included in the current cluster.
    i =  $\text{argmin}(\Delta MSR_i(Q, I))$ 
    I= $I \cup \{ FV_i \}$ ;
  End;
End.

```

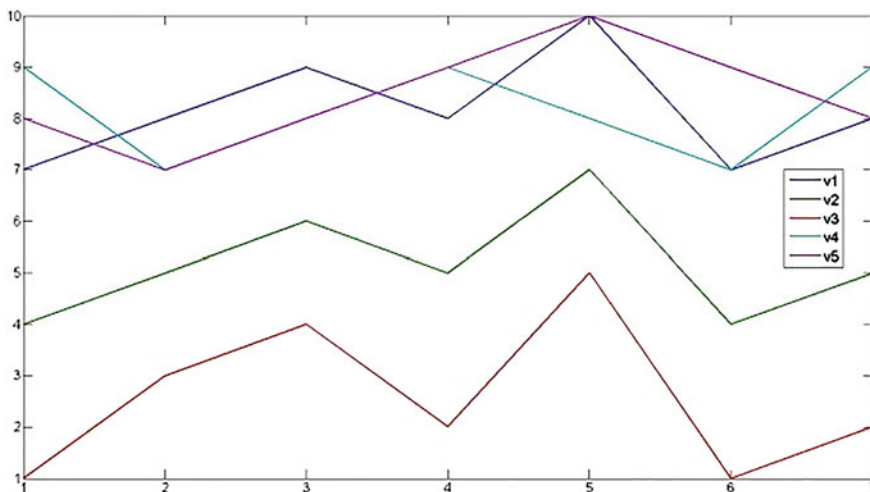


Fig. 2 Example, the five vectors

For example, let the following five vectors (Fig. 2):  $V_1, V_2, V_3, V_4,$  and  $V_5$  such that:

$$V_1 = [7, 8, 9, 8, 10, 7, 8].$$

$$V_2 = [4, 5, 6, 5, 7, 4, 5].$$

$$V_3 = [1, 3, 4, 2, 5, 1, 2].$$

$$V_4 = [9, 7, 8, 9, 8, 7, 9].$$

$$V_5 = [8, 7, 8, 9, 10, 9, 8].$$

We also assume that we have a query vector  $V_Q$ , such that:

$$V_Q = [7, 8, 9, 10, 7, 8].$$

If we match the vector  $V_Q$  with the above five vectors using a classical distance metric such as Euclidean distance (Eq. 7) they will be ranked according to their distances from  $V_Q$  as follow  $V_1$  ( $d = 0$ ),  $V_5$  ( $d = 2.83$ ),  $V_4$  ( $d = 3.46$ ),  $V_2$  ( $d = 7.94$ ), and  $V_3$  ( $d = 14.8$ ).

Now, using the proposed method based on the MSR. At the first step (initialization) we have only the query vector  $V_Q$ . In the second step, we search for the vector among the database vectors (not included yet) that has the lowest cost (MSR difference ( $\Delta MSR$ )). So, according to the vectors that we have,  $V_1$  is the one which verifies this constraint ( $\Delta MSR_{V_1} = 0$ ). We repeat the process, we have  $Fv_Q = V_Q$  and  $I = \{V_1\}$ , the vector which has the lowest cost when it is included to the set  $I$  is  $V_2$  ( $\Delta MSR_{V_2} = 0$ ), then  $V_3$  ( $\Delta MSR_{V_3} = 0.0459$ ), and after that  $V_5$  ( $\Delta MSR_{V_5} = 0.1957$ ). In this step  $Fv_Q = V_Q$  and  $I = \{V_1, V_2, V_3, V_5\}$  and the inclusion of  $V_4$  has the cost ( $\Delta MSR_{V_4} = 0.1926$ ). At the end, the resulted vectors will be ranked as follow:  $V_1, V_2, V_3, V_5,$  and  $V_4$ .

$$d_{euc}(x, y) = \sqrt{\sum_i (x_i - y_i)^2} \quad (7)$$

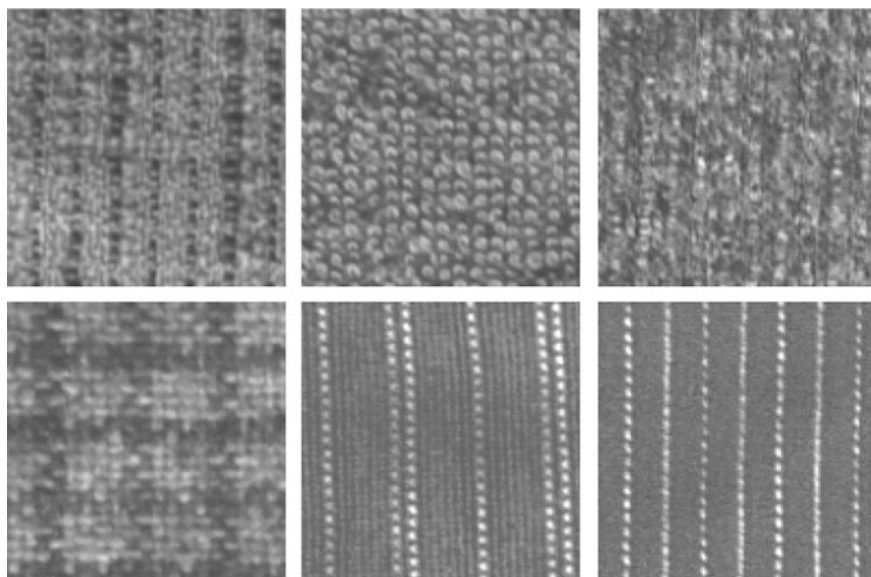
## 4 Experimentations

Our experimentations were conducted on two databases of textured images. The first one is Outex\_tc\_00000 test suite of *Outex*<sup>1</sup> database. This suite is composed of 480 images, distributed on 24 classes, 20 images for each class, with a size of  $128 \times 128$  pixels. Some samples from this database are shown in Fig. 3.

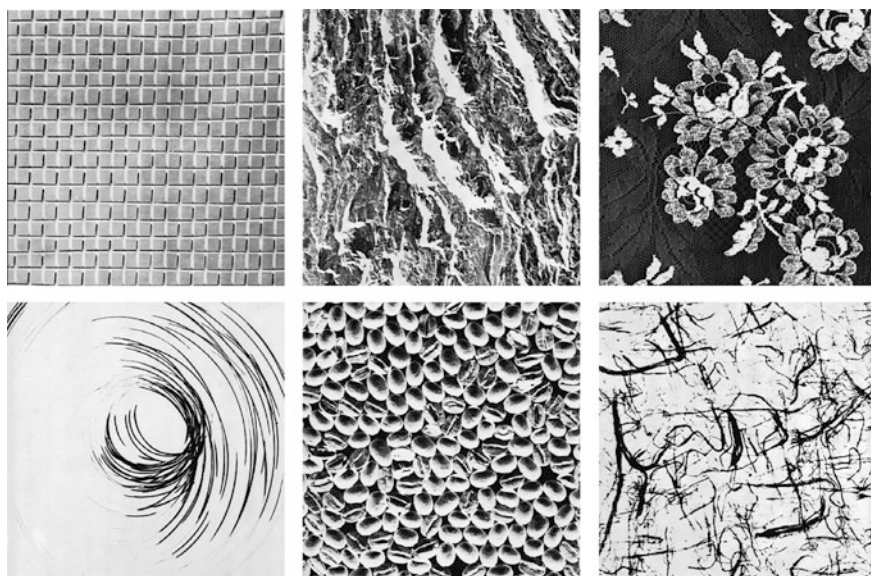
The second database is *Brodatz*<sup>2</sup> database. This dataset is composed of 112 textured images, having  $640 \times 640$  pixels size. In this paper, we have divided each image into 16 non-overlapping sub-images ( $4 \times 4$ ). Thus, the total number of images is 1792 images, 16 images in each class. Figure 4 presents some samples from this database.

<sup>1</sup>[http://www.outex.oulu.fi/db/classification/tmp/Outex\\_TC\\_00000.tar.gz](http://www.outex.oulu.fi/db/classification/tmp/Outex_TC_00000.tar.gz).

<sup>2</sup>[http://multibandtexture.recherche.usherbrooke.ca/images/Original\\_Brodatz.zip](http://multibandtexture.recherche.usherbrooke.ca/images/Original_Brodatz.zip).



**Fig. 3** Some samples from Outex database ( $128 \times 128$  px)



**Fig. 4** Some samples from Brodatz database ( $640 \times 640$  px)



The performance evaluation is done through the Average Precision (AP) criterion. The AP of texture class  $I$ , which contains  $m$  samples, within a window of  $k$  images (the number of retrieved images), is calculated as follows:

$$AP(I, k) = \frac{\sum_i^m p(i, k)}{m} \quad (8)$$

$$p(i, k) = \frac{\text{Nbr Relevant Retrieved Images}}{k} \quad (9)$$

## 5 Results and Discussion

Table 1 presents the results of the retrieval using the proposed algorithm based on the MSR versus Euclidean distance metric in term of the average precision of the top 20 images retrieved (i.e.  $k = 20$ ), over all database. The table shows clearly that the MSR is more effective than Euclidean metric, where an AP of 87.68 % overall the database is reached against 85.18 % for Euclidean distance. More of that, the results analysis by class show that when Euclidean reaches 90 % of AP, the MSR gives a perfect AP (100 %) (With the exception, the class C3).

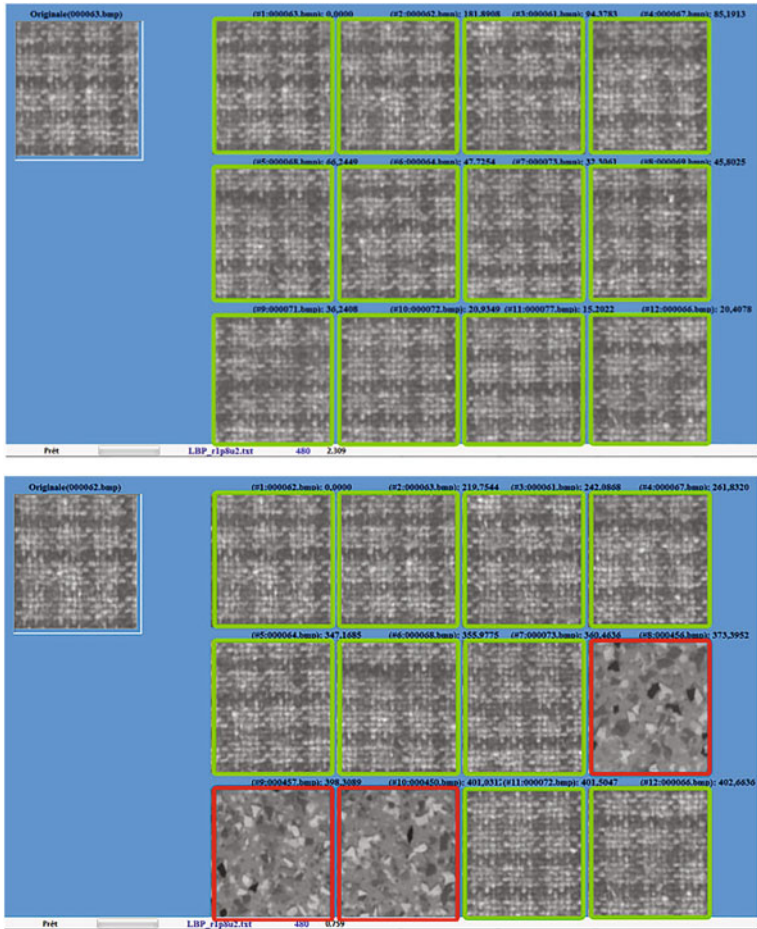
The second table (Table 2) presenting the AP for the second database (Brodatz) of the top 16 retrieved images, also shows an interesting performance for the

**Table 1** Outex\_tc\_00000 database (precision, window = 20)

Texture	Proposed	Euclidean	Texture	Proposed	Euclidean
C0	<b>100</b>	96.5	C12	<b>100</b>	95.5
C1	<b>100</b>	96	C13	50	<b>50.3</b>
C2	<b>100</b>	90.5	C14	40	<b>50.5</b>
C3	<b>99.5</b>	90.5	C15	<b>74</b>	67.5
C4	100	100	C16	56.3	<b>57</b>
C5	100	100	C17	<b>58</b>	55.3
C6	100	100	C18	<b>100</b>	97.3
C7	100	100	C19	<b>78.8</b>	74.5
C8	<b>100</b>	98.3	C20	<b>100</b>	96
C9	<b>77.8</b>	68.3	C21	<b>100</b>	99.8
C10	100	100	C22	<b>95</b>	89
C11	<b>100</b>	99	C23	<b>75</b>	72.5
			<b>Total</b>	<b>87.68</b>	85.18

**Table 2** Brodatz database (16 sub-images \* 112)

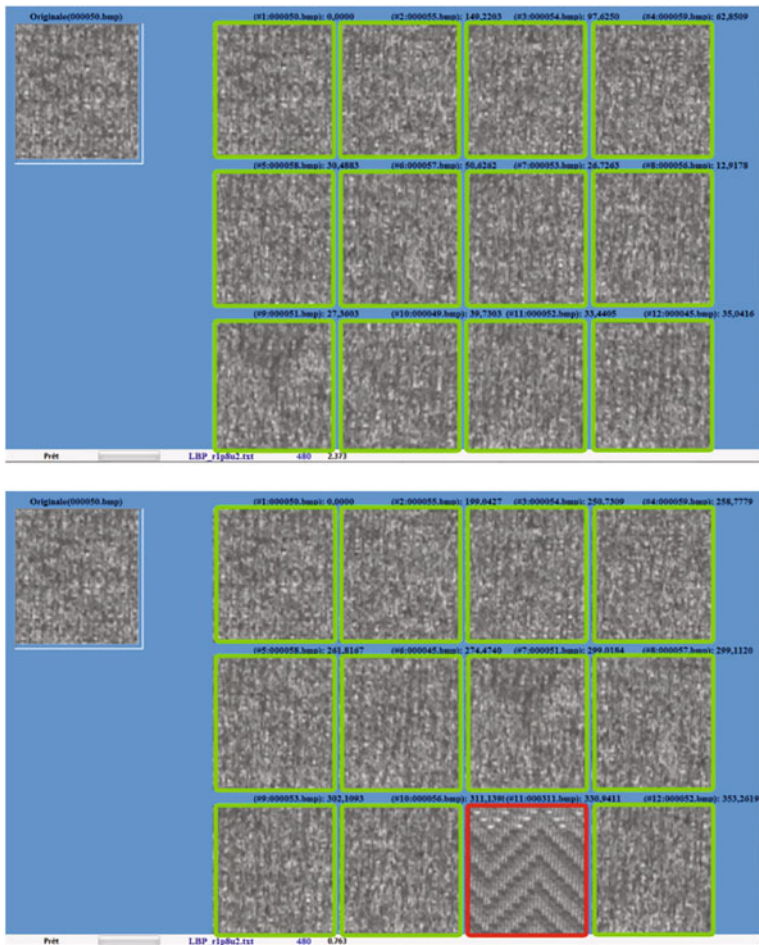
Texture	Proposed	Euclidean	Texture	Proposed	Euclidean	Texture	Proposed	Euclidean
D1	<b>94.5</b>	89.8	D39	25	<b>32.8</b>	D77	100	100
D2	43.4	<b>44.1</b>	D40	<b>99.2</b>	86.7	D78	<b>100</b>	85.2
D3	63.7	<b>72.7</b>	D41	<b>93.8</b>	85.2	D79	<b>94.1</b>	85.5
D4	<b>74.2</b>	73	D42	58.6	<b>66.4</b>	D80	<b>100</b>	89.1
D5	45.3	<b>49.6</b>	D43	13.3	<b>17.6</b>	D81	<b>100</b>	94.9
D6	100	100	D44	19.1	<b>21.9</b>	D82	<b>100</b>	95.3
D7	43	<b>46.1</b>	D45	14.1	<b>23</b>	D83	100	100
D8	39.8	<b>41.4</b>	D46	<b>94.1</b>	82.4	D84	<b>100</b>	99.2
D9	<b>59.4</b>	55.9	D47	<b>100</b>	96.5	D85	<b>100</b>	99.2
D10	<b>94.5</b>	85.2	D48	<b>71.1</b>	62.9	D86	<b>100</b>	98.8
D11	60.2	<b>63.3</b>	D49	100	100	D87	94.1	<b>94.9</b>
D12	<b>89.5</b>	78.9	D50	<b>94.5</b>	80.9	D88	26.2	<b>40.6</b>
D13	25	<b>36.7</b>	D51	<b>83.6</b>	81.6	D89	39.8	<b>49.6</b>
D14	94.1	<b>94.9</b>	D52	<b>100</b>	99.2	D90	48.8	<b>50</b>
D15	<b>58.2</b>	56.6	D53	100	100	D91	33.2	<b>40.2</b>
D16	100	100	D54	44.5	<b>48.4</b>	D92	<b>98</b>	94.1
D17	<b>100</b>	94.5	D55	100	100	D93	50	<b>66</b>
D18	<b>100</b>	89.5	D56	100	100	D94	61.3	<b>62.9</b>
D19	67.6	<b>69.9</b>	D57	100	100	D95	<b>89.1</b>	85.2
D20	100	100	D58	28.9	<b>33.2</b>	D96	<b>87.9</b>	84
D21	100	100	D59	14.8	<b>23.4</b>	D97	50.4	50.4
D22	<b>53.9</b>	52.7	D60	<b>72.7</b>	66.4	D98	<b>61.7</b>	57
D23	33.2	<b>41.4</b>	D61	<b>69.1</b>	63.3	D99	36.7	<b>41</b>
D24	<b>82.8</b>	72.3	D62	<b>65.6</b>	63.7	D100	36.7	<b>39.5</b>
D25	63.3	<b>66.4</b>	D63	31.3	<b>35.5</b>	D101	<b>100</b>	97.3
D26	<b>87.5</b>	80.9	D64	100	100	D102	<b>100</b>	98.8
D27	<b>50</b>	49.2	D65	100	100	D103	<b>100</b>	97.3
D28	<b>94.1</b>	85.2	D66	<b>94.9</b>	89.5	D104	<b>94.1</b>	87.1
D29	<b>100</b>	92.2	D67	<b>88.7</b>	80.5	D105	76.6	<b>79.7</b>
D30	41	<b>48</b>	D68	<b>97.7</b>	96.1	D106	60.5	<b>70.3</b>
D31	29.3	<b>36.3</b>	D69	48	<b>49.6</b>	D107	47.3	<b>53.1</b>
D32	100	100	D70	<b>100</b>	97.3	D108	<b>68</b>	67.2
D33	<b>100</b>	98.8	D71	<b>71.1</b>	68.8	D109	<b>99.2</b>	91.8
D34	<b>98</b>	86.7	D72	30.1	<b>38.7</b>	D110	<b>100</b>	99.2
D35	28.9	<b>33.2</b>	D73	32.8	<b>41.4</b>	D111	<b>100</b>	79.7
D36	29.7	<b>41</b>	D74	<b>93</b>	77.3	D112	<b>83.2</b>	74.6
D37	<b>82</b>	80.9	D75	<b>92.6</b>	86.7			
D38	36.7	<b>42.2</b>	D76	<b>100</b>	93.4	<b>Total</b>	<b>73.59</b>	72.67



**Fig. 5** Results obtained by querying with image #000062; *top* proposed method (precision = 12/12), *bottom* retrieval using Euclidean distance (precision = 9/12)

proposed method against Euclidean distance. Actually, the proposed method beats the Euclidean distance 57 times, and loses 40 times, and shows comparable performance to the Euclidean distance in 15 classes.

The screenshots of the results obtained using the proposed method and Euclidean distance on two different queries are shown in Figs. 5 and 6.



**Fig. 6** Results obtained by querying with image #000050; *top* proposed method (precision = 12/12), *bottom* retrieval using Euclidean distance (precision = 11/12)

## 6 Conclusion

In this paper, we have proposed a new algorithm for image retrieval based on texture. Specifically, we have used the uniform-LBP for extracting texture features. The proposed algorithm is based on the Mean Squared Residue measure, an existing measure originally proposed for biclustering of gene expressions data. Our algorithm starts by initialization of the result set to empty. Then, in each iteration, a new image is selected from the database images and added to the result set, so that the overall homogeneity of the result set is preserved most. The algorithm is distinguished by the fact that all images in the result set contribute to the selection of the new image through the difference of the MSR measures.

The obtained results of the conducted experimentation on Outex and Brodatz databases show an interesting performance (Average Precision) compared to the uniform-LBP combined to Euclidean distance.

In the future, we plan investigation of the proposed algorithm performance using other descriptors, such as color histograms, and also combination with other standard metrics (Canberra, Manhattan, etc.). Furthermore, the adaptation of the proposed algorithm for features selection is also envisaged.

## References

1. Cheng, Y., Church, G.M.: Biclustering of expression data. In: Proceedings of the Eighth International Conference on Intelligent Systems for Molecular Biology (2000)
2. Liu, Y., Zhang, D., Lu, G., Ma, W.-Y.: A survey of content-based image retrieval with high-level semantics. *Pattern Recogn.* **40**, 262–282 (2007)
3. Haralick, R.M., Shanmugam, K., Dinstein, I.H.: Textures features for image classification. *IEEE Trans. Syst. Man Cybern.* **SMC-3**, 610–621 (1973)
4. Ojala, T., Pietikäinen, M., Mäenpää, T.: Multiresolution gray-scale and rotation invariant texture classification with local binary patterns. *IEEE Trans. Pattern Anal. Mach. Intell.* **24**, 971–987 (2002)
5. Ojala, T., Pietikäinen, M., Harwood, D.: A comparative study of texture measures with classification based on feature distributions. *Pattern Recogn.* **29**, 51–59 (1996)
6. Ahonen, T., Hadid, A., Pietikäinen, M.: Face description with local binary patterns: application to face recognition. *IEEE Trans. Pattern Anal. Mach. Intell.* **28**, 2037–2041 (2006)
7. Yang, Z., Ai, H.: Demographic classification with local binary patterns. In: Lee, S.-W., Li, S. (eds.) *Advances in Biometrics*, vol. 4642, pp. 464–473. Springer, Berlin (2007)
8. Tang, Z., Su, Y., Er, M.J., Qi, F., Zhang, L., Zhou, J.: A local binary pattern based texture descriptors for classification of tea leaves. *Neurocomputing* **168**, 1011–1023 (2015)
9. Jin, H., Liu, Q., Lu, H., Tong, X.: Face detection using improved LBP under Bayesian framework. In: Proceedings of the Third International Conference on Image and Graphics (ICIG'04) 2004
10. Tan, X., Triggs, B.: Enhanced local texture feature sets for face recognition under difficult lighting conditions. *Anal. Model. Faces Gestures* **4778**, 168–182 (2007)
11. Liao, S., Law, M.W.K., Chung, A.C.S.: Dominant local binary patterns for texture classification. *IEEE Trans. Image Process.* **18**, 1107–1118 (2009)
12. Takala, V., Ahonen, T., Pietikäinen, M.: Block-based methods for image retrieval using local binary patterns. In: Kalviainen, H., Parkkinen, J., Kaarna, A. (eds.) *Image Analysis*, vol. 3540, pp. 882–891. Springer, Berlin (2005)
13. Bougueroua, S., Boucheham, B.: Ellipse based local binary pattern for color image retrieval. In: ISKO-Maghreb: Concepts and Tools for knowledge Management (ISKO-Maghreb), 2014 4th International Symposium, pp. 1–8. Algiers, Algeria (2014)
14. Bougueroua, S., Boucheham, B.: GLIBP: gradual locality integration of binary patterns for scene images retrieval. Accepted for publication in the Journal of Information Processing Systems (JIPS), ISSN: 1976-913x(print), ISSN: 2092-805x(online), the official international journal of the Korea Information Processing Society
15. Huang, Z.-C., Chan, P.P.K., Ng, W.W.Y., Yeung, D.S.: Content-based image retrieval using color moment and Gabor texture feature. In: Ninth International Conference on Machine Learning and Cybernetics (ICMLC), 2010. Qingdao (2010)
16. Jasmine, K.P., Kumar, P.R.: Integration of HSV color histogram and LMEBP joint histogram for multimedia image retrieval. In: *Intelligent Computing, Networking, And Informatics*, vol. 243, pp. 753–762. Springer, India (2014)

17. Palm, C.: Color texture classification by integrative co-occurrence matrices. *Pattern Recogn.* **37**, 965–976 (2004)
18. Zhou, J., Xu, T., Gao, W.: Content based image retrieval using local directional pattern and color histogram. In: *Optimization and Control Techniques and Applications*, vol. 86, pp. 197–211. Springer, Berlin (2014)
19. Wang, X.-Y., Zhang, B.-B., Yang, H.-Y.: Content-based image retrieval by integrating color and texture features. *Multimedia Tools Appl.* **68**, 545–569 (2014)
20. Huang, P.W., Dai, S.K.: Image retrieval by texture similarity. *Pattern Recogn.* **36**, 665–679 (2003)
21. Tiecheng, S., Hongliang, L., Bing, Z., Gabbouj, M.: Texture classification using joint statistical representation in space-frequency domain with local quantized patterns. In: *2014 IEEE International Symposium on Circuits and Systems (ISCAS)*, pp. 886–889 (2014)
22. Ma, W.Y., Manjunath, B.S.: Texture features and learning similarity. In: *1996 IEEE Computer Society Conference on Computer Vision and Pattern Recognition, 1996. Proceedings CVPR '96*, pp. 425–430 (1996)
23. Swain, M.J., Ballard, D.H.: Color indexing. *Int. J. Comput. Vision* **7**, 11–32 (1991)
24. Rubner, Y., Tomasi, C., Guibas, L.: The Earth mover's distance as a metric for image retrieval. *Int. J. Comput. Vision* **40**, 99–121. 2000/11/01 2000
25. Wei-Ta, C., Wei-Chuan, L., Ming-Syan, C.: adaptive color feature extraction based on image color distributions. *IEEE Trans. Image Process.* **19**, 2005–2016 (2010)
26. Zhang, Q., Canosa, R.L.: A comparison of histogram distance metrics for content-based image retrieval, pp. 902700–902700-9 (2014)
27. Patil, S., Talbar, S.: Content based image retrieval using various distance metrics. In: Kannan, R., Andres, F. (eds.) *Data Engineering and Management*, vol. 6411, pp. 154–191. Springer, Berlin (2012)
28. Madeira, S.C., Oliveira, A.L.: Biclustering algorithms for biological data analysis: a survey. *IEEE/ACM Trans. Comput. Biol. Bioinform.* **1**, 24–45 (2004)

# Clustering to Enhance Case-Based Reasoning

Abdelhak Mansoul and Baghdad Atmani

**Abstract** In this article, we propose an approach to improve CBR processing mainly in its retrieval task. A major difficulty arise when founding several similar cases and consequently several solutions, hence a choice must be done involving an appropriate strategy focusing the best solution. This main difficulty has a direct impact on the adaptation task. To overcome this limitation many works related to the retrieval task were conducted as hybridizing CBR with data mining methods. Through this study, we provide a combining approach using CBR and clustering to reduce the search space in the retrieval step. The objective is to consider only the most interesting cases and the most interesting solution to support decision and provide an intelligent strategy that enables decision makers to have the best decision aid. We also present some preliminary results and suggestions to extend our approach.

**Keywords** Decision • Support • Case-based reasoning • CBR • Clustering

## 1 Introduction

The traditional CBR approach has been widely used for enhancing decision aid systems. However it presents some drawbacks mainly in the retrieval task [1–3]. A major drawback is that if process found several similar cases and consequently several solutions which involve looking for a strategy to choose the best solution. Several works were conducted to overcome this drawbacks [2, 4–8] by using

---

A. Mansoul (✉)

Department of Computer Science, University of Skikda, Skikda, Algeria  
e-mail: mansoul21@gmail.com

A. Mansoul

Lio Laboratory, University of Oran 1 Ahmed Ben Bella, Oran, Algeria

B. Atmani

University of Oran 1 Ahmed Ben Bella, Oran, Algeria  
e-mail: atmani.baghdad@gmail.com

different strategies with the aim to impact positively the CBR process. In this work, we experiment collaboration between CBR and clustering. Case-based reasoning approach emerged, it was appropriated and widely used to solve problems and support decision in health care, however it presents also some drawbacks in the two mean tasks: the retrieval and the adaptation (reuse and revision) tasks [1–3]. Thus, and as the two tasks are interrelated several works have been conducted on the retrieval task using different strategies which deals with suitable solutions with the aim to impact positively the adaptation task. These solutions are range from simple sequential calculation to non-sequential indexing, classification algorithms such as ID3 and Nearest Neighbor matching. For the retrieval task, a major drawback is that if process found several similar cases and consequently several solutions, hence choice arises for the process and involves looking for a strategy to choose the best solution. Schmidt et al. suggested clustering cases into prototypes and remove redundant ones to avoid an infinite growth of case base, the retrieval searches only among these prototypes [2]. This solution can simplify the adaptation task. Missing similar cases can also occur and may lead to less robust decision due to large number of features. Marling et al. suggested a solution at retrieval task using a three matching algorithms and combined three different measures and fuzzy similarity and they also proposed another solution using a reutilisability measure to select and retrieve a case in addition to check of constraints and a scoring. This method gives the easiest case to adaptation task. This solution was used to propose a menu planer system based on CBR and RBR [6]. Thus, it becomes imperative to review traditional approaches of knowledge processing and to propose new solutions based on new paradigms.

In this work, we experiment a new method by using collaboration between CBR and clustering to propose an available strategy at retrieval task which permits choosing the best solution from a set of solutions found by clustering a case base. We present some preliminary results and suggestions to extend and improve our approach. The rest of this paper is structured as follows: in Sect. 2 we give some notions on CBR and data mining. In Sect. 3 we give a survey on most important related works showing particularly the use of case-based reasoning and data mining that have contributed in decision aid. We continue by presenting our approach in Sect. 4. In Sect. 5 we give a presentation of experimentation and interpretation of results and finally in Sect. 6 we give the conclusion which summarizes the paper and point out a possible trend.

## 2 Background

Before describing our approach we will give some notions related to decision support to help for understanding the continuation of the paper:

**Decision support:** “Decision support is the activity that is supported by models clearly explained but not necessarily completely formalized, which helps to obtain some answers to questions asked by an intervener in a decision process,...” [9].



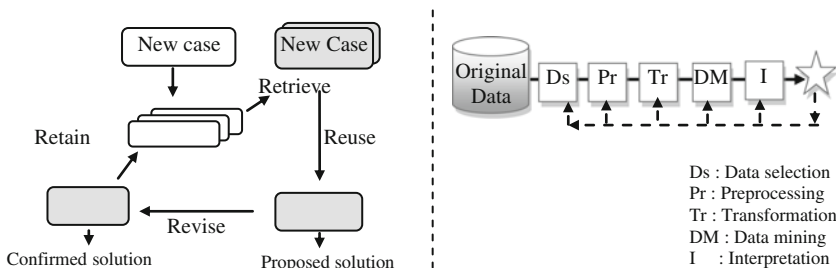
This decision aid is often supported by methods such as statistics, operations research, multi-criteria methods, etc. The decision support involves the development of an action plan or a decision model.

**CBR:** Reasoning by reusing past cases is a powerful and frequently applied approach to solve problems. The case-based reasoning uses this principle. It is conventionally based on four tasks: retrieve, reuse, revise and retain as shown in Fig. 1. It is widely used in medicine, because of the reasoning method used, which is close to the physician reasoning against a pathological situation. Indeed, finding a medical solution is based on reminding previous cases already experienced for being guided toward a similar situation [10]. Figure 1 shows four steps that a case-based reasoner must perform according to Aamodt and Plaza [11]:

- (a) retrieve cases which are similar to the problem description from a case base, this task involves analogy-making or case matching, it is based on reminding,
- (b) reuse a solution suggested by the retrieved cases in order to make it applicable to the current case,
- (c) revise or adapt the solution to better fit the new case,
- (d) retain the new solution once it has been confirmed or validated.

**Data mining:** Data mining uses a variety of methods and a large volumes of data in order to discover useful knowledge for decision making. Thus, it constitutes a decision aid support in various sectors. We mention here some data mining methods commonly used in the medical field:

- Decision trees. These are structures that represent sets of decisions. These decisions generate rules for the classification of a data set.
- Neural networks. They are at the origin of mathematical modeling of the human brain. They use existing data with a known result to form a model that can later be used to make predictions upon data with unknown result.
- Bayesian networks. They are a directed acyclic graph where each node represents a random variable and the arcs represents probabilistic dependencies between a node and its parents.



**Fig. 1** The CBR cycle and standard data mining process

- The K-nearest neighbors. It is a case reasoning method dedicated to the classification. It allow making decisions by searching for similar cases already resolved.
- Logistic regression. It is a method derived from statistics. It is an extension of ordinary regression.
- Clustering. Its divides data into meaningful groups (clusters) that share common characteristics. It is used in information retrieval.

## ***2.1 Data Mining and CBR***

Data Mining can be used for a variety of purposes in Case-Based Reasoning. Some uses are listed here:

- Find features for a case (in a case base): It might be interest to classify the cases for use.
- Find features for a case (in a database): A data base can be searched to complete the information given in a case.
- Find domain knowledge: Domain knowledge might be mined from the data in the form of functions, rules or causal graphs which can be used later by a CBR process.
- Construct “artificial cases”: We should be able to build cases from a database.

## **3 Related Works**

As mentioned in introduction, there is a large body of work attempting to use CBR in medical fields particularly in the diagnosis of diseases. Many works have addressed directly the use of CBR while other works were conducted with other approaches and many recent works have emerged and have contributed to the advancement of research. We notice the following concerns.

### ***3.1 Use of Case-Based Reasoning***

Many studies concerning CBR in decision support were conducted. Marling et al. presented an approach for treatment of patients suffering from diabetes [12]. Jha et al. presented a work for diabetes detection and care [13]. Bresson and Lieber created CASIMIR, a system for treatment of breast cancer [14]. Shanbezadeh et al. proposed an oriented decision support system for treatment of asthma [15]. Song et al. proposed a system for dose planning in radiotherapy for prostate cancer [16].

Begum et al. presented a decision support system to help physicians to diagnose the state of stress [17]. De Paz et al. presented a decision support system for the diagnosis of different types of cancer [18]. Schwartz et al. used also CBR to enhance care on insulin therapy [19]. This list is not exhaustive but it shows the diversity of utilization of CBR and underlines the interest for this approach to improve the care of patients by providing physicians with information technology tools for medical decision support.

### ***3.2 Use of Data Mining***

Owing to the large volume of data manipulated by health structures, it became imperative to take into account this mass of medical data to improve medical practice and at the same time improve the care practiced by clinicians. These methods and particularly the decision trees and the neural networks have been used in many studies in medicine [17, 20]. We give a non-exhaustive list of some research works which uses data mining methods in a medical field. Sivakumar presented a method based on the neural networks to classify subjects with diabetic retinopathy (common complications of diabetes) [21]. This algorithm generates a set of rules for the diagnosis and prediction of diabetes. Kiezun et al. have used logistic regression to help clinicians in the diagnosis of myocardial infarction (heart attack) in patients presenting chest pain [22]. Malyshevska studied the problem of cancer diagnosis using the neural networks [20]. The aim of this study is to classify different types of tissue that are used to determine the risk of cancer. Sung and Seong recently done a study based on the building of a hybrid method, combining methods of data mining (association rules, classification trees) to help clinicians to classify more faster and more accurate chest pain diseases [23]. Xu Li used an indexing/matching module based on retrieving only cases that match the important indices of the new case, calculate an aggregate match score for the comparable cases and retrieve only those comparable cases with higher aggregate match scores [7]. Kumar et al. used two distances (Weighted Euclidean, Mahalanobis) to perform retrieval task and eliminate bad cases with an eliminating score [8]. Macura and Macura used a retrieval-only system to avoid the adaptation task, because the users wish to see and interpret all specific details of the cases themselves without going until adaptation task [24]. Bichindaritz and Marling have used combination of RBR and model based components but this strategy can't be seen as solution for CBR drawbacks (for retrieval or adaptation), but as an opportunity to enhance CBR subtasks instead of using an older technique. Recently, a major trend seems to be the extending of CBR applications beyond the traditional diagnosis or treatment toward the applicability of CBR to new reasoning tasks [1].

### 3.3 Combining CBR with Other Approaches

Combining CBR with other approaches (Multi-Modal Reasoning) represents another way used to avoid the adaptation problem, mainly by combining the retrieval task with other reasoning strategies, to provide decision support. The interest in multi-modal approaches involving CBR has reached the medical areas [2]. This is an issue of current concern in CBR research in different fields as medicine and others [10]. The first multi-modal reasoning system in the health care was CASE, it integrated CBR with model-based reasoning (MBR) for diagnosis of heart failures [6]. Araujo et al. have combined rule-based reasoning (RBR) and CBR to recommend neuroleptic drugs for Alzheimer's patients [25]. Althoff et al. have integrated induction and CBR for diagnostic [4]. Janetzko and Strube also tried to combine CBR with knowledge processing [26]. Li and Sun hybridized multi-criteria and CBR to enhance a data mining process for improving detection of disease [27]. Armaghan and Renaud used also combination of CBR and multi-criteria to study diabetes [5]. Angehrn and Dutta used also this combination to study diabetes [28]. Royes used multi-criteria and CBR for strategic planning support [29]. Araujo de Castro et al. used a hybrid model based on multi-criteria and CBR to diagnosis of Alzheimer's disease [25]. Other researchers have proposed hybrid solution by combining CBR with other techniques as reasoning by rules and many works emerged among these studies [6, 30].

## 4 The Proposed Approach

The medical situation we advocate is described by the decision maker (physician) is in front of a diagnosis of a situation and will have to explore possible options (diagnosis) to choose the best therapy. This situation is characterized by: a problem definition more or less complete, an exhaustive survey of possible diagnosis and the existence of specific signs for each patient such as for example "elderly patient", "allergy to penicillin", etc. these specific signs can indicates that a desired therapy will be more or less compliant as an elderly patient may be less compliant with a salt diet for example. Moreover, it is well recognized today that diagnosis decisions related to each patient must take into account particular signs (drug risk, medication side effects, dosages, etc.). Moreover, the physician reasons when searching for a therapy such a system which uses old situations (cases) in order to propose a similar or a best therapy.

Thus, the physician defines his medical situation with a set of symptoms and an environmental context described by the specific signs. The medical situation becomes a medical case composed of  $u$  specific signs, and  $v$  symptoms which are descriptive of the case and  $w$  descriptors giving the "diagnosis/therapy" considered for the case in question.

Thus, the medical situation will be defined as follows:

```

Medical_situation={Specific_Signs, Symptoms, Diagnosis}.
Medical_case
Specific_Signs : ss1=value1 , ..., ssu=valueu
Symptoms : symptom1=value1 , ..., symptomv=valuev
Diagnosis : Diagnosis1 , ..., Diagnosisw
End_medical_case.

```

**The contribution of data mining.** However, specific signs can guide search space reduction while using a clustering technique. Clustering does not aim at labeling the cases in a group with a specific tag (as it happens in classification), where the tag represents a piece of generalized domain knowledge, extracted from the subsumed cases. In clustering specific signs remains enables collecting the most similar cluster (s) allow the identification of the cases collected under similar circumstances, and the limitation of retrieval just to them. In result we can have exploitation of prototypes which are a generalization from single to clustered typical cases. Their main purposes are to structure the case base and to guide and speedup the retrieval process.

## 4.1 Processing

In this work, we experiment a new method by using collaboration between CBR and data mining to propose an available strategy at retrieval task which permit choosing the best solution from a set of solutions found by mining cases by a so called constraint based clustering.

**The constraint based clustering process:** We chose a rational approach for retrieval task: instead of a massive retrieval of cases that is the classic recipe of reasoning, we analyze the cases rationally and we focus research on particular perimeters with specific cases that are the subject of suspicion or potential cases. Our aim is to find closest cases on all previously treated cases in order to avoid complication at the adaptation phase and make it arduous. Indeed, it doesn't matter to collect all the closest cases, but it should rather focus on a small perimeter of cases. So, we must proceed otherwise than by classical method. Thus, our approach focuses on reducing the perimeter of research, and then retrieve. We will call it: *MineR* for Mining and Retrieve.

From there, the clustering operation is guided by specific signs to select a subset of cases contained in the case base. Thus, reducing the search space solutions (diagnoses) for the retrieval step becomes an essential operation for the CBR process. This choice can clearly make retrieval computationally better regarding to only interesting solution for the case being processed and hopefully more meaningful, since only cases taken under comparable circumstances are retrieved. The set of closest diagnoses (*Closest\_Diags*) is received from the CBR\_Process to join it to proposed diagnoses (*Proposed\_Diags*) that the user has already defined in the medical situation as described below (see also step C). This process will be handled by the following steps:

**Step A: Cases selection**

A this step, the specific signs help to filter the cases so as to keep only cases which meet only those constraints, then we proceed successively by steps B and C.

**Step B: Preprocessing**

At this step, we will only prepare data for clustering as cleaning data or appropriate treatment.

**Step C: Clustering**

At this step, we will launch the suitable clustering method. This entire step will be initiated by the following pseudo\_algorithm which will generate the best cluster (Best\_cluster) for processing later the best diagnosis (Best\_Diag) by the CBR.

**The CBR process:** This process has a main task: the matching. It consists in finding the  $n$  closest cases to the proposed case by using a similarity measure. We used the K-nn method for the simplicity of its implementation. The process will select closest or similar cases from the best cluster (Best\_cluster) proposed by clustering process, and will extract the preliminary closest diagnoses (Closest\_Diags) that have been considered for the  $n$  similar cases, and then those preliminary closest diagnoses are considered to determine the best diagnosis (Best\_Diag).

All this two process will be handled by the following pseudo-algorithm.

```
Pseudo_algorithm : CBR_Miner_Process
1: Input : Closest_Diags • ∅
2: New_Case (Ss, Sy, Proposed_diags)
3: Begin MineR_Process ()
  a) Best_cluster • Clustering ()
  b) Closest_cases • Extraire (Best_cluster)
  c) Accept_or_refuse (Best_cluster)
  d) If accept = "yes" then go to step 5
      Else Review any step: 2 or 3
  Endif
4: End MineR_Process ()
5: Initialize k
6: Closest_Diags=Proposed_diags
7: Closest_cases•Retrieve (New_Case, Best_Cluster, K-
  nn)
8: If Closest_Cases•∅ then
  For each Current_Case in Closest_Cases
  For i=1 to n
    {Closest_Diags• Closest_Diags U Current_Case (
    Diagnosisi)}
  Endfor
  Endfor
  Else
  EndIf
9: Reuse ()
10: Revise ()
11: If confirmed_solution="yes" then
  Specific_Signs =Ss
  Symptoms=Sy
  Diagnosis=Best_Diag
  Produce_New_Case (Specific_Signs, Symptoms, Diagnosis)
  Retain_New_Case ()
  Endif
  New_Case (∅, ∅, ∅)
12: End
```

## 5 Implementation and Experimentation

The proposed approach has been applied to a medical datasets the Vertebral Column Data Set of orthopaedic patients, we project to use the presumptive diagnosis of diseases of orthopaedic patients data set which is a data set containing values for six biomechanical features used to classify orthopaedic patients into 3 classes (normal, disk hernia or spondylolisthesis) [31]. Each patient is represented in the data set by six biomechanical attributes derived from the shape and orientation of the pelvis and lumbar spine (in this order): pelvic incidence, pelvic tilt, lumbar lordosis angle, sacral slope, pelvic radius and grade of spondylolisthesis. The following convention is used for the class labels: DH (Disk Hernia), Spondylolisthesis (SL), Normal (NO) and Abnormal (AB).

### 5.1 Data Description

This data contains information about diseases of orthopaedic patients (normal, disk hernia or spondylolisthesis) of a patient based on his characteristics. Figure 2 gives an overview of data set sample.

Each patient is described by seven descriptors, with the last attribute that contains the results of the diagnosis. It contains [31]:

1. pelvic incidence (numerical)
2. pelvic tilt (numerical)
3. lumbar lordosis angle (numerical)
4. sacral slope (numerical)
5. pelvic radius (numerical)
6. grade of spondylolisthesis (numerical)
7. diagnosis: DH (Disk Hernia), Spondylolisthesis (SL), Normal (NO) and Abnormal (AB).

Data Set sample
39.05695098,10.06099147,25.01537822,28.99595951,114.4054254,4.564258645,Hernia
68.83202098,22.21848205,50.09219357,46.61353893,105.9851355,-3.530317314,Hernia
83.93300857,41.28630543,61.99999999,42.64670314,115.012334,26.58810016,Spondylolisthesis
78.49173027,22.1817978,59.99999999,56.30993248,118.5303266,27.38321314,Spondylolisthesis

Fig. 2 Overview of presumptive diagnosis of diseases of orthopaedic patients sample [31]

**Table 1** Case base descriptors

Descriptor	Label
$X_1$	Pelvic incidence
$X_2$	Pelvic tilt
$X_3$	Lumbar lordosis angle
$X_4$	Sacral slope
$X_5$	Pelvic radius
$X_6$	Grade of spondylolisthesis
Y	Diagnosis

For the purposes of our experimentation we have transformed Presumptive diagnosis of diseases of orthopaedic patients data set descriptors into a case base descriptors and each case will be described by the set of variables  $X_1, X_2, \dots, X_6$ , called descriptive variables and we have associated a target attribute denoted Y corresponding to diagnosis. The following Table 1 shows case base descriptors.

## 5.2 Construction of Case Base $\Omega_N$ and Partial Case Bases $\Omega_L, \Omega_T$

To evaluate the efficacy of our approach, we have transformed the presumptive diagnosis of diseases of orthopaedic patients date set into a case base named  $\Omega_N$ . It contains a number of cases  $\omega_i \cdot \Omega_N = \{\omega_1, \omega_2, \dots, \omega_n\}$ , each case is described by the set of variables  $X_1, X_2, \dots, X_6$ , called descriptive variables. For each case  $\omega_i$  we associate a target attribute denoted Y, which takes its values in the set  $Y = \{DH, SL, NO, AB\}$  corresponding to diagnosis where DH = "Disk Hernia", SL = "Spondylolisthesis", NO = "Normal" and AB = "Abnormal". Table 2 shows some cases noted  $\omega_1, \omega_2, \dots, \omega_n$  of Vertebral Column Case Base.

After construction of case base  $\Omega_N$ , we subdivide it on a learning case base  $\Omega_L$  (80 % of  $\Omega_N$ ) and a test case base  $\Omega_T$  (20 % of  $\Omega_N$ ) by separating the population  $\Omega_N$  as follows in Table 3.



**Table 2**  $\Omega_N$

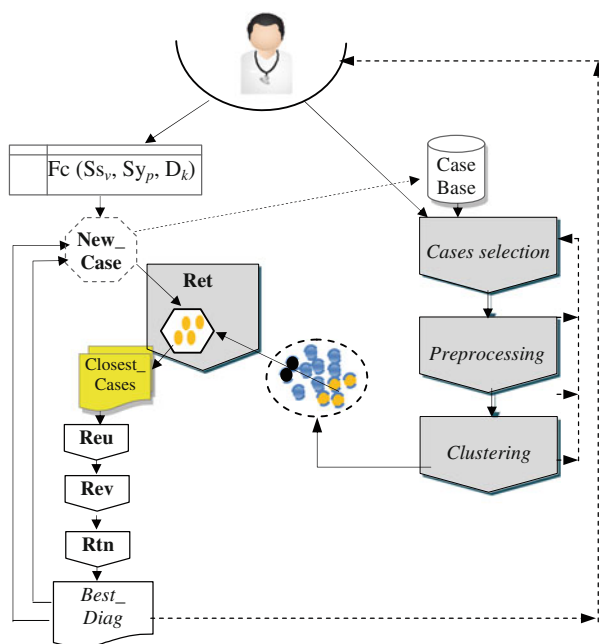
$\omega$	$X_1(\omega)$	$X_2(\omega)$	$X_3(\omega)$	$X_4(\omega)$	$X_5(\omega)$	$X_6(\omega)$	$Y(\omega)$
$\omega_1$	63.0278175	22.55258597	39.60911701	40.47523153	98.67291675	-0.254399986	Hernia
...							
$\omega_i$	44.529051	9.433234213	51.99999999	35.09581679	134.7117723	29.10657504	Spondylolisthesis
...							
$\omega_h$							

**Table 3** Partial case bases

Case base $\Omega_N$	Learning case base $\Omega_L$ 80 %	Testing case base $\Omega_T$ 20 %
310	248	62

### 5.3 Implementation/Experimentation

Experiments are conducted on an interactive system developed in JAVA with an interconnection module to JCOLIBRI system [32]. This system is essentially based on an engine described by Fig. 3. We use the JCOLIBRI platform to build the case base and all the relative operations for CBR process. In first step clustering process is initiated, this operation is done under WEKA platform, helped with the specific signs to reach the different clusters, then the results of this platform is the generation of the best cluster (Best\_cluster) that will be returned to CBR process for collaboration to improve the decision support. The final objective of the whole process is to collaborate for deciding about the best diagnosis to each new case (medical situation) given as input.



**Fig. 3** Overview of the different steps involved by the approach. *Rtv* Retrieve similar cases, *Reu* Reuse a suggested solution, *Rev* Revise or adapt the solution, *Rtn* Retain the new solution, *Fc (Ss<sub>v</sub>, Sy<sub>p</sub>, D<sub>k</sub>)* Formulation\_of\_case (*v* Specific\_Signs, *p* Symptoms, *k* Diagnosis)

**Table 4** Comparison results of three data sets using the error rate (ER)

Number of Cases tested from $\Omega_T$	Type of diagnosis for tested cases	Misclassified cases	ER (%)
20	Normal	4	20
20	Disk Hernia	7	35
20	Spondylolisthesis	8	40

We have considered 20 cases randomly taken from the testing case base  $\Omega_T$  without any hypothesis of diagnosis. A comparison of each case under  $\Omega_T$  is done with the learning case base  $\Omega_L$  as follows:

$$\forall \omega_i \in \Omega_T \quad \text{and} \quad \forall \omega_j \in \Omega_L \quad \text{if} \quad \begin{cases} y(X(\omega_i) = y(X(\omega_j))) & \text{then good matching} \\ \text{else} & \text{mismatch} \end{cases} \quad (1)$$

Thereafter, with the conditional structure (1), we calculate the rate of correct matching. This rate represents the number of correctly identified cases in learning case base  $\Omega_L$  and identically diagnosed in testing case base  $\Omega_T$ . The test results are presented in Table 4.

## 5.4 Evaluation of Results

To evaluate the efficiency of our approach, a comparison of each case tested from  $\Omega_T$  is made in  $\Omega_L$ . We calculate the error rate of each type of diagnosis. From results presented in Table 4, we note that the error rate is relatively low (lower than average) which indicates that our system tends to give answers close to reality.

According to these results, we note that the rate of correct matching (similar diagnosis) is relatively high compared to the average which indicates that the system provides results closer to the reality as declared in testing case base  $\Omega_T$  answers particularly for good matching cases. We note also that the rate of good matching is more over than the average which indicates that our system tends to recognize and make a good matching of diagnosis.

## 6 Conclusion and Future Trends

This study provides the theoretical basis of an approach that tends to solve a problem of CBR reasoning. Later, we intend to evolve our approach in another orientation by using the concept of clustering in a form a rule and where each rule define a cluster then make a comparative study.

## References

1. Bichindaritz, I., Marling, C.: Case-based reasoning in the health sciences: foundations and research directions. *Computational Intelligence in Healthcare* 4, pp. 127–157. Springer, Berlin (2010)
2. Schmidt, R., Montani, S., Bellazzi, R., Portinale, L., Gierl, L.: Cased-based reasoning for medical knowledge-based systems. *Int. J. Med. Inform.* **64**(2), 355–367 (2001)
3. Montani, S.: Exploring new roles for case-based reasoning in heterogeneous AI systems for medical decision support. *Appl. Intell.* **28**(3), 275–285 (2008)
4. Althoff, K.D., Bergmann, R., Maurer, F., Wess, S., Manago, M., Auriol, E., Conruyt, N., Traphoner, R., Brauer, M., Dittrich, S.: Integrating inductive and case-based technologies for classification and diagnostic reasoning. In: *Proceedings ECML-93 Workshop on Integrated Learning Architectures* (1993)
5. Armaghan, N., Renaud, J.: An application of multi-criteria decision aids models for case-based reasoning. *Inf. Sci.* **210**, 55–66 (2012)
6. Marling, C., Rissland, E., Aamodt, A.: Integrations with case-based reasoning. *Knowl. Eng. Rev.* **20**(3), 241–245 (2005)
7. Xu, L.D.: An integrated rule-and case-based approach to AIDS initial assessment. *Int. J. Biomed. Comput.* **40**(3), 197–207 (1996)
8. Kumar, K.A., Singh, Y., Sanyal, S.: Hybrid approach using case-based reasoning and rule-based reasoning for domain independent clinical decision support in ICU. *Expert Syst. Appl.* **36**(1), 65–71 (2009)
9. Roy, B.: *Méthodologie multicritère d'aide à la decision*. Paris Economica (1985)
10. Begum, S., Ahmed, M., Funk, P., Xiong, N., Folke, M.: Case-based reasoning systems in the health sciences: a survey of recent trends and developments. *IEEE Trans. Syst. Man Cybern. Part C Appl. Rev.* **41**(4), 421–434 (2011)
11. Aamodt, A., Plaza, E.: Case-based reasoning: foundational issues, methodological variations, and system approaches. *AI Commun.* **7**(1), 39–59 (1994)
12. Marling, C., Jay, S., Schwartz, F.: Towards case-based reasoning for diabetes management: a preliminary clinical study and decision support system prototype. *Comput. Intell.* **25**(3), 165–179 (2009)
13. Jha, M.K., Pakhira, D., Chakraborty, B.: Diabetes detection and care applying CBR techniques. *Int. J. Soft Comput. Eng.* **2**(6), 132–137 (2013)
14. Bresson, B., Lieber, J.: Raisonement à partir de cas pour l'aide au traitement du cancer du sein. *Actes des journées ingénierie des connaissances*, pp. 189–196 (2000)
15. Shanbezadeh, M., Soltani, T., Ahmadi, M.: Developing a clinical decision support model to evaluate the quality of asthma control level. *Middle-East J. Sci. Res.* **14**(3), 387–393 (2013)
16. Song, X., Petrovic, S., Sundar, S.: A case-based reasoning approach to dose planning in radiotherapy. In: *7th International Conference on Case-based Reasoning ICCBR*, pp. 348–357 (2007)
17. Begum, S., Ahmed, M.U., Funk, P., Xiong, N., Von Schéele, B.: A case-based decision support system for individual stress diagnosis using fuzzy similarity matching. *Comput. Intell.* **25**, 180–195 (2009)
18. De Paz, F.J., Rodriguez, S., Bajo, J., Corchado, M.J.: Case-based reasoning as a decision support system for cancer diagnosis: a case study. *Int. J. Hybrid Intell. Syst.* **6**(2), 97–110 (2009)
19. Schwartz, F.L., Shubrook, J.H., Marling, R.: Use of case-based reasoning to enhance intensive management of patients on insulin pump therapy. *J. Diab. Sci. Technol.* **2**(4), 603–611 (2008)
20. Malyshevska, K.: The usage of neural networks for the medical diagnosis. *International Book Series. Inf. Sci. Comput* 77–80 (2009)
21. Sivakumar, R.: Neural network based diabetic retinopathy classification using phase spectral periodicity components. *ICGST-BIME J.* **7**(1), 23–28 (2010)

22. Kiezun, A., Lee, I.T.A., Shomron, N.: Evaluation of optimization techniques for variable selection in logistic regression applied to diagnosis of myocardial infarction. *Bioinformatics* **3**, 311–313 (2009)
23. Ha, S.H., Joo, S.H.: A hybrid data mining method for the medical classification of chest pain. *Int. J. Comput. Inf. Eng.* **4**(1) 33–38 (2010)
24. Macura, R.T., Macura, K.J.: *Macrad: radiology image resource with a case-based retrieval system*. Case-Based Reasoning Research and Development, pp. 43–54. Springer, Berlin (1995)
25. Araujo de Castro, A.K., Pinheiro, P.R., Dantas Pinheiro, M.C.: Towards the neuropsychological diagnosis of Alzheimer’s disease: a hybrid model in decision making. *WSKS, CCIS* **49**, 522–531 (2009)
26. Janetzko, D., Strube, G.: Case-based reasoning and model-based knowledge-acquisition. *Contemp. Knowl. Eng. Cogn. Lect. Notes Comput. Sci.* **622**, 97–114 (1992)
27. Li, H., Sun, J.: Hybridizing principles of the Electre method with case-based reasoning for data mining: Electre-CBR-I and Electre-CBR-II. *Eur. J. Oper. Res.* **197**(1), 214–224 (2009)
28. Angehm, A.A., Dutta, S.: Integrating case-based reasoning in multi-criteria decision support systems. *INSEAD* (1992)
29. Royes, G.F.: A hybrid fuzzy-multicriteria-CBR methodology for strategic planning support. In: *Processing NAFIPS’04, Annual Meeting of the Fuzzy Information*, vol. 1, pp. 208–213 (2004)
30. Verma, L., Srinivasan, S., Sapra, V.: Integration of rule based and case-based reasoning system to support decision making. In: *International Conference on Issues and Challenges in Intelligent Computing Technics (ICICT)*, pp. 106–108. IEEE (2014)
31. <http://archive.ics.uci.edu/ml/datasets/Vertebral+Column#>
32. Bello-Tomás, J.J., González-Calero, P.A., Díaz-Agudo, B.: *Jcolibri: an object-oriented framework for building CBR systems*. *Advances in Case-Based Reasoning*, pp. 32–46. Springer, Berlin (2004)
33. Bouhana, A., Abed, M., Chabchoub, H.: An integrated case-based reasoning and AHP method for personalized itinerary search. In: *4th International Conference on Logistics*, pp. 460–467. IEEE (2011)
34. John, D.A., John, R.R.: A framework for medical diagnosis using hybrid reasoning. In: *Proceedings of the International Multi Conference of Engineers and Computer Scientists*, vol. 1 (2010)
35. Bichindaritz, I., Montani, S.: Introduction to the special issue on case-based reasoning in the health sciences. *Comput. Intell.* **25**(3), 161–194 (2009)
36. Pandey, B., Mishra, R.B.: Data mining and CBR integrated methods in medicine: a review. *Int. J. Med. Eng. Inform.* **2**(2) (2010)
37. Zhuang, Z.Y., Churilov, L., Burstein, F., Sikaris, K.: Combining data mining and case-based reasoning for intelligent decision support for pathology ordering by general practitioners. *Eur. J. Oper. Res.* **195**(3), 662–675 (2009)
38. Yuan, G., Hu, J., Yinghong, P.: Research on CBR system based on data mining. *Appl. Soft Comput.* **11**(8) 5006–5014 (2011)
39. Hall, M., Frank, E., Holmes, G., Pfahringer, B., Reutemann, P., Witten, I.H.: The WEKA data mining software: an update. *ACM SIGKDD Explor. Newslett.* **11**(1), 10–18 (2009)
40. Holmes, G., Donkin, A., Witten, I.H.: Weka: a machine learning workbench. In: *Proceedings of the 1994 Second Australian and New Zealand Conference on Intelligent Information Systems*, pp. 357–361. IEEE (1994)

# Improving the Method of Wrist Localization Local Minimum-Based for Hand Detection

Sofiane Medjram, Mohamed Chaouki Babahenini,  
Mohamed Ben Ali Yamina and Abdelmalik Taleb-Ahmed

**Abstract** Nowadays, hand detection and gestures recognition have become very popular in human computer interaction systems. Several methods of hand detection based on wrist localization have been proposed but the majority work only with short sleeves and they are not efficient in front of all the challenges. Hand detection based on wrist localization proposed by Grzejszczak et al. (Proceedings of the 8th International Conference on Computer Recognition Systems CORES 2013 439–449, 2013), Nelpa et al. (Man Mach Interact 3(242):123–130, 2014) [3, 4] use the property of local minima along the contour of the skin mask obtained in the first stage to detect the wrist position. Although this technique provides good results where the skin mask contains the hand and the forearm, it still sensitive to the short contour where the skin mask contains the hand region only which generate false detection of the hand. We present in this paper an assessment of this method where the skin mask contains the hand region only. The main idea is based on the 2D shape properties of the hand and its components. Using 134 color images with their ground- truth, we evaluated the method enhanced and the results obtained were very satisfactory compared to the original one.

**Keywords** Hand detection · Wrist localization · Skin detection · Gestures recognition

---

S. Medjram · M.B.A. Yamina  
University of Badji Mokhtar Annaba, Annaba, Algeria  
e-mail: medjram.sofiane@gmail.com

M.B.A. Yamina  
e-mail: benaliyam2@yahoo.fr

M.C. Babahenini  
University of Mohamed Khider Biskra, Biskra, Algeria  
e-mail: babahenini@yahoo.com

A. Taleb-Ahmed (✉)  
University of Valenciennes, Valenciennes, France  
e-mail: Abdelmalik.Taleb-Ahmed@univ-valenciennes.fr

## 1 Introduction

Human-computer interaction aims to provide a better communication with a computer system. Furthermore, hands are spontaneous mean for a user to communicate with his environment, they are easy to use and correspond to the human nature. The use of hands in the human computer interaction domain may greatly improve the communication between the user and the computer.

Several methods of hand detection have been proposed; we can divide them in two categories: material- and vision-based approaches. The first methods [1, 2] impose to the user to wear a device on his hand for interaction. Effectively, these methods offer high detection results, but they are unnatural and not suitable for daily applications. The second methods [3–14] apply one or more techniques of computer vision on the acquired images, the skin segmentation is usually the first step and the skin mask obtained contains the hand region only or the hand and the forearm.

Among the vision-based methods of hand detection, they exist a number of methods based on wrist localization incorporating: local minima analysis and method width-based. The method using the local minima concept [3, 4] detects the hand of the user without imposing constraints on the length sleeves or background color, but it remains sensitive where the skin mask contains the hand region only. In this paper, we propose an enhancement for this method in order to detect well the hand where the skin mask contains the hand region only.

The paper is structured as follows. Section 2 introduces the different techniques of wrist localization presented in the literature. Section 3 presents the main contribution of the paper. Section 4 illustrates the experimental results and Sect. 5 concludes the work.

## 2 Related Work

Hand detection based on wrist localization has been widely studied recently in order to facilitate the interaction between the user and its machine.

In [1, 15], the authors proposed a wrist localization method for hand detection where the skin-mask contains the hand and the forearm. They localized the wrist by analyzing the forearm width with respect to the mask orientation. The minimum distances between symmetric contour points will represent the wrist location, and the side which contains several value changes of width-distance will be the side of the hand region (Fig. 1). The hand is well detected in these two methods but the width property loses its efficacy with the change of gestures and it does not work where only the hand region is presented in the scene.

In [4], the authors proposed a new method of hand detection based on wrist localization that works without any constraints on the sleeves length. After rotating the skin mask horizontally (using the longest cord of contour points) (PQ Fig. 2),



Fig. 1 The method of wrist localization proposed in [1, 15]

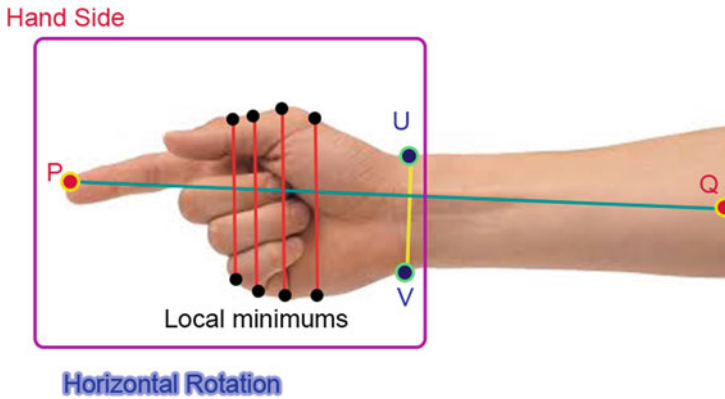


Fig. 2 The method of wrist localization proposed in [4]

they determined the position of the wrist by finding the local minimum (UV Fig. 2) of the contour of the skin mask. And the hand region is detected by finding the side which contains the high number of local minimum from the points UV of the wrist (Fig. 3).

Although this method detects the hand well where the skin mask contains the hand and the forearm, it still sensitive to the case of hand region only.



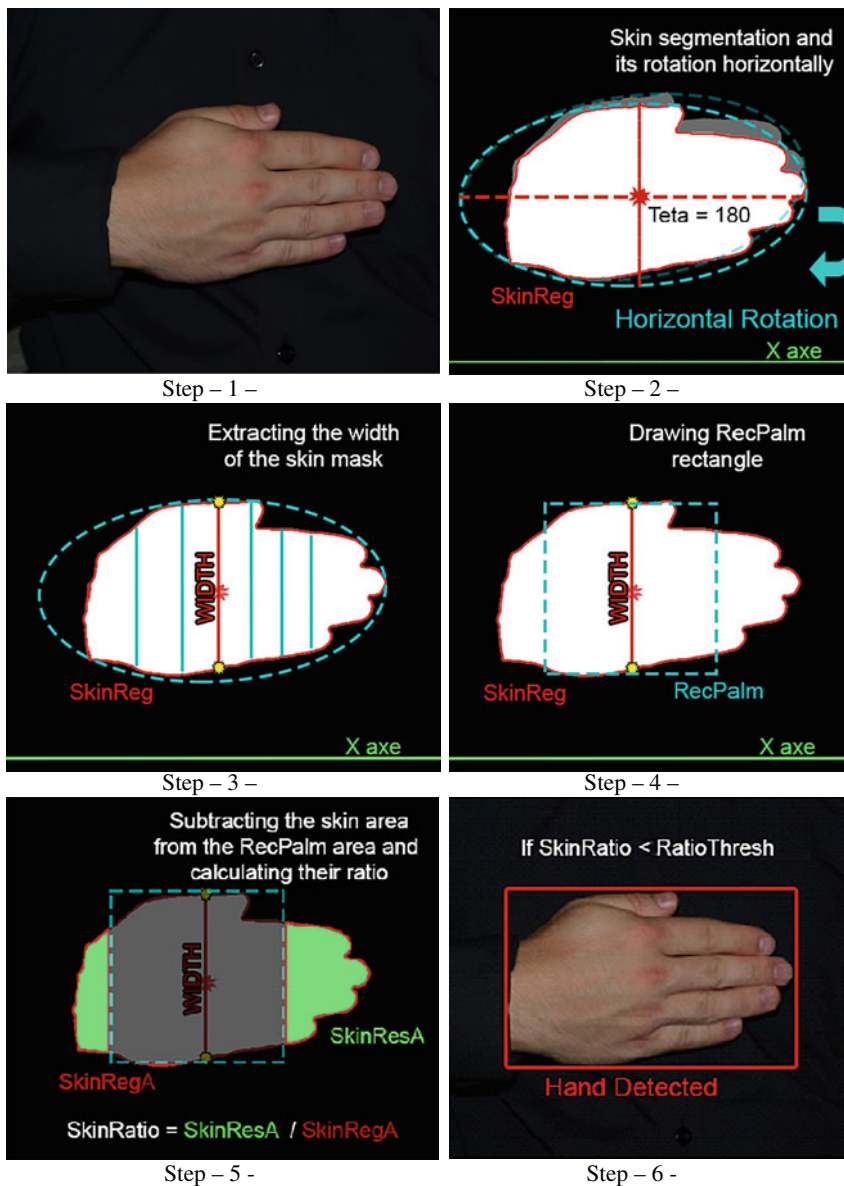


Fig. 3 Different steps used by the enhanced method for hand detection

### 3 Enhancement Proposed

The main idea of our proposed method is inspired from the 2D shape properties of the hand. A hand is a deformable object composed of fingertips, wrist and a hand palm that represents the majority of the hand area. This last property was used for the enhancement of the wrist localization local minima-based method where the skin mask contains the hand region only.

After the skin region segmentation and its rotation horizontally, we used the area property of hand palm to verify if this skin mask contains the hand with or without the forearm. The algorithm of the hand region verification is presented as follow:

Begin

- 1 - Skin region segmentation **SkinReg**.
- 2 - Rotate the skin mask **SkinReg** horizontally.
- 3 - Get out the width **SkinWidth** of the skin mask **SkinReg**.
- 4 - Draw a rectangle **RecPalm** with a length = **SkinWidth** and with same center as the skin mask **SkinReg**.
- 5 - Remove the skin mask **SkinReg** from the rectangle **RecPalm** and save the result in **SkinRes**.

$$\mathbf{SkinRes} = \mathbf{SkinReg} - \mathbf{RecPalm}.$$

- 6 - Calculate the ratio **SkinARatio** between the initial area **SkinRegA** of the skin mask and the skin area **SkinResA** resulted after subtraction.

$$\mathbf{SkinARatio} = \mathbf{SkinResA} / \mathbf{SkinRegA}.$$

- 7 - If **SkinARatio** < **RatioThresh**, then the **SkinReg** contains the hand region only, hand detected.

Elsewhere, the **SkinReg** contains the hand and the forearm region; apply the original algorithm of hand detection based on wrist localization (local minimum)

End.

## 4 Implementation Test and Results

Our experimental results are conducted on HP G62 notebook equipped with an Intel processor Core™ i3 CPU 2.27 GHz, 4G of RAM and windows 7 OS. The method of wrist localization based on local minima was re-implemented on Matlab2013a and assessed using the database1 of hand gesture recognition created by [4].

We defined the threshold **RatioThresh = 0.4**, the corresponding results of hand detection are showed in the Figs. 4 and 5 the results of the original method are presented.

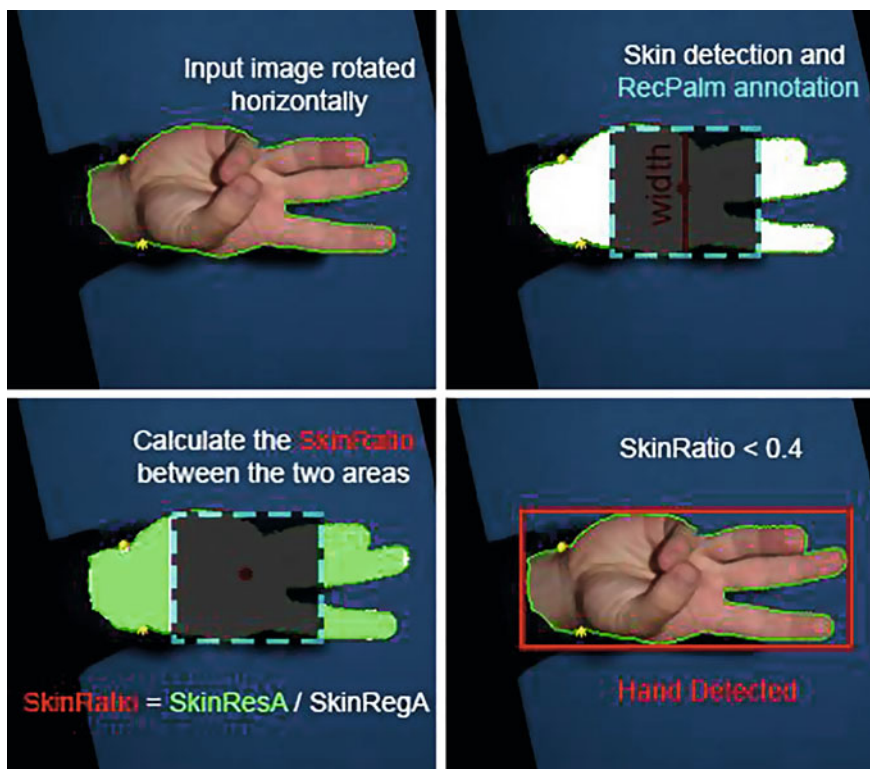


Fig. 4 Hand detection result by the enhanced method

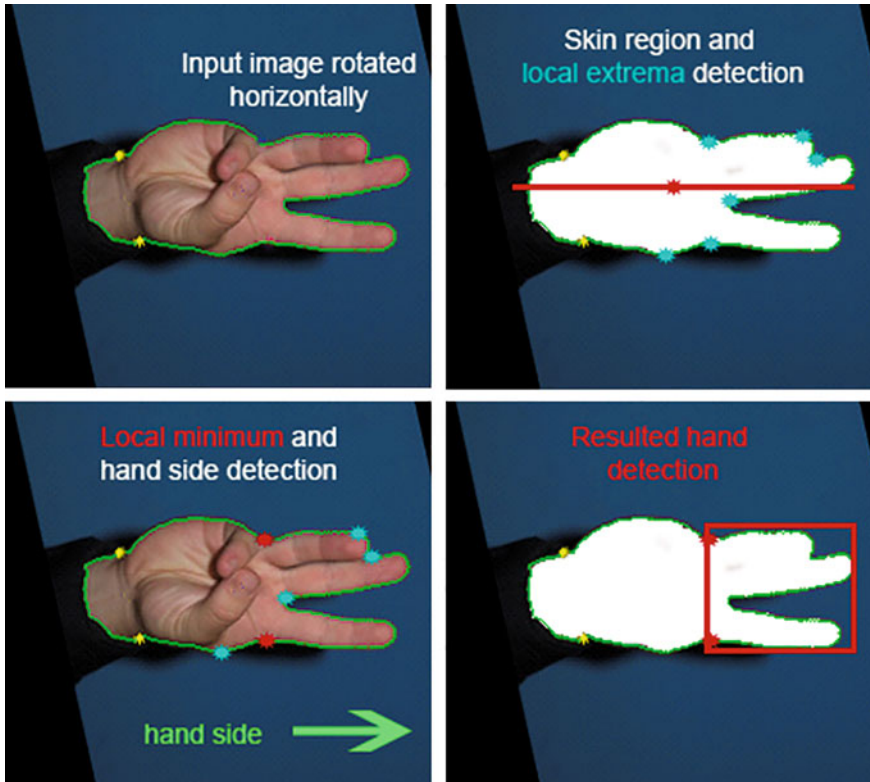


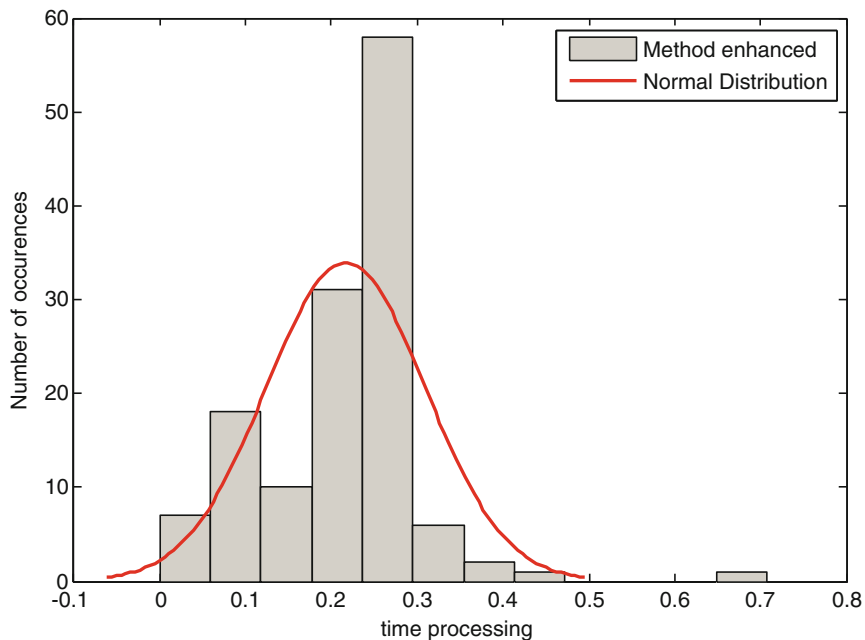
Fig. 5 Hand detection result by the original method of wrist localization

## 5 Evaluation

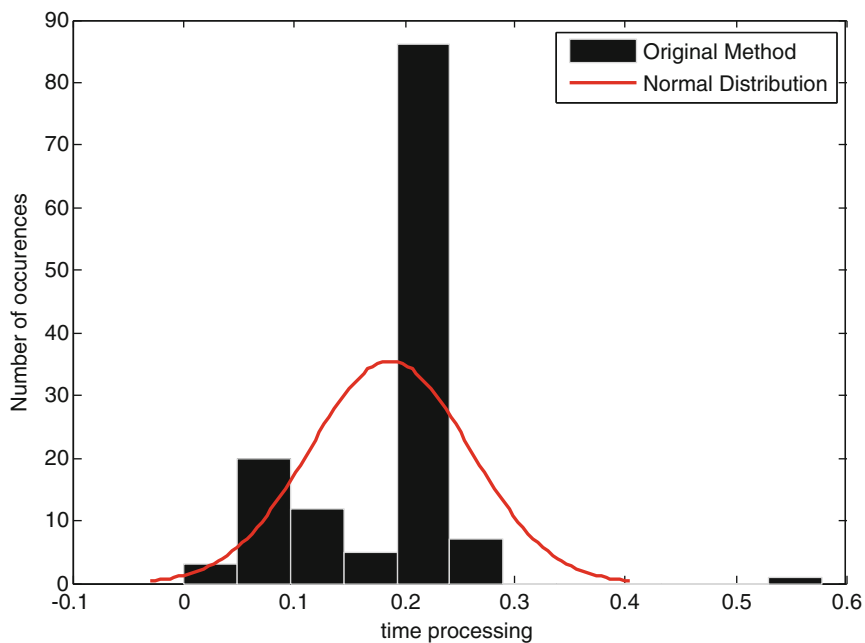
The database used for the evaluation contains 899 color images of hand gestures with both cases (hand, hand and forearm). However, as our method improve the detection of the hand where the skin mask contains the hand region only, we chosen from this database only the images containing the case studied. In result, we obtained 134 images with their ground-truth (Figs. 6, 7 and 8).

We compared the results of the original method of hand detection by wrist localization with the enhanced one using these 134 color images in measures of time processing, wrist error statistics and rate of correct hand detection (Table 1).

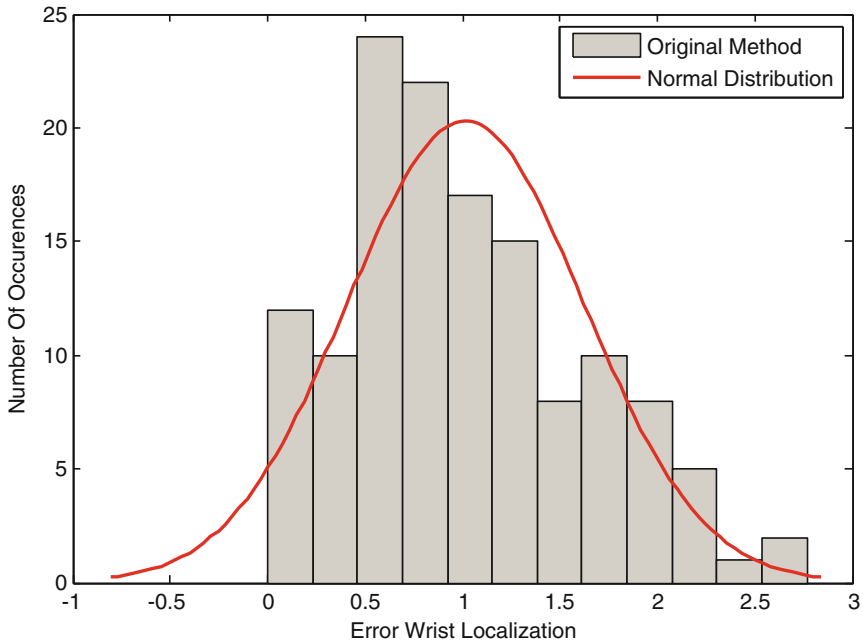
The time-processing results obtained by the method of wrist localization before and after the enhancement are very close. From the corresponding graphs, we can notice that the majority of the images in the original method have been executed in 0.2 s only, and in the enhanced method, the majorities are distributed between 0.2 and 0.3 s.



**Fig. 6** Histogram of time processing for the 134 color images of the database using the enhanced method



**Fig. 7** Histogram of time processing on the 134 color images of the database using the original method



**Fig. 8** Error statistics of wrist localization resulted by the original method

**Table 1** Time processing comparison between the original method of hand detection and the enhanced method

		The original method of wrist localization [4] (s)	The original method after enhancement (s)
Processing Time	time_avg	0.1786 ± 0.0716	0.2192 ± 0.0934
	time_max	0.6103	0.7206

**Table 2** The rate of the successful hand detection and error statistic for the original and the enhanced methods of hand detection

	The original method of wrist localization [4]	The original method after enhancement
Correct hand detection	46	<b>86</b>
	34.41 %	64.17 %
Error statistic	88	<b>48</b>
	65.67 %	35.82 %

The Table 2 shows the rate of the correct hand detection obtained by both methods. For the original method, we consider a correct hand detection if the error wrist localization  $E$  compared to the annotated ones are inferior to  $E < 0.8$ . For the second method, we consider a correct hand detection if the **RatioThresh < 0.4**.

We can notice from the results obtained that the enhanced method recovers 30 % of the misclassified hand images from the original one.

## 6 Conclusion

We presented in this paper an enhancement of the method of hand detection by wrist localization based on local minimum. We confirmed in the experiments that the proposed method performs in short times and recovers 30 % of the misclassified hand images of the original method. We conclude from the results obtained that there is no need to localize the wrist where the hand region is presented in the scene only.

## References

1. Paulson, B., Cummings, D., Hammond, T.: Object interaction detection using hand posture cues in an office setting. *Int. J. Hum. Comput. Stud.* **69**, 19–29 (2011)
2. Wang, R.Y., Popović, J.: Real-time hand-tracking with a color glove. *ACM Trans. Graph.* **28**, 1 (2009)
3. Grzejszczak, T., Nalepa, J., Kawulok, M.: Real-time wrist localization in hand silhouettes. In: *Proceedings of the 8th International Conference on Computer Recognition Systems CORES 2013*, pp. 439–449 (2013)
4. Nelpa, J., Grzejszczak, T., Kawulok, M.: Wrist localization in color images for hand gesture recognition. *Man Mach. Interact.* **3**(242), 123–130 (2014)
5. Yeo, H.S., Lee, B.G., Lim, H.: Hand tracking and gesture recognition system for human-computer interaction using low-cost hardware. *Multimed. Tools Appl.* 1–29 (2013)
6. Toni, B., Darko, J.: IPRO: A robust hand detection and tracking algorithm with application to natural user interface (2012)
7. Xie, S., Pan, J.: Hand detection using robust color correction and gaussian mixture model. In: *2011 Sixth International Conference on Image and Graphics*, pp. 553–557. IEEE (2011)
8. Choi, J., Seo, B.: Robust hand detection for augmented reality interface. In: *Proceedings of the 8th International Conference on Virtual Reality Continuum and its Applications in Industry*, pp. 319–322 (2009)
9. Vidya, K., Deryl, R., Dinesh, K., Rajabommanan, S., Sujitha, G.: Enhancing hand interaction patterns for virtual objects in mobile augmented reality using marker-less tracking. In: *2014 International Conference on Computing for Sustainable Global Development, INDIACom 2014*, pp. 705–709 (2014)
10. Grzejszczak, T., Kawulok, M., Galuszka, A.: Hand landmarks detection and localization in color images. *Multimed. Tools Appl.* (2015)
11. Mittal, A., Zisserman, A., Torr, P.: Hand detection using multiple proposals. *Proc. Br. Mach. Vis. Conf.* **75**, 1–75.11 (2011)
12. Kerdvibulvech, C.: A methodology for hand and finger motion analysis using adaptive probabilistic models. *EURASIP J. Embed. Syst.* **2014**, 18 (2014)
13. Stergiopoulou, E., Papamarkos, N.Å.: Engineering applications of artificial intelligence hand gesture recognition using a neural network shape fitting technique. *Eng. Appl. Artif. Intell.* **22**, 1141–1158 (2009)

14. Mao, G.-Z., Wu, Y.-L., Hor, M.-K., Tang, C.-Y.: Real-time hand detection and tracking against complex background. In: 2009 Fifth International Conference Intelligent Information Hiding and Multimedia Signal Processing, pp. 905–908 (2009)
15. Licsar, A., Sziranyi, T.: Hand gesture recognition in camera-projector system. Lect. Notes Comput. Sci. 83–93 (2004)



# Parkinson's Disease Recognition by Speech Acoustic Parameters Classification

D. Meghraoui, B. Boudraa, T. Merazi-Meksen and M. Boudraa

**Abstract** Thanks to improvement of means of communication performance and intelligent systems, research works to detect speech disorders by analysing voice signals are very promising. This paper demonstrates that dysarthria in people with Parkinson's disease (PWP) can be diagnosed using a classification of the characteristics of their voices. For this purpose, we have experimented two types of classifiers, namely Bernoulli and multinomial naïve Bayes in order to select the most pertinent features parameters for diagnosing PWP. The prediction accuracy achieved by using multinomial naïve Bayes (NB) classifier model reaching 95 % is very encouraging.

**Keywords** Speech analysis · Parkinson's disease recognition · Naïve Bayes · Bernoulli naïve Bayes · Multinomial naïve Bayes

## 1 Introduction

Parkinson's disease (PD) is progressive neuro-degenerative disorder that involves the death of neurons. It results in compromised muscular coordination as well as a specific form of dysarthria [1]. Because of the existence of large disparity between subjective voice problem reports and those resulting from clinical examination, acoustic analysis has become a promising approach for providing an objective evaluation [2, 3].

---

D. Meghraoui (✉) · B. Boudraa · T. Merazi-Meksen · M. Boudraa  
Faculty of Electronics and Informatics, University of Science and Technology Houari  
Boumediene USTHB, BP 32, El Alia, Bab Ezzouar, Algiers, Algeria  
e-mail: d.meghraoui@usthb.dz; djamila.meghraoui@gmail.com

It is generally observed in elderly people and causes speech disorders of ninety percent of the Parkinson's patients [4]. These patients suffer from hypokinetic dysarthria that manifests itself in all aspects of speech production, respiration, phonation, articulation, nasality and prosody. They have also dysphonia problem which include impairment in the normal production of vocal sounds [1, 2]. To discriminate these pathological states, clinicians have always payed attention to perceptive and objectives evaluation methods of acoustical analysis [3, 5]. However, these analytical methods are generally unpractical for routine clinician usage and do not always yield correct diagnosis [3]. For these reasons, recent studies have shown promising results of voice disorders detection with machine learning techniques using acoustic measurements (features) of dysphonia which could be useful to evaluate speech disorders [2, 3, 6, 7]. Little et al. [2] aimed to extract PD dysphonia measures from the phonations to analyze stage of the disease by telemonitoring. Rahan et al. have compared sustained vowel phonations of PD subjects with those of control subjects by quantifying the standard perturbation of voice parameters such that jitter and shimmer using nonlinear dynamic analyses [6]. Hernandez et al. [3] applied neural networks techniques using several acoustic parameters to distinguish between pathologic and non-pathologic voices. Support Vector Machine (SVM) and K-Nearest Neighbors (k-NN) have also been exploited in classification methods to discriminate the healthy subjects from subjects with PD [7].

This research aims to give a help in diagnosing the patients with Parkinson's disease (PWP). In a first step, acoustic features have been extracted from voice samples by using Praat acoustic analysis software [7, 8]. Then, in a learning stage, pertinent ones that allowed PWP detection with high accuracy were selected in order to be used as inputs for a model containing both normal and pathological acoustic parameters using Bernoulli and multinomial naive Bayes (NB) classifiers. In order to evaluate the performance of these models in discriminating healthy subjects from people with PD, we calculated both error rate and accuracy scores.

In the second section of this paper an overview of the voice features characterizing a speech signal is presented. The third section describes the classifiers tested in this work. Methodology and results are presented in Sect. 4 and conclusions are given in Sect. 5.

## 2 Voice Features

The main parameters that characterize human voices are:

### (A) *Jitter*

The jitter in a person's voice corresponds to how much one period differs from the next in the speech signal. This is a useful measure in speech pathology, because pathological voices often have a higher jitter than healthy voices [9, 10].

There are five different jitter measurements [8]:

- Jitter (local) is the average absolute difference between consecutive periods, divided by the average period for the precise procedure, expressed as.
- Jitter (local, absolute) represents the cycle-to-cycle variation of fundamental frequency. It is computed as the average absolute difference between consecutive periods, in seconds.
- Jitter (rap) represents the relative average perturbation, computed as the average absolute difference between a period and its average when considered with its two neighbours, divided by the average period.
- Jitter (ppq5) represents the five-point period perturbation quotient, defined as the average absolute difference between a period and its average of and its four closest neighbours, divided by the average period.
- Jitter (ddp) is the average absolute difference between consecutive periods, divided by the average period. The value is three times rap.

### *(B) Shimmer*

The Shimmer is similar to jitter, but instead of looking at periodicity, it measures the difference in amplitude from cycle to cycle. Once again, this is a useful measure in speech pathology, as pathological voices will often have a higher shimmer than healthy voices [11, 12].

Praat calculates six different measurements of shimmer:

- Shimmer (local) is the average absolute difference between the amplitudes of consecutive periods, divided by the average amplitude, expressed as percentage.
- Shimmer (local, dB) represents the variability of the peak-to-peak amplitude in decibels, computed as the average absolute base-10 logarithm of the difference between the amplitudes of consecutive periods, multiplied by 20.
- Shimmer (apq3) is the three-point amplitude perturbation quotient, it is expressed as the average absolute difference between the amplitude of a period and the average of the amplitudes of its neighbours, divided by the average amplitude.
- Shimmer (apq5) is the five-point amplitude perturbation quotient, represents the average absolute difference between the amplitude of a period and the average of the amplitudes of its four closest neighbours, divided by the average amplitude.
- Shimmer (apq11) represents the 11-point amplitude perturbation quotient, defined as the average absolute difference between the amplitude of a period, and the average of the amplitudes of it, and its ten closest neighbours, divided by the average amplitude.
- Shimmer (ddp) is the average absolute difference between consecutive differences between the amplitudes of consecutive periods. The value is three times apq3.

### *(C) Harmonicity*

The harmonics-to-noise, and noise to-harmonics, ratios are derived from the signal-to-noise estimates from the autocorrelation of each cycle. The harmonic to noise ratio (HNR) is expressed as the degree of acoustic periodicity, and is calculated by the ratio of the energy of the periodic part, related to the noise energy [8].

#### *(D) Pitch*

The pitch is the rate of the vibration of vocal folds of the larynx during phonation of voiced sounds [13]. The set of pitch variations during an utterance is defined as intonation. Typically, men pitches' are lower than those of women, who have a lower pitch than children [11]. Pratt calculates five measures of pitch: Median, Mean, Standard deviation, Minimum and Maximum pitch [8].

#### *(E) Pulse*

The glottal pulse is a single period, corresponding to a puff of air at the glottis. Praat calculates four pulse measurements: number of pulses, number of periods, mean period, standard deviation of period (in seconds) [8].

#### *(F) Voicing*

The fraction of locally unvoiced pitch frames represents the fraction of pitch frames that are analysed as unvoiced. The normative value for the fraction of unvoiced frames is 0, which means that the normal healthy voices should have no trouble maintaining voicing during a sustained vowel. Every non-zero value can be considered as a sign of pathology [8, 10].

- Number of voice breaks is the number of distances between consecutive pulses that are longer than 1.25 divided by the pitch floor [8].
- Degree of voice breaks is the total duration of the breaks between the voiced parts of the signal, divided by the total duration of the analysed part [8].

### **3 Classification**

#### *A. Principle*

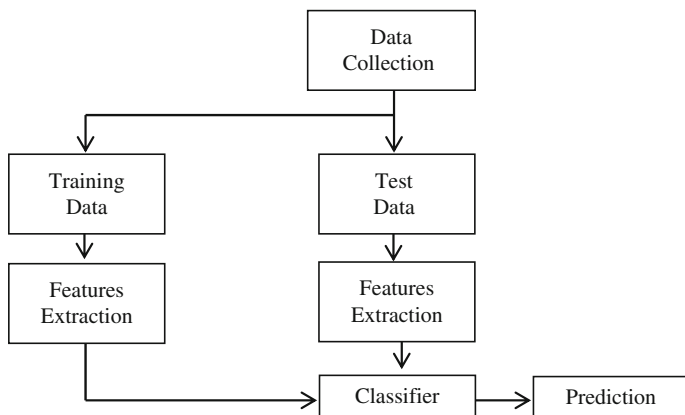
Classification is a data meaning task of predicting the value of target. This is done by building a model based on one or more predictors' variable or features. The data for a classification project is typically divided into two data sets: one for training the model, the other for testing the model.

Classification models are tested by comparing the features values to known target values in a set of test data. There are tested by applying them to test data with known target values and comparing the predicted values with the known ones [12].

Figure 1 shows a simplified diagram of the general model building procedure for classification.

Classification algorithms use different techniques for finding relationships between the values of the predictors and the values of the target.

In this paper we used the NB classifier because of its simplicity and stability. The NB model is based on the conditional independence model of each predictor given the target class [14, 15]. It classifies data in two steps: The first step uses the training data which estimates the parameters of a probability distribution, assuming that predictors are conditionally independent given the class. In the second step, the method computes the posterior probability of that sample belonging to each class. The test data is classified according to the largest posterior probability.



**Fig. 1** Process of data classification

The Bayes theorem allows the inversion of the generative model and computation of posterior probabilities. The final classification is performed by selecting the model yielding the maximum posterior probability [14]. By Bayes theorem, the posterior probability of class  $c$  given predictor  $x$  is:

$$P(c|x) = \frac{P(x|c)P(c)}{P(x)} \quad (1)$$

$$P(c|x) = P(x_1|c) \times \dots \times P(x_n|c) \times p(c) \quad (2)$$

where  $P(c|x)$  is the posterior probability of class of given predictor and  $P(c)$  is the prior probability of class.  $P(x|c)$  is the likelihood which is the probability of predictor, given class.  $P(x)$  is the prior probability of predictor [15].

The multinomial and Bernoulli Naive Bayes Classifiers differ mainly by the assumptions they make, regarding the distribution of  $P(x|c)$ :

### B. Multinomial Naive Bayes

Multinomial NB is a specialised version of NB where each  $P(x_i|c)$  is multinomial distribution. This distribution is parameterized by vectors  $\theta_c = (\theta_{c1}, \dots, \theta_{cn})$  for each class  $c$ , where  $n$  is the number of features and  $\theta_{ci}$  is the probability  $P(x_i|c)$  of feature  $i$  appearing in a sample belonging to class  $c$  [16].

The parameter  $\theta_c$  is estimated by a smoothed version of maximum likelihood:

$$\theta_{ci} = \frac{N_{ci} + \alpha}{N_i + \alpha n} \quad (3)$$

where  $N_{ci}$  Count of observing feature  $i$  appears in a sample of class  $c$  in the training set, and  $N_i$  is the total count of all features for class  $c$ , and the additive smoothing

parameter  $\alpha$  which can be used in order to avoid the problem of zero probabilities. The most common variants of additive smoothing are the Lidstone smoothing ( $\alpha < 1$ ) and ( $\alpha = 1$ ) for Laplace smoothing.

### C. Bernoulli Naive Bayes

Bernoulli NB is used for the NB training classification algorithms for data that are distributed according to multivariate Bernoulli distributions. This class requires samples to be represented as binary-valued feature vectors [15]. The decision rule for Bernoulli NB is given by:

$$P(x_i|c) = P(i|c)x_i + (1 - P(i|c))(1 - x_i) \quad (4)$$

Which differs from multinomial Naive Bayes' rule is that it explicitly penalizes the non-occurrence of a feature  $i$  which is an indicator for the class  $c$ . The multinomial variant would simply ignore a non-occurring feature.

## 4 Application and Results

Described approaches of automatic classification have been tested in this work in order to compare their performances in decision making for Parkinson disease recognition.

### A. Data sets

The dataset used was created by Olcay Kursun et al. from the Department of Computer Engineering at Istanbul University, Istanbul (Turkey) who recorded the speech signals. All the recordings were made in stereo-channel mode and saved in WAVE format [7]. Figure 2 illustrates an example of speech signal of respectively sustained vowel /a/ of PWP and healthy subject extracted from this data base. It can be observed on the Parkinson's acoustic signal that an additional noise is superimposed.

Praat acoustic analysis software is exploited for the measurements of jitter, shimmer, harmonicity, pitch, pulse, and voicing features [8].

### B. Methodology

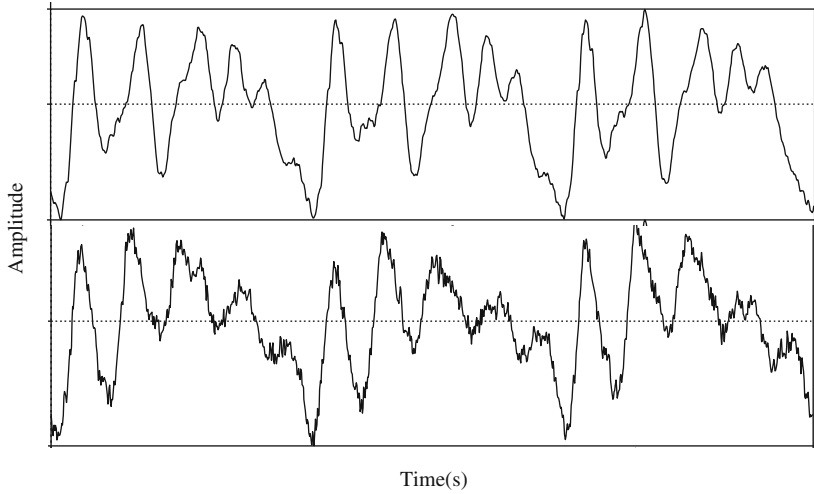
The data are constituted by training and test groups of signals. The training data belongs to 20 patients with Parkinson (6 female, 14 male) and 20 healthy subjects (10 female, 10 male). The sound recordings include: sustained vowels (/a/, /o/, /u/), numbers, words and short sentences.

The different features values described in Sect. 2 have been used as inputs for the classification.

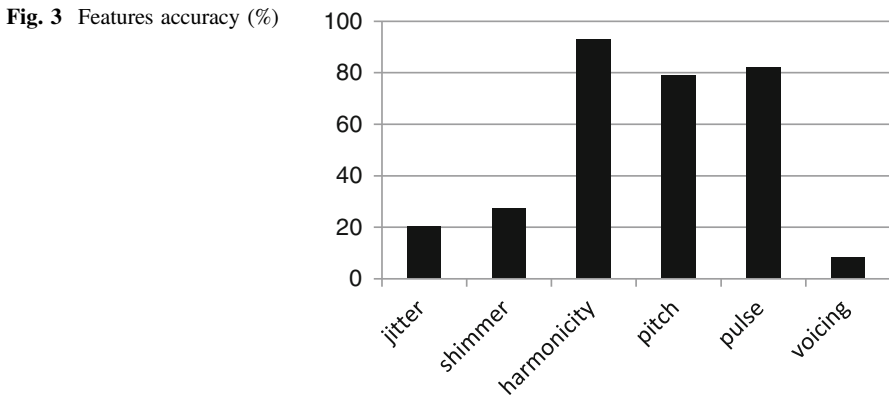
Both optimized feature selection algorithm and NB classification method have been implemented in MATLAB environment.

Figure 3 shows that harmonicity, pulse and pitch features give a higher accuracy than other acoustics features.

As best classification has been obtained by using harmonicity, pitch, and pulse features. These pertinent features will be used for training Bernoulli and



**Fig. 2** Waveforms of a sustained vowel /a/ belonging to a healthy individual (*top*) and PWP (*bottom*)



Multinomial NB classifiers for Parkinson's disease diagnosis with two groups (PD and healthy).

To verify the accuracy of a classification that uses only these three pertinent features, a test had been performed by using 28 voicing samples of patients with PD who were asked to pronounce only the sustained vowels /a/ and /o/.

In order to measure the accuracy of those classifiers, Mean Squared Error (MSE) and accuracy measures have been calculated [17]:

$$MSE = \frac{1}{n} \sum_n (\hat{y}_i - y_i)^2 \tag{5}$$

**Table 1** Bernoulli and multinomial NB accuracies

Classifiers	MSE	Accuracy (%)
Bernoulli NB	0.375	62.5
Multinomial NB	0.047	95.23

$$Accuracy (\%) = 100 \times (1 - MSE) \quad (6)$$

where  $\hat{y}_i$  is a vector of  $n$  predictions, and  $y_i$  is the vector of observed values corresponding to the inputs to the function which generated the predictions. The results are summarised in Table 1.

The results seen from Table 1 show that a classification accuracy of 95.23 % has been achieved using NB multinomial classifier.

Considering the research results, it is reported in Ref. [7] that a classification accuracy of 85 % has been achieved for 26 features using SVM and K-NN classifiers. Other results from this research include 91.4 % of classification accuracy with introducing pitch period entropy (PPE) as new feature using kernel support vector machine [2]. It is clearly seen that the multinomial NB algorithm outperforms this method by selecting the best features that have had the most influence on data classification process between both healthy and PD data.

## 5 Conclusion

Parkinson's disease is known as the second common neurological disorder after Alzheimer. It influences several aspects of human's functions in which speech disorder is the most prominent. In this paper, Parkinson's disease recognition based on voice analyses has been experimented. The principle consists in classifying various features of voice signals corresponding respectively to healthy people and people with Parkinson in order to develop a valid model for diagnosing other subjects independently and give a help in the decision making.

Two approaches of automatic classification have been tested, namely Multinomial and Bernoulli NB. It has been seen that the most pertinent features are the harmonicity, the pitch and the pulse that allowed the highest accuracy by using Multinomial NB classifier. It is observed that, this method outperforms the SVM based one, described in reference [7], in terms of accuracy. In future works the stability and reliability of this method will be studied.

**Acknowledgment** We thank Mr Benba Achraf, from the university Mohamed five, Rabat, Morocco, and Miss Hadjaj Hassina from the university of Science and Technology Houari Boumediene, Algiers, Algeria for helpful discussions.



## References

1. Ishihara, L., Brayne, C.: A systematic review of depression and mental illness preceding Parkinson's disease. *Acta Neurologica Scandinavica* 211–220 (2005)
2. Little, M.A. et al.: Suitability of dysphonia measurements for telemonitoring of Parkinson's disease. *IEEE Trans. Biomed. Eng.* 1015–1022 (2009)
3. Hernandez-Espinosa, C., et al.: Diagnosis of vocal and voice disorders by the speech signal. In: *Proceedings of the IEEE-INNS-ENNS International Joint Conference, Italy*, pp. 253–258 (2000)
4. O'Sullivan, S.B., Schmitz, T.J.: Parkinson disease. In: *Physical Rehabilitation*, 5th edn, pp. 856–894. F. A. Davis Company, Philadelphia, PA, USA (2007)
5. Kent, R.D.: Hearing and believing: some limits to the auditory-perceptual assessment of speech and voice disorders. *Am. J. Speech Lang. Pathol.* 5(3), 7–23 (1996)
6. Rahn, D.A., Chou, M., et al.: Phonatory impairment in Parkinson's disease: evidence from nonlinear dynamic analysis and perturbation analysis. *J. Voice* 21(1), 64–71 (2005)
7. Sakar, B.E., et al.: Collection and analysis of a Parkinson speech dataset with multiple types of sound recordings. *IEEE J. Biomed. Health Inf.* 828–834 (2013)
8. Styler, W.: Using praat for linguistic research, University of Colorado at Boulder Phonetics Lab, Last Update: March (2014)
9. Farrús, M., et al.: Jitter and Shimmer measurements for speaker recognition. In: *Proceedings of International Conference Interspeech*, pp. 778–781 (2007)
10. ArefiShirvan, R., Tahami, E.: Voice analysis for detecting Parkinson's disease using genetic algorithm and KNN classification method. *Biomed. Eng.* 14–16 (2011)
11. Hart, J.T., Collier, R., Cohen, A.: *A Perceptual Study of Intonation*. Cambridge University Press (2006)
12. Yongjian, F.: Data mining: tasks, techniques and applications. *IEEE Potentials* 16, 18–20 (1997)
13. Mary, L., Yegnanarayana, B.: Extraction and representation of prosodic features for language and speaker recognition. *Speech Commun.* 50(10), 782–796 (2008). Elsevier
14. Bayes, T.: An essay towards solving a problem in the doctrine of chances. *Philos. Trans. R. Soc. Publ.* 53 370–418 (2012)
15. Manning, C., et al.: *Introduction to Information Retrieval*. Cambridge University Press, USA, April (2009)
16. Metsis, V., et al.: Spam filtering with Naive Bayes—Which Naive Bayes? In: *3rd Conference on Email and Anti-Spam (CEAS)*, July (2006)
17. Wang, Z., Bovik, A.: Mean squared error: love it or leave it? *IEEE Signal Process. Mag.* 98–117 (2009)

**Part III**  
**Networking and Cloud Computing**

# The Finger-Knuckle-Print Recognition Using the Kernel Principal Components Analysis and the Support Vector Machines

S. Khellat-Kihel, R. Abrishambaf, J. Cabral, J.L. Monteiro and M. Benyettou

**Abstract** In the computer networks explosion's time, the need to identify individuals increasingly becomes necessary to perform various operations, such as access control and secure payments. So far, inputting alphanumeric code remains the most used solution. This solution, in spite of having the merit to be very simple, has the disadvantage to certify only the individual who enters the correct code. Another possibility that is open to us is to use biometric identification, by identifying directly the physical traits of the user. Biometric identification is defined as a science allowing the identification of people using their behavioral or physiologic characteristics. It seems like an evident solution to the problem explained previously: the identity of a person is then related to who he/she is and not to what he/she possesses or knows. In this work, we propose a biometric system based on a very recent biometric trait, which consists in the finger-Knuckle-Prints. This recognition is based on a mathematical model.

**Keywords** Finger-Knuckle-Print · SVM · Kernel principal components analysis · Recognition

---

S. Khellat-Kihel (✉) · M. Benyettou  
Laboratory of Modelization and Optimisation of the Industriel Systems,  
Departement of Informatics, University of Science and Technologies Mohamed-Boudiaf,  
Oran, Algeria  
e-mail: souad.khellat@univ-usto.dz

J. Cabral · J.L. Monteiro  
Centro Algoritmi, School of Engineering, University of Minho, Campus of Azurém,  
4800-058 Guimarães, Portugal

R. Abrishambaf  
Department of Engineering Technology, Miami University, Hamilton, OH 45011, USA

## 1 Introduction

Recently, it has been discovered that the outer part of the finger or the Finger-Knuckle-Print, which refers to the inherent forms of the outer surface around the finger and especially the high part of the finger, is unique and can be used as a distinctive biometric modality. The Finger-Knuckle-Print is still in the development phase and can be considered as a new trend in biometrics. The Finger-Knuckle-Print can add new information to the texture of the finger. This biometric trait has the merit of a great acceptance from the user part.

Previously, many researchers were interested in the Finger-Knuckle-Print biometrics modality. The systems that were developed were based on the Subspace reduction methods, Coding methods, and fusion methods. The main methods used in the systems based on the Subspace are the PCA (Principal Component Analysis), LDA (Linear Discriminant Analysis), ICA (Independent Component Analysis) [1], OLDA (Orthogonal Linear Discriminant Analysis) [2], KPCA (Kernel Principal Analysis) [3], and also Fisher Analysis which consists of the fusion of the PCA with LDA [4]. The multimodality has found great results and performances comparing to the unimodal systems, for that we found in the literature that researchers have done the multimodality not only in terms of the fingers fusion but also in terms of algorithms fusions. In [5], the researchers proposed a multiple algorithm for the feature extraction. The algorithms are LG (Log Gabor filters), LPQ (Local phase Quantization), PCA (Principal Components Analysis), and LPP (Locality Preserving Projections). Hence, the best fusion was the LG with the LPP.

In this paper we do not propose only the space reduction by different methods (PCA, LDA and KPCA) but also we propose the application of the Gabor filter that have shown a good performances on the veins' recognition [6], and we propose the use of Mahalanobis distance, the KNN (K Nearest Neighbors) and the SVM (Support Vector Machines) for the classification.

## 2 Definition, Characteristics

The Finger-Knuckle-Print one of the physical biometrics that refers to the inherent skin in the outer part of the finger. This modality catch big researchers' attention for the last period. Even if the Finger-Knuckle-Print is one of the hand based biometrics that has a high acceptability from the user, but this new trait has an added advantage of not getting the damage easily since the normal use necessitates the inner part or the fingerprint. It is not easy to be forged since people do not leave traces of their FKP on the objects touched [7]. The finger-Knuckle-Print has a high textured characteristic, easily accessible at the same time it is non-criminal stigma like the fingerprint.

### 3 Finger-Knuckle-Print Acquisition

The first FKP sensor developed by the Woodard and Flynn [7] was used for the 3D FKP. This sensor captures both  $640 \times 480$ -range image and a registered  $640 \times 480$  24-bit color intensity image nearly simultaneously. The sensor dimensions are  $213 \text{ mm} \times 413 \text{ mm} \times 271 \text{ mm}$  and it weights 11 kg. These previous characteristics less the practical use of this sensor. From the next Fig. 1, we remarked that the quality of the obtained finger image are very weak and necessitate a huge preprocessing.

Kumar and Ravikanth [1], developed a system, Fig. 2, for acquiring the Finger-Knuckle-Print that uses a digital camera. The camera was set and fixed about 20 cm from the imaging space, non-uniform illumination and this distance can reduce the images quality.

The biometric research center at Hong Kong Polytechnic University has developed a real time device for capturing the FKPs. They provide a big database for the research, which contains 7920 images in total with 165 individuals. For each individual four fingers with 12 catches for each finger. Therefore, it is a big available database for this modality. Most of the newest works on this modality works on this database. For that, we used in our work this database.

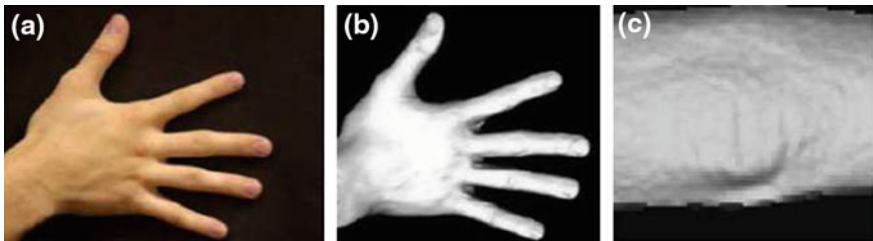


Fig. 1 a Intensity image, b range image, c range

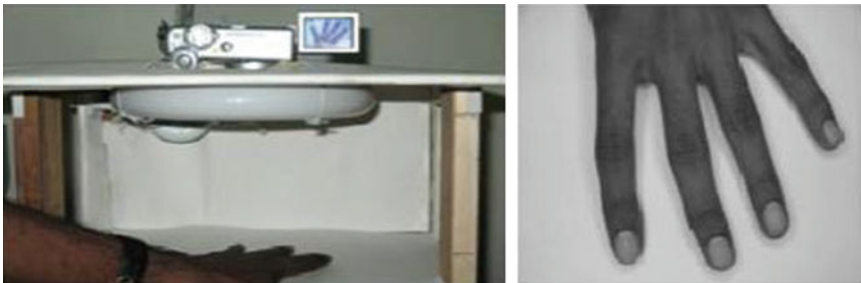


Fig. 2 a Acquisition sensor, b the acquired image

### 4 Proposed Method, Databases

Since the biometric system is a pattern recognition system, then it consists of different parts. In our approach, we tried to improve each part, Fig. 3 shows the general architecture of the proposed Finger-Knuckle-Print recognition system:

In the first, we used two different databases, the first one is composed of 165 individual, each individual has 12 catches of the index. This data base is available on the internet (PolyU FKP database) [8]. However the second is composed of 158 individual, each individual has 5 caches, available on the internet (Delhi FKP database). Figure 4 represents examples for images from the different FKP databases.

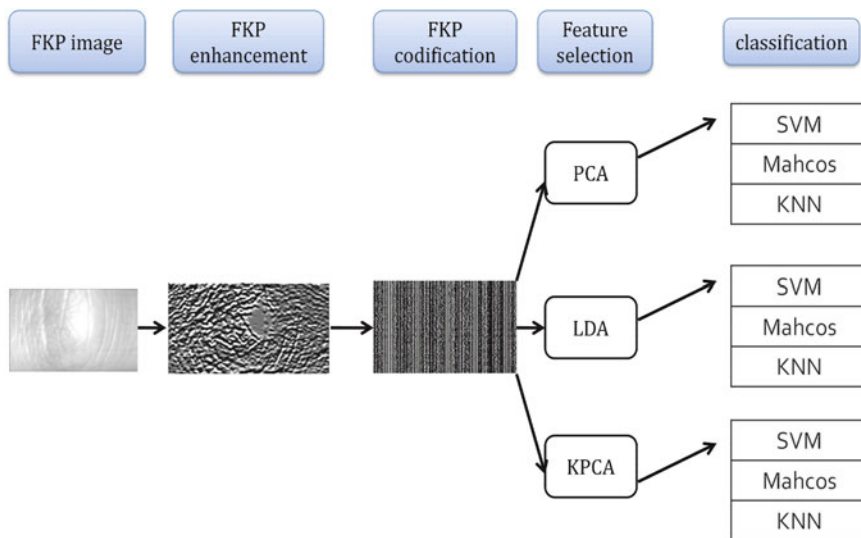


Fig. 3 The general architecture of the Finger-Knuckle-Print recognition system

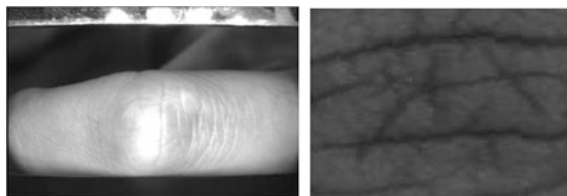


Fig. 4 Examples of the acquired FKP images

## 4.1 Pre-processing

In our system the pre-processing consist of the application of the Gabor filter 2D: This Bi-dimensional filter has shown great efficiency for the finger vein images enhancement in [6]. Also this filter has been used for the different images on a multimodal system that combined the fingerprint, finger vein and also the Finger-Knuckle-Print [9]. Fusing the phase and direction features to identify the Finger-Knuckle-print. Because the finger-knuckle-print consists of many lines, it has stable and obvious direction which makes it suitable to be viewed as a texture image. 2-D Gabor filter is widely used in extracting the features of textured images. This version of the 2D Gabor filter is basically a bi-dimensional Gaussian function centered at origin (0,0).

## 4.2 Codification

For the feature extraction or the codification of the preprocessed images the Bank of Gabor filters was used. The latter had already shown a great performance on the facial images [10] by constructing a bank of 40 Gabor filters. For implementation we used the PhD toolbox [11]. These codes are used in the next stage that represent the reduction dimension or the feature selection. The Gabor filter used by [10] is presented by the following mathematical formula:

$$\psi(\mathbf{x}, \mathbf{y}) = \frac{f_u^2}{\pi k \eta} e^{-\left(\left(\frac{f_u^2}{k^2}\right)x^2 + \left(\frac{f_u^2}{\eta^2}\right)y^2\right)} e^{j2\pi f_u x'}, \quad (1)$$

In this stage of feature extraction with the Gabor\_bank filter, we obtained 640 features; so for a database of 165 individuals with 12 catches a feature selection is indispensable, based on the existing works in the literature we used the PCA, LDA and the KPCA.

## 4.3 Feature Selection

It is a crucial step in pattern recognition system, more importantly; it is one of data preparation steps. It provides certain number of characteristics or parameters (most important) i.e. describes each form with the smallest of relevant attributes. There are two principal reasons to keep the number of attributes as small as possible: costs of measurement and precision of classification. A small group of selected attributes simplifies the patterns representation as well as classifiers, which are built around them. Consequently, the resulting classifier will be faster and will use less resources memories. In addition, The FKP database require feature selection or space

reduction because of its big size. For this reason, we propose the use of the most common methods on the uni-modal traits that is LDA (Linear Discriminant Analysis) the PCA (Principal Components Analysis) and the KPCA (Kernel Principal Components Analysis).

Despite the fact that the PCA reduces the redundancy and minimizes the noise, it doesn't take into consideration whether these features are in the same database. However the LDA covers this point by focusing on the discrimination between the classes for the feature selection. So the LDA doesn't reduce only the space but also it preserves the class information discrimination as much as possible.

#### 4.4 Classification

In the phase of the classification that give the biometric system decision, we proposed the use of a mathematical method that has a solids mathematic tools, that consists of the Support Vector Machines. The general idea of the SVM is to find the best hyper plan that separate perfectly the classes, and achieves maximum separation between the classes. In this system a Gaussian kernel has been used for resolve the problem of the non-linearity. The SVM has shown their efficiency on the finger vein recognition [6], also on multimodal biometric system [9].

We proposed also a distance calculation for the FKP recognition. That is the Mahalanobis (or within cosine) similarity measure and the KNN (K Nearest Neighbors). The following formula represents the distance calculation between two vectors  $X = (x_1, x_2, \dots, x_n)$  and  $Y = (y_1, y_2, \dots, y_n)$ :

$$D(\mathcal{X}_n, \mathcal{Y}_n) = \sqrt{(\mathcal{X}_n - \mathcal{Y}_n)^T \text{cov}(\mathcal{X}_n - \mathcal{Y}_n)^{-1}}, \quad (2)$$

where,  $X_n$  and  $Y_n$  are the normalized or the means of two groups of data. cov is the covariance.

### 5 The Results

In this part the different obtained results on the differer databases are presented. The results presentation was with the ROC (*Receiver Operating Characteristics*) and also the recognition rate obtained by the SVM and the KNN.

The Figs. 5 and 6 consist of curves that correspond to the obtained results on the different databases, with the features obtained by the Gabor filter, PCA, LDA and the KPCA.

The recognition rates obtained by the distance calculation, the SVMs and also the KNN were presented on the Tables 1 and 2:



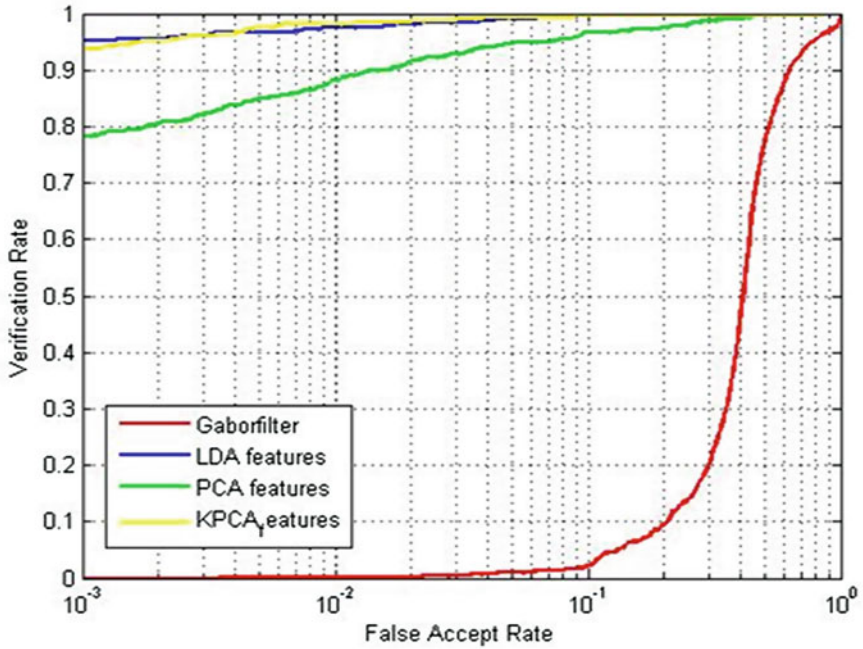


Fig. 5 The ROC curve for the Gabor filter, PCA, LDA and KPCA features, PolyU database

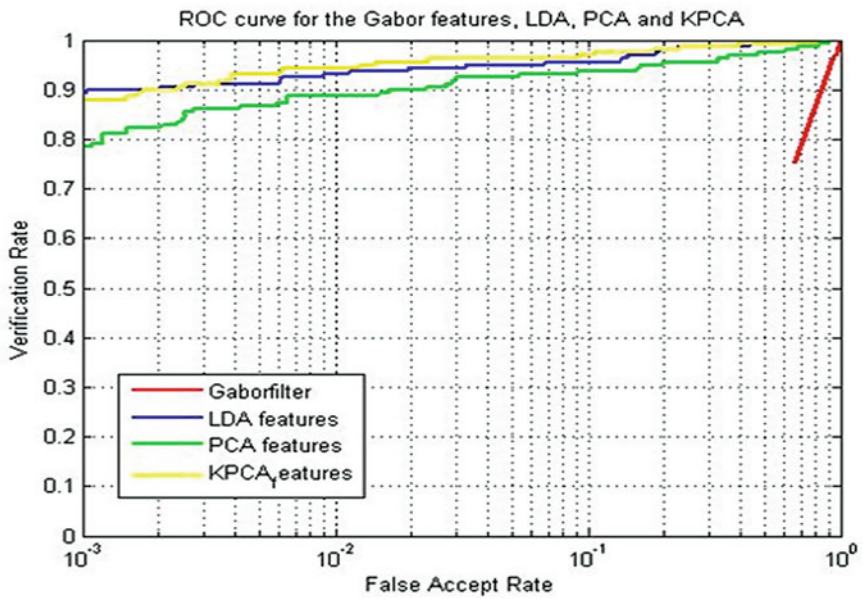


Fig. 6 The ROC curve for the Gabor filter, PCA, LDA and KPCA features, Delhi database

**Table 1** The recognition rates DB1

The recognition rate	SVM (%)	KNN (%)	Distance Mahcos (%)
Gabor filter's features	91.92	94.24	42.59
The PCA features	91.62	94.24	68.18
The LDA features	90.81	91.01	94.24
The KPCA features	86.26	87.07	94.39

**Table 2** The recognition rates DB2

The recognition rate	SVM (%)	KNN (%)	Distance Mahcos (%)
Gabor filter's features	85.76	87.97	96.20
The PCA features	86.71	85.76	80.06
The LDA features	83.33	78.80	86.39
The KPCA features	83.23	77.53	87.03

The DB1 consists of the PolyU database, the DB2 consist of the Delhi database. The Gabor features was reduced from 640 features to 211 by the PCA however more reduction is done by applying the LDA which gives only 105 features. The characteristic vectors obtained after the KPCA application are vectors with only 90 features.

The results obtained have clearly seen that the characteristics of KPCA gave good performance by comparing to the features without selection or just the attributes obtained by the Gabor filter codification and the characteristics obtained by other selection methods (PCA and LDA). The curves and the tables presented ensure the robustness of this biometric method as a modality with a reliable texture.

## 6 Conclusion

In this work one of the most recent biometric traits have been presented, which consists of the Finger-Knuckle-Print. Different methods have been applied in the paper with various curves and tests presentations. Two large databases have been used to test the robustness of this method and the proposed algorithm for recognition. Different methods for the space reduction (PCA, LDA, KPCA) were applied in the feature selection phase and a small comparison between these methods was represented. We suggest the use of bio-inspired methods for the selection of the best attributes.

## References

1. Baldonado, M., Chang, C.-C.K., Gravano, L., Paepcke, A.: The Stanford digital library metadata architecture. *Int. J. Digit. Libr.* **1**, 108–121 (1997)
2. Bruce, K.B., Cardelli, L., Pierce, B.C.: Comparing object encodings. In: Abadi, M., Ito, T. (eds.) *Theoretical Aspects of Computer Software*. Lecture Notes in Computer Science, vol. 1281, pp. 415–438. Springer, Berlin (1997)
3. Van Leeuwen, J. (ed.): *Computer Science Today. Recent Trends and Developments*. Lecture Notes in Computer Science, vol. 1000. Springer, Berlin (1995)
4. Michalewicz, Z.: *Genetic Algorithms + Data Structures = Evolution Programs*, 3rd edn. Springer, Berlin (1996)
5. AlMahafzah, H., et al.: Multi-algorithm decision-level fusion using Finger-Knuckle-Print biometric. Springer, India (2014)
6. Ravikanth, C., Kumar, A.: Biometric authentication using finger-back surface. In: *CVPR'07*, pp. 1–6 (2007)
7. Yang W.: Finger-Knuckle-Print recognition using Gabor feature and OLDA. In: *Proceedings of the 30th Chinese Control Conference*, Yantai, China (2011)
8. Swati, M.R., Ravishankar, M.: Finger Knuckle Print recognition based on Gabor feature and KPCA + LDA. In: *International Conference on Emerging Trends in Communication, Control, Signal Processing and Computing*, Bangalore (2013)
9. Khellat-Kihel, S., et al.: Multimodal fusion of the finger vein, fingerprint and the finger-knuckle-print using Kernel Fisher analysis. doi:[10.1016/j.asoc.2016.02.008](https://doi.org/10.1016/j.asoc.2016.02.008)
10. Khellat-Kihel, S., et al.: Finger vein recognition using Gabor filter and support vector machine. In: *IPAS'14 International Image Processing Applications and Systems Conference*. IEEE (2014)
11. Shariatmadar, Z.S., Faez, K.: A novel approach for Finger-Knuckle-Print recognition based on Gabor feature fusion. In: *4th International Congress on Image and Signal Processing*. IEEE (2011)
12. Woodard, D.L., Flynn, P.J.: Finger surface as a biometric identifier. *CVIU* **100**, 357–384 (2005)
13. <http://www.comp.polyu.edu.hk/~biometrics/FKP.htm>

# An Intelligent Management of Lighting in an Ambient Environment with a Multi-agent System

Aouatef Chaib, Boussebough Imen and Chaoui Allaoua

**Abstract** The home automation is one of the most customers of electrical energy after the industry. Lighting represents on average about 15 % of the annual electricity bill excluding gas and hot water. Different studies have been made to reduce the electrical energy consumption like automatic switching and time programming. But all these techniques have not an important rate in reducing the electrical energy consumption. So we note that an intelligent lighting which varies with the users need remains important source of economy of the energy. The intelligent lighting is obtained by using ambient intelligence (AmI). Multi agent System (MAS) have become the important paradigm to develop an ambient system because they have important characteristics like autonomy, proactivity and mobility to respond better to the main characteristic of ambient intelligence like the adaptability to the context. In this area, we propose an adaptive and intelligent lighting system in which each light source is represented by a software agent and the set of agents compose and coordinate their competences in order to illuminate a region with minimum energy consumption.

**Keywords** Ambient intelligence · Multi agent system · Intelligent lighting · Home automation · Context-aware

---

A. Chaib (✉) · C. Allaoua  
MISC Laboratory, Constantine 2 University, 25000 Constantine, Algeria  
e-mail: chaibaouatef@gmail.com

C. Allaoua  
e-mail: chaoui@umc-misc.org

B. Imen  
Lire Laboratory, Constantine 2 University, 25000 Constantine, Algeria  
e-mail: iboussebough@yahoo.fr

## 1 Introduction

Ambient intelligence (AmI) [1] is defined like an environment having the ability to perceive, reason, act and interact to provide services improving the quality of life of persons [2]. The main characteristic of an AmI system is the ability to take into account the context aware of the users and adapt her functionality on this context information [3, 4].

The General mended of AmI is the integration of computer science technologies in the objects of our environment in order to assist person in their everyday activities. It is situated in a junction of different and important fields like: artificial intelligence and distributed artificial intelligence, electronic architecture and nanotechnology, Networks and telecommunications and HMI.

The main objective of AmI is to make our environment [5, 6]:

- Attentive to the specific characteristics of each one;
- Able to adapt her behavior to the users needs;
- Able to respond intelligently to spoken or gestural indications and even to engage in dialogue.

Ambient intelligence is used in several areas like: Crisis management [7], the assistance of the elderly [7–11], intelligent transport, Home Automation: [12–14].

The Home automation includes all techniques and technologies, electronic, computer science and telecommunication means to automate tasks and improve in a house [15]. This automation is carried out with the integration of communicating sensors in the home. This allows knowing the status of the objects of the home at any time: the lamps are lit, the temperature in each room, the state of openings/closures (doors, windows) The main objectives of home automation are:

- Comfort (lights, automation housework...)
- Security (smoke detectors, alarms, video surveillance...)
- Energy savings (heating management, consumption analysis...).

Multi Agent System (MAS) [16] are the more adequate paradigm to develop a context-aware ambient environment. Mainly because they respond more to the main characteristic of ambient intelligence concerning: the adaptability to the context. MAS allows realizing multiple device agents that obtain the context information and they perform their own context inferences to rapidly detect context information changes [4, 17]. More of that, softagents offer several useful characteristics to AmI like: autonomy, reactivity, proactively, reasoning and coordination.

Coordination is one of the main characteristics of MAS for developing an ambient environment. It implements a combination of organizations, interactions, agents and environmental models [16]. Each agent uses its knowledge and resources to solve a sub-problem. The cooperative agents need to avoid as much as possible the conflicting position to solve a problem. Negotiation is a conflict resolution technique. It is considered as a process for improving the agreements.

In this area, we propose an adaptive multi agent system to automate an intelligent lighting system in which each light source is represented by a software agent and the set of agents compose and coordinate their competences in order to illuminate a region with minimum energy consumption. Our system is a context aware, because it take into account some context information of the environment like: the location of the user and the intensity of ambient lighting.

The rest of this article is organized as follows: Sect. 2 presents some related works. In Sect. 3 we present our proposed system and the general structure of agents. In Sect. 4 we introduce a case study going from scenario description to it actual execution. Finally, we draw the conclusions and we present some perspectives to extend it in Sect. 5.

## 2 Related Works

Several projects use MAS in the field of AmI for home automation:

In [12] the authors present a project called MavHome that aims to build a smart home with various functions such as adaptive control of temperature, water, light, clean and multimedia (audio and video) leisure. The authors use a soft ware agent to control the devices in the home. The organization of agents is dynamic because it may change. Agents predict the movements and activities of habitants of the house to automate their activities, assist the elderly, detect anomalies, predict problems and make decisions to solve them. The main inconvenient of this project relates to the structure of agents is not modular (addition or suppression difficult to make) which makes the system closed. Moreover, there is no cooperation between agents then no auto organization in the system.

iDorm [14] is a room for several purposes to: to sleep, to leisure, to work, etc. The piece includes several objects and more sensors are integrated in the room as temperature sensor, occupancy sensor, humidity sensor, etc... iDorm make life easier for residents. The project uses two types of agents. The first one is embarked on static objects; it receives the sensor values, learns user preferences and control actuators. Controlled parameters are the date, the level of indoor and outdoor light, indoor and outdoor temperature, the activities and movements of user and the status of each object in the room. The second one is embarked on a robot that learns and adapts the needs of user. The agents of this project cooperate between them but the system is not fully distributed because the chief agent must wait until the robot has finished its tasks; The system risk of inter locking situation.

In [13], the authors proposed a multi-agent system for intelligent management of home automation context. This intelligent system can fully manage the habitat or simply make proposals for action he thinks is best for management of the real environment. The authors use the approach centered interactions for cognitive agents located. These agents have goals they must solve by acting in simulated environment. These actions are then reflected in the real environment. Three types of agents are used: Active agent: capable of performing interactions, liabilities agent: may undergo

**Table 1** The comparison between projects

Project	Dynamicity	Adaptability	MAS	Distribution	Context aware
[12]	–	+	+	+	–
[14]	+	++	+	–	–
[13]	–	+	+	–	+
Our project	++	++	++	++	++

interactions and Artifact agent who can neither suffer nor make any interaction. This project is context aware, because the system is able to plan and perform actions based on the context data; but it is not distributed because there's always access to a central simulator.

Table 1 summarizes and compares these different projects with our proposed system.

### 3 Proposed System

#### 3.1 General Presentation

We proposed an intelligent lighting system. This later contains several and different light sources. The main objective of our system is to illuminate a region where a user is situated with the desired lighting intensity to satisfy the users lighting need with minimum energy consumption. For example; if we want to light up a region with certain intensity; this intensity can be obtained in different ways.

- 1st way: with a single source light that is close to the region to be illuminated and it has this intensity;
- 2nd way: by the combination of several source lights that are capable together to produce the desired intensity.

Our system must give a solution that should save energy consumption. The system must:

1. Perceive the ambient lighting intensity to calculate the missing need of light to satisfy the user need light;
2. Locate the user to obtain the region to be illuminated and the set of light sources which can contribute to supply the missing need of light.

Figure 1 presents the general representation of our system.

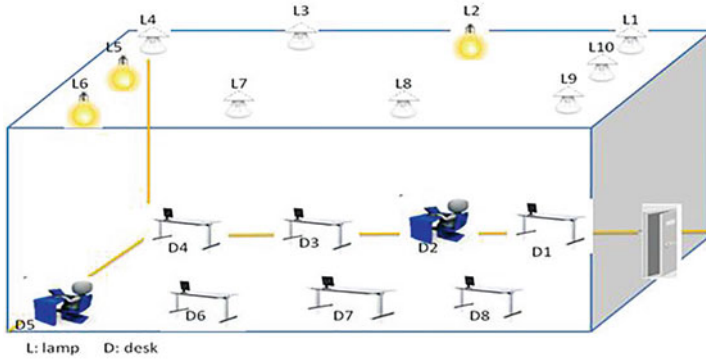


Fig. 1 The general representation of the system

### 3.2 The Agents of Our System

Each light source is represented by a software agent, the set of agent coordinate between them and compose their competences in order to satisfy the users light need. We have two types of agents:

1. *The initiator agent*: represent the closest light source to the user.
2. *The ambient agent*: represent the rest of light sources which can coordinate with the initiator agent to give de desired light.

The initiator agent sent message to the ambient agents contains her need to supply the desired lighting. Each ambient agent tries to answer favorably alone, if its capacity is insufficient, he becomes another initiator and it sent a message to ambient agent contains as parameters the capacity which misses to satisfy the need of the first initiator. The process of sending messages is terminated if the initial need is satisfied. The ambient agents sent their propositions to the initiator; this later evaluate this proposition and the select the proposition witch satisfy the desired lighting with minimum energy consumption. Figure 2 represents the structure of the agents of our system.

- **Perception module**: this module perceives the ambient environment, it contains two sub modules and a data bases:
  - The Sensor captures the localization of the user and the ambient lighting intensity and it transmits these values to the interpreter;
  - The interpreter: it interprets the context values and it saves them in a data bases;
  - Context information: it is a data bases for storage of context information for a later use.

We define the context-aware information by a set of  $(Var_i, Val_i)$  pairs,  $Var_i$  is the variable name and  $Val_i$  is the value of  $Var_i$ . For example, the context aware information of our ambient environment at a given moment is  $\{(AmbInt, 45 \text{ lux}), (Loc, D3)\}$ .



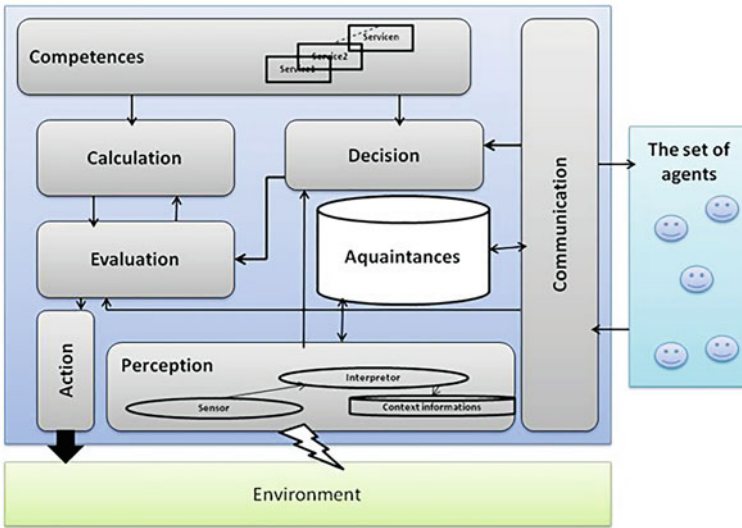


Fig. 2 The structure of the agents

(*AmbInt*, 45 lux) indicates that the ambient lighting intensity of an environment is 45 Lux.

(*Loc*, D3) indicates that the user is in the desktop D3.

- **Communication module:** if this agent is a trigger; this module is responsible for sending/receiving messages to/from the agents of the system.
- **Evaluation module:** Evaluates the proposals of ambient agents and it selects the best one. The evaluation is done according to certain criteria.
- **Decision module:** choose the adequate action according to the competences of the agent.
- **Competences module:** it contains all the services that this agent can perform it.
- **Calculation module:** calculate the need of the agent.
- **Action module:** performs the adequate action decided by Decision module.
- **Aquaintances:** This data base defines the list of the ambient agents which are in the proximity of this agent and which can cooperate with him.

Figure 3 details the operation of the initiator agent and Fig. 4 details the operation of the ambient agent.

## 4 Case Study

We propose an intelligent lighting system of a room office. This later has the conception showing in Fig. 5 it contains 8 lamps, 2 roof lights and a neon of different power lighting. Table 2 summarizes the dimensions of the room office. Table 3 summarizes

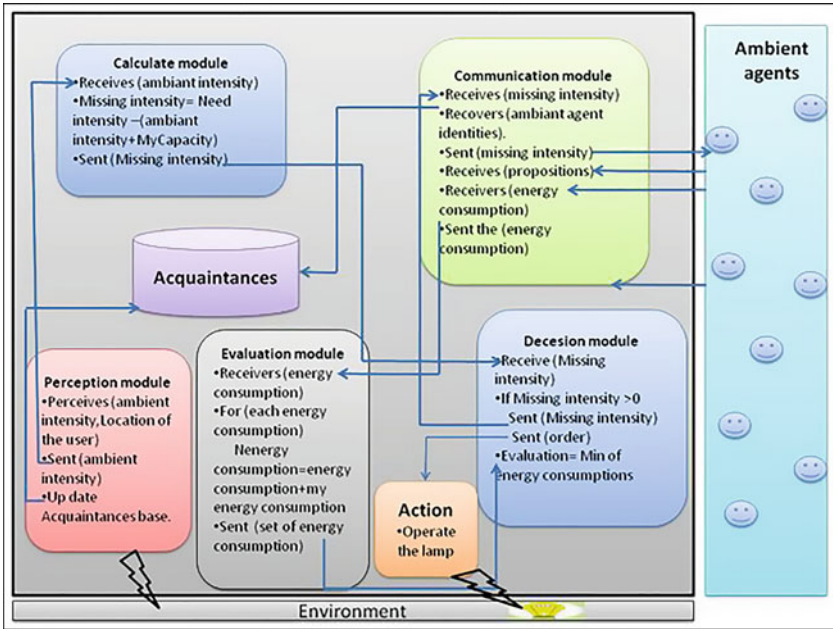


Fig. 3 The operation of the initiator agent

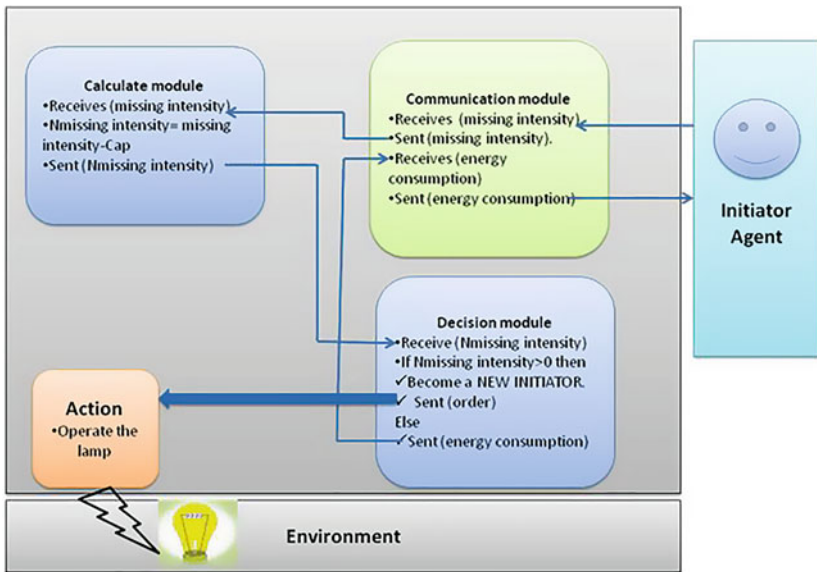
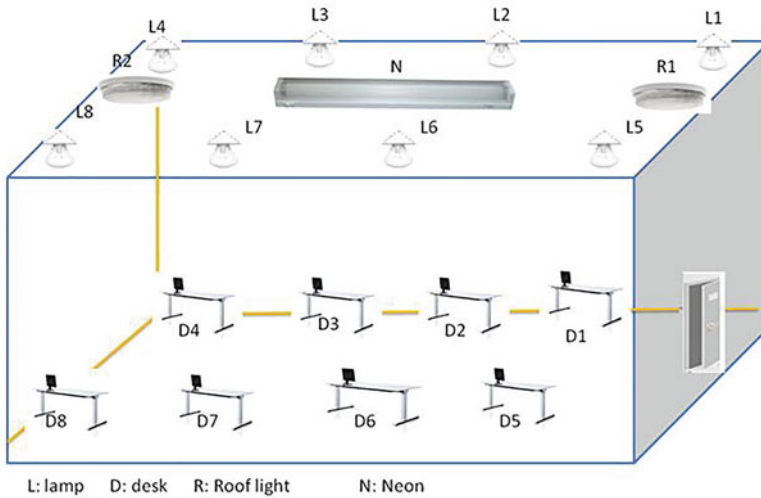


Fig. 4 The operation of the ambient agent



**Fig. 5** The conception of the room office

**Table 2** The dimension of the room office

Length (m)	Width (m)	Length of desktop (m)	Between desktops (m)	Between lamps (m)	Between roof lights (m)
13.5	5	1.5	2.5	3.3	8

**Table 3** The characteristics of the lamps, the roof lights and a neon

	Lighting intensity (Lm)	Surface to be illuminated (m <sup>2</sup> )	Amount of light (Lux)	Energy consumption (W)
Lamp: L1, L2, L3, L4, L5, L6, L7, L8	1000	10	100	75
Roof light: R1, R2	1500	50	30	100
Neon: N	2800	70	40	150

the characteristics of the lamps, the roof lights and a neon. Each lamp, roof light and a neon are represented by an agent called a *LampAgent*, *RoofAgent* and *NeonAgent*.

**Lumen(Lm):** is a luminous power unit indicate the flow of light emitted by the lamp.

**Lux:** indicate the amount of light received by a surface **1 Lux=1 Lm/m<sup>2</sup>**

Assume the following scenario: The user is in the second desktop (D2) and the ambient intensity is 250 lux, According to the **NF EN 12464-1 norm**, the recommended minimum value for Writing, typing, reading and data processing is **500 lux**.

The context information:  $\{(AmbInt, 250lux), (Loc, D2)\}$  The initiator agent is: AgentLamp2 **Missing intensity = Need intensity (AmbInt + MyCapacity) = 500 - (250 + 100) = 150 lux**

- Missing intensity: the intensity wich mises AgentLamp2 to complete the need of the user;
- Need intensity: the intensity needed by the user;
- AmbInt: the value of the ambient intensity;
- MyCapacity: the value of the intensity offered by AgentLamp2.

The founded plans are:

1. Plan1: LampAgent2, LampAgent1, RoofAgent1, LampAgent3.  
Energy consumption =  $75 + 75 + 100 + 75 = 325$  W.
2. Plan 2: LampAgent 2, LampAgent 1, RoofAgent1, RoofAgent2.  
Energy consumption =  $75 + 75 + 100 + 100 = 350$  W.
3. Plan 3: LampAgent 2, LampAgent 1, RoofAgent1, NeonAgent.  
Energy consumption =  $75 + 75 + 100 + 150 = 400$  W.

The system must execute Plan 2 because it has the minimum of energy consumption.

#### ***4.1 The Implementation of the System***

We have chosen Java Agent DEvelopment framework (JADE) platform to implement our system because:

- Jade facilitates the development of multi agent systems
- Jade is easy to use
- Jade runs on all operating systems
- Jade realize the applications conform to the FIPA standard to facilitate communication of Jade agents with non JADE agents.

We have simulated our system by a graphic interface, where a user can indicate her localization and the ambient intensity Fig. 6.

Figure 7 shows the class diagram of the lamp agent if it is an initiator agent and Fig. 8 shows the class diagram of the lamp agent if it is an ambient agent.

Sniffer agent of JADE is useful to sniff, monitor and debug conversations between agents [9]. Figure 9 shows the sniffer agent at the moment of sending of the first message and the sending the propositions.

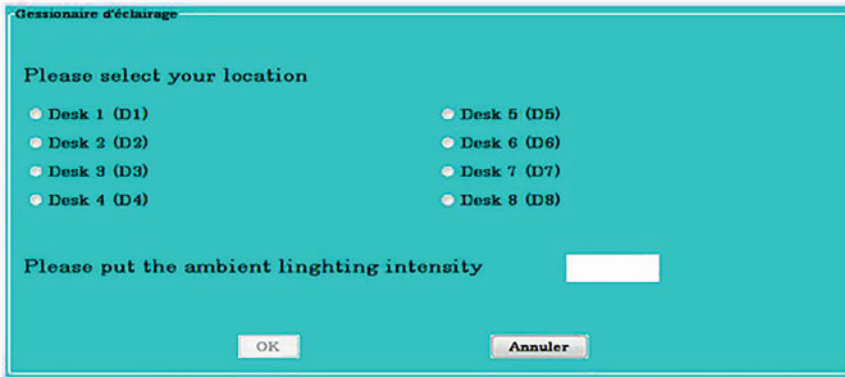


Fig. 6 The interface of our system

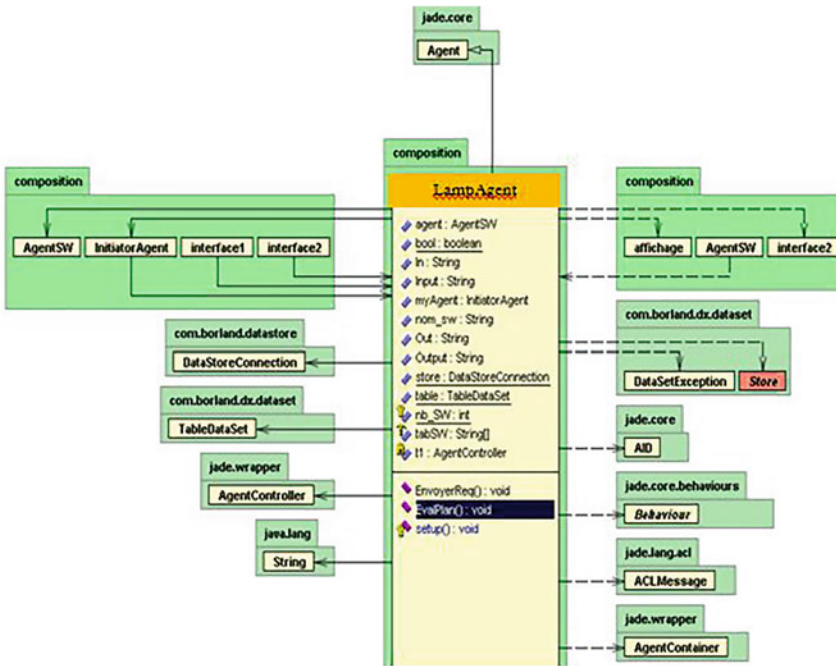


Fig. 7 The class diagram of the initiator agent

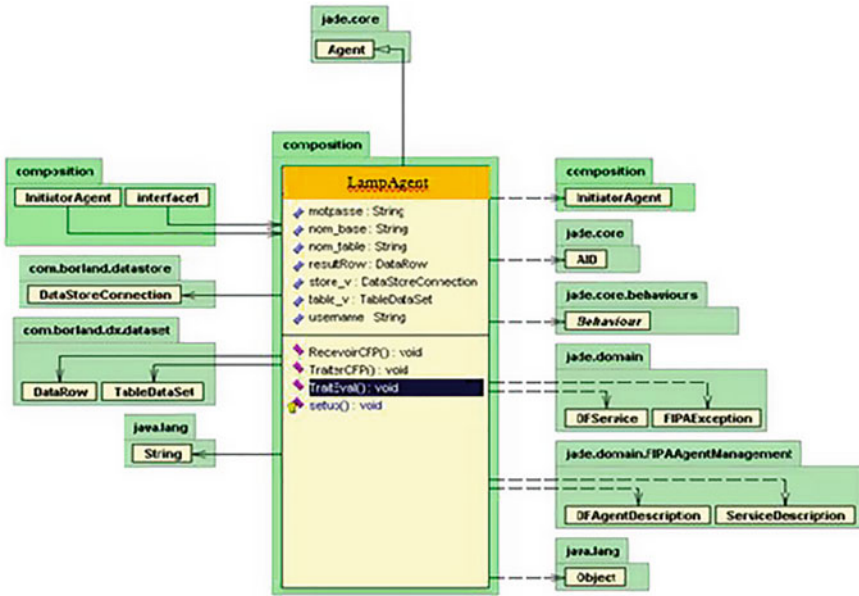


Fig. 8 The class diagram of the ambient agent

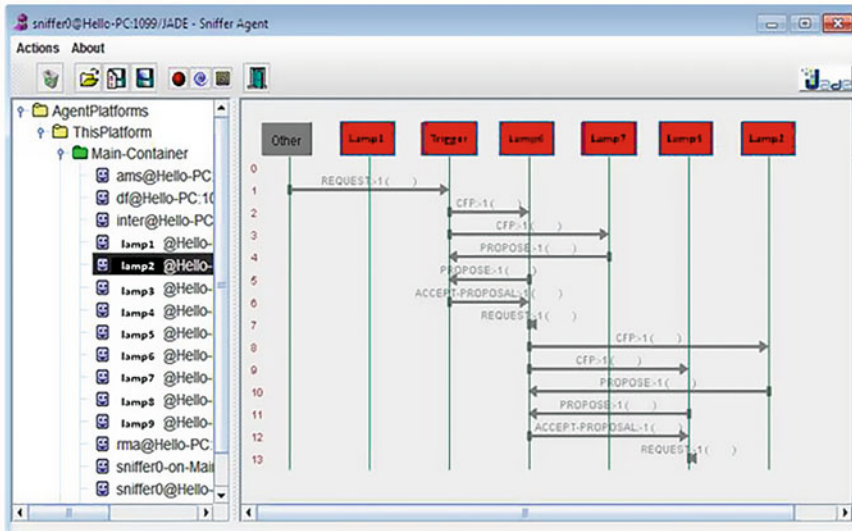


Fig. 9 The sniffer agent at the moment of sending of CFP and resaving of propositions

**Table 4** Some obtained results

Localization	Ambient intensity (Lux)	Needed intensity (Lux)	Operates lamps	Energy consumption (W)
D2	250	250	P1: L2, L1, R1, R2	350
			P2: L2, L1, R1, L3	325
			P3: L2, L1, R1, N	400
D1	450	50	P1:L1	75
			P2: R1, R2	200
			P3: L2	75
			P4: N, R1	250
D8	70	430	P1: L8, L7, L3, L4, R1, R2	500
			P2: L8, L7, L3, L4, N	550
D5	300	200	P1: L5, L1	150
			P2: L5, L6	150
			P3: L5, R1, R2, N	425
D6	0	500	P1: L6, L5, L1, L2, L7	375
			P2: L6, L5, L7, N, R1, R2	575
D3	20	480	P1: L3, L4, L2, L7, L8	375
			P2: L3, L4, L2, L7, N, R1, R2	650
D7	360	140	P1: L7, L8	150
			P2: L7, R1, R2	275
			P3: L7, L6	150
			P4: L7, N	225

## 4.2 Results and Discussion

We have executed our system and we have obtained the encouraging results. Table 4 summarizes some obtained results.

We assume that the desired intensity is 500 lux. Figure 10 presents a histogram that shows schematically the obtained results of the execution of the system.

In each localization of the user and in accordance with the ambient intensity; the system provides several combination of light sources but it executes the combination which consumes less. Whatever light sources used and whatever their characteristics; our system select the combination that uses electrical energy.

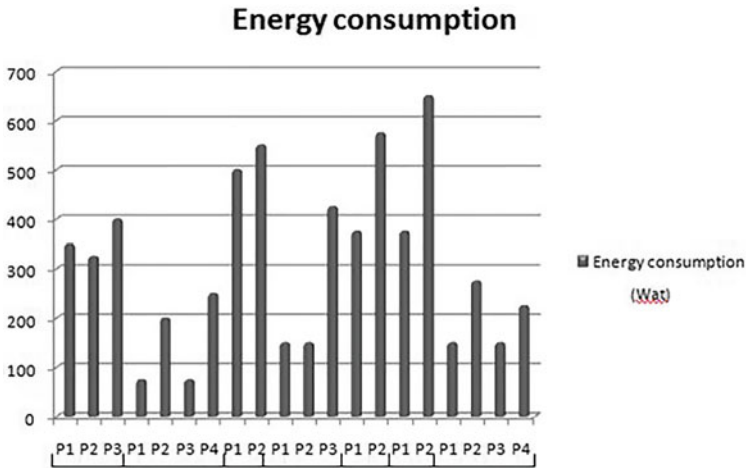


Fig. 10 The energy consumption

## 5 Conclusion

This paper illustrated how a Multi Agent System can be used in a smart field such as ambient environment. MASs became the principal paradigm for developing an ambient system because they offer several useful characteristics like: reactivity, proactivity, reasoning, autonomy and coordination to create an adaptive environment.

We presented here a MAS for an intelligent management of lighting. The main objective of our contribution is to provide the desired lighting intensity to satisfy the users lighting need with minimum energy consumption.

Our system is context awareness. It uses several contextual information. It must perceive the environment to get the ambient lighting intensity to calculate the missing light and the localization of the user to obtain the region to be illuminated.

Each light source is represented by an agent and the set of agents coordinate and cooperate between them to give the best lighting with minimum consumption of energy.

We have taken the example of the intelligent lighting of a room office to validate our proposition. The room office has several light sources (Lamp, Roof light, Neon) of different power lighting and different energy consumption. We have implemented our system in JADE platform because it facilitates the development of multi agent systems. We have executed the system and we have obtained encouraging results.

As future work, we plan to adapt our system to other complex domains like a health-care, compare the obtained results and create a general framework for service composition in ambient environment using the paradigm of Multi Agent System.



## References

1. Weiser, M.: Some computer science issues in ubiquitous computing. *Commun. ACM* **36**(7), 75–84 (1993)
2. Crowley Coutaz, J.: Plan intelligence ambiante: Defis et opportunités. Document de réflexion conjoint du comité d'experts Informatique Ambiante du département ST2I du CNRS et du Groupe de Travail Intelligence Ambiante du Groupe de Concertation Sectoriel (GCS3) du Ministère de l'Enseignement Supérieur et de la Recherche **36**(7), 75–84
3. Baldauf, M., Dustdar, S., Rosenberg, F.: A survey on context-aware systems. *IJAHUC* **2**(4), 263 (2007)
4. Ferrando, S.P., Onaindia, E.: Context-aware multi-agent planning in intelligent environments. *Inf. Sci.* **227**, 22–42 (2013)
5. Bogdanowicz, M., Scapolo, F., Leijten, J., Burgelman, J.C., Ducatel, K.: Istag scenarios for ambient intelligence. Technical report, IST Advisory Group (2010)
6. Ramos, C., Augusto, J.C., Shapiro, D.: Ambient intelligence and mathsemicolon the next step for artificial intelligence. *IEEE* **23**(2), 15–18 (2007)
7. Bergmann, R.: Ambient intelligence for decision making in fire service organizations. In: *Lecture Notes in Computer Science*, pp. 73–90. Springer Science Business Media (2007)
8. Aouatef, C., Iman, B., Allaoua, C.: Multi-agent system in ambient environment for assistance of elderly sick peoples. In: *Proceedings of the International Conference on Intelligent Information Processing, Security and Advanced Communication (IPAC 15)*. Association for Computing Machinery (ACM) (2015)
9. Bellifemine, F., Caire, G., Greenwood, D.: *Developing Multi-agent Systems with JADE*. Wiley (2007)
10. Corchado, J.M., Bajo, J., de Paz, Y., Tapia, D.I.: Intelligent environment for monitoring alzheimer patients, agent technology for health care. *Decis. Support Syst.* **44**(2), 382–396 (2008)
11. Moraitis, P., Spanoudakis, N.: Argumentation-based agent interaction in an ambient-intelligence context. *IEEE Intell. Syst.* **22**(6), 84–93 (2007)
12. Cook, D.J., Youngblood, M., Das, S.K.: A Multi-agent Approach to Controlling a Smart Environment, chapter *Designing Smart Homes*. Springer (2006)
13. Dujardin, T.: *Gestion intelligente d'un contexte domotique par un Systeme Multi-Agents*. Ph.D. thesis, Université Lille 1—Sciences et Technologies, France (2011)
14. Remagnino, P., Hagra, H., Monekosso, N., Velastin, S.: Ambient intelligence. In: *Ambient Intelligence*, pp. 1–14. Springer Science Business Media
15. Mezzano, T.: *Veille Technologique en Informatique-SmartHome-*. Ph.D. thesis, Université Libre de Bruxelles Faculté des sciences Département d'informatique (2006)
16. Ferber, J.: *Les Systèmes Multi Agents: vers une intelligence collective* (1995)
17. Olaru, A.: *A context-Aware Multi-Agent System for AmI Environments*. Ph.D. thesis, University politehnica of Bucharest. Romania. University Pierre et Marie curie (Paris 6). France (2011)

# A Proposal for Shared VMs Management in IaaS Clouds

Sid Ahmed Makhoulf and Belabbas Yagoubi

**Abstract** The progress of Cloud computing as a new model of service delivery in distributed systems encourages researchers to study the benefits and drawbacks about scheduling scientific applications such as workflows. Cloud computing allows users to scale their workflow applications dynamically according to negotiated service level agreements (SLA). However, the resources available in one cloud data center are limited, e.g. in Amazon 20 VMs is available. So if a high demand for a workflow Application is observed, a cloud provider will not be able to deliver consistent quality of service to process the application and the SLA can be violated. Our approach to avoid such a scenario is to allow the growing of resource requests by scaling Workflows applications on multiple independent data centers. Our approach is achieved by the installation of agents called *CloudCoordinators* and a special agent called *CloudExchange*. These agents follow economic market policies to get virtual machines across multiple data centers. In our approach, a user can offer his resources already obtained while waiting the end of an input/output operation in a Workflow. The discovery of offers and requests is done via the specific services offered by the *CloudExchange* agent. Clouds providers and users access the *CloudExchange* via there *CloudCoordinator*.

**Keywords** Cloud computing • Workflow • DAG • Resources brokering • Resources sharing • Distributed system • Workflow management system

---

S.A. Makhoulf · B. Yagoubi (✉)  
Department of Computer Sciences, University of Oran 1-Ahmed Ben Bella,  
Oran, Algeria  
e-mail: byagoubi@gmail.com

S.A. Makhoulf  
e-mail: sidahmed.makhoulf@gmail.com

# 1 Introduction

Cloud Computing is one of the latest technology in the literature distributed systems that provides software and hardware infrastructure as a service. Users can consume these services on the basis of a service level agreement (SLA) that defines the required quality of service (QoS), following the “pay-as-you-go” pricing model. The multi-objective nature of the scheduling problem in the Clouds is difficult to solve, especially in the case of complex applications such as Workflow. In addition, the pricing model of the most common commercial Clouds, makes the scheduling problem more complex.

Workflows constitute a common model to describe a wide range of scientific applications. Typically, a workflow is described by a directed acyclic graph (DAG) in which each computer task is represented by a node, and each set of data or control dependency between tasks is represented by a directed edge between the corresponding nodes.

Currently, there are several commercial Clouds, such as Amazon, which provide computing power and virtualized storage hardware, so users can deploy their own applications and services. This new service model in distributed systems, which is known as Infrastructure as a Service (IaaS), has potential benefits for the execution of scientific workflows [6]. First, users can get the resources dynamically on demand, and will be billed on the basis of pay-as-you-go system. This allows the workflow management system to increase or decrease its purchased resources according to the needs of workflow and user budget. The second advantage of the Clouds is the direct provisioning of resources compared to the best-effort method to provide resources in the grids. This feature can significantly improve the scheduling performance of the workflow interdependent tasks. The third advantage is the illusion of unlimited resources [9]. It means that the user can request a resource whenever he needs it.

Scheduling workflow is the problem of assigning each task to a suitable resource and control tasks in each resource to meet performance criteria. The task scheduling is NP-complete problem [8], many heuristics have been proposed for heterogeneous distributed systems such as grids [5, 11]. These methods of scheduling attempt to minimize the Workflow execution time (makespan). The most of current workflow management systems uses such planning methods. However, in the Clouds, there is another important parameter other than the execution time, namely, the execution cost. Generally, the fastest resources are more expensive than slower, so the scheduler is faced with a time-cost trade-off to choose the appropriate services. The resources in a cloud can be acquired in different levels of abstraction. On this paper, we are interested at the “Infrastructure as a Service” (IaaS). However, the resources available in a single data center is limited even if the data center may contain thousands of physical machines capable of hosting tens of thousands of virtual machines each. High demand put pressure on the capacity of the Cloud data center and its resources are overloaded; resulting in a degradation of data center performance and SLA violations from the workflow applications.

One approach to avoid the situation above is to allow Workflow applications to scale across multiple independent data centers. This approach, proposed in InterCloud [2] project includes data centers and brokers trading the resources to meet transparently the application requirements. InterCloud offers policies based on the economic market for the provisioning of virtual machines across multiple data centers. Key elements of the InterCloud are *CloudCoordinators*, which represent the providers and users of the market economy and the *CloudExchange* which acts as a system of resource discovery and publication of resources offers/requests.

## 2 Related Works

Works that share the vision and goals of the *InterCloud* are in the research domain of computational grids, and grids/clouds federation.

### 2.1 Federation of Grids and Cloud

The Intergrid [7] project uses virtualization technology to allow the sharing of resources between the grids. Resources are sought in remote grids whenever an incoming allocation request cannot be served by local resources. Resources grids and clouds are usually assigned differently. While grids federation is usually based on cooperation and resource sharing with allocations limited time, clouds allocations are not limited time; customers can explicitly request resources at any time because in the Clouds customer financially compensate resource providers. Therefore, solutions for the federation to the grid cannot be directly applied to the Clouds, and therefore cannot be directly applied in the context of InterCloud project.

Several Federation Cloud platforms have recently been proposed. Reservoir [12] has a modular and extensible architecture that supports cloud management enterprise services and federation of Cloud. Claudia [13] provides an abstract layer for running applications through a transparent federation of cloud providers. OpenCirrus [1] is a closed association between universities and research centers to facilitate research into design, procurement and management of services across multiple data centers. Sky Computing [10] introduced a virtual site of distributed resources dynamically provisioned from multiple data centers and managed by a model of closed federation, where resource sharing is based on cooperation as in the grids.

### 2.2 Workflow and Cloud Computing

One of the most recent work in this field was introduced by Byun et al. [3, 4]. They first proposed algorithm BTS (Balanced Time Scheduling) [3], which plans the

workflow in resource provisioning system on demand in a Cloud. The BTS algorithm attempts to estimate the minimum number of resources required to run the workflow. The algorithm has three main phases: (i) initialization, in which it calculates the initial values of some basic parameters, (ii) the placement of tasks in which calculates a preliminary schedule for the tasks of the workflow, (iii) and redistribution of tasks in which refines the preliminary schedule by moving tasks in the areas that require more resources.

The BTS algorithm has two main drawbacks: (i) considers the environment as homogeneous, i.e., all resources have the same task performance, (ii) it uses a fixed number of resources throughout the execution of the workflow, i.e., it does not use the elastic characteristics of current resources provision systems. In [4], Byun et al. propose the PBTS algorithm (Partitioned Balanced Time Scheduling) which is an extension of the BTS algorithm for elastic resources, i.e., they eliminate the second gap. The algorithm considers the billing policy of the time intervals of the current trade Clouds. This algorithm aims to find the minimum number of resources required for each time interval, so that the entire workflow is completed before the deadline set by the user.

### 3 Proposed Model

#### 3.1 Workflows Model

A workflow

$$wf_{(c)} = \left\langle X, U, StageNb, Stage^{(i,n)} \mid i = \overline{1, StageNb}, VmNb \right\rangle$$

is a set of tasks  $X$  oriented by a set of dependencies  $U$  and organized in number of stages  $StageNb$  which each stage  $Stage^{(i,n)} = \left\{ Task^{(j,d)} \mid j = \overline{1, n} \right\}$  contains  $n$  parallel tasks, see Fig. 1. Each task  $j$  has an execution time  $d$ .  $D_i$  is the execution time of stage  $i$  which

$$D_i = d_{Max} (Task^{(j,d)} \mid j = \overline{1, n} \mid i = \overline{1, StageNb}).$$

In our approach, the  $VmNb$  is the number of VM created for the execution of each Workflow.

Consider the Workflow of Fig. 1,  $X$  contains 20 tasks,  $U$  contains 29 dependencies,  $StageNb = 9$ . The main idea in our work is the possibility that workflow can share its VM with other workflow while waiting the end of an  $I/O$  operations; or get temporarily free VMs from other workflow to accelerate its execution. Example; for the execution of workflow in Fig. 1, if we create 04 VMs, then the workflow will be executed according to the following stages:

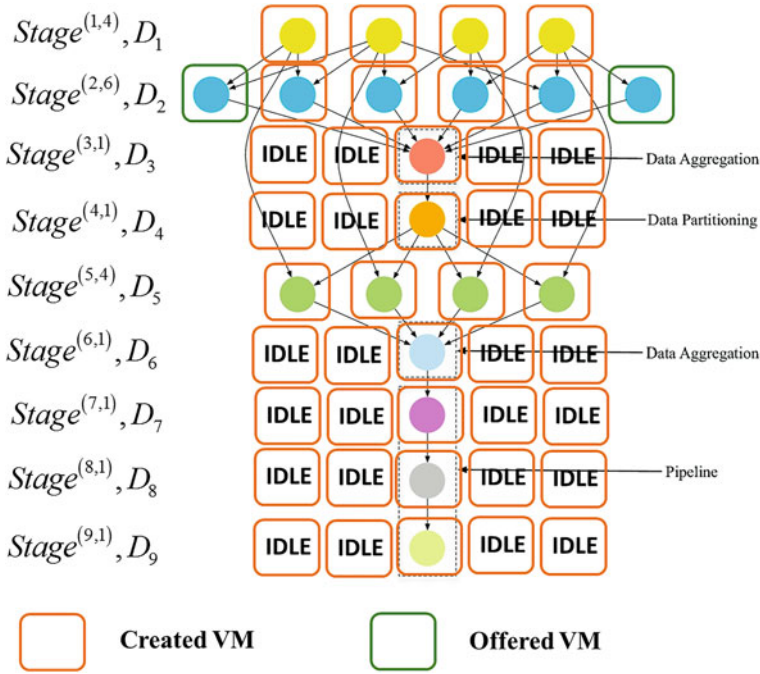


Fig. 1 Execution of workflow stages

- $Stage^{(1,4)}$ : The number of created VMs is sufficient to complete the execution of the 04 tasks as fast as possible.
- $Stage^{(2,6)}$ : The number of VMs is insufficient to complete the execution of the 06 tasks as fast as possible because it lacks 02 VMs. In our approach, Workflow can call other Workflows find at most 02 other free VMs to speed up its execution.
- $Stage^{(3,1)}$ : During this stage, the workflow requires only one VM to perform the execution of one task. In our approach, the workflow is allowed to propose to other workflow the using of its free VM, namely 03 VMs, but for determined period  $D_3 = d$ .  $d$  is the execution time of the unique tasks of the stage 3 and  $D_3$  is the execution time of the stage 3.

### 3.2 CloudExchange Model

Figure 2 shows the general organization of our approach. This is an implementation of market economy to allow brokers and providers the execution of workflow applications by exploiting resources from multiple Clouds.

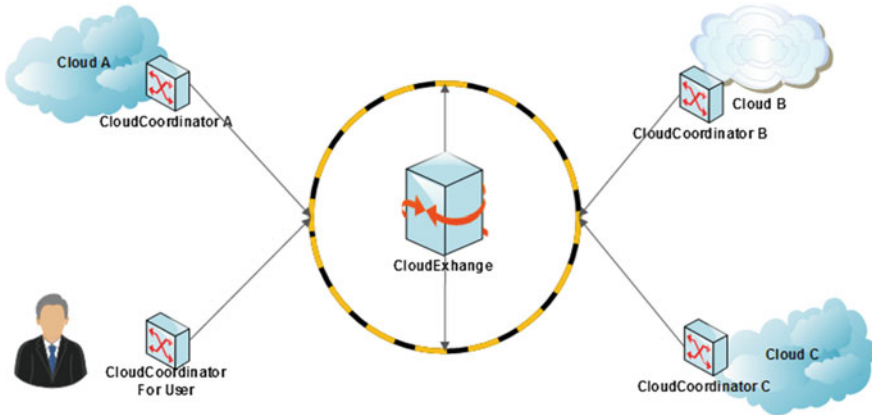


Fig. 2 System model

The *CloudExchange* is at the heart of the model. This component acts as the exchange of the economic market by providing a register for negotiation between the various parties of the economic market. Resource providers query the *CloudExchange* to discover other parts of the economic market components. In our approach, we assume that providers have **dynamic billing policies**.

### 3.3 *CloudCoordinator Model*

Resource providers communicate with the *CloudExchange* and other component of the economic market via *CloudCoordinator*, Fig. 2. The *CloudCoordinator* is a service oriented agent for sending to *CloudExchange* offers and receive requests from other parts of the economic market component. **No specific economic mechanism is imposed by our model to resource providers**. Therefore, each provider defines its own resource usage price and applies its own billing mechanisms. The resources exchanged on the market are virtual machines.

This paper focuses on the operation of *CloudCoordinator* as an agent in charge of workflow applications in the cloud, so users do not need to discover and acquire direct resources from multiple data centers for their workflows. In our model, the *CloudCoordinator* must be present at each data center and each user in the cloud. The *CloudCoordinator* is used by users and brokers who want to acquire resources; in this case, the *CloudCoordinator* can be considered as a data center that has no available local resources, so its always buys resources on the market in response to changes in the workflow application. The *CloudCoordinator* also offers services to enter into communication with other *CloudCoordinators* to share resources according to the billing mechanisms of the data center and to access the services of *CloudExchange*.

In this sense, the *CloudCoordinator* acts as a commercial agent. *CloudCoordinator* is the component of our system that implements the communication with other *CloudCoordinators*.

In our approach, the *CloudCoordinators* may propose the sharing of VMs that are temporarily *IDLE*. For example, a user can share VMs already obtained via its *CloudCoordinator* while waiting the completion of an *I/O* operation in a workflow. Figure 3 shows the publishing process of VMs in our model. The *CloudCoordinators* who want to publish a VMs offer (*DC1* in Fig. 3) or a resource request (User in Fig. 4) publish their offer/request via *CloudExchange*. Optionally, the *CloudCoordinators* query the *CloudExchange* about the availability of offers that match their needs.

Offer  $O_{(c,m)}^{(s,D)}$  of *CloudCoordinator*  $c$  is a list of Virtual Machines (VM) such as  $O_{(c,m)}^{(s,D)} = \{VM_{(i,c,p)}^{(s,D)} | i = \overline{1, m}\}$ , Where  $s$  is the offer submission time,  $m$  is the number of offers,  $D$  the offer duration time and  $p$  is the price of the virtual machine  $i$ . In the case of a resource provider, the duration  $D$  is unlimited but in the case of a single workflow broker it is limited.

Offers for resources are described in terms of numbers, characteristics and prices of available virtual machines. Providers and users send their own offerings or requests of resources to *CloudExchange* containing the following information:

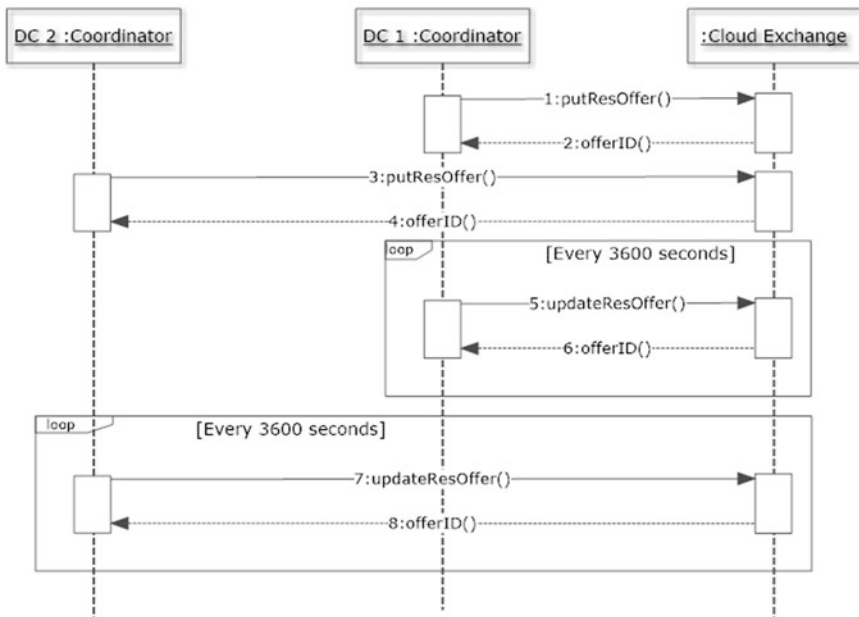


Fig. 3 Resource publication process



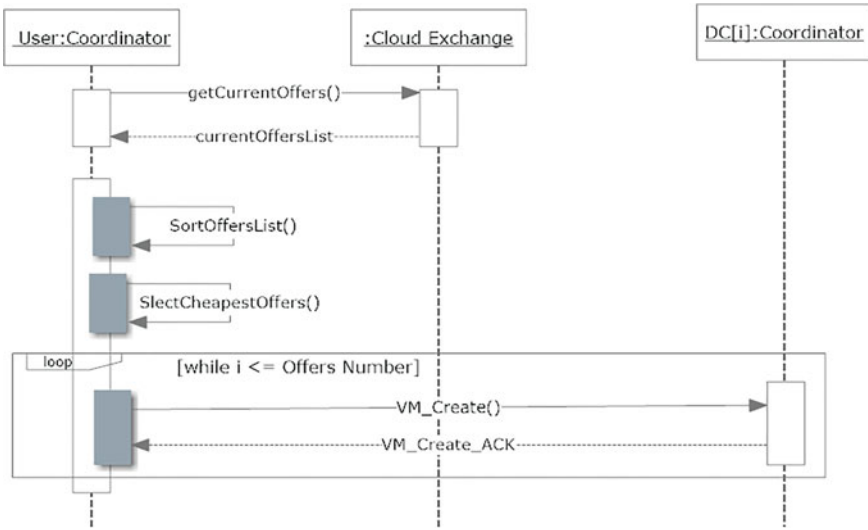


Fig. 4 Virtual machine creation process

- Number of available or required virtual machines
- Amount of memory virtual machines
- Number of cores per virtual machine
- computing capacity of each core
- Price of each virtual machine (per hour for the resource provider)

The discovery of offers and requests is available via specific services offer by the *CloudExchange*.

In our model, we suppose that the Cloud Data Center review the prices of their resources every 3600 s (1 h), and contact the *CloudExchange* to update their new prices. These can increase or decrease depending on offers and query.

In Fig. 4, the user (workflow) request *CloudExchange* for the list of available offers

$$OfferList = \bigcup_{c=1}^N o_{(c)}^{(s,D)}.$$

The user sort the *OfferList* by price in ascending order  $SortedOfferList = Sort_{price}^{\uparrow}(OfferList)$ . Then it selects the  $VmNb$  cheapest offers  $cheapestOffer \subseteq SortedOfferList$  that meet its needs for the creation of virtual machines.

Figure 5 models the submission of a subset of workflow (Algorithm 1, Appendix A). The *CloudCoordinator* starts by checking if the number of its *idle* virtual machines is sufficient to makes a direct allocation of tasks. If the number of idle virtual machine is not sufficient, then the user request *CloudExchange* for a list of

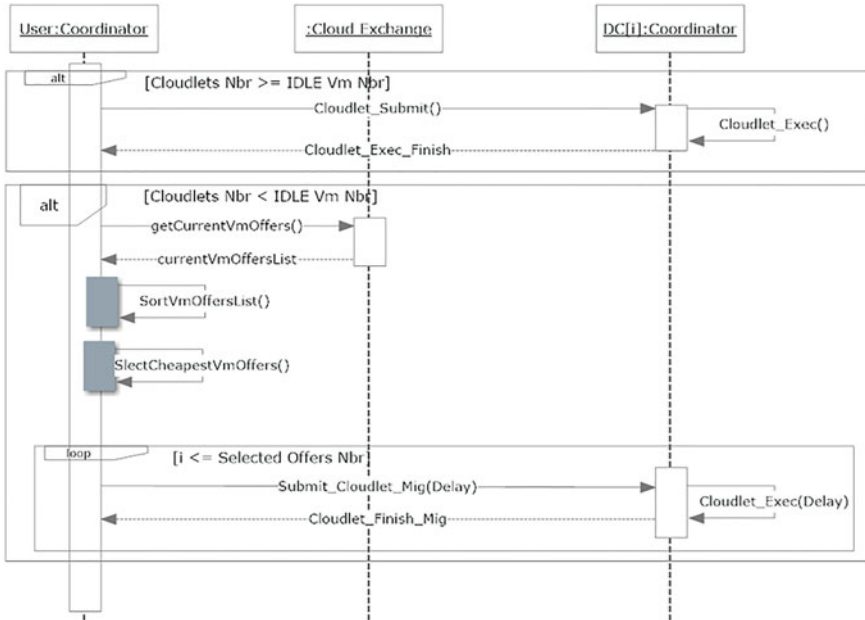


Fig. 5 Tasks submission process

available virtual machines offered temporarily by other *CloudCoordinator*. This last one will sort the offer list by price in ascending order (Algorithm 2, Appendix A). It then selects the cheapest virtual machines offered that meet its needs. In this case, allocation of virtual machine to the tasks is done during a period of time (Delay in Fig. 5). The Delay is period during which Offer is valid before it expires. It is possible that the Delay expires before the end of the execution of the task. If the number of idle virtual machine is sufficient, then the user do a local allocation by using its VMs (Algorithm 3, Appendix A).

Figure 6 models the return of a task after the expiration of the offer Delay (Algorithm 4, Appendix A). If the job has not finished, then, the user re-execute the diagram of Fig. 5. Figure 7 models the offer mechanism implemented by the *CloudCoordinator* that represent a user. After allocating set of tasks in set of virtual machines, the user checks if he has already an *idle* virtual machines to offers, to do, its call *CloudExchange* to offer his idle virtual machines during a period of time (Delay in Fig. 5) while waiting the return of previously submitted tasks.

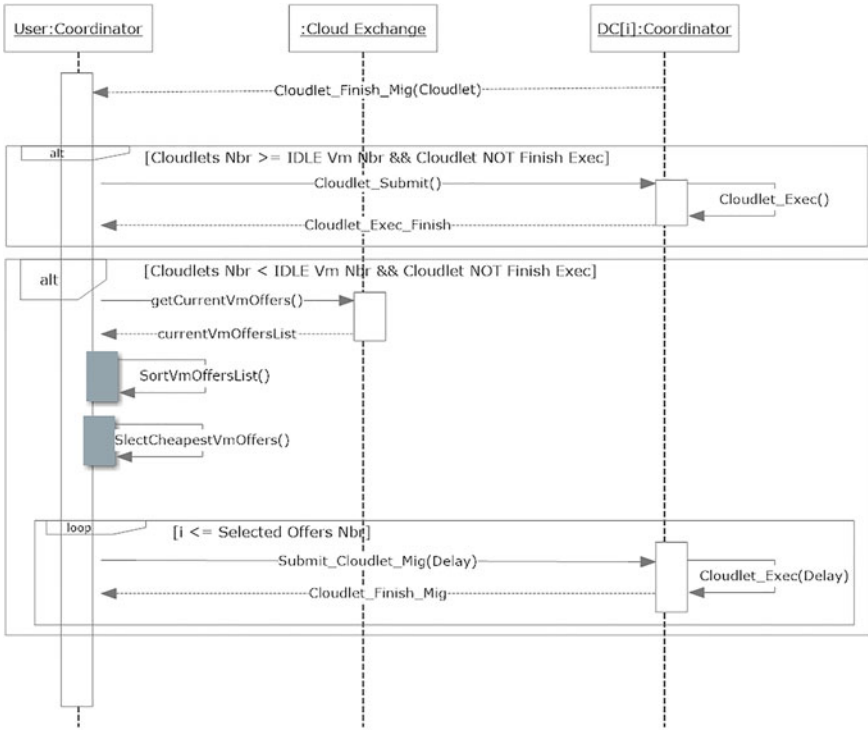


Fig. 6 Tasks return process

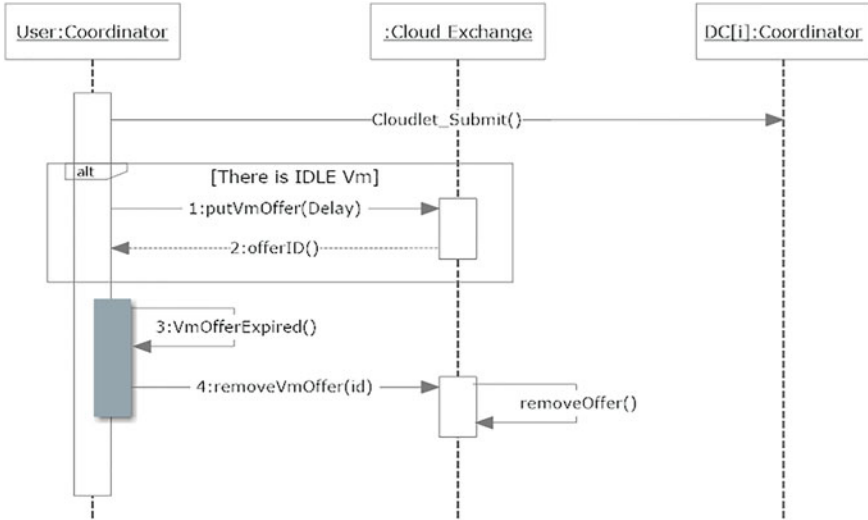


Fig. 7 Virtual machines offers process

## 4 Implementation and Experimentation

In order to validate the proposed model, we implemented a discrete event simulator using *CloudSim*. The simulator has a general architecture of IaaS Cloud.

We simulated the arrival of 100 *Montage* workflows each of them contains 1000 tasks. Figure 8 describe the most used scientific workflows [3]. The arrival of workflow follows the *Poisson* distribution with  $\lambda = 1800$  s. For each workflow we have varied the number of VMs between 4 and 16 VM and measure the time and cost of workflows execution. We implemented in the *CloudSim* simulator the architecture of virtual machines offered by the Amazon *EC2* Cloud. As in the *EC2* Cloud, the prices of virtual machines dynamically change every 3600 s. We conducted our simulation in a server with 48 GB of RAM, an Intel Xeon E5-2620 processor 2.10 GHz and Windows Server 2012. We have compared our “*Vm Sharing*” model with the “*No Vm Sharing*” model that does not share the *idle* virtual machines.

In Table 1, we have varied the number of VM for each workflows and calculate the average execution time. We can see that as the number of VM increases more execution time decreases. And we can see that between 4 and 8 VM, our model gives a good result. It can reduces the execution time by 1 h.

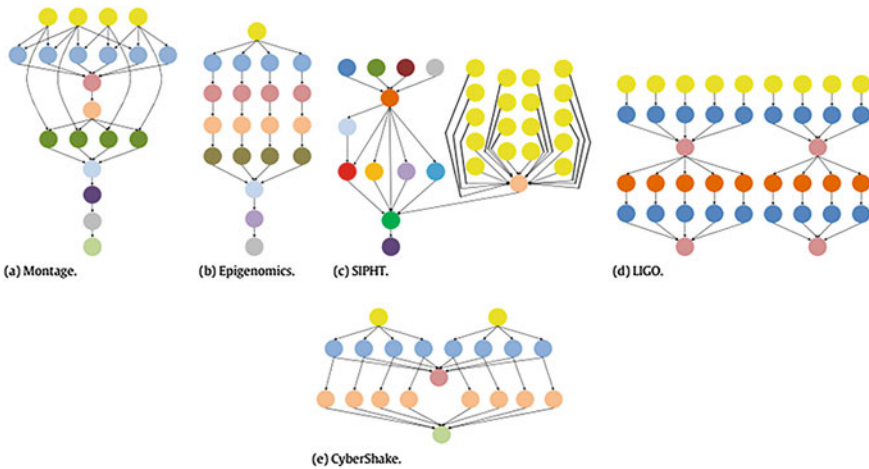


Fig. 8 Structure of five scientific workflows [3]

Table 1 Average workflows execution time (hours)

Number of VMs	Vm sharing	No Vm sharing
4	83.22	84.25
8	46.5	47.42
16	28.6	28.67

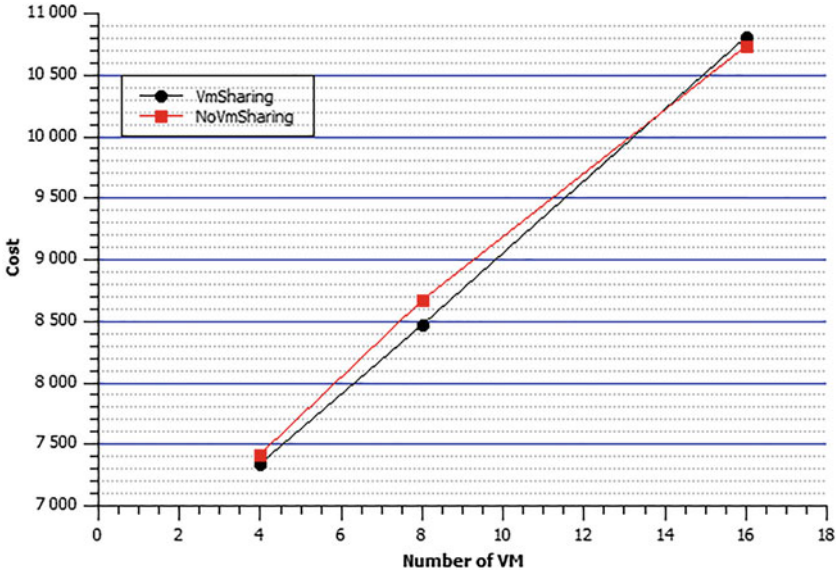


Fig. 9 Average execution cost

Table 2 Average workflows execution cost

Number of VMs	Vm sharing	No Vm sharing
4	7336	7416
8	8469	8677
16	10811	10771

In Fig. 9, we varied the number of VM for each workflows and calculate the average execution cost. We can see that as the number of VMs increases more the cost increases. And we can see that between 4 and 8 VM, our model gives a good result; it can reduce cost of 200 unit (e.g. 200 €). Table 2 shows the detailed costs of Fig. 9.

## 5 Conclusion

One of the most difficult problems in the Clouds Computing is workflow scheduling. In this paper, we proposed a model of *interCloud* workflow management system based on a *CloudExchange* agent and a set of *CloudCoordinators* agents. The *CloudCoordinator* represents data centers and brokers in a Cloud market, and is responsible of offers, publishing and requests of resources and discovery of potential resource providers. To do this, the *CloudCoordinator* interacts with *CloudExchange*.

*CloudExchange* is a directory service that receives requests and offers of *CloudCoordinator* to be published in the system. *CloudExchange* does not impose any billing mechanism to Cloud providers. The main idea of our approach is to allow users to execute their workflow applications across multiple providers via their *CloudCoordinator*. Our model is based on the principle of virtual machines sharing, for example, a user can temporarily offer its resources pending the completion of an I/O operation via its *CloudCoordinator*.

In order to show the efficiency of our proposed approach, we have built in a simulator adapted to the simulation of workflows applications. We made a series of simulations and the results show that it is possible to reduce the time and cost of execution with sharing idle virtual machines.

The Clouds IaaS offer various pricing options on different types of instances (virtual resources) such as Reserved Instances. The problem of users using the cloud-based services is to minimize the costs of the allocations instances choosing from the different pricing options according to their needs. So, as future work, we plan to develop resource allocation policies that support advance reservation.

## Appendix A: Algorithmic Modelisation

---

### Algorithm 1 Task Submission

---

```

1: procedure TASKSUBMISSION( $wf = \langle X, U, StageNb, Stage^{(i,n)} | i = \overline{1, StageNb}, VmNb \rangle$ )
2:   for  $i = 1; i \leq StageNb; i \leftarrow i + 1$  do
3:      $Stage^{(i,n)} \leftarrow getStage(wf)$ 
4:     if  $|Stage^{(i,n)}| \leq IDLE(VmList[VmNb])$  then ProcedureCall :
       localVmAllocation ( $Stage^{(i,n)}, VmList[VmNb]$ )
5:     end if
6:     if  $|Stage^{(i,n)}| \geq IDLE(VmList[VmNb])$  then ProcedureCall :
       sharedVmAllocation ( $Stage^{(i,n)}, VmList[VmNb]$ )
7:     end if
8:   end for
9: end procedure

```

---

---

**Algorithm 2** Shared VMs Allocation
 

---

```

1: procedure SHAREDVMALLOCATION( $Stage^{(i,n)}$ ,  $VmList[VmNb]$ )
2:    $offerList \leftarrow getCurrentOffer()$ 
3:   if  $offerList = \phi$  then
4:     for  $j = 1; j \leq VmNb; j \leftarrow j + 1$  do
5:        $Task^{(j,d)} \leftarrow get(Stage^{(i,n)})$ 
6:       if  $IDLE(VmList[VmNb]) > 0$  then
7:          $taskSubmit(Task^{(j,d)}, VmList[j])$ 
8:       else
9:          $taskWaitingList \leftarrow taskWaitingList \cup \{Task^{(j,d)}\}$ 
10:      end if
11:    end for
12:   else
13:      $SortedOfferList \leftarrow Sort_{price}^{\uparrow}(OfferList)$ 
14:     for  $j = 1; j \leq VmNb; j \leftarrow j + 1$  do
15:       if  $IDLE(VmList[VmNb]) > 0$  then
16:          $taskSubmit(Task^{(j,d)}, VmList[j])$ 
17:       else
18:         if  $SortedOfferList \neq \phi$  then
19:            $O_{(x,1)}^{(s,d_x)} \leftarrow \min(SortedOfferList)_{price}$ 
20:            $SubmitTaskMig(Task^{(j,d)}, O_{(x,1)}^{(s,d_x)}, d_x, x)$ 
21:            $SortedOfferList \leftarrow SortedOfferList - \{O_{(x,1)}^{(s,d_x)}\}$ 
22:         else
23:            $taskWaitingList \leftarrow taskWaitingList \cup \{Task^{(j,d)}\}$ 
24:         end if
25:       end if
26:     end for
27:   end if
28: end procedure

```

---

**Algorithm 3** Local VMs Allocation
 

---

```

1: procedure LOCALVMALLOCATION( $Stage^{(i,n)}$ ,  $VmList[VmNb]$ )
2:    $D_i \leftarrow 0$ 
3:   for  $j = 1; j \leq n; j \leftarrow j + 1$  do
4:      $Task^{(j,d)} \leftarrow get(Stage^{(i,n)})$ 
5:     if  $d > D_i$  then
6:        $D_i \leftarrow d$ 
7:     end if
8:      $taskSubmit(Task^{(j,d)}, VmList[j])$ 
9:   end for
10:   $m \leftarrow IDLE(VmList[VmNb])$ 
11:  if  $m > 0$  then
12:     $O_{(c,m)}^{(CurrentTime,D_i)} \leftarrow getIDLE(VmList[VmNb])$ 
13:     $putVmOffer(O_{(c,m)}^{(CurrentTime,D_i)})$ 
14:  end if
15: end procedure

```

---

**Algorithm 4** Task Return

---

```

1: procedure TASKRETURN( $Task^{(j,n)}$ ,  $VmList[VmNb]$ )
2:   if
            $NotFinished (Task^{(j,d)})$ 
       then
3:      $taskWaitingList \leftarrow taskWaitingList \cup \{Task^{(j,d)}\}$ 
4:   end if
5:   if  $|taskWaitingList| \leq IDLE (VmList [VmNb])$  then
6:     Procedurecall :  $localVmAllocation (taskWaitingList, VmList [VmNb])$ 
7:   end if
8:   if  $|taskWaitingList| > IDLE (VmList [VmNb])$  then Procedurecall :
        $sharedVmAllocation (taskWaitingList, VmList [VmNb])$ 
9:   end if
10: end procedure

```

---

**References**

1. Avetisyan, A., Campbell, R., Gupta, I., Heath, M., Ko, S., Ganger, G., Kozuch, M., O'Hallaron, D., Kunze, M., Kwan, T., Lai, K., Lyons, M., Milojicic, D., Lee, H.Y., Soh, Y.C., Ming, N.K., Luke, J.Y., Namgoong, H.: Open cirrus: A global cloud computing testbed. *Computer* **43**(4), 35–43 (2010)
2. Buyya, R., Ranjan, R., Calheiros, R.N.: Intercloud: Utility-oriented federation of cloud computing environments for scaling of application services. In: Algorithms and Architectures for Parallel Processing, 10th International Conference, ICA3PP 2010, Busan, Korea, May 21–23, 2010. Proceedings. Part I, vol. 6081. Springer (2010)
3. Byun, E.K., Kee, Y.S., Kim, J.S., Deelman, E., Maeng, S.: BTS: resource capacity estimate for time-targeted science workflows. *J. Parallel Distrib. Comput.* **71**(6), 848–862 (2011)
4. Byun, E.K., Kee, Y.S., Kim, J.S., Maeng, S.: Cost optimized provisioning of elastic resources for application workflows. *Future Gen. Comput. Syst.* **27**(8), 1011–1026 (2011)
5. Daoud, M.I., Kharma, N.N.: A high performance algorithm for static task scheduling in heterogeneous distributed computing systems. *J. Parallel Distrib. Comput.* **68**(4), 399–409 (2008)
6. Deelman, E.: Grids and clouds: making workflow applications work in heterogeneous distributed environments. *Int. J. High Perform. Comput. Appl. (IJHPCA)* **24**(3) (2010)
7. di Costanzo, A., de Assunção, M.D., Buyya, R.: Harnessing cloud technologies for a virtualized distributed computing infrastructure. *IEEE Internet Comput.* **13**(5), 24–33 (2009)
8. Garey, M.R., Johnson, D.S.: Computers and Intractability; A Guide to the Theory of NP-Completeness. W.H Freeman (1979)
9. Juve, G., Deelman, E., Vahi, K., Mehta, G., Berriman, B., Berman, B.P., Maechling, P.: Scientific workflow applications on amazon EC2 (2010)
10. Keahey, K., Tsugawa, M.O., Matsunaga, A.M., Fortes, J.A.B.: Sky Comput. *IEEE Internet Comput.* **13**(5), 43–51 (2009)
11. Nadeem, F., Fahringer, T.: Optimizing execution time predictions of scientific workflow applications in the grid through evolutionary programming. *Future Gen. Comput. Syst.* **29**(4), 926–935 (2013)
12. Rochwerger, B., Breitgand, D., Epstein, A., Hadas, D., Loy, I., Nagin, K., Tordsson, J., Ragusa, C., Villari, M., Clayman, S., Levy, E., Maraschini, A., Massonet, P., Muñoz, H., Toffetti, G.: Reservoir—when one cloud is not enough. *IEEE Comput.* **44**(3), 44–51 (2011)
13. Rodero-Merino, L., Gonzalez, L.M.V., Gil, V., Galán, F., Fontán, J., Montero, R.S., Llorente, I.M.: From infrastructure delivery to service management in clouds. *Future Gen. Comput. Syst.* **26**(8), 1226–1240 (2010)



# Cloud Simulation Model Based on Large Numbers Law for Evaluating Fault Tolerance Approaches

Oussama Hannache and Mohamed Batouche

**Abstract** Cloud computing is an emerging paradigm that consists of hosting and delivering computing services across the web. The availability is one of the security features such as integrity and confidentiality. Certainly endorsing high availability by the improvement of fault tolerance techniques is one of the major concerns of the cloud. Elsewhere we cannot afford to directly evaluate new approaches for cost reason. For this reason we introduce in this paper a probabilistic model for simulation based on the principle of “Large Numbers Law”. The idea is to simulate a scenarios of cloud virtual environment in which faults can occur in a random way following failure occurrence probabilities. The global unavailability measured is faithful to unavailability average known of Cloud providers. The model allows live virtual machine migration in order to evaluate proactive fault tolerance approaches based on preemptive migration.

**Keywords** Cloud computing · High availability · Fault tolerance · Probabilistic model · Simulation · Large numbers law · Virtual machine migration

## 1 Introduction

In this last few years, cloud computing has been one of the new emerging topics representing the ability to consume computing services across the large web, it refers to the delivery of computing resources on demand [1]. The cloud itself is not a new technology but a new way of seeing due to the mobility of the consumers and flexibility and scalability of the computing resources. The cloud has no place to be

---

O. Hannache (✉) · M. Batouche  
MISC Laboratory, Computer Science Department, College of NTIC,  
Constantine University 2, Constantine, Algeria  
e-mail: oussama.hannache@univ-constantine2.dz

M. Batouche  
e-mail: mohamed.batouche@univ-constantine2.dz

without previous technologies on which he is based, we quote mainly web 2.0, open source software and virtualization. Of course, virtualization techniques bid to the cloud the aptitudes to be flexible and scalable allowing high availability by mutualizing physical resources [2]. Increase the availability is very essential, it represents one of the main features of cloud security such as integrity and confidentiality. Multicore processing, virtualization, distributed storage systems and an overarching management framework that enable the cloud offer a plethora of possibilities to provide high availability using commodity systems [3]. Besides that, critical processes can be lost over the time compromising the availability of some critical services, for this reason, fault tolerance and load balancing technics used must be effective. Researches in fault tolerance aim to increase the failure prediction accuracy or to decrease the recovery time, but we cannot afford to directly implement and evaluate new approaches for cost and time reasons. Elsewhere, existing cloud simulation tools for evaluating algorithms do not take into consideration the fault occurrence which makes the evaluation inaccurate. The lack of benchmarks or standard models for evaluating fault tolerance approaches in the cloud brings us to think more about modeling the cloud environment for evaluating reactive and proactive fault tolerance approaches. For this purpose, we propose in this work a probabilistic model for simulation based on “Law of large Numbers” for evaluating fault tolerance approaches. The proposed model illustrates multi-layer virtual environment allowing live virtual machine migration.

The paper is organized as follows: First, we introduce in Sect. 2 cloud concept. In Sect. 3 we provide a review of virtualization technics used in the cloud illustrating live virtual machine migration. In Sect. 4 we speak about the role of VM migration for increasing high availability in the cloud. Section 5 is devoted to the cloud benchmarking works. Section 6 we introduce our simulation model followed by results obtained in Sect. 7. Finally, conclusions and future directions of the work are drawn.

## 2 Cloud Computing

In this last decade, a debate took place within the computer science community between those who think that the cloud is just “the natural evolution of computing” and those who consider the cloud itself a new model. But incontestably the cloud computing emerges like one of the hot topics nowadays. The real question is: what is the cloud computing? That is what we will see in this section.

Cloud Computing has recently emerged as new paradigm for hosting and delivering services over the Internet. Cloud Computing is the use of computing resources such as hardware and software that are delivered as service over the internet [4]. A special publication by the US National institute of standard and technology has given a complete definition of the cloud computing. According to NIST [5] “Cloud computing is a model for enabling ubiquitous, convenient, on-demand network access to a shared pool of configurable computing resources

(e.g., networks, servers, storage, applications, and services) that can be rapidly provisioned and released with minimal management effort or service provider interaction. This cloud model is composed of five essential characteristics, three service models, and four deployment models”.

Again according to NIST there are 3 service models and 4 deployment models. The users interact with the cloud through services: Software as a Service (SaaS), Platform as a Service (PaaS) and Infrastructure as a Service (IaaS). The SaaS layer is devoted to the large users offering a plethora of applications which are running in the cloud infrastructure. These applications can be accessible from any location and the consumers does not care about managing or controlling the underlying cloud infrastructure including network, servers, operating systems, storage, or even individual application capabilities [5]. The PaaS layer concern mainly developers, the capability provided to the consumer is to deploy onto the cloud infrastructure consumer-created or acquired applications created using programming languages and frameworks supported by the cloud provider [5]. In the IaaS cloud provider provide infrastructure services in term of processing, storage, networks, and other fundamental computing resources where the consumer is able to deploy and run arbitrary [6]. The consumer does not manage or control the underlying cloud infrastructure but has control over operating systems, storage, and deployed applications; and possibly limited control of select networking components [5] (Table 1).

The NIST publication brings out also 4 deployment models: Private cloud, Community cloud, Public cloud and the Hybrid cloud. In the private cloud the infrastructure is reserved for the exclusive use of a single organization. In the community cloud The cloud infrastructure is provisioned for exclusive use by a specific community of consumers from organizations that have shared concerns. In the public cloud the infrastructure can be used by the general public, on the pre-mises of the providers it can be operated, owned or managed by d by a business, academic, or government organization. In the hybrid cloud the infrastructure is

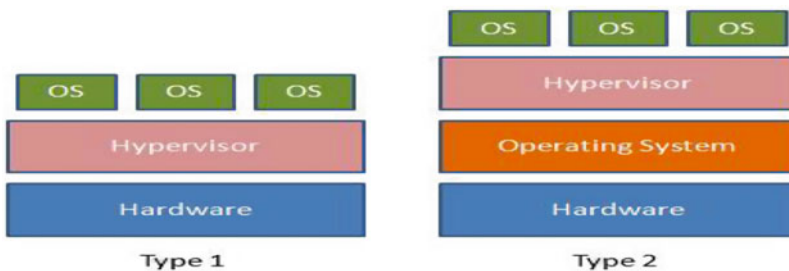
**Table 1** The cloud computing according to NIST [5]

Five essential characteristics	1. On demand self-service
	2. Broad network access
	3. Resource pooling
	4. Rapid elasticity
	5. Measured services
Three service models	1. Software as service (Saas)
	2. Platform as service (Paas)
	3. Infrastructure as service (Iaas)
Deployment models	1. Public cloud
	2. Private cloud
	3. Hybrid cloud
	4. Community cloud

composed by of two distinct or more cloud infrastructure (private, community, or public) [5].

### 3 Virtualization in the Cloud

As stated before, the virtualization concept bid to the cloud the ability to dynamically scale as the demand grow, A virtualized server environment allows computing resources to be shared among multiple performance isolated platforms called virtual machines (VM) [7]. The efficiently managing server hardware and system resources leads to an effective use of IT infrastructure. VM is an essential component in most of the cloud/data-center system software stacks. By employing virtualization platform, the cloud provides virtualized computing hardware architecture (IaaS) employing so flexible and scalable virtualization platform. Virtualized environments are usually implemented with the use of a Hypervisor, which is a software layer located below the VMs and above physical hardware layer. The Hypervisor allocates resources to the VMs, such as main memory and peripherals. It is in charge of providing each VM with the illusion of being run on its own hardware, which is done by exposing a set of virtual hardware devices (e.g. CPU, Memory, NIC, Storage) whose tasks are then scheduled on the actual physical hardware [8]. Hypervisors can be classified into two types—Type 1 and Type 2 hypervisors. Type 1 hypervisors run directly above the host hardware and monitor operating systems that run above the hypervisor. These are also called bare metal hypervisors [9], this type of virtualization offers logically a better performance because of the direct interaction with the physical layer, for this reason the Type 1 hypervisors are the most use in the cloud environment. One of the major advantages too is that any fault that can occur in any VM does not affect the other VMs running on the hypervisor. In Type 2 hypervisors, the hypervisor is installed on an operating system and then supports other operating systems above it [9], this type of virtualization unlike the Type 1 hypervisors offers less performance. Any problems in the base operating system affects the entire system as well even if the hypervisor running above the base OS is secure [9] (Fig. 1).



**Fig. 1** Types of hypervisors [9]

The virtualized environment of the cloud computing has the aptitude to be flexible and scalable as stated before, and that is likely due to the live virtual machine migration between physical hosts achieving so load balancing, fault tolerance and energy efficiency increasing by the way the high availability of the cloud [10]. Live virtual machine migration is a technique that consists of migrating the whole operating system and all the applications running on it from one physical machine to another. The process runs lively without disrupting the global system. This process can be performed by two techniques: Pre-copy and Post-copy migration [10].

In Pre-Copy migration technique majorities of memory pages are copied from source to destination while the process is executing on the source machine, the newly written pages are transferred in each iteration and this process is repeated until either the limit on iteration reaches or the final data is too small for causing any network transfer overhead [11, 12].

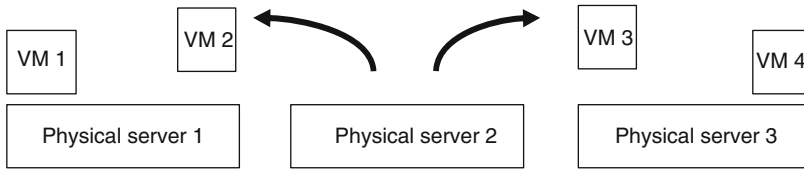
1. Memory and VCPUs are reserved on the destination host.
2. When the migration is issued, a check on page writes is initiated and all the RAM contents are transferred to the destination. This is the first iteration.
3. In the subsequent steps, only the pages that have been dirtied since the last iteration are transferred until the iteration limit is reached or the memory of dirty pages in an iteration is low enough.
4. The execution of VM on source is stopped and CPU state, registers, Virtual devices state and last memory pages are transferred to the destination.
5. VM is resumed at the destination.

In Post-copy migration technique, initially the processor state and minimal memory pages that are required to operate the VM at the destination server are copied in contrary to pre-copy [11, 13].

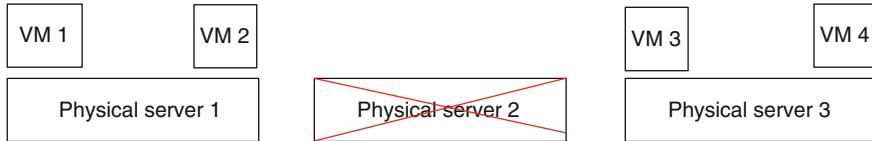
1. Stop the VM at the source.
2. VCPU registers and states of devices are copied to the destination VM.
3. Resume the execution at the destination.
4. If the VM tries to access a not yet fetched page, then a network page fault occurs and the page is transferred to the destination (on-demand paging).

## 4 Live Migration and Fault Tolerance

The live migration of virtual machines mechanism aims to endorse the cloud high availability by achieving mainly fault tolerance and load balancing. Of course, in order to balance the load among servers VMs are migrated following policies that vary from a method to another. Besides that, one of the most interesting aspect of the live migration is Fault tolerance. Fault tolerance is a major concern to guarantee availability and reliability of critical services as well as application execution, it permits a system to keep performing actually when one of its parts falls flat [14].



**Fig. 2** Proactive fault tolerance with preemptive VM migration [migration decision]



**Fig. 3** Migration of VM 2 and VM 3 before server 3 failure

Based on fault tolerance policies, there are two types of fault tolerance: reactive fault tolerance and proactive fault tolerance.

- The reactive fault tolerance techniques are used to reduce the impact of failures just after their occurrence, in other terms, the processes are triggered reactively. The most classic known techniques are: Check pointing/Restart, Replication, Job migration, User defined exception handling [15].
- The proactive fault tolerance techniques aim to avoid the recovery from faults that can occur by predicting them. Based on what we call failure predictor module, the process of avoiding faults is triggered according to predictions provided by the failure predictor [15]. Techniques based on this policy are: Software Rejuvenation-It with a periodic reboots, self-healing and mainly Preemptive Migrations

As shown in the Figs. 2 and 3, the physical server 2 is about to fail, the failure predictor module predicts that fail few times before it occurrence and triggers the migration of all the VMs running on it to physical server 1 and 3 while maintaining load balancing.

## 5 Benchmarking in the Cloud

In order to assess the performance of the cloud computing in terms of availability, benchmarks are more necessary than ever, by the increasing of the adoption of the cloud we cannot afford to directly implement and evaluate new fault tolerance or load balancing algorithms in real cloud infrastructure for evident cost reasons. For this purpose, we need more initiatives for benchmarking the cloud in order to know what are the best rules, the best policies to follow in order to have the best

performances [16]. The major task of a benchmark is to give us the best system in a given domain which is the cloud in our context, Benchmarks pick a representative scenario for the given domain. They define rules how to setup and run the scenario, and how to obtain measurement results [16]. We talk also about SUT (System Under Test), a SUT is a collection of components necessary to run the benchmark scenario. In the cloud the basic idea is to determine the main actors defining with them a complete application architecture. After that, the benchmark proceeds to evaluate the complete behavior of the SUT (Figs. 4, 5 and 6).

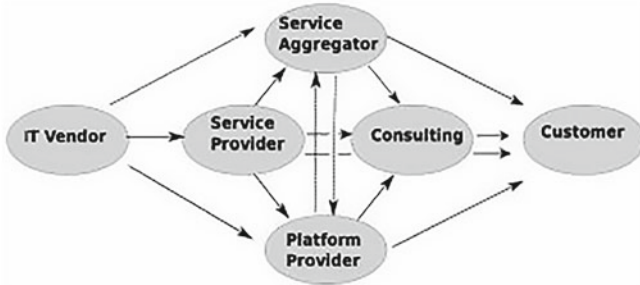


Fig. 4 Cloud Actors and their Value Network [16]

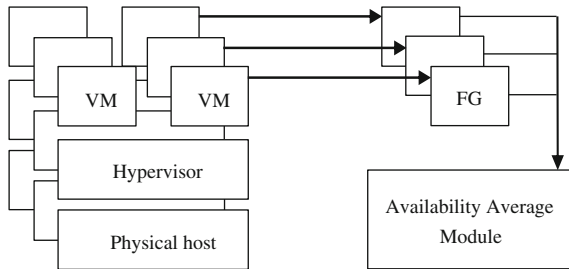


Fig. 5 Global system architecture

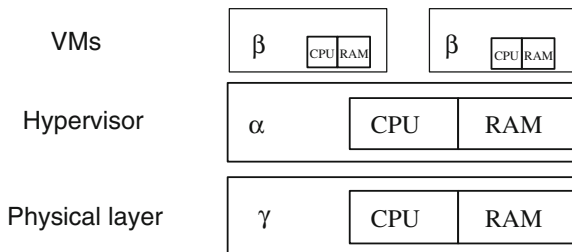


Fig. 6 Virtual environment with  $\alpha$ ,  $\beta$  and  $\gamma$  resources vectors

## 6 Proposed Work

In this section, we introduce our proposed simulation model of the cloud computing. The basic idea is to simulate a scenario in a virtual environment in which faults can occur in the physical nodes or hypervisors over the time causing downtimes, and the unavailability of the global system during the simulation can be measured and should be faithful to “n-nine” availability metrics (90, 99, 99.9, 99.99 and 99.999 % of availability) known in the SLAs for cloud providers as shown in the following table.

We had advanced in a previous work [17] a similar model for evaluating a proactive fault tolerance approach. The aim of this model is to permit evaluating of fault tolerance approaches especially proactive fault tolerance approaches based on preemptive virtual machine migration. This is possible because our simulation model allow live migration of virtual machines during the simulation and the downtime of nodes whose VMs have migrated to another physical nodes is not recorded. On top of that, we have introduced in this work for the model the notion of the load related to each physical node that can increase the probability of fail occurrence.

### 6.1 Description

The model aims to implement a minimalist system of the cloud computing in which fails can occur and the availability average can be measured [17].

The model includes many physical nodes. Each node is modeled according to type-2 virtualization. (i.e., physical layer, Hypervisors and VMs) Each node is provided with a failure generator. The failure generator has as task to generate faults that cause downtimes. All the unavailability time is measured by the availability average module.

### 6.2 Virtual Environment

The virtual environment contains for each node

- Physical host
- Hypervisor
- VMs

Each component is provided with a vector containing information about resources in term of CPU and Memory utilization. For load management we use a metric proposed by Emmanuel and David [18] for load balancing. The proposed idea is to assign weight to all the resources utilized by the servers. The resources utilized by



virtual machines are known only by the hypervisor layer. The Virtual Server Load (VSL) is metric that is computed (Eq. 1) using the resources utilized at the hypervisor layer.

$$VSL = \sum \alpha \frac{\sum \beta}{\sum \gamma} \tag{1}$$

where  $\alpha$  indicates the weight allotted to resources of physical server,  $\beta$  indicates the utilization of resources by virtual machines running in a physical server and  $\gamma$  indicates the resource capacity of a physical server. The VSL value is calculated for each Server in the cloud Data center. Based on the VSL values the virtual machines are migrated from highly utilized servers to less utilized servers. The VSL metric in this work is not used for migration decision for load balancing. The idea is that the Failure Occurrence Probability (FOP) that we will describe in the next section is influenced by VSL of each physical node. We have also based our resources measurements on a study from Li et al. [19] called “Performance Overhead Among Three Hypervisors: An Experimental Study using Hadoop Benchmarks” the work done by Jack li et al. is to conduct experimental measurements of several benchmarks using Hadoop MapReduce to evaluate and compare the performance impact of three popular hypervisors. They also proceeded to run four benchmarks (Word Count, KMeans Clustering, Hive aggregate and Hive join) and compared the obtained results in term of CPU and memory utilization as shown in Fig. 7.

In order to compute VSL, we have used this results such as, for each benchmark algorithm we know the resources utilizations in hypervisor and VM level.

### 6.3 Failure Generator

The objective of this module is to generate fails randomly following a fault occurrence probability (FOP). Based on “Law of large Numbers” we can be sur to reaches a very high accuracy with the correlation of all the fails occurring in the

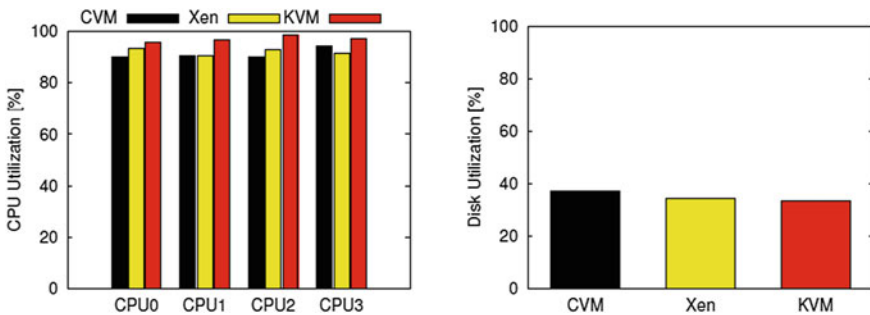


Fig. 7 CPU and Disk utilization recorded for CVM, Xen and KVM hypervisors [19]

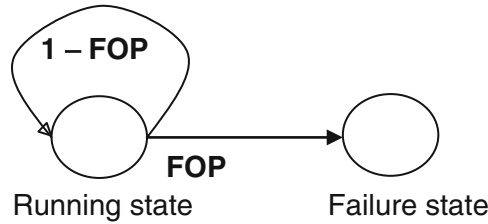


Fig. 8 Failure generator automat

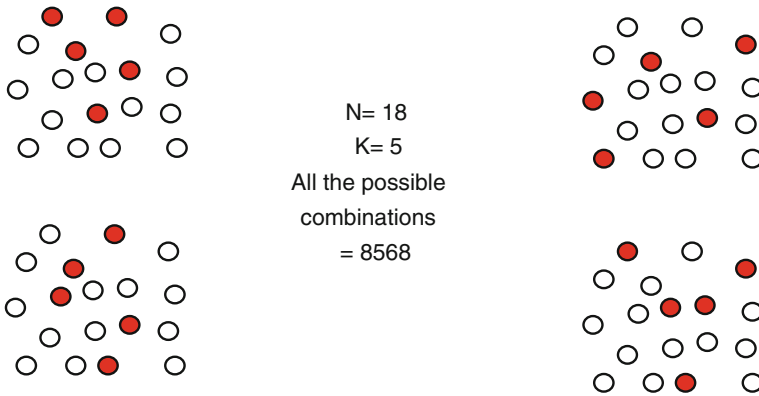


Fig. 9 Illustration of four examples of combinations of 5 nodes from 18 nodes

physical nodes even if they are totally random. FOP is calculated from a “n-nine” availability of the cloud. We suppose that the system contains  $N$  nodes and  $K$  is the minimal number of fail nodes required for the unavailability of all the system. In order to calculate FOP we have to consider all the possible combinations (Eq. 2) of  $K$  nodes among total nodes  $N$  (Figs. 8 and 9).

$$\text{All combinations} = C_N^K = \frac{N!}{(N - K)!K!} \tag{2}$$

The degree of availability “n” expresses also the probability of unavailability such as:

In 2 nines availability for example, at time  $t$ : there is a probability of 0.01 for unavailability. In general, at time  $t$  there is a probability of  $\frac{1}{10^n}$  for unavailability while  $n$  is the availability degree. The probability that  $K$  nodes generates faults at the same time is:  $FOP^K$ . considering all the combinations, the probability of unavailability at time  $t$  is:

$$C_N^K * FOP^K = \frac{1}{10^n} \tag{3}$$

So the FOP value is:

$$FOP = \frac{1}{\sqrt[k]{C_N^k * 10n}} \quad (4)$$

As stated before, FOP can be influenced by the load related to physical server. The idea is that the fail probability increase with the increasing of the load measured by VSL. If VSL reaches maximum value MVSL then FOP will be:

$$FOP' = FOP + VSL - FOP * VSL \quad (5)$$

The failure generator pseudo code is as follows:

```
begin
Calculate FOP ;
While (true)
    For each nodes
        Generate random r; / r e [0 , 1]
    If ( r ≤ FOP)
        Notify AAM;
End.
```

## 6.4 Availability Average Module

The main role of this module is to calculate availability metrics during the simulation and the global unavailability time. This module calculates:

- MTBF (Mean time Between failure): The value of this indicator shows, how long it takes before the service delivery is interrupted. Because there are no 100 % available components to build IT systems, this value is always a positive, finite amount of time.
- MTBR (Mean time Between recover): Shows how long it takes, to recover from a complete service outage back to normal operations. This value can be infinite, but is mostly a finite, positive amount of time.

$$\text{Availability average} = \frac{MTBF}{MTBF + MTBR} \quad (6)$$

The pseudo code related to availability average module is as follows:

```

Begin

MTBR, MTBF, Day, NumberFail = 0 ;
C = 1;
safeNumber = N - K ;
Initialize(D) ; /*simulation time*/
While(Day ≤ D)
    Begin
        Day++;
        C++;
        If(notify)
            N--;
            NumberFail++;
        If( N ≤ safeNumber)
            MTBR = MTBR + C*(60*24) * 1/10n ;
            N = N + K ;
            C=1;
        Else
            MTBF = MTBF + 60*24 ;
            N = N + NumberFail;
            NumberFail = 0 ;
    End (while);
AA= MTBF/(MTBF + MTBR);
End.

```

## 7 Results

The model aims to reaches the “n-nine” availability of the cloud as described in the SLAs. In another words for a year simulation for example the simulation should achieve around 90 % of availability for  $n = 1$ , 99 % for  $n = 2$  and so on (Eq. 7).

$$input(n, simun\ time) \rightarrow (100 - \frac{10}{10^{n-1}}) \quad (7)$$

After several executions of a year simulation, with a different variation of number of nodes  $N$  and fails nodes requierd  $K$  we have obtained results for parameters ( $n = 1, 2, 3$ ) reaching a high accuracy as shown in the Tables 2 and 3.

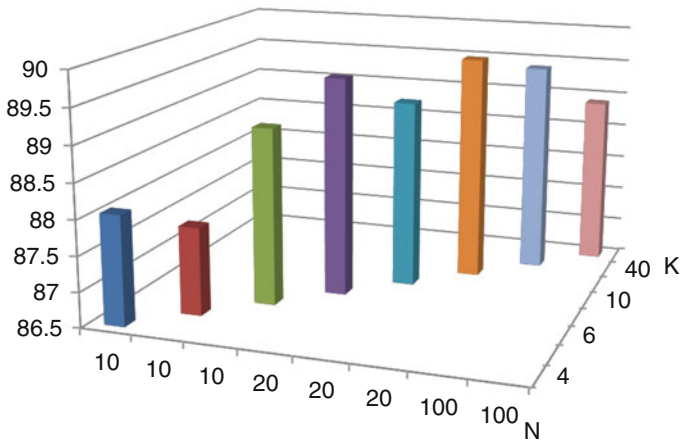
The Figs. 10 and 11 shows the availability average measured for each parameter ( $n = 1, 2, 3$ ). As we can see a high accuracy is reached for several combination of

**Table 2** High availability “n-nine”

Availability in %	Unavailability per year
90 % (one nine)	36.5 days
99 % (two nines)	3.65 days
99,9 % (three nines)	8.76 h
99,99 % (four nines)	52.56 min
99,999 % (five nines)	5.26 min
99,9999 % (six nines)	31.5 s

**Table 3** Availability average obtained

N	K	FOP	AA n = 1 (%)	AA n = 2 (%)	AA n = 2 (%)
10	4	0.147	88.06	99.06	99.906
10	5	0.208	87.75	99.18	99.920
10	6	0.279	89.02	99.04	99.912
20	8	0.173	89.62	98.98	99.901
20	10	0.236	89.18	99.03	99.903
20	14	0.368	89.72	99.06	99.901
100	40	0.156	89.51	99.78	99.905
100	60	0.281	88.90	98.64	99.908



**Fig. 10** Availability average with n = 1 illustrated with organ pipes

physical node number N and minimal number of fail nodes required for the unavailability of all the system K.

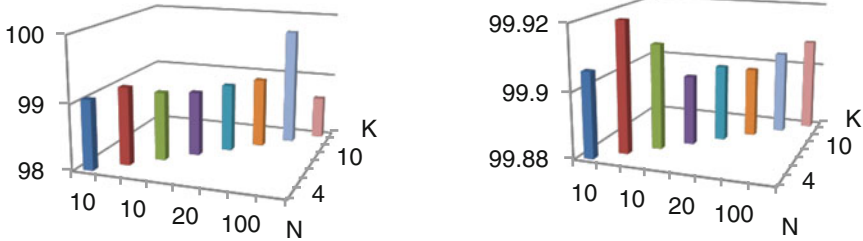


Fig. 11 Availability average with n = 2 and n = 3 (99 and 99.9 %)

## 8 Conclusion

In this paper we have proposed a simulation model of the distributed and virtual cloud environment based on “the law of large numbers”. The principle of the large numbers law is that the correlation of random behaviors of a large population invidious will certainly converge into a predictable result. We know that cloud providers has a known availability average, based on that we have proposed a probabilistic model with different virtualization layers. The model includes failure generator that generates randomly faults following a failure occurrence probability (FOP). In addition to that, FOP can be influenced by the load on each physical node which can increase the failure probability. After the simulation we have reached unavailability times which are very faithful to “n-nine” availability know in the SLAs (90, 99, 99.9 %...) as the large numbers principle states. The simulation model allows live virtual machine migration in order to evaluate proactive fault tolerance approaches based on preemptive virtual machine migration. The possibility of evaluation proactive fault tolerance approaches is the main aim of this model. The model presented and described in this work can lead to design and evaluate as future work proactive fault tolerance approaches base on live VM migration and failure prediction (Table 4).

Table 4 Global accuracy

n	Global accuracy (%)
1	98.90
2	99.21
3	98.34
4	98.46
5	97.48

## References

1. Foster, I., Zhao, Y., Raicu, I., Lu, S.: Cloud computing and grid computing 360-degree compared. In: Grid Computing Environments Workshop, 2008. GCE'08, pp. 1–10 (2008)
2. Wang, Q., Varela, C.A.: Impact of cloud computing virtualization strategies on workloads' performance. In: 2011 Fourth IEEE International Conference on Utility and Cloud Computing (UCC), pp. 130–137 (2011)
3. Pham, C., Cao, P., Kalbarczyk, Z., Iyer, R.K.: Toward a high availability cloud: techniques and challenges. In: 2012 IEEE/IFIP 42nd International Conference on Dependable Systems and Networks Workshops (DSN-W), pp. 1–6 (2012)
4. Kaushal, V., Bala, A.: Autonomic fault tolerance using haproxy in cloud environment. *J. Adv. Eng. Sci. Technol.* **7**(2), 54–59 (2011)
5. Mell, P., Grance, T.: The NIST definition of cloud computing. National Institute of Standards and Technology, Information Technology Laboratory (2011)
6. Shankarwar Mahesh, U., Pawar Ambika, V.: Security and Privacy in Cloud Computing: A Survey, vol. 2, pp. 1–11. Springer International Publishing, Switzerland (2015)
7. Kusic, D., Kephart, J.O., Hanson, J.E., Kandasamy, N., Jiang, G.: Power and performance management of virtualized computing environments via lookahead control. In: International Conference on Autonomic Computing, 2008. ICAC'08, pp. 3–12 (2008)
8. Perez-Botero, D., Szefer, J., Lee, R.B.: Characterizing hypervisor vulnerabilities in cloud computing servers. In: Proceedings of the 2013 International Workshop on Security in Cloud Computing (Cloud Computing'13), pp. 3–10. ACM, New York (2013)
9. Riddle, A.R., Chung, S.M.: A survey on the security of hypervisors in cloud computing. In: 2015 IEEE 35th International Conference on Distributed Computing Systems Workshops (ICDCSW), pp. 100–104 (2015)
10. Leelipushpam, P.G.J., Sharmila, J.: Live VM migration techniques in cloud environment: a survey. In: 2013 IEEE Conference on Information and Communication Technologies (ICT), pp. 408–413 (2013)
11. Sahni, S., Varma, V.: A hybrid approach to live migration of virtual machines. In: 2012 IEEE International Conference on Cloud Computing in Emerging Markets (CCEM), pp. 1–5 (2012)
12. Clark, C., Fraser, K., Hand, S., Hansen, J.G., Jul, E., Limpach, C., Pratt, I., Warfield, A.: Live migration of virtual machines. In: Proceedings of the 2nd Conference on Symposium on Networked Systems Design and Implementation, vol. 2, pp. 273–286 (2005)
13. Hines, M.R., Gopalan, K.: Post-copy based live virtual machine migration using adaptive pre-paging and dynamic self-ballooning. In: Proceedings of the 2009 ACM SIGPLAN/SIGOPS International Conference on Virtual Execution Environments, pp. 51–60. ACM (2009)
14. Kaushal, V., Bala, A.: Autonomic fault tolerance using haproxy in cloud environment. *J. Adv. Eng. Sci. Technol.* **7**(2), 54–59 (2011)
15. Amin, Z., Sethi, N., Singh, H.: Review on fault tolerance techniques in cloud computing. *Int. J. Comput. Appl.* **116**(8), 13 (2015) (0975–8887)
16. Folkerts, E., Alexandrov, A., Sachs, K., Iosup, A., Markl, V., Tosun, C.: Benchmarking in the cloud: what it should, can, and cannot be. In: 4th TPC Technology Conference, TPCTC Volume pp. 173–188 (2013)
17. Hannache, O., Batouche, M.: Probabilistic model for evaluating a proactive fault tolerance approach in the cloud. In: 2015 IEEE International Conference on Service Operations and Logistics, and Informatics (SOLI), pp. 94–99 (2015)
18. Arzuaga, E., Kaeli, D.R.: Quantifying load imbalance on virtualized enterprise servers. In WOSP/SIPEW'10: Proceedings of the First Joint WOSP/SIPEW International Conference on Performance Engineering, pp. 235–242. ACM, New York (2010)
19. Li, J., Wang, Q., Jayasinghe, D., Park, J., Zhu, T., Pu, C.: Performance overhead among three hypervisors: an experimental study using Hadoop benchmarks. In: 2013 IEEE International Congress on Big Data (BigData Congress), pp. 9–16 (2013)

# Towards an Inter-organizational Collaboration Network Characterization

Kahina Semar-Bitah and Kamel Boukhalfa

**Abstract** Nowadays in the international trade, there are many aspects that influence the interactive relationships between several types of organizations. Modeling such kinds of organizational interactions needs the consideration of a maximum of concepts related to the inter-organizational collaboration in general, in order to cover any kind and any case of collaboration. For this purpose, we present in this paper an inter organizational collaboration Meta Model dedicated to the generation of a knowledge-based used for inter organizational collaborative process modeling. The purpose is to build an inter-organizational collaboration Meta-model which covers the majority of the aspects and the concepts related to the inter-organizational collaboration, found in the literature. At this level it's necessary to identify and extract the objectives and knowledge about the collaboration environment. These knowledge can be acquired from many different sources in many different ways such as interview, conversation, software, documentation, experiences, professional social web, etc. This knowledge acquisition is done to define the collaboration Meta-Model. At the end of this paper we are going to present the instantiation of our meta-model through a case study.

**Keywords** Inter-organizational collaboration • Modeling • Meta-model • Collaborative business process • MDA

---

K. Semar-Bitah (✉)

Centre de Développement des Technologies Avancées CDTA,  
Div.Telecom, UBMA, Lab.Lrs, Annaba, Algeria  
e-mail: ksemar@cdta.dz; ksemar1@yahoo.com

K. Boukhalfa

Department of Computer, Lab.Lsi, USTHB, Annaba, Algeria  
e-mail: kboukhalfa@usthb.dz



## 1 Introduction

Now days, the trend is to be organized into one or several kinds of industrial networks, in which interact many organizations. In order to have access to a broader range of opportunities (e.g. Canada Business Network, US Corporate Networks, etc.). The capacity of partners to collaborate in an efficient way becomes an important factor for their evolution and their ability to survive. The heterogeneities of partners (e.g. location, language, politic, information system) and of knowledge which can be exchanged between them make it difficult to achieve this collaboration. This collaboration must be well planned and well modeled, so that organizations engage in it and seek to maintain it. The partners have no prior idea about how this collaboration will be done. This means that they can express informally and partially, their requirements but how can they formalize and achieve this collaboration?

In this paper, we focused on how we can characterize and model the inter-organizational collaboration. Many studies have been conducted, these last years, in order to propose a solution for the inter-organizational collaboration modeling.

All the research works found in literature do not take into account all the concepts and the all aspects related to the inter-organizational collaboration, but only combined a few of them. Therefore, the problem is not completely solved and remains topical.

For example according to [2–13] collaboration has an individual and collective aspect. The individual aspects concern the actors who accomplish the collaboration tasks such as role. The collective aspect concerns the strategies, goals, relationships, such as typology. As show in (Fig. 1), no concept according to the resource or to the collaboration process are introduced in this model. Therefore, to cover all collaboration concepts, it is necessary to gather all knowledge about partner, collaboration and the collaborative process.

In our previous work [8–12] we presented a general approach (Fig. 2) to model the inter-organizational collaborative process. In [8–12] we proposed an approach, which allows afterward creating an inter-organizational platform composed of three parts (Fig. 2): (1) the gathering of information concerning partners, collaboration and inter-organizational collaborative process (presented in detail in this paper), (2) the generation of a knowledge base and (3) the reasoning process to model the inter-organizational collaborative process.

In [8–12] a general approach allowing the inter-organizational collaborative process modeling was presented in a global way. In [8–12] we presented the relationship between the three parts of our approach. In this paper, we deal only with the knowledge gathering step (part bordered with red dotted in Fig. 2). In our ingoing works we will present our contribution according to the second and the third step.

So, in this paper, we will present the first step in detail, beginning with the proposal of a meta-model that characterizes the inter-organizational collaboration

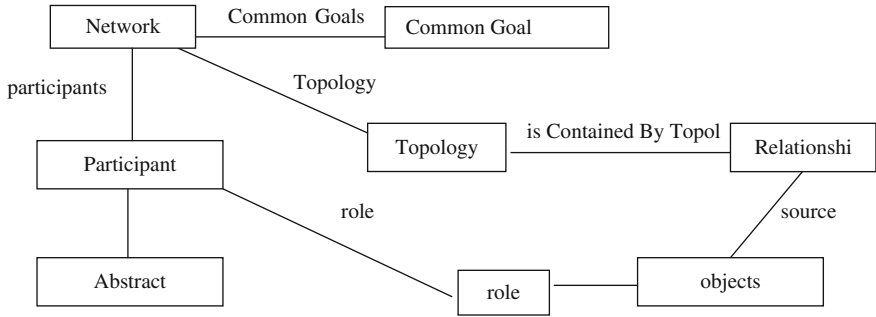


Fig. 1 Summary of the concepts used in Rajsiri Domain model [2]

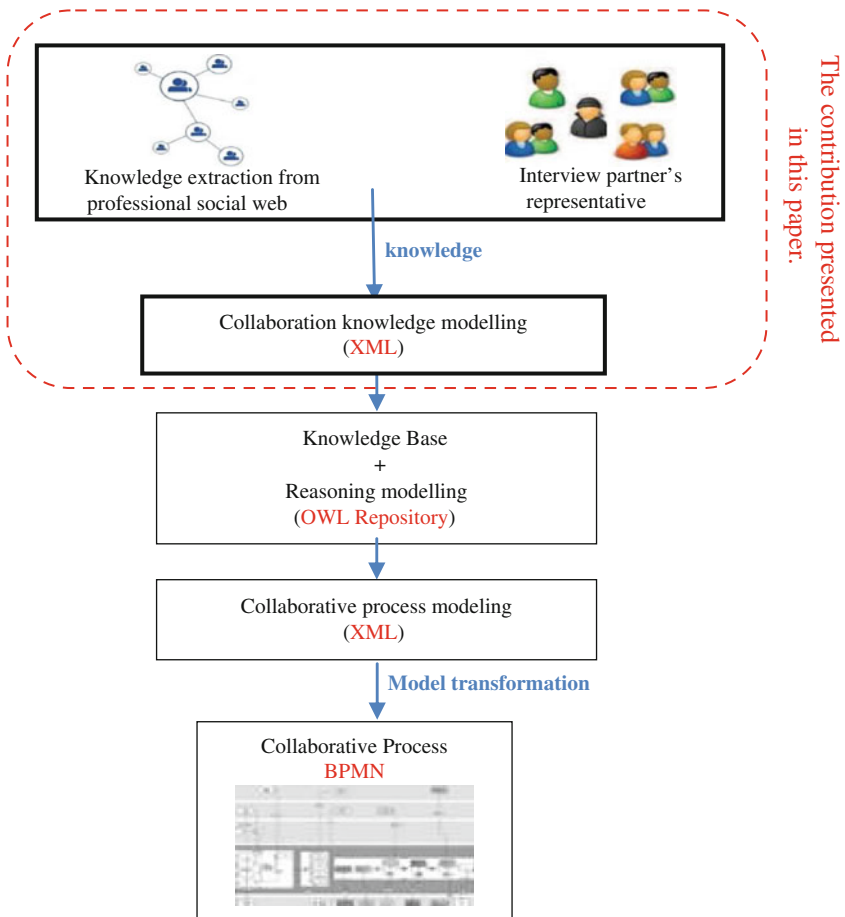


Fig. 2 Approach for defining BPMN collaborative process

until the instantiation of this one with a graphical editor of collaboration models (which is based on this meta-model). This meta-model is generic and covers a large number of concepts related to inter-organizational collaboration. The editor allows the design and the graphical modification of collaboration models according to the knowledge gathered from the collaboration network.

We start our work by gathering knowledge about partner, collaboration and collaborative process. As we have already said these knowledge can be acquired from many different sources in many different ways such as interview, conversation, software, documentation, experiences, professional social web, etc. The ability to capture this knowledge and seamlessly share them between different partners is often limited by the heterogeneity, the organization and the structure of data and technologies. Therefore, it is necessary to make this knowledge homogeneous in a single meta-model, which include all concepts. For that we combine the majority of the factors, found in the literature, related to the organization, collaboration and to the collaborative business process (such as the nature of the relationship between the partners, the network topology, the common goal, etc.).

We considered necessary the introduction of the collaborative business process concepts because the objective in our ingoing works is the inter-organizational collaborative process modeling. So that, we allow partners to give, if they want, parts of their detailed or abstract process; according to their role and the common goal to achieve. In the next sections of this paper, we will present our inter-organizational collaboration meta-model.

The paper is structured as follows: Sect. 2 discusses some related works dealing with the modeling of the inter-organizational collaboration, Sect. 3 presents the collaboration concepts taken into count in this work. In Sect. 4 a detailed description of all the aspects included in our meta-model is presented. Section 6 concludes this paper and presents our in-going works.

## 2 Related Works

As shows the (Fig. 2), we present our global approach, it's a model-driven approach used to design the inter-organizational collaborative process. Our collaborative platform is constructed so that at each level the associated models are used to build the models of the next level. We should provide the transformation of models from the collaboration network model (knowledge about collaborative environment) until we obtain an inter-organizational collaborative processes model. The MDA (Model Driven Architecture) is an approach of software design, based on models and favors the approach of transforming a model to another. It is designed for complex systems. This approach seems most adapted to the work we want to achieve [22]. The MDA proposed by the OMG (Object Management Group) [4], support the development of complex and distributed systems. The approach proposes to divide the development process into three distinct layer, and transform (automatically or semi-automatically) the models from a layer to the other [5].

The inter-organizational collaboration is a very complex system (Voluminous, Scalable, Heterogeneous) that changes frequently. A considerable research work where interested in the collaboration concept, it illustrates the big variety of the possible designs of the collaboration. From methods of management until the engineering of the processes, there is a rich range of conceptualizations which affect various aspects of the inter-organizational collaboration.

We are interested in the research works those are close to our work, using MDA to transfer the collaboration knowledge from a model to the other. Since the MDA allows guaranteeing, a high level of flexibility and a great capacity for re-use [11].

The approach, which we have already proposed in [8–12], is an enrichment of two existing approaches Rajsiri [2] and Saib [9], the choice was justified in detail in [8–12].

According to Mertins [21], the deduction of the collaborative process of Rajsiri [2] has an important lack; it considers only some characteristics of collaboration and does not care about the possible options in the collaborative process.

In [2], Rajsiri affirmed that they may need to enrich their inter-organizational collaborative process modeling by taking into account some missing elements that they have to include for example: *event*.

In the next section of this paper, we focus first on gathering a maximum number of knowledge from collaboration environment, second characterizing and modeling this knowledge into a collaboration network and finally instantiate collaboration models via a graphical collaboration models Editor.

The characterization and the modeling of the collaboration network is done in, as generic as possible, way; including a maximum of concepts found until now in the literature according to the inter-organizational collaboration. In the next sections we deal with concepts we used to model the inter-organizational collaboration model.

### 3 The Inter-organizational Collaboration Network Characterization

To cover all collaboration concepts, we consider necessary the gathering of all knowledge about Partners, Collaboration and the Collaborative Process.

In order to take in count the maximum of aspects related to the inter-organizational collaboration, our approach focused on collaboration in general including its definitions and classifications.

The main contribution in this work is to propose a characterization for meta modeling the collaboration networks which supports and combines a maximum of aspects found in the literature, related to the inter-organizational collaboration.

So to deal with that we propose that our meta model must support a maximum of concepts relating to: (1) *the inter-organizational collaboration*, (2) *the organizations* and (3) *the collaborative process*.

As we have demonstrated in our previous works [8–12], that we adopt MDA for models transformation in our collaboration platform. We said that our approach is an enrichment of two existing approaches Rajsiri [2] and Saib [9].

Now we present in Tables 1, 2 and 3 the concepts included in our collaboration network characterization and those used by Rajsiri [2] Saib [9] related to collaboration, organization and collaborative process respectively.

Table 1 presents the concepts of inter-organizational collaboration: its structure, the collaborative network and its topology.

Table 2 presents the concepts related to the organization: the profile, types, resources and inter-organizational relationships.

And finally Table 3, which presents aspects related to the collaborative process, those we have include to allow partners, if they want, the sharing of parts of their business processes, according to their respective roles and their collaboration goal. So that we can include these parts of business process, in our future works, in order to model the collaborative process.

According to these three tables (Tables 1, 2 and 3) we notice that in the case of Rajsiri [2], they take in count only the case of “the virtual enterprise”. Therefore, they considered only concepts related to this collaboration structure. Saib [9], proposed a collaboration between business processes of enterprises systems, so they take into count aspects related to “network of enterprises” collaboration structure. We notice that [2, 9], take into account the concepts according to their collaboration needs.

**Table 1** Collaboration aspects taken in count at the gathering knowledge stage

Research works concepts	Rajsiri [2]	Saib [9]	Our work
<b>Collaboration</b>			
<i>The collaboration structures</i>			X
– Virtual organization VO [14]			X
– Virtual dynamic organization VDO [14]			X
– Virtual enterprise [6]	X		X
– Extended enterprise [7]			X
– Network enterprise [10]			X
– Network of enterprises [3]		X	X
<i>Collaboration network [2]</i>	X		X
– Common goal	X	X	X
– Relationship	X	X	X
– Duration	X		X
– Stability			
<i>Collaborative network topologies pologies [13]</i>	X		X
– Chain topology	X		X
– Star topology	X		X
– Peer-to-peer topology	X		X
– Decision making power	X	X	X

**Table 2** Organization aspects taken in count at the gathering knowledge stage

Research works concepts	Rajsiri [2]	Saib [9]	Our work
<b>Organizations [15]</b>			
<i>The types of organization</i>			X
– Enterprise	X	X	X
– Public organization			X
– Non-profit organization			X
<i>General criteria</i>	X		X
– A name	X	X	X
– A description			X
– A location (city, state, country)	X		X
– A nationality			X
– A constitution (individual organization or group)			X
– The size (number of employees)	X		X
– A business			X
– A business sector	X		X
<i>Resources</i>			X
– Financial resources			X
– Human resources		X	X
– Hardware resources	X	X	X
– Software resource	X	X	X
<i>Inter-enterprise relationships [16, 17]</i>			X
– Competition or horizontal relationship	X	X	X
– Subcontracting, supplier-customer, or vertical relationships	X	X	X
– Group interests or transversal relationships	X	X	X

In our research work, since that in our approach [8–12] the purpose is to design, as an output, an inter-organizational collaborative process, we considered necessary the introduction of the collaborative business process concepts in our collaboration network meta model. Some partners accept to communicate, in an abstract or a detailed way, a few portion of their process, it seems necessary to take in count these knowledge.

In our case, we want to support several types of collaboration structures, so we tried to take into count a maximum of concepts. So that our collaboration meta model will be as generic as possible, supporting a maximum of inter-organizational collaboration case.

Thus, to realize our meta-model we have make a state of the art study, in which we listed and counted the concepts relative to organizations types; different collaboration structures, relations, topology and types; and also business processes concepts to enable partner to share parts of their business processes (those which can be included in the collaborative process).

**Table 3** Collaborative process concepts taken in count at the gathering knowledge stage

Research works concepts	Rajsiri [2]	Saib [9]	Our work
<b>(C) Collaborative process [1, 9, 18–20]</b>			
Activities			X
Role	X		X
Task			X
Transition controls			X
Resources			X
An event			X
– An internal event			X
– A temporary even			X
– An external event			X
A specialization of the event			X
– A trigger event			X
– An interrupter event			X
– A modifier event			X
A result			X
An entry			X
A scenario			X
A condition			X
A global process		X	X
A detailed process			X
Process type			X
– The main process			X
– The secondary process			X
– The management process			X

We also would like to say that at this stage we don’t support network “stability” factor. Because we start our research work from the hypothesis that all partners are previously selected in professional social networks.

In the next section we will present the meta model including these aspects.

## 4 Inter Organizational Collaborative Meta-Model

We present in this section our inter-organizational Meta-model (see Fig. 3). It is oriented business process, describing the collaborative system and the interactions between partners.

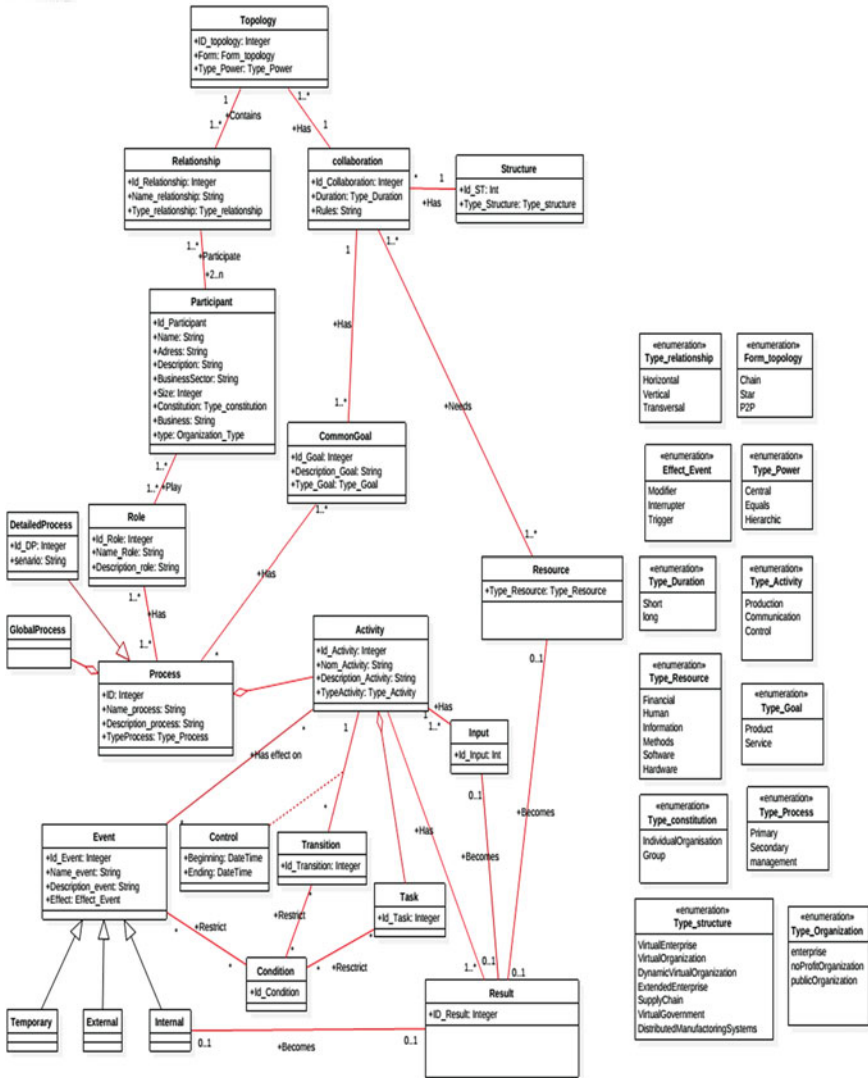


Fig. 3 Collaboration Meta model

Our Meta Model will include all the concepts described in the last section. These concepts are presented according the three aspects above mentioned: organization, collaboration and collaborative process.



## 4.1 The Organization

The aim is to specify the nature of the partners and the relationships between them (according to their collaboration). The organization is described by the following classes:

- The *participant* class: describes the nature of the partners: **enterprise, public organization** or **non-profit organization**.
- The *relationship* class: describes the type of relationship between each two partners. Three types are considered: **horizontal** (collaboration between companies that are in the same sector or the same industry), **vertical** (collaboration between the company with its partners, supplying it a necessary complementary service) or **transverse** (combines horizontal and vertical relationship).
- The *role* class: describes the functions performed by each participant.

A participant can supply several processes; it plays several roles (seller, producer, executor, negotiator, coordinator, buyer, etc.). The Collaboration must have at least two participants (two different organizations); each two participants are linked by a relationship (customer-supplier/vertical competition/horizontal, interest groups/cross).

## 4.2 The Collaboration

In the meta model we include all characteristics related to the collaboration in a generic way. It is described by the following classes:

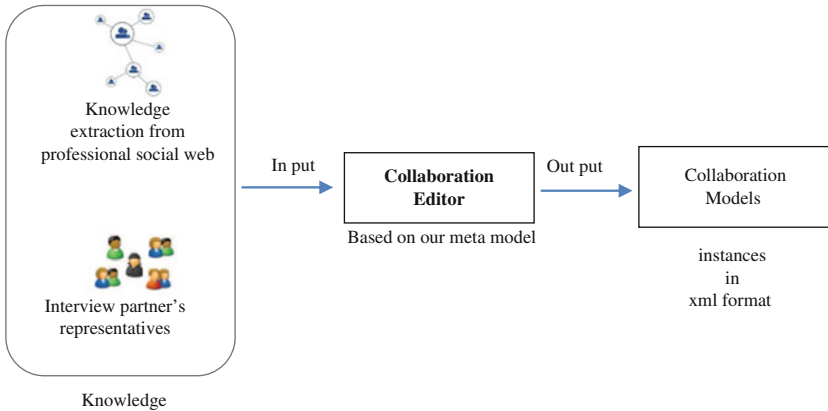
- The *collaboration* class: represents the collaborative network. This class is defined by two main attributes: duration and rules. The attribute *duration* describes the period duration, for which the partners will stay in collaboration in the same network, to achieve the common goal of the collaboration. A network can have a *short* (in the case of a collaboration activated by an collaboration opportunity, e.g.: virtual enterprise VE) or a *long* (e.g.: supply chain collaboration case) life cycle. The attribute *rules* refers to measures, which regulate the relationship between partners (taken from collaboration contracts between partners).
- The *structure* class describes the form of the collaboration which can be:
  - *virtual enterprise VE*: enterprises form a temporary alliance their skills and resources,
  - *virtual organization VO*: like VE but partners are public organizations or non-profit organization,
  - *virtual dynamic organization VDO*: it is a VE where the alliance is dissociated when the common goal is accomplished,

- **extended enterprise EE**: an enterprise extends its boundaries to encompass its suppliers, customers, and other business partners),
  - **enterprise networks EN**: is a vertical collaboration characterized by the dependence of the lower level on the upper level, with a pivot firm: pyramid shape,
  - **network of enterprises NOE**: It is a kind of horizontal agreements between enterprises in diverse forms according, to the partner type. In this network the decision-making is not centralized. For example alliance between big multinational groups.
  - Several other types of organizations cited in [23], have been taken into consideration.
- The **resource** class refers to various means necessary to make successful the collaboration. It can be **hardware, software, methods, information, human, financial**, etc....
  - The **common goal** class: describes the reason why the collaboration exists; it can be a **service** or a **product**.
  - The **topology** class describes the shape of the collaboration network. It can be a **chain** (or process-oriented) depends essentially on its superiors and inferiors hierarchical, a **star** (or main contractor) in which one enterprise pilots the collaboration, **peer to peer** where there are several relations between all the knots without hierarchy, it can be also a combination of these three structures. The attribute **power** (take a decision): every topology has a concept of decision-making which can be central, equals or hierarchic.
  - A **topology** can contain one or several **relations** which can be provider/costumer (vertical), concurrence (horizontal) or groups of interests (transversal).

### 4.3 The Collaborative Process

The **collaborative process** class describes the characteristics of business process and its collaborative concepts. This part modeled the abstract or detailed business process, which can be provided by partners in their respective roles in order to achieve the common goal. It is represented by the following classes:

- The **process** class represents the execution of a set of instructions to achieve a common goal. The purpose of the process is **primary, secondary** or **management**.
- Several **processes** can form a **global process**. A process can be described by a **detailed process**. It can be simulated by a scenario, which is a text describing the execution of a process instance.
- The **activity** class: represented the functional decomposition unit of a process, it expresses the transformation of an input to an output. It describes the purpose



**Fig. 4** Collaboration Network editor operating

that a detailed process can be achieved. It can be made in several **tasks**. An activity can have **inputs** and **results** and can be a set of activities.

- The **transition** class: the set of transitions of a process is the scheduling of its activities. It can be used simultaneously with or instead of the event concepts
- The **condition** class: the condition expresses a restriction of the task execution, or the starting of the transition. It can be associated to an event.
- The **event** class: the event is a stimulus which provokes a reaction in an activity. The event can be divided into three categories: **internal**, **external** or **temporary** events. The effect provoked by an event is the release of the corresponding activity. However, in certain cases, the type of event may be taken into account in the implementation of the activity. Therefore, that leads to a second specialization of the event according to its goal purpose: **modifier**, **trigger** or **interrupter**.
- The **result** stemming from the execution or a system state change can become an input, a resource or an internal event for an activity.

In this section we tried to present in details the meta model that we have proposed. It includes the maximum of concepts related to the inter-organizational collaboration; in order to have as generic as possible model, modeling several possible collaboration cases.

In the next section we will introduce a tool allowing users to graphically instantiate this meta model so that they can characterize many particular inter-organizational collaboration cases.

The main reason for developing the Network Editor (NE) is to support the knowledge gathering and formalization functionality for collecting the essential knowledge, and modeling the collaboration network graphically.

Our editor has as an input **knowledge** gathered from collaboration environment and provided as an output **collaboration models** in XML format (Fig. 4), these files will be transformed and imported into the Knowledge Base afterwards (Fig. 2).

## 5 Collaboration Editor: Example Scenario

Our Collaboration Editor (CE) is a collaboration models design tool based on our meta model. It is created with GMF (Graphical Modeling Framework), it provide a sort of design space with tools which allow users to create, and characterize their collaboration in a graphic way. This editor support the knowledge gathering, formalization functionality and modeling collaboration.

To illustrate principles of knowledge representation, in this section, we introduce a sample example scenario taken from customer-supplier use case.

We will start, in the scenario (Table 4), by describing the collaborative situation which is our input knowledge.

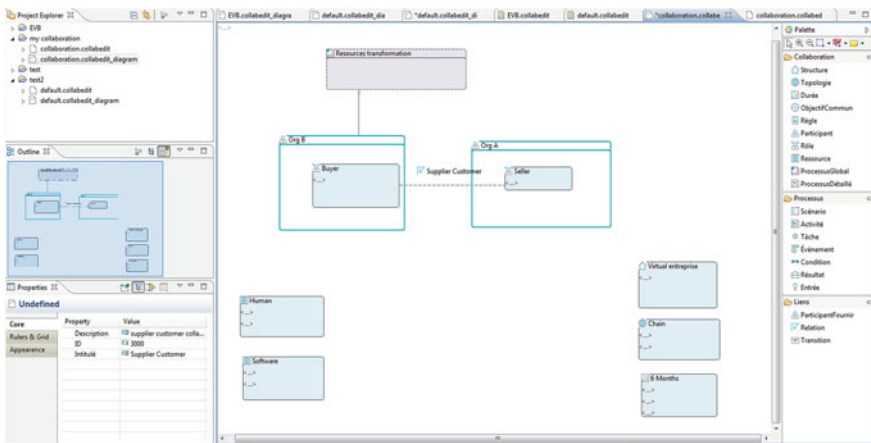
In this scenario, we have two participants Org A and Org B. They perform a supply chain network so that partners are in customer-supplier relationship: Org A is a seller and Org B is the buyer.

Table 4 represent the collaboration network customer-supplier. The structure of this collaboration is Virtual Enterprise; the resources used are human and software. The duration of this collaboration is 6 months.

The diagram (Fig. 5) is a graphical representation of our collaboration model through the CE. The details on relationships and on some collaboration aspects are

**Table 4** Interpretation of the supplier-customer collaboration

Participant	Org A	Org B
Role	Seller	Buyer
Common goal	Buy products	
Topology	Chain	
Relationship	Customer-supplier	
Duration	6 months	
Resources	Human, software	
Structure	Virtual enterprise VE	
Abstract process	Resources transformation	



**Fig. 5** Collaborative network diagram of the supplier-customer collaboration

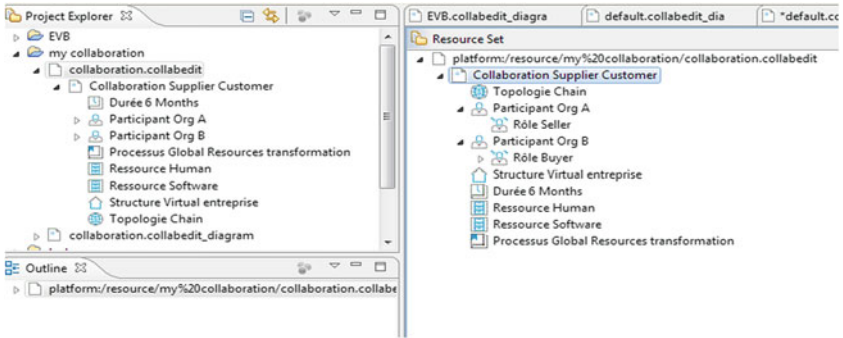


Fig. 6 Collaboration XML structure

```

<xmlns:collaboration.editeur.collabedit="http://collaboration/editeur/collabedit"  intitulé="Supplier
Customer" description="supplier customer collaboration">
  <topologies nom="Chain"/>
  <participants nom="Org A ">
    <rôles nom="Seller"/>
  </participants>
  <participants nom="Org B" fournir="//@processus.0">
    <rôles nom="Buyer ">
      <relations source="//@participants.1/@rôles.0" cible="//@participants.0/@rôles.0"
nom="Supplier Customer"/>
    </rôles>
  </participants>
  <ID>3000</ID>
  <structure nom="Virtual entreprise"/>
  <durée nom="6 Months"/>
  <ressources nom="Human"/>
  <ressources nom="Software"/>

```

Fig. 7 Collaboration XML file (text Editor view)

accessed via the properties view (Fig. 5). The (Fig. 6) represents the collaboration model in XML schema. The associated XML file (Fig. 7) will be transformed and imported into the Knowledge Base afterwards (Fig. 2), in our future works. The definition of the collaborative network depends mostly on the interpretation and experience of the CE’s users. For the same knowledge (e.g.: captured by interview), users may interpret it differently. Thus, it is possible to define more than one potential collaborative model in order to obtain an appropriate collaborative process that satisfies the partners as much as possible.

## 6 Conclusion

The objective of this paper is to present in details the meta model designed for the network collaboration characterization and modeling. Based on this meta model a graphical editor was conceived, to allow users the gathering of knowledge and the graphical instantiation of the meta model. To obtain collaboration models of many specific inter-organizational collaboration cases.

In our ongoing works, collaboration network models provided by this editor (in XML format) will be converted automatically to OWL (Web Ontology Language) file used as an input for building inter-collaboration knowledge-based. The later will be used to define an inter-organizational collaborative process.

In this paper, the first part of the system [8–12] was presented. The creation of the whole system, the specification of its features and the development of the full proposed prototype [8], are a very important part of our future works.

**Acknowledgment** This article could not be realized without the precious contributions of several students. We are very grateful to Selma Bounsiar, Amel Sandjak and Wissam Maamar Kouadri.

## References

1. Touzi, J.: Aide à la conception de Système d'Information Collaboratif support de l'interopérabilité des entreprises. Thèse en Informatique, Centre de Génie Industriel, Ecole des Mines d'Albi Carmaux (2007)
2. Rajsiri, V.: Knowledge-based system for collaborative process specification. Ph.D. Thesis, Dept, Industrial Engineering, Université de Toulouse (2009)
3. Burlat, P., Peillon, S., Vincent, L.: Quels modèles pour une firme sans frontières. Actes du 2e Congrès International Franco-Québécois de Génie Industriel: le génie industriel dans un monde sans frontières (1997)
4. Object Management Group. <http://www.omg.org> (2006)
5. Jardim-Goncalves, A., Grilo, A., Garcao, S.: Challenging the interoperability between computers in industry with MDA and SOA. *Comput. Ind.* (2006)
6. Luczak, H., Hauser: Knowledge management in virtual organizations. In: Proceedings of ICSSSM'05. s.l.: International Conference on Services Systems and Services Management (2005)
7. D1.1 SYNERGY, Deliverable. State of the Art and As-Is Analysis (2008)
8. Semar-Bitah, K., Abbassene, A.: Vers une architecture de modélisation des processus collaboratifs inter-organisationnels. In: SYSCO'14, Hamamet, Tunisie (2014). doi:10.13140/RG.2.1.1622.3760
9. Sara, S., Rachid, B., Kenza, B.: Modeling of mediation system for enterprise systems collaboration through MDA and SOA approaches. *J. Theor. Appl. Inf. Technol.* **54**(3), 2013 (2013)
10. Lizarraga, V., Leonor, C.: Contribution au pilotage des projets partagés par des PME en groupement basée sur la gestion des risques. s.l.: Ecole des Mines d'Albi-Carmaux (2005)
11. David, C., Stewart, L.: Collaboration 2.0 Technology and Best Practice for Successful Collaboration in a Web 2.0 World. Silicon Valley, California (2008)
12. Semar-Bitah, K., Boukhalfa, K.: Vers une Plateforme d'aide à la Modélisation de la Collaboration Inter-organisationnelle. In: Conférence Internationale sur le Traitement de

- l'Information Multimédia (CITIM'2015), Mascara, Algeria, Mai (2015). doi:[10.13140/RG.2.1.1098.0883](https://doi.org/10.13140/RG.2.1.1098.0883)
13. Katzy, B., Zhang, C., Löh, H.: Reference Models for Virtual Organizations. Working Paper No 2704, Working Paper Series. s.l.: CeTIM (2000)
  14. Camarinha-Matos, L.M., Afsarmanesh, H.: Taxonomy of Collaborative Networks Forms (2012)
  15. Yolande, B.: MODELE de GRILLE DE CARACTERISATION. Site Economie-Gestion Académie de Lyon (2008). [http://www2.ac-lyon.fr/enseigne/ecogestion/legt/IMG/pdf/GRILLE\\_DE\\_CARACTERISATION.pdf](http://www2.ac-lyon.fr/enseigne/ecogestion/legt/IMG/pdf/GRILLE_DE_CARACTERISATION.pdf)
  16. Jean-Marc, F., François, D., Sophie, D.: Collaboration et Outils Collaboratifs pour la PME Manufacturière. s.l.: Université Laval (2003)
  17. Fombrun, C.J., Astley, W.G.: The telecommunication community: an institutional overview. *J. Commun.* (1982)
  18. Alida, E.: Intégration des approches SOA et orientée objet pour modéliser une orchestration cohérente de services. s.l.: Institut National des Sciences Appliquées de Lyon (2010)
  19. Aubert, B.A., Dussart, A.: Systèmes d'information inter-organisationnels: CIRANO (2002)
  20. Morley, C., Hugues, J., Leblanc, B., Hugues, O.: Processus Métiers et SI: Evaluation, modélisation, mise en oeuvre. Paris, France, Dunod (2005)
  21. Kai, M., et al.: Enterprise Interoperability VI Interoperability for Agility, Resilience and Plasticity of Collaborations, p. 227. s.l.: Springer, (2014)
  22. Bénaben, F., Touzi, J., Rajsiri, V., Pingaud, H.: Collaborative information system design. In: AIM Conference, pp. 281–296 (2006)
  23. Camarinha-Matos, L.M., Afsarmanesh, H.: Taxonomy of Collaborative Networks Forms. Report (2012)

# Asymmetric End-to-End Security for Human-to-Thing Communications in the Internet of Things

Somia Sahraoui and Azeddine Bilami

**Abstract** The Internet of Things (IoT) vision is a groundbreaking networking evolution that connects all things that were not meant to be connected to the Internet. Thus, identification technologies and Internet-enabled wireless sensor nodes will be incorporated in homes, cities, vehicles, watches, etc. making them uniquely identified and able to process and communicate information via Internet. Hence, the emergence of the Internet of Things paradigm will bring a lot of smartness to our daily life and will improve the way people monitor their goods, expenses, environment and health status. The smart connected things in the IoT interact with each other and/or with the regular Internet hosts according to two communications styles: Thing-to-Thing(s) (T2T) and Human-to-Thing (H2T). Enabling security for such communications is a real issue especially in H2T interactions. This is mainly due to scarce resources of the connected objects and the asymmetric nature of the communications between those smart things and the ordinary Internet hosts. In this paper we address this problematic and we propose an asymmetric security model that mitigates H2T communication heterogeneities and provides reasonable security costs.

**Keywords** Internet of things (IoT) · Wireless sensor networks (WSNs) · Human to thing communications · End-to-end security · IPsec

---

S. Sahraoui (✉) · A. Bilami  
LaSTIC Laboratory, Computer Science Department, University of Batna 2,  
Batna, Algeria  
e-mail: somiasahraoui@gmail.com

A. Bilami  
e-mail: abilami@yahoo.fr



## 1 Introduction

The Internet of Things [1] will bring worldwide seamless and transparent interconnection of a sheer number of heterogeneous devices belonging to different types of networks. This allows novel and added-value perspectives in numerous urban, rural, military and civil applications [2], namely, smart cities, smart healthcare, etc. where comfort, smartness, the enhancement of the quality of different services and the rationalization of expenditures are the principal goals of IoT deployments.

Wireless sensor networks [3] that are already well-known by their efficiency in terms of accurate sensing for environmental and behavioral remote monitoring, are a cornerstone technology in IoT. Indeed, it is forecasted that billions of smart objects and places will be connected to the Internet, in the near future, mainly through the Internet-enabled sensors appended to them. Hence, these smart objects will be able to sense relevant information, process and communicate them in the Internet as if they were ordinary Internet hosts. In this context, we distinguish two main communication styles that emerge with the appearance of the Internet of Things, so we refer to Human-to-Thing (H2T) [4] and Thing-to-Thing(s) (T2T). T2T communications, also termed Machine-to-Machine (M2M) [5], refer to the communications between autonomous entities without human involvement. Such interactions are very useful in many applications of the IoT, like manufacturing, smart cities, smart grid, ... In another side, H2T transactions, in which we are interested in this work, are initiated by the human that explicitly solicits (using a laptop, tablet or smart phone) the connected objects (sensors) to take advantage of well-determined services. H2T interactions are very common in numerous applications namely, smart city, connected home, u-healthcare and legacy building control applications [6]. This type of interactions is heterogeneous; the communicating entities (sensors and laptops, smart phones) are of different natures, belong to non-equivalent networks and are not submitted to similar constraints.

Right now, the greatest concern is related to the fact that the switching to the Internet of Things exhibits its users, as well as, the implied networks and devices to severe security problems. This imagination can become a reality, unless robust security countermeasures are in place. Many research works and projects are being carried out in order to provide effective solutions for communications security and end-users privacy protection in the context of the IoT.

In this paper we highlight the security of the communications with the connected smart things in the IoT. We address particularly Human-to-Thing communications which are very interesting from security perspective. This, as such kind of transactions is often the source of DoS (Denial of Service) attacks that are among the most harmful threats targeting the Internet of things in general and Internet-enabled WSNs in particular [7].

In this paper, we propose an optimized security policy for Human-to-Thing interactions in the IoT. The proposed solution exploits the several forms of

heterogeneities (material and technological) characterizing H2T communications between ordinary Internet hosts and connected sensors, while enabling efficient end-to-end security.

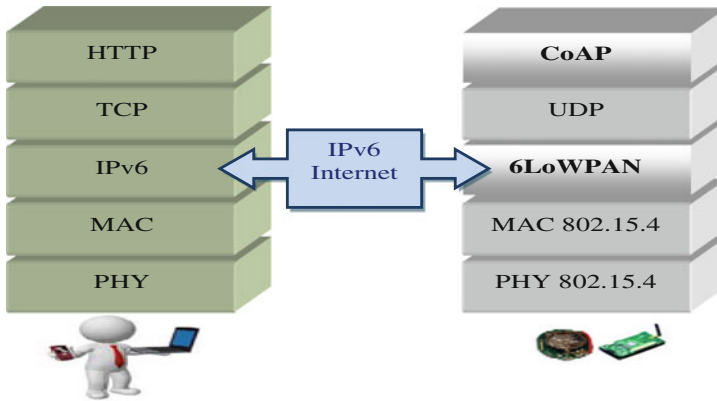
The rest of the present paper is organized as follows: Sect. 2 describes the communication model and preliminaries concerning the standards allowing the integration of WSNs into the IoT. In Sect. 3, we present the security issues related to Human-to-Thing communications in the future Internet. Section 4 presents a state-of-the-art of the proposed solutions secure Human-to-Thing communications in the Internet of things. In Sect. 5, we highlight the essence of the proposed solution, and in Sect. 6 we present the assessment results. Finally we conclude the paper.

## 2 Communication Model and Background

In the Internet of Things side we consider an IPv6-enabled wireless sensor networks, so-called 6LoWPAN networks. They derive this name from the 6LoWPAN (IPv6 over Low power Wireless Personal Area Networks) [8] adaptation layer that is specified and standardized by IETF working group. The main purpose behind the adoption of IP infrastructure for the Internet of Things is to unify the integration of the sensor networks (with sensor nodes deployed independently or integrated into smart objects) to the Internet and allow a flexible end-to-end communications. From another side, IPv6 is used rather than IPv4 to fulfill the need for a wide range of IP addresses that will be assigned to each sensor node joining the IoT.

6LoWPAN standard makes possible the communication of IPv6 datagrams within IEEE 802.15.4-based WSNs, through header compression and packets fragmentation techniques. Consequently, communication costs are significantly reduced and, IPv6 packets could safely fit in IEEE 802.15.4 frames.

The 6LoWPAN header compression standard aims to revoke redundant and unnecessary information in the header of IPv6 protocol (and even UDP protocol). Accordingly, the header size may decrease from 40 bytes down to only 2 bytes. The compression technique is enough beneficial, as it decreases the overall messages sizes. Consequently, the energetic costs, as well as, the memory requirements for packets communication and memorization are respectively amortized. Besides, the compression and decompression procedures are both handled by the 6LoWPAN border router (6BR) that compresses incoming IPv6 datagrams, split them into small fragments. The resulting 6LoWPAN fragments are thereafter communicated within the WSN, towards their final destination. Conversely, the 6BR reassembles the received fragments related to the same outgoing IPv6 datagram and then, it decompresses the corresponding header.



**Fig. 1** The protocol stacks of sensor nodes in an internet-integrated WSN (on the *right side*) and ordinary internet hosts (on the *left side*)

From an applicative perspective, CoAP (Constrained Application Protocol) [9] protocol that brings web services for WSNs integrated in IoT. Consequently, the connected sensor nodes will be able to behave as web clients or servers. CoAP is standardized to be the first and the HTTP equivalent web transfer protocol in the web of things (WoT). It operates over UDP protocol (that is suitable for WSN deployments) and manages optionally the communication reliability at the application layer. Besides that, COAP implements the HTTP's REST model, while getting rid of a large part of HTTP protocol complexities. Figure 1 shows the protocol stack of an Internet connected sensor node compared to the one of a regular host.

At this level, it is worthy to mention that CoAP is especially tailored to support machine-to-machine communications between CoAP speaking entities, in the Internet of Things. For example, a CoAP client may send this request to a CoAP server to get the current reading of temperature: CON Get coap://temp.example.com/temperature. Where, CON refers to a confirmable request. The response would be like: ACK 23. Nevertheless, Human-to-Thing communications between HTTP and CoAP nodes in the Internet are also possible. However, in this case a CoAP-HTTP cross proxy [6] should intervene to perform the required translations because the two protocols are not quite compatible. The proxy may also act as a forward proxy that stores locally the server's resources that do not change frequently. Hence, the proxy replies on behalf of the CoAP server by forwarding the cached resource to the client, so that to reduce the response delay and network overhead. Figure 2 depicts an example of Human-to-Thing communication between HTTP client and CoAP server.

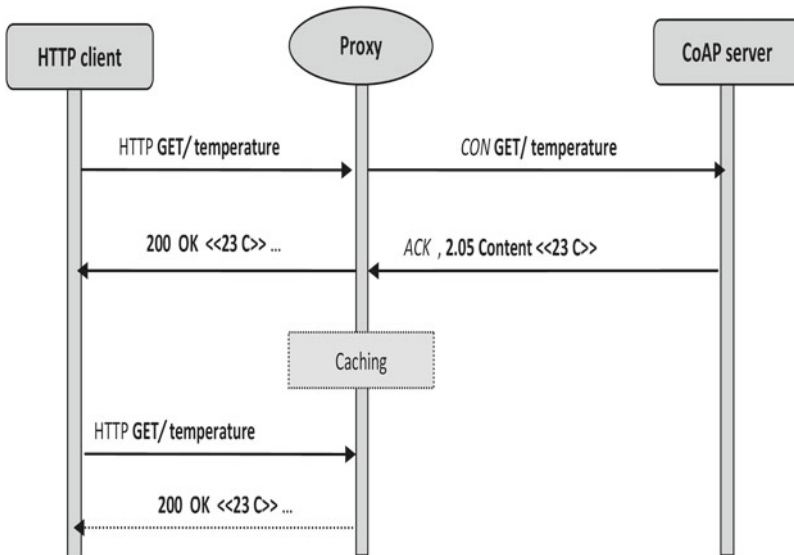


Fig. 2 Example of H2T communication between HTTP-CoAP entities in the IoT

### 3 Security Considerations Related to Human-to-Thing Communications in the Internet of Things

Human-to-Thing interactions are by nature vulnerable to severe security threats. The communication between external powerful hosts (desktops, laptops, tablets, smart phones, ...) and the constrained and resource-limited sensor nodes in the IoT is challenging because of the several forms of heterogeneities that might be maliciously exploited by strong hosts to easily launch denial of service attacks over certain connected sensor nodes acting as web servers or over the entire sensor networks integrated into the Internet. Indeed, DoS attacks are considered as the first and even the most dangerous risk facing WSNs security in the IoT. This is mainly due to the fact that WSNs are service-oriented networks where the services are usually critical enough. So, the sensor nodes have to keep themselves secure and safe throughout their lifetime.

The common and the simplest way to exercise DoS attacks targeting Internet-integrated WSNs is to exploit the big differences between the maximal IEEE 802.15.4 MTU that is fixed to 127 bytes, and the minimal MTU in IPv6 networks that is equal to 1280 bytes. So, attackers (or only one attacker) can concentrate even small amount of amplified messages that will introduce huge set of fragments in the WSN side which will increase the network overhead and weigh down WSN's services. If the transmission of huge IPv6 packets towards the WSN is frequently repeated, then the impact of the attack gets deeper and the services risk to become rapidly disrupted. Figure 3 illustrates the discussed threat models.

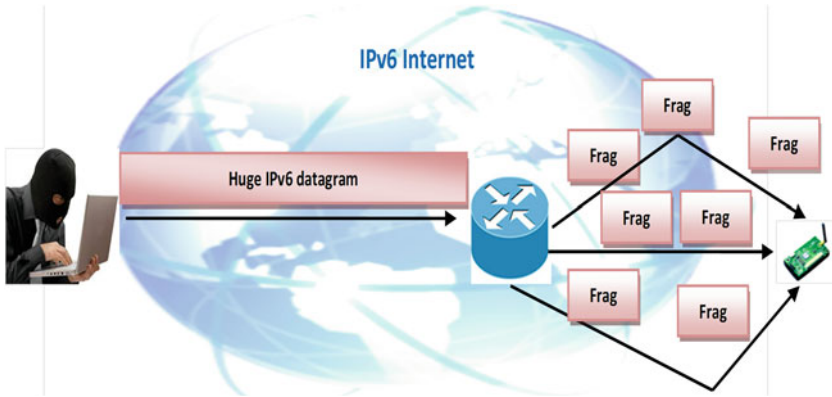


Fig. 3 DoS attack in the IoT

## 4 Related Works

In this section we highlight the solutions proposed to address security issue in Human-to-Thing communications turning between HTTP clients (ordinary Internet hosts) and CoAP servers (connected sensors) in the IoT.

In [10], authors suggest the adoption of IPsec protocol. To adapt such security protocol to WSN's constraints, the solution defines a compression model for AH (Authentication Header) [11] and ESP (Encapsulating Security Payload) [12] headers. The security session between the communicating peers (sensor/sensor or sensor/ordinary Internet host) is either static (the session key is pre-shared as assumed in [10]) or dynamically established by another protocol IKE (Internet Key Exchange) [13] or HIP (Host Identity Protocol) [14]. As the dynamic approach is much more convenient to IoT scenarios, some recent research works have issued the adaptation of IKE and HIP protocols for the connected WSNs [15, 16].

Authors in [17] propose to use TLS (Transport Layer Security) to secure WSN applications in the transport layer. The most computationally-expensive operations in the security handshake in TLS protocol are delegated to powerful entities in the network. But, as TLS focuses on TCP protocol that is judged ill-suited for WSN environments, these solutions seem to be not practical, especially for 6LoWPANs where CoAP protocol is tightly tailored to operate on UDP protocol.

Rather than using TLS to secure transactions with WSN nodes in the IoT, another security approach in the transport layer consists in the use of DTLS protocol that is based on UDP. This last is known to be more adapted than TCP for WSN constraints. In [18], authors propose 6LoWPAN compression extensions for DTLS messages when they are communicated within the connected WSNs to reduce the communication energetic costs. Later, other complement adaptation solutions have been proposed for DTLS in the context of the IoT (e.g. [19]). One of

the most important shortcomings of this trend is that contrary to TLS, DTLS isn't widely adopted in the Internet. Accordingly, authors in [20] propose to continue to use DTLS for Internet-integrated WSNs while mapping between it and TLS protocol in the border router (the base station). Although the solution solves the problem of TLS/DTLS coexistence, the communication, and the computational costs remain substantial.

With all the stated solutions, the WSN's base station (so called 6BR for 6LoWPAN border router) should intervene between the communicating hosts (the ordinary Internet host and the connected sensor) in order to perform the required protocol mapping between HTTP and CoAP and translates also, in some cases, between different security protocols (TLS/DTLS).

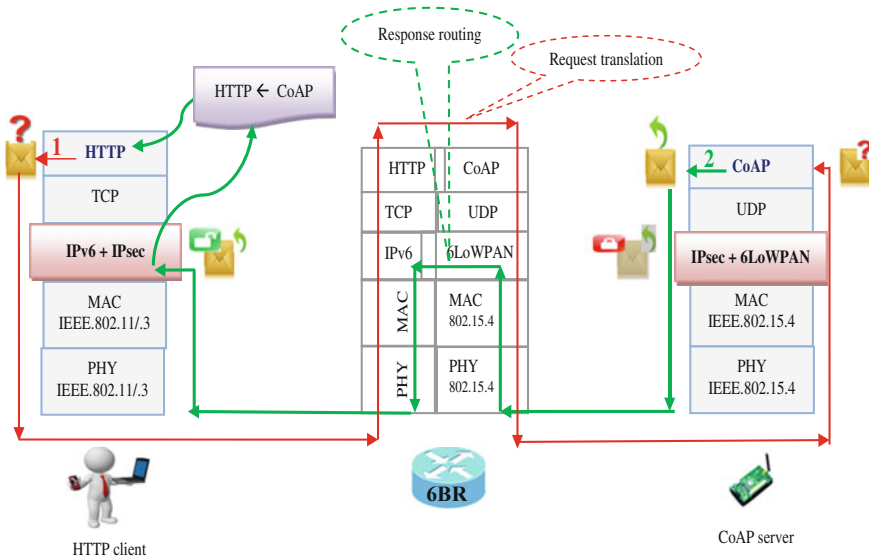
## 5 Overview of the Proposed Solution

Despite its importance, H2T communication security has attracted less attention in the existing IoT security solutions. Also, the current H2T communication security schemes are based on broken end-to-end security at the proxy, for protocol translation reasons. Those schemes share another shortcoming which is the symmetry of the security; security is applied in an equal way from and towards the CoAP servers (sensor nodes) which is not really practical since CoAP responses are much more interesting from security point of view than CoAP requests.

In order to address the raised issues, in this paper, we propose an asymmetric and end-to-end security solution for Human-to-Thing communications.

The asymmetric security is inspired by ADSL (Asymmetric digital Subscriber Line) [21] technique that provides an asymmetric throughput, as data flow is much more important in one communication sense than in the other. Following this concept, we propose to concentrate the security on the server-to-client communication sense. That is to say that only the CoAP responses that carry the sensitive sensory data are concerned by the end-to-end security between the CoAP server and the HTTP client. Figure 4 illustrates the proposed asymmetric security mechanism.

With all incoming HTTP requests, the 6LoWPAN border router behaves as a HTTP-CoAP proxy and performs the required protocol translations to transform the HTTP request to a CoAP request. But, the 6BR handles the outgoing secured CoAP responses just as a router that should not share the secret security key with the remote HTTP client and the CoAP server. In order to avoid the translation between different security protocols, we encourage the adoption of network layer security with IPsec protocol. The border router is prevented from accessing the content of the outgoing CoAP responses that are secured from end to end. So, we propose to shift the CoAP-to-HTTP mapping task to the client that is generally much more



**Fig. 4** Model of the proposed asymmetric security policy for H2T communications

powerful. The figure below shows an abstracted scheme of the proposed security model for HTTP request/CoAP reply communication.

By securing only the critical messages, the proposed asymmetric security solution allows an equitable and balanced security in human-to-thing interactions, in the future Internet. This reduces the security costs on the constrained CoAP servers and helps to mitigate the effect of denial of service attacks that are among the most severe threats targeting 6LoWPAN networks in the IoT.

## 6 Performance Evaluation

This section, we present the preliminary evaluation results conducted on Cooja simulator [22] of Contiki OS version 2.5, where we make use of a wireless sensor network composed of emulated Tmote Sky sensor nodes (10 kB of RAM and 48 kB of ROM) with IEEE 802.15.4 transmission technology. The considered WSN is multimodal, and each sensor node is able to report temperature and light measures. Besides, we have implemented the HTTP-CoAP translation rules onto the border

**Table 1** Current draw values with Tmote Sky platform

Functionality	Current value (mA)
Low power mode (LPM)	0.0545
CPU operation	1.8
Transmission	17.7
Listening	20

router as defined in [6], and we have used the compressed IPsec solution, proposed in [10], at the network layer of the 6LoWPAN network.

We assume a HTTP client sending requests to a CoAP server at regular and massive rates. And we evaluate the induced energy overhead on the CoAP server in accordance with the following equation:

$$Energy(mJ) = \frac{Time}{STicks} * Current(mA) * Voltage(V) \quad (1)$$

where,  $STicks$  represents the number of ticks per second that the timer generates. In Contiki 2.5, the timer produces 32768 ticks per second. The supply voltage is about 3 V in Tmote Sky platform, and current draw values are as indicated in Table 1.

Figure 5 presents the energy consumption by a CoAP server each 50 s with the standard and the asymmetric security solutions in the following cases: (a) one HTTP request is sent once each five seconds, and (b) a HTTP request is sent once per second, and (c) the case when five HTTP requests are sent per second. The simulation time is fixed to 700 s.

Figure 5 shows that the proposed system ensures a reasonable security costs, compared to the standard policy that is especially expensive with increasing Human-to-thing interaction frequencies. Consequently, the proposed solution is sufficiently DoS-resistant.

We have also estimated the communication overhead (see Table 2) that is expected to be reduced with the proposed solution, as the incoming requests are all not encapsulated by IPsec protocol. Although the adopted IPsec is compressed, the obtained results show enhanced communication costs, especially in case of initiated DoS attack (5 requests per second).



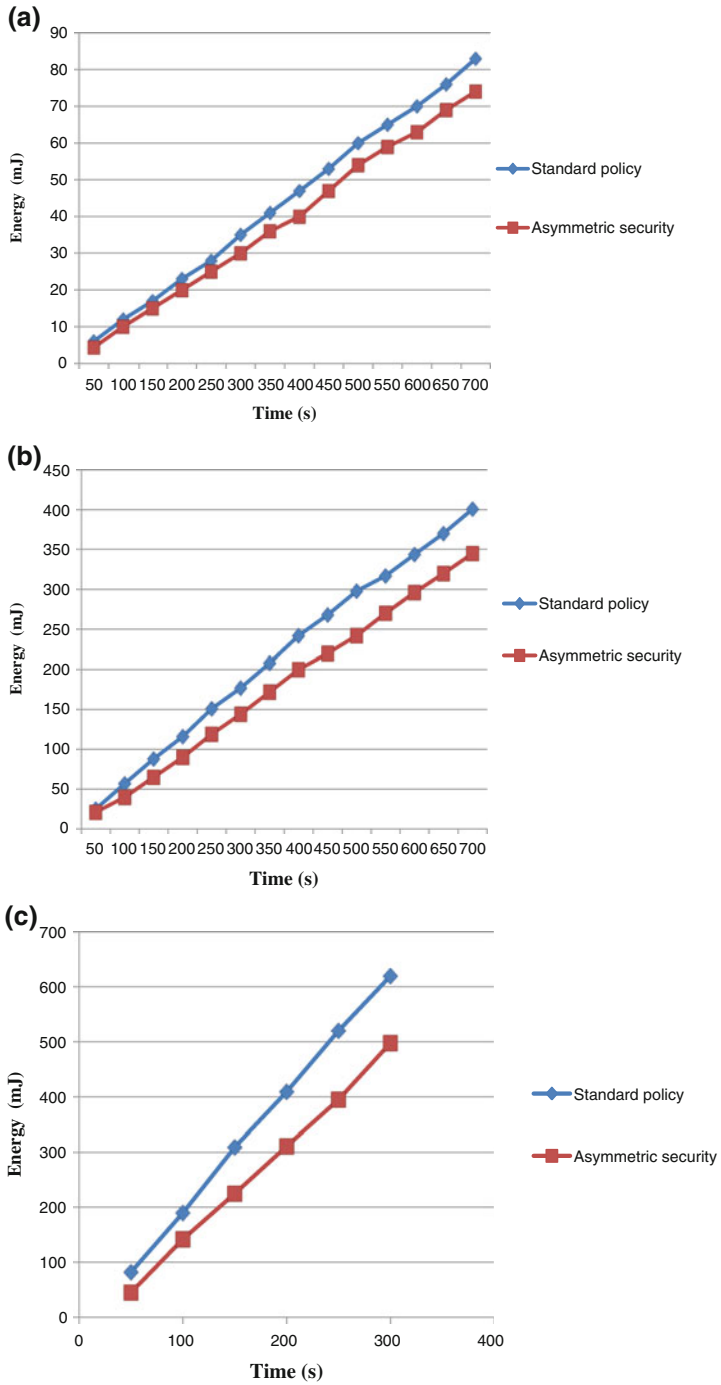


Fig. 5 The obtained evaluation results of the proposed H2T security strategy

**Table 2** Summarize of obtained assessment evaluation results of computational and communication costs

Communication frequency	Solution	Overall computational overhead (mJ)	Overall communication overhead (m)
1 Req/5 s	Standard policy	83	242
	Asym. security	74	231
1 Req/1 s	Standard policy	426	867
	Asym. security	345	839
5 Reqs/1 s	Standard policy	620	1204
	Asym security	498	1161

## 7 Conclusion

We have proposed an efficient solution that is able of ensuring end-to-end alleviated security for human-to-thing communications. This is achieved through an asymmetric ADSL-inspired security scheme that concentrates security only on server (CoAP)-to-Client (HTTP) communication sense which carries the critical and/or user's privacy-informing sensorial reports. Thus, IPsec protocol is used in network layer to avoid the translation between upper non-identical security protocols (DTLS and TLS) with a UDP/CoAP-to-TCP/HTTP translation shifting to the HTTP client that is supposed to be a powerful entity.

The obtained results have confirmed the efficiency of the proposed security strategy that can even mitigate the impact of Denial of Service attacks that might be destined to overcharge CoAP web servers (sensor nodes) by sending HTTP requests intensively.

Finally, we state that the proposed solution can be applied for optimized security of machine-to-machine communications turning between CoAP devices in the Web of Things (WoT).

## References

1. Vans, D.E.: The Internet of things: how the next evolution of the internet is changing everything. Cisco Internet Business Solutions Group (IBSG) (2011)
2. Miorandi, D., Sicari, S., Pellegrinia, F.D., Chlamtaca, I.: Internet of things: vision, applications and research challenges. *Ad Hoc Netw.* **10**(7), 1497–1516 (2012)
3. Akyildiz, I.F., Su, W., Sankarasubramaniam, Y., Cayirci, E.: Wireless sensor networks: a survey. *Comput. Netw.* **38**(4), 393–422 (2002)

4. Garcia-Morchon, O., Keoh, S., Kumar, S., Hummen, R., Struik, R.: Security Considerations in the IP-based Internet of Things. draft-garcia-core-security-04 (2012)
5. Geng, W., Talwar, S., Johnsson, K., Himayat, N., Johnson, K.D.: M2M: from mobile to embedded internet. *IEEE Commun. Mag.* **49**(4), 36–43 (2011)
6. Castellani, A., Loreto, S., Rahman, A., Fossati, T., Dijk, E.: Guidelines for HTTP-CoAP Mapping Implementations. draft-ietf-core-http-mapping-06 (2015)
7. Kasinathan, P., Pastrone, C., Spirito, M. A., Vinkovits, M.: Denial-of-service detection in 6LoWPAN based internet of things. In: 9th International Conference on Wireless and Mobile Computing, Networking and Communications (WiMob), pp. 600–607. IEEE (2013)
8. Hui, J., Thubert, P.: Compression format for IPv6 datagrams in 6LoWPAN networks. Technical report, Internet Engineering Task Force (IETF) draft-ietf-6lowpan-hc-05 (2009)
9. Shelby, Z., Hartke, K., Bormann, C., Frank, B.: The Constrained Application Protocol (CoAP). Request For Comments: 7252 (2014)
10. Raza, S., Voigt, T., Roedig, U.: 6LoWPAN Extension for IPsec. In: The Interconnecting Smart Objects with the Internet Workshop (2011)
11. Kent, S.: IP Authentication Header. Request for Comments: 4302 (2005)
12. Kent, S.: IP Encapsulating Security Payload (ESP). Request for Comments: 4303 (2005)
13. Frankel, S., Kishnan, S.: IP Security (IPsec) and Internet Key Exchange (IKE) document roadmap. Request for Comments: 6071 (2011)
14. Moskowitz, R., Nikander, P., Jokela, P., Henderson, T.: Host Identity Protocol. IETF RFC 5201 (2008)
15. Raza, S., Voigt, T., Jutvik, V.: Lightweight IKEv2: a key management solution for both the compressed IPsec and the IEEE 802.15.4 security. In: The IETF Workshop on Smart Object Security (2012)
16. Sahraoui, S., Bilami, A.: Efficient HIP-based approach to ensure lightweight end-to-end security in the internet of things. *Comput. Netw.* **91**, 26–45 (2015)
17. Ben-Saied, Y., Olivereau, A., Zeglache, D., Laurent, M.: Lightweight collaborative key establishment scheme for the internet of things. *Comput. Netw.* **64**, 273–295 (2014)
18. Raza, S., Tralbalza, D., Voigt, T.: 6LoWPAN compressed DTLS for CoAP. In: The 8th International Conference on Distributed Computing in Sensor Systems, pp. 287–289. IEEE (2012)
19. Shafagh, H., Hithnawi, A.: Poster abstract: security comes first, a public-key cryptography framework for the internet of things. In: The 10th International Conference on Distributed Computing in Sensor Systems. DCSS'14, pp. 135–136. IEEE (2014)
20. Kothmary, T., Schmitt, C., Hu, W., Brunig, M., Carle, G.: DTLS based security and two-way authentication for the internet of things. *Ad Hoc Netw.* **11**(8), 2710–2723 (2013)
21. Asymmetric Digital Subscriber Line (ADSL). AG Communication Systems 1–14
22. Sehgal, A.: Using the Contiki Cooja Simulator (2013)

# Mobile User Location Tracking with Unreliable Data

Samia Zouaoui and Abdelmalik Bachir

**Abstract** We present an architecture of a location tracking system based on the deployment of completely passive monitors that capture WiFi messages transmitted by mobile users for reasons other than localization, such as those messages transmitted for connectivity management (e.g. probe request messages). Being completely passive, our system has the main advantage of being potentially able to track any WiFi equipped devices without the device contributing to the tracking or even being aware of it. However, the feature of complete passivity comes with the challenge of getting accurate localization at regular time intervals, because some devices may not transmit any WiFi message if they are not being actively used. In addition, some messages transmitted by the device might not be captured by monitors due to many reasons such as collision with another message, temporarily changing channel conditions, or software glitches due to the driver of capturing system. The missing of those messages affects the location accuracy of our tracking system because sometimes, the system has to rely on messages captured by less than three monitors. Therefore, we present two techniques to compensate for that missing data by estimating the current position of the user based on its previous positions. The first technique is called Direction and it targets selecting the most probable current position that minimizes the direction change compared to the past positions. The second method is called Speed; it takes as the most probable position the one that leads to the least speed change compared to previous speeds. Both Direction and Speed are inspired from the assumption that humans tend not to make abrupt changes in their speeds and directions while moving under normal circumstances. We evaluate our proposed techniques in comparison with Dead Reckoning technique by simulation with computer generated mobility data and with real mobility data from the CRAWDAD project. By using NS3 we evaluated our techniques with log-normal and indoor propaga-

---

S. Zouaoui (✉)

LINFI Laboratory, Department of Computer Science,  
University of Biskra, P.O. Box 145 RP, 07000 Biskra, Algeria  
e-mail: s.zouaoui@univ-biskra.dz

A. Bachir (✉)

LMA Laboratory, Department of Mathematics,  
University of Biskra, P.O. Box 145 RP, 07000 Biskra, Algeria  
e-mail: a.bachir@univ-biskra.dz

© Springer International Publishing Switzerland 2016  
S. Chikhi et al. (eds.), *Modelling and Implementation of Complex Systems*, Lecture Notes in Networks and Systems 1, DOI 10.1007/978-3-319-33410-3\_19

tion models. NS3 simulations on both log-normal and indoor propagation models show that both methods can lead to satisfactory results and missing of data can be compensated by the proposed heuristics.

**Keywords** Location tracking · Trilateration · WiFi · NS3 simulation

## 1 Introduction

The development of high capacity and performance computer systems coupled with the democratization of storage and the improvement of data manipulation methods has encouraged many data gathering and analytics applications with the goal of understanding various phenomena. One of the emerging and most prominent of these applications is the collection and analysis of crowd movements in confined areas where various techniques other than WiFi-based one have been used with more or less success [1].

However, with the increasing deployment of WiFi hot-spots and the democratization of smart-phones, tablets, and other hand-held WiFi-equipped devices, it has become possible to collect data on those users by capturing the signals transmitted by their devices. Indeed WiFi devices transmit some management frames from time to time searching for preferred access points and seeking association with them with the goal of accelerating hand-off between those access points. Those management frames are transmitted without encryption and thus can be captured and analyzed by any WiFi device with monitoring capabilities. Those frames are always transmitted with the same physical identifier (the MAC address of the device) and thus can be used track the movement of the user.

One of the most straightforward way to track the movements of a user is to perform proximity based localization where the user is deemed to be located near the access point with which it is associated or with the one from which it is receiving the strongest signal. While this proximity-based localization is sufficient in some tracking applications, having a better accuracy is required for a larger amount of applications. Therefore, there is a need for finer-grained WiFi-based location tracking systems.

Although there has been extensive research in the area of WiFi localization, particularly in indoor environment, with more or less satisfactory results due to the challenging constraints of radio propagation characteristics, location tracking causes much more challenges particularly in the case of completely passive tracking where the user does not need to cooperate or help the tracking nor does it even need (technically) to be aware of the tracking process. These additional challenges are mainly due to the irregularity and the small amount of suitable WiFi frames expected from the users. Those frames can be more or less frequent depending on the activity of the user with his hand-held device. If the device is not actively used it may go to sleep mode and refrain from transmitting messages for an extended period of time. The other challenge is the possibility of missing messages at the monitors. If an area is

overcrowded, the high number of frames captured by each monitor can lead to saturation thereby causing the missing of a number of those frames. These challenges make the tracking even more challenging than traditional localization systems where the user is receiving regular powerful signals from anchors which help averaging them and getting a better estimate of the signal strength.

In this paper, we present an architecture of a completely passive location tracking system based on the capture of WiFi frames transmitted by mobile users. We discuss the expected performance of multilateration which is one of the most practical techniques for WiFi devices. We run simulation with NS3 to assess the performance of the position tracking in a general propagation model (log-normal) and an indoor propagation model (IUT-R P.1238). We consider the problem of missing data that occurs at the monitors and propose two techniques to compensate for those missing data to estimate the current position of the user based on its previous position. The first technique is called Direction and it aims to select the most probable current position that minimizes the direction change among past positions. The second method is called Speed; it takes as the most probable position the one that leads to the least speed change compared to previous speeds. Both Direction and Speed are inspired from the assumption that humans tend not to make abrupt changes in their speeds and directions while moving. NS3 simulations on both log-normal and indoor propagation models show that both methods can lead to satisfactory results and missing of data can be compensated by the proposed heuristics.

## 2 Mobile User Location Tracking

### 2.1 Localization Versus Location Tracking

Localization is one of the technical areas that have received increasing attention in recent years due to the boom for location-based services that mobile users can benefit from and the wealth of localization applications in WiFi, ad-hoc, and sensor networks [2, 3]. Localization is defined as the process of determining the position of a mobile device at a given time. The localization process involves the use of wireless signals, to be exchanged with the non located node, in order to get some physical measurements that help in inferring the node's position.

Location tracking is a system that can follow the user mobility by measuring user movements (sequence of locations) over a period of time [4]. It can be achieved by logging the user's historical locations. Tracking applications are numerous including understanding shopping behaviors in malls, schools, public safety, disaster areas, airport, museums, campuses, and exhibitions [1].

There are two types of location tracking: active and passive. In active location tracking, the user performs positioning as in traditional localization technologies and then shares its positions to the tracking system. In passive location tracking, the user does not participate in the tracking procedure. The difference between those two

tracking types is that active tracking may lead to better accuracy as the user receives regular messages from anchors nodes thus leading to a better localization. However, this comes with the constraint of requiring the user to actively collaborate with the tracking system.

## ***2.2 Indoor Location Tracking***

Location tracking can be applied in two contexts: outdoor and indoor. For outdoor or (LOS: Line-Of-Sight) localization, GPS (Global Positioning System) is the most famous active location tracking system used. It works very well in open sky. However, its performance drop in other environments because GPS signals can be blocked by buildings, thick forests and other types of physical obstacles like walls, roofs, floors, etc. Thus, GPS does not work well in indoor or NLOS (Non-Line-Of-Sight) environments due to the complex structure and dynamic nature of indoor environments that affect the wireless signal propagation characteristics making it complex and hard to model. Multipath interference is a problem that exists in indoor environment which happens when the transmitted signal from a satellite is reflected due to barriers such as buildings or trees. Weak signals also affect the accuracy of the position.

## ***2.3 User Detection Accuracy***

An indoor environment is quite different from an outdoor environment. The propagation of a wireless wave can be influenced by some factors that would affect the accuracy of the location estimation of mobile users. In an indoor environment, walls, furniture, or walking people will change the propagation of the wireless wave and introduce variance to the wireless signal received by the user [3]. The RSS (Received Signal Strength) is usually quantified by RSSI (Received Signal Strength Indicator) which is a value that can be read from the wireless radio device. The accuracy of the measure provided by the RSSI is affected by the following factors.

- The Access Point (AP) may be blocked by an object, thus the received signal strength by AP from a terminal may be lower than it should be. Therefore, relying only on the RSSI to estimate a mobile user location becomes unreliable.
- Different environments have different levels of interference. The noise in one environment may be higher than in another due to the existence of many wireless devices transmitting electromagnetic waves.
- There could be refraction, reflection, diffraction, absorption, and scattering of radio signals, which causes the signal strength to be weakened.
- The signal strength can be affected by multipath fading or shadow fading.

### 3 WiFi-Based Location Tracking

The use of WiFi has many attractive features such as: (i) existing low-cost hardware, (ii) large-scale deployment of WiFi, (iii) free software, (iv) no need for sophisticated special hardware, (v) no need for users to install applications or even be aware of the passive location tracking.

#### 3.1 *Frame Types*

WiFi networks use radio technologies called IEEE 802.11 to provide secure, reliable, fast wireless connectivity. A typical WiFi set-up includes one or more access points (APs) and one or more clients. An AP broadcasts its SSID (service set identifier, or “network name”) via packets that are called beacons, which are usually broadcast every 100 ms. The beacons are transmitted at 1 Mbit/s, and are of relatively short duration and therefore do not have a significant effect on performance.

A mobile user running WiFi transmits many types of frames: data, control, and management. While data frames are most likely to be encrypted, management frames are transmitted in clear and thus reveal the identity of the user which can be used to track its movements.

All of these frames contain a frame header, which includes the source and destination MAC addresses. It also contains information such as beacon interval and Service Set Identifier (SSID), which is the name of the WLAN. The SSID is important for a terminal to know which network it is trying to establish a connection with. Management frames perform supervisory functions. They are used for the purpose of establishing a connection between an AP and a terminal. A terminal in a WLAN, with multiple APs deployed, may move around and as a result, the terminal may need to switch association from one AP to the next using management frames. They perform the following operations: (i) join and leave wireless networks, and (ii) move associations from access point to access point. In addition to management frames, control frames are used to coordinate data frame exchange. Although, location tracking can be done on any type of frames, we focus on management frames as they are transmitted in clear without encryption.

#### 3.2 *Wireless Modes*

Most wireless users only use their wireless cards as a station to an AP. In managed mode, the wireless card and driver software rely on a local AP to provide connectivity to the wireless network. Another common mode for wireless cards is ad-hoc mode. Two wireless stations that want to communicate with each other directly can do so by sharing the responsibilities of an AP for a limited subset of wireless LAN services.



Ad-hoc mode is used for short-term connectivity between stations, when an AP is not available to provide connectivity.

Many wireless cards also support master mode, where the wireless card provides the services of an AP when paired with the appropriate software. Managed mode allows to configure a wireless card to connect to an AP. Finally, wireless cards support monitor mode functionality. When configured in monitor mode, the wireless card stops transmitting data and sniffs the currently configured channel, reporting the contents of any observed packet to the host operating system. This mode is useful for completely passive location tracking systems as the entire contents of wireless packets, including header information can be analyzed [5].

## 4 Positioning Approaches

Positioning systems can be classified according to the measurement techniques they employ to determine the user's location. There are many approaches: triangulation, multilateration, area-based, and fingerprinting [6–9]. In this paper, we focus on multilateration as it is the most practical among localization approaches.

In the multilateration, the localization is based on turning RSSI measures into distances from the mobile user to the anchors. The conversion from RSSI to distance is based on a path loss model (also called radio propagation or attenuation model) which predicts the loss in signal strength in function of the distance between the source and destination nodes. The loss in signal strength is caused by (i) distance, (ii) multipath (reflected, diffracted, or scattered copy of the transmitted signal) and (iii) shadowing (blockage of signal due to obstacles). To predict the loss in signal in different environments, different propagation models have been developed and can be categorized into two classes; theoretical (deterministic) and experimental (statistical) models. Theoretical models try to simplify the complex behavior of path loss, multipath and shadowing using mathematical models [7]. A widely used model is the log-normal path-loss that predicts the path loss a signal encounters inside a building or densely populated areas over distance. Mathematically, the received power over a distance  $d$  between the transmitter and the receiver according to the log-normal model is given in (1). We have:

$$P_r(d) = P_r(d_0) - 10n \log \left( \frac{d}{d_0} \right) - X_\sigma \quad (1)$$

where  $d_0$  is the reference distance generally taken equal to 1 m,  $n$  is path-loss exponent,  $X$  is a Gaussian random noise variables of average for 0 (dBm) and standard deviation of  $\sigma$  (dBm).  $P_r(d)$  is received signal power (dBm) and  $P_r(d_0)$  is the received signal power at the reference distance (dBm). Multilateration algorithms aim at providing a good estimate of the user location given the exact anchor locations and distances the user to each anchor. Multilateration requires at least three non collinear anchors to be able to estimate the position of the user. To estimate the position of

the tracked user, the monitors obtain RSS measures and turn them into distances required to apply the multilateration algorithm. These distances can be obtained by solving (1) for  $d$  which results in:

$$d = d_0 * \exp \frac{P_r - P_r(d_0) - X_\sigma}{10 * n} \tag{2}$$

Let  $(x, y)$  be the coordinates of Monitor  $i$  and  $d_i$  the distance between the user and Monitor  $i$ . We have the following:

$$\begin{cases} d_1^2 = (x_1 - x)^2 + (y_1 - y)^2 \\ \dots \\ d_n^2 = (x_n - x)^2 + (y_n - y)^2 \end{cases} \tag{3}$$

Equation (3) can be rewritten to as:

$$\mathbf{AX} = \mathbf{b} \tag{4}$$

where

$$\mathbf{A} = \begin{pmatrix} 2(x_1 - x_n) & 2(y_1 - y_n) \\ \vdots & \vdots \\ 2(x_{n-1} - x_n) & 2(y_{n-1} - y_n) \end{pmatrix}, \mathbf{X} = \begin{pmatrix} x \\ y \end{pmatrix} \tag{5}$$

$$\mathbf{b} = \begin{pmatrix} x_1^2 - x_n^2 + y_1^2 - y_n^2 + d_1^2 - d_n^2 \\ \vdots \\ x_{n-1}^2 - x_n^2 + y_{n-1}^2 - y_n^2 + d_{n-1}^2 - d_n^2 \end{pmatrix} \tag{6}$$

By adopting the minimum variance estimation method, the coordinates  $(x, y)$  of the user can be calculated. We have:

$$\mathbf{X} = (\mathbf{A}^T \mathbf{A})^{-1} \mathbf{A}^T \mathbf{b} \tag{7}$$

Note that multilateration is a very efficient technique. Its main weakness is caused by the inefficiency of the RSSI measure to be turned into a distance, because this depends on the knowledge of the environment constraints that may change from one region to another closed region and from time to time.

## 5 Location Tracking with Unreliable Data

### 5.1 *The Problem of Missing Data*

When using monitors to capture packets transmitted by a user, it is not uncommon that a capture is missed by a monitor. This can be caused by many factors such as obstacles obstructing the signal, hardware problems at the radio transceiver, saturation due to a high number of packets being captured, etc. To evaluate the amount of those missed captures, we run experiments with three monitors placed in an office environment in a Professional Education Institute. We installed three monitors M1, M2, and M3 in various locations of the office. In the experiments scenario, we let a user move in the office and transmit packets from time to time, and let every monitor capture those packets and measure their corresponding RSSIs. At the end of the experiments, the monitors collected 497 packets in total. Monitors 2 and 3 observed a loss of 6 and 41 packets respectively, which makes the total loss rate of 9.46 %.

### 5.2 *The Effect of Missing Data*

With missing RSSI readings, it becomes difficult to estimate the location of the user. We consider the case where there are two RSSI readings which could be turned into two distances. Therefore, (4) will not necessarily have a unique solution. The results of that equation will depend on the positions of the two circles centered at the two monitors with ranges as distances obtained from the RSSI readings. There will be multiple cases: no solutions when the two circles do not intersect, infinity of solutions if the two circles are the same, one solution if the two circles touch at a single point and two solutions if the two circles intersect at two different points.

### 5.3 *Estimating Position with Missing Data*

We consider the case where there are two solutions and aim at finding the best methods to eliminate the unlikely location and keep the most probable one. For the multilateration technique, we use two heuristics to estimate the most probable position of the user. These metrics are as follows.

#### 5.3.1 **Direction Method**

We assume that humans are less likely to make abrupt changes in their movements. Therefore, in our selection of the most suitable point, we take the one with the least direction changes among potential candidate points. We calculate the movement

vectors of all potential candidates and take the one with the minimum direction change. Mathematically this reduces to taking the vector the maximum *cosine* value with the previous movement vector. Assume that the user was at Location  $L_{-2}$ , then  $L_{-1}$ , and we want to eliminate  $L_0$  or  $L'_0$  the two potential current locations resulting from the intersection of the two circles. We take the location estimate  $\hat{L}$  which results in the minimum cosine value among the following:

$$\hat{L} = \begin{cases} L_0 & \text{if } |\cos(L_{-2}L_{-1}, L_{-1}L_0)| < |\cos(L_{-2}L_{-1}, L_{-1}L'_0)| \\ L'_0 & \text{otherwise} \end{cases} \quad (8)$$

### 5.3.2 Speed Method

We assume that humans are likely to change the pace of their movements abruptly. Therefore, we take the point that is closest to the history of the speed of movement of users. Technically we calculate the distances of all potential candidates from the current point. For all these points we calculate the corresponding velocities and take the point whose the corresponding velocity is closest to the previous speed. The basic idea is to measure the minimum distance between the mobile node and the two points of intersection of two circles by using Euclidean distance. If we assume that the user was at Location  $L_{-2}$  (resp.  $L_{-1}$ ,  $L_0$ ,  $L'_0$ ) at time  $t_{-2}$  (resp.  $t_{-1}$ ,  $t_0$ ,  $t_0$ ), we calculate the velocities  $v_0$  and  $v'_0$  and compare them to the previous velocity  $v_{-1}$ .

$$v_{-1} = \frac{\|L_{-2}L_{-1}\|}{t_{-2} - t_{-1}}, v_0 = \frac{\|L_{-1}L_0\|}{t_{-1} - t_0}, v'_0 = \frac{\|L_{-1}L'_0\|}{t_{-1} - t_0} \quad (9)$$

where  $\|X\|$  is the norm of the vector  $X$ . Thus, the user is assumed to be at the location that minimizes the difference in velocity. We have:

$$\hat{L} = \begin{cases} L_0 & \text{if } |v_{-1} - v_0| < |v_{-1} - v'_0| \\ L'_0 & \text{otherwise} \end{cases} \quad (10)$$

### 5.3.3 Dead Reckoning

Is a localization technique proposed in [10]. In Dead Reckoning, nodes are localized during a time interval called checkpoint. There are two localization phases in Dead Reckoning. The first phase is called initialization phase during which a node is localized using the multilateration mechanism. A node remains in the initialization phase until it localizes using the multilateration mechanism. The subsequent localization phase is called sequent phase. In this phase, a node localizes itself using only two anchor nodes. Bezouts theorem [11] is used to estimate the node's locations. Let  $(x, y)$  be the position of an unknown node and  $(a_1, b_1)$ ,  $(a_2, b_2)$  be the position of

two of its neighboring anchor nodes. Moreover, let the distance between an unknown node and the respective anchor nodes be  $d_1$  and  $d_2$ , respectively. Then

$$\begin{cases} (x - a_1)^2 + (y - b_1)^2 = d_1^2 \\ (x - a_2)^2 + (y - b_2)^2 = d_2^2 \end{cases} \quad (11)$$

After solving the Eq. (11), the algorithm estimates two positions  $P_1(x_1, y_1)$  and  $P_2(x_2, y_2)$ . Next, the node computes the correction factors ( $Cf_1$  and  $Cf_2$ ) to select one of the two estimated positions  $P_1$  and  $P_2$ . The correction factor is computed by using  $P(\hat{x}, \hat{y})$  which the position of the node using multilateration in the first time. After that, it use the previous position at the checkpoint  $t_i$  to estimate its location in the next checkpoint at  $t_{i+1}$ .

$$\begin{cases} Cf_1 = \sqrt{(\hat{x} - x_1)^2 + (\hat{y} - y_1)^2} \\ Cf_2 = \sqrt{(\hat{x} - x_2)^2 + (\hat{y} - y_2)^2} \end{cases} \quad (12)$$

The correct position of the node is  $P_1$  if ( $Cf_1 < Cf_2$ ). Otherwise, it will be  $P_2$ . This is because, the calculated position  $P(\hat{x}, \hat{y})$  always deviate from the actual position by a small margin.

## 5.4 Error Estimation

To evaluate the accuracy of our location tracking system, we calculate the estimation error between the real location  $L$  and the estimated one returned by our system  $\hat{L}$ . We have:

$$\epsilon = \|L - \hat{L}\| \quad (13)$$

## 6 Simulation

To evaluate the performance and the accuracy of our location tracking methods, we run extensive simulations with NS3 which is a discrete-event network simulator where the simulation core and models are implemented in C++. NS3 is open source and licensed under the GNU GPLv2 license and therefore has benefited from a growing community base which contributed to adding more radio propagation models and network protocols. Since its release in 2008 it is one of the most important and widely used network simulation tools. Creating a NS3 simulation consists of four basic steps. These basic component types of a network are nodes, applications, net devices, channels and topology helpers [12, 13]. An important part of any wireless network simulation is the appropriate choice of the propagation loss model to be used

**Table 1** Description of real mobility DataSets used

	Environment size	Environment	User type	Sample size
CRAWDAD DataSet1 [14]	400 m <sup>2</sup>	Office	Mobile robot	1689
CRAWDAD DataSet2 [15]	15 m × 36 m	Office	User	60
KIOS DataSet3 [16]	500 m <sup>2</sup>	Office	User	96
CRAWDAD DataSet4 [17]	50 m × 75 m	Office	User	180

to model the performance of a wireless network. These models are needed for the simulator to compute the signal strength of a wireless transmission at the receiving stations. There are a variety of such models in NS3.

The indoor radio propagation model we used with NS is implemented according to the description of ITU-R P.1238. We considered two cases ( $\sigma = 0$  and 1) to reflect various environments. The area that we used in our simulations is an office  $10 \times 20 \times 10$  building with concrete windows. This building has one floors and an internal  $20 \times 2$  grid of rooms of equal size.

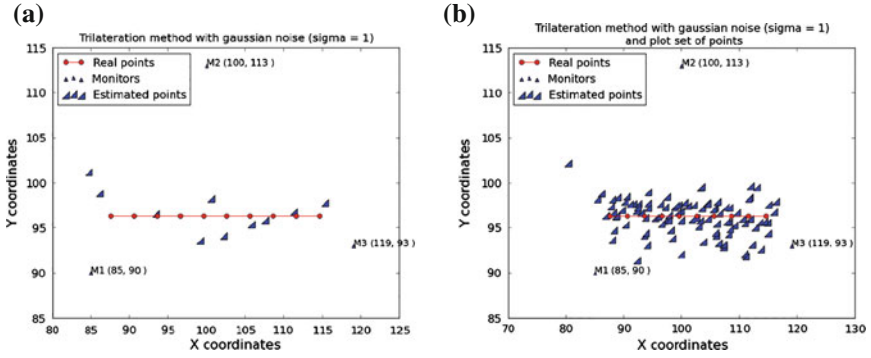
For the user mobility, we considered computer generated mobility data and real mobility traces. In the computer generated data, we considered an ideal mobility model where the user is simulated to move along constant direction with a constant speed. We also considered the indoor mobility model that comes with the NS3 package. For the real mobility data, we considered 4 data sets from the CRAWDAD and KIOS projects. The main characteristics of these datasets (DS) are summarized in Table 1.

For all these mobility scenarios, we use three monitor places at non collinear positions. For each position of the user we simulate the transmission of a message from the user that will be captured by the monitors. Each monitor that captures a message, reads its RSSI and turns it into a distance that is used to estimate the user position according to one the techniques tested: Dead Reckoning, Distance, and Speed.

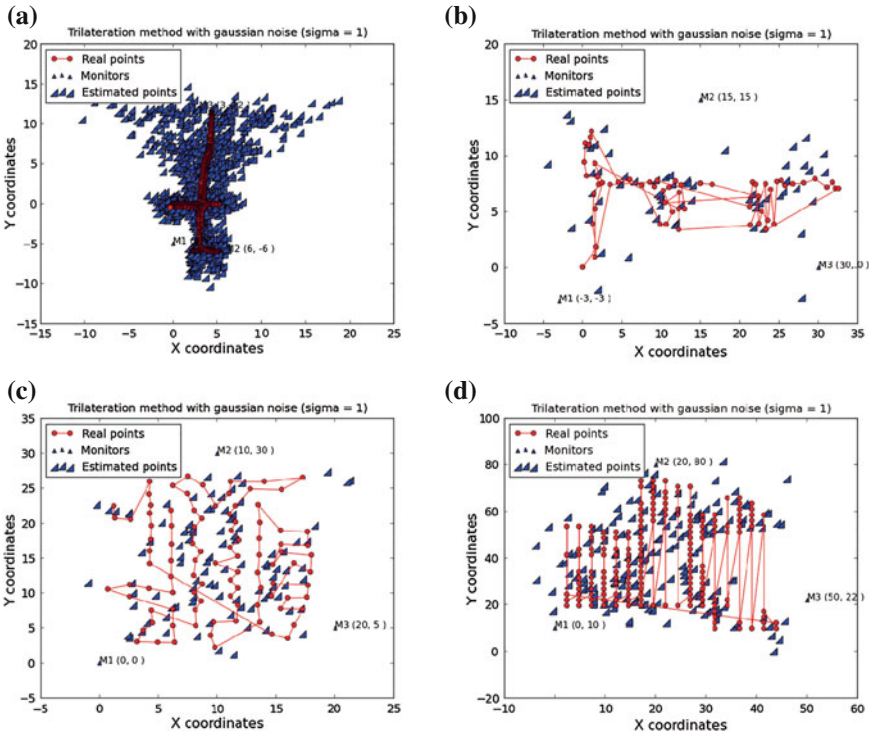
To simulate unreliable data, we introduce random losses at the monitors. We introduce a probability of missing a message for each monitor. Initially we assume that only one monitor misses a message at a time so there are always at least two other monitors receiving the same message, and we aim to estimate the position of the user based on the available two RSSI measures.

## 6.1 Location Tracking Without Missing Data

In the case ideal mobility model and  $\sigma = 0$ , all the positions can be correctly estimated and the estimated positions perfectly match the real ones. In a little more complex situation where  $\sigma = 1$ , the estimated positions do not match the real ones even with an ideal mobility model (see Fig. 1). However, as we notice in the same



**Fig. 1** Coordinates of estimated position calculated based on RSS measures. Ideal mobility with  $\sigma = 1$ . **a** Each position is used to calculate 1 coordinate estimate. **b** Each position is used to calculate 10 coordinate estimates

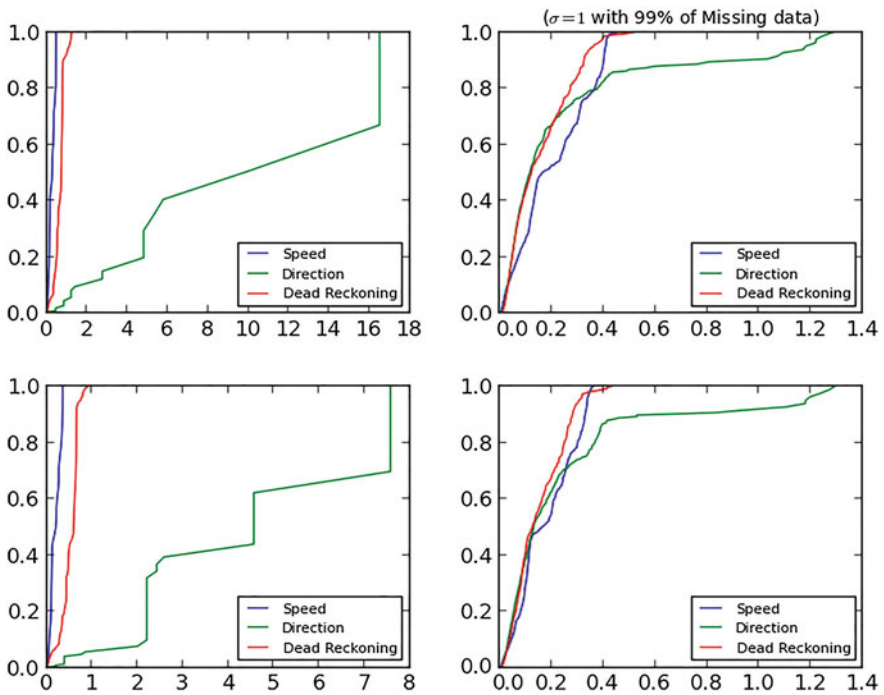


**Fig. 2** Position coordinates from real mobility data and their corresponding position estimated without missing data and with  $\sigma = 1$ . **a** DataSet1. **b** DataSet2. **c** DataSet3. **d** DataSet4

**Table 2** Summary of the obtained results

DS	Pos.	Method	$\sigma = 0$		$\sigma = 1$		Trilateration	
			Mis. = 74 %	Mis. = 99 %	Mis. = 74 %	Mis. = 99 %	$\sigma = 0$	$\sigma = 1$
1	1689	Direction	0.121511	0.264769	1.645680	1.602990	0.0026119	1.6618
		Speed	4.268930	5.645070	4.865160	5.904530		
		Dead reckoning	0.706925	0.849137	1.789630	2.006390		
2	60	Direction	1.526920	1.946580	3.763000	3.848790	4.74E-06	2.3797
		Speed	4.692470	5.564970	5.818530	6.378680		
		Dead reckoning	3.564433	4.127600	4.578430	4.997270		
3	96	Direction	0.837704	0.611903	2.547160	2.084700	4.45E-06	2.14042
		Speed	1.858930	0.327840	4.009810	2.300220		
		Dead reckoning	2.018800	2.108680	3.117430	2.823130		
4	180	Direction	5.537220	3.412730	6.861800	6.921910	1.13E-05	4.77129
		Speed	8.400200	8.615250	9.903870	10.850200		
		Dead reckoning	3.929080	9.361340	7.637980	9.929080		

CDF for DataSet1



**Fig. 3** CDF with DataSet1



figure, the difference between these values quantified by the by the estimation error is low.

In the case of real mobility data and  $\sigma = 1$ , we plotted the graphs in Fig. 2 to show the effect of RSSI fluctuations of the estimation of positions in the case of real mobility data. The mean errors in position estimation with these scenarios are summarized in Table 2.

### 6.2 Location Tracking with Missing Data

We run various scenarios for missing data. In the first one, Missing0 already discussed above, there are no missing data and all the messages transmitted by the user will be captured by the monitors. In the second and third scenarios only a proportion of the messages are captured by the monitors. For example, in Missing74 and Missing99 scenarios, 74 and 99 % of the localization estimations are based on the RSSI readings of only two monitors, respectively. For various setting, we plot the CDF of the error in position estimation expressed in meters as shown in Figs. 3, 4, 5 and 6.

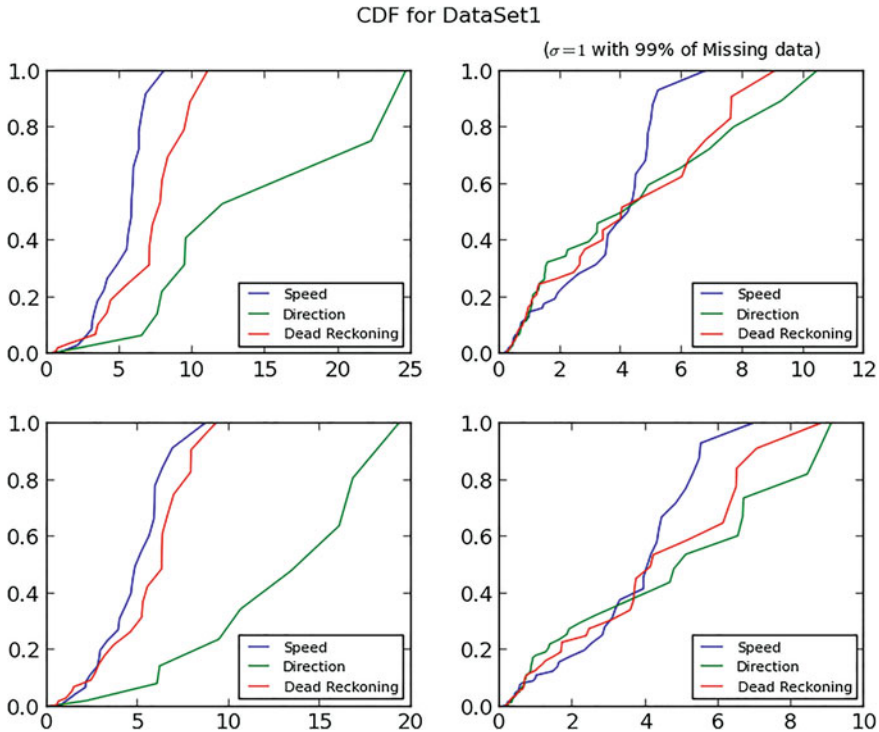


Fig. 4 CDF with DataSet2

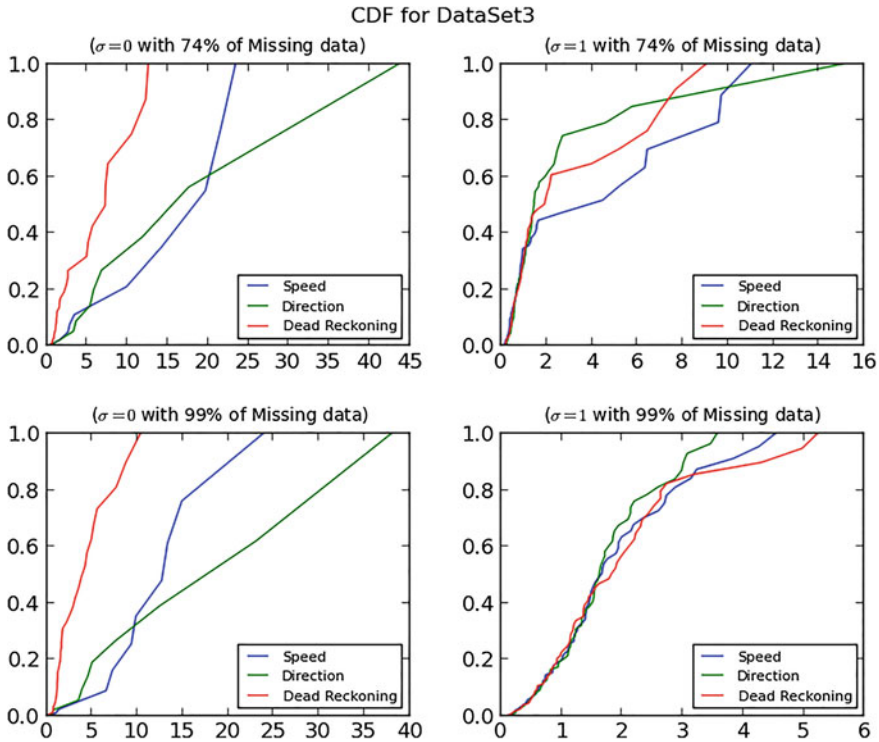


Fig. 5 CDF with DataSet3

In general, we also notice that when  $\sigma$  increases the error in position estimation also grows as explained earlier in the case of no missing data. We also show that Direction method achieves the best position estimation followed by Dead Reckoning followed by Speed and that there is not a big difference in position estimation when the ratio of missing data increases from 74 to 99%. In some situations such as in DataSet3 (Fig. 5), we show that Speed achieves good position estimate. The reason is that in DataSet3, the user movements are regular. For the DataSet4, we show that all methods return higher errors in position estimation. This is because user movements are not regular as the users seems to make vertical movements due to the large time interval between recorded positions. There is another reason why position estimates are less good in DataSet4 compared to the other data sets, which is due to the placement of monitors that farther away from the positions to be estimated. We also show that Direction method is the best in situation where we have short intervals between positions recording such as in DataSet1 (Fig. 3).

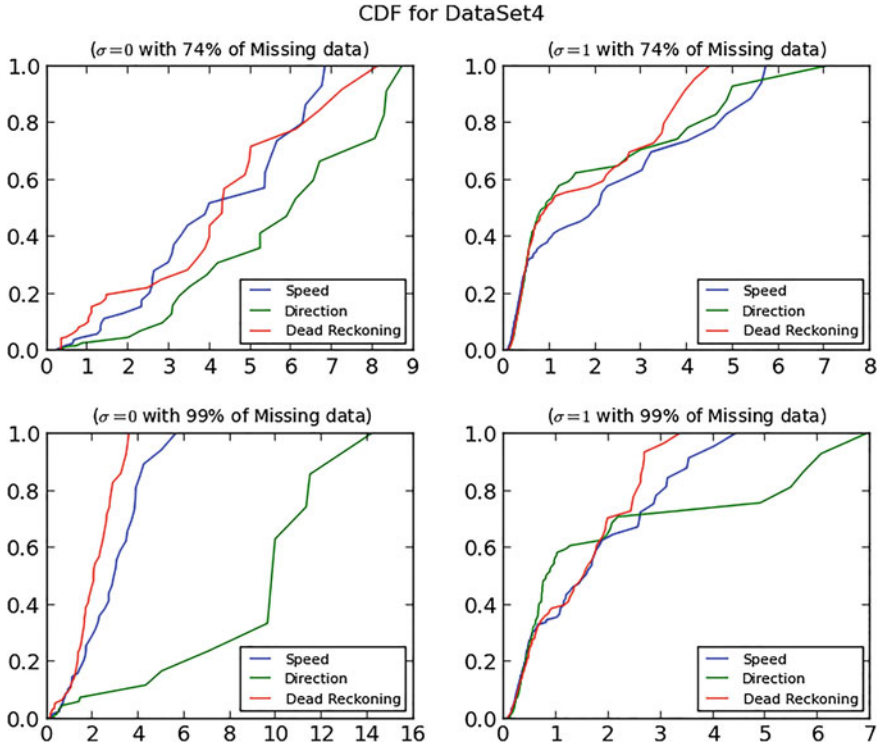


Fig. 6 CDF with DataSet4

## 7 Conclusions

We have presented a completely passive location tracking system that allows finding WiFi equipped mobile user locations. We analyzed the performance of the proposed system in a general environment governed by a log-normal path loss model with both real and computer generated data sets. We presented the problem of missing data that occurs at the monitors which we validated with experiments based on WiFi-enabled Raspberry Pi monitors. To cope with the problem of missing data, we proposed two heuristics in relation with the direction and speed change of mobile user with the assumption that humans users are likely to keep nearly constant speed and direction in their movements. NS3 simulations on both a general path-loss model and an indoor model on both computer generated and real mobility data have shown that Direction method achieves better results in general compared to Speed and Dead Reckoning.

**Acknowledgments** This work is funded in part by the Algerian Ministry of Higher Education and Scientific Research under contract B\*01420130132. We gratefully acknowledge the use of wireless data from the CRAWDAAD archive at Dartmouth College.

## References

1. Larson, J.S., Bradlow, E.T., Fader, P.S.: An exploratory look at supermarket shopping paths. *Int. J. Res. Mark.* **22**(4), 395–414 (2005)
2. Schiller, J., Voisard, A.: *Location-Based Services*. Elsevier (2004)
3. Lasla, N., Younis, M.F., Ouadjaout, A., Badache, N.: An effective area-based localization algorithm for wireless networks. *IEEE Trans. Comput.* **64**(8), 2103–2118 (2015)
4. Zhang, D., Xia, F., Yang, Z., Yao, L., Zhao, W.: Localization technologies for indoor human tracking. In: 2010 5th International Conference on Future Information Technology (FutureTech), pp. 1–6. IEEE (2010)
5. IEEE standard for information technology–telecommunications and information exchange between systems local and metropolitan area networks–specific requirements Part 11: wireless LAN Medium Access Control (MAC) and Physical Layer (PHY) Specifications. IEEE Std 802.11-2012 (Revision of IEEE Std 802.11-2007), pp. 1–2793, March (2012)
6. Cisco Systems. Location tracking approaches. In: *Wi-Fi Location-Based Services 4.1 Design Guide*. Cisco Systems (2008)
7. Chuan-Chin, P., Chuan-Hsian, P., Lee, H.-J.: Indoor location tracking using received signal strength indicator. In: *Emerging Communications for Wireless Sensor Networks*. InTech (2011)
8. Guvenc, I., Abdallah, C.T., Jordan, R., Dedeoglu, O.: Enhancements to rss based indoor tracking systems using kalman filters (2003)
9. Lasla, N.: *Toward an efficient localization system for wireless sensor networks*. PhD Thesis, USTHB (2015)
10. Rashid, H., Turuk, A.K.: Dead reckoning localisation technique for mobile wireless sensor networks. *IET Wirel. Sens. Syst.* **5**(2), 87–96 (2015)
11. Bezouts theorem. <http://www.sjsu.edu/faculty/watkins/bezout.htm>. Accessed 28 Jan 2016
12. NS3 project. <https://www.nsnam.org/docs/release/3.9/manual.pdf>. Accessed 15 July 2015
13. Rampfl, S.: Network simulation and its limitations. In: *Proceeding zum Seminar Future Internet, Innovative Internet Technologien und Mobilkommunikation und Autonomous Communication Networks*, vol. 57 (2013)
14. Parasuraman, R., Caccamo, S., Baberg, F., Ogren, P.: CRAWDAD dataset kth/rss (v. 2016-01-05) (2016). <http://crawdad.org/kth/rss/20160105>
15. King, T., Kopf, S., Haenselmann, T., Lubberger, C., Effelsberg, W.: CRAWDAD dataset mannheim/compass (v. 2008-04-11) (2008). <http://crawdad.org/mannheim/compass/20080411>
16. Panayiotou, C., Laoudias, C., Piche, R.: Device self-calibration in location systems using signal strength histograms. *J. Location Bas. Serv.* **7**(3), 165–181 (2013). KIOS WiFi RSS dataset (PDF Download Available). doi:10.1080/17489725.2013.816792. Accessed 6 Feb 2016
17. Bauer, K., Anderson, E.W., McCoy, D., Grunwald, D., Sicker, D.C.: CRAWDAD dataset cu/rssi (v. 2009-05-28) (2009). <http://crawdad.org/cu/rssi/20090528/text>

**Part IV**  
**Software Engineering and Formal**  
**Methods**

# Two Stages Feature Selection Based on Filter Ranking Methods and SVMRFE on Medical Applications

Hayet Djellali, Nacira Ghoualmi Zine and Nabiha Azizi

**Abstract** This paper investigates feature selection stage applied to medical classification of disease on datasets from UCI repository. Feature selection methods based on minimum Redundancy Maximum Relevance (mRMR) filter and Fisher score were applied, each of them select a subset of features then the selection criteria is used to get the initial features subset. The second stage Support vector machine recursive feature elimination is performed to have the final subset. Experiments show that the proposed method provide an accuracy of 99.89 % on hepatitis dataset and 97.81 % on Wisconsin Breast cancer dataset and outperforms MRMR and Support vector machine recursive feature elimination SVM-RFE methods, as well as other popular methods on UCI database, and select features that are relevant in discriminating cancer class (malign/benign).

## 1 Introduction

Feature selection (FS) plays an important role in pattern recognition and data mining. FS algorithms consider that the feature set contains redundant features or irrelevant. Irrelevant features are not discriminative for the classification problem, and redundant features contain information which is present in more informative

---

H. Djellali (✉) · N.G. Zine  
Computer Science Department, Annaba, Algeria  
e-mail: hayetdjellali@yahoo.fr

H. Djellali · N.G. Zine  
LRS Laboratory, Annaba, Algeria

N. Azizi  
Labged Laboratory, Annaba, Algeria

H. Djellali · N.G. Zine · N. Azizi  
Badji Mokhtar University, Annaba, Algeria

features. We can investigate the remaining relevant features to determine the effect to the class label. Thus, classification performance is improved [1, 2].

FS for medical application serves many purposes like helping in efficient identification of disease (as example cancer disease from a subset of features), also helps to construct a robust classifier with discriminative features and non redundant one [3–5]. In this paper, Feature Selection methods have been studied and tested on medical application.

Considering only robustness of a feature selection technique is not an appropriate strategy to find good subsets of features, and also model performance should be taken into account to decide which features to select. Therefore, feature selection needs to be combined with a classifier in order to get the best performance [6].

FS algorithms suffer from instability. The perturbation of the data such as removal of a few samples may cause a FS algorithm to select a different set of features [5, 7].

The present work is focused on feature selection in automatic classification system of disease (malign and benign). In this paper, we propose a scheme to improve robustness using in first stage the feature selection based on MRMR filter and fisher score, then select the common features. The second stage we use Support Vector Machine recursive feature elimination SVMRFE to remove the worst features and estimate accuracy.

The manuscript is organized as follows. Section II describes features selection methods: filter ranking methods, MRMR and SVM-RFE methods and related work. Section III gives a detailed description of the proposed algorithm: FS methods combine SVM-RFE with MRMR and fisher score Filter. The numerical experiments on medical datasets from UCI database like hepatitis and breast cancer are demonstrated in Section IV and evaluating the performance of our algorithm and comparison with SVMRFE and MRMR approaches are presented. Finally, in section V and VI the results were discussed followed with conclusion.

## 2 Feature Selection Methods

In this section, we describe different feature selection approaches like filter, wrappers and embedded methods. We describe these methods to highlight their ability to build an efficient classification system.

Feature selection (FS) is a widely-used technique in pattern recognition applications. Feature selection is the process of selecting an optimum subset of features from the huge potential features available in a given classification problem [4]. It removes irrelevant and redundant features from the original data; FS reduce the problem of over fitting and the performance of the resulted model is improved. More importantly, we can compare the features and keep only the relevant ones.

FS algorithms are divided into three categories: filters, wrappers and embedded methods, based on how they interact with classifiers [4]. Filters methods often employ only a heuristic approach where the criterion function is not related to

particular classifier. The filters are evaluated based on criteria like Pearson correlation, entropy, probabilistic distance measures, and mutual information [3, 8].

Feature ranking were the first approaches used and still applied for too high dimensionality problems. The best ranked features may be selected as input of a classifier. All the filter methods are fast and computationally simple and independent of the classifiers. The principal disadvantage is they ignore the interaction with the classifier and most proposed technique is univariate (each feature is considered separately thereby ignoring feature dependencies) which may lead to worse classification performance when compared to other types of FS techniques [1].

Wrappers methods aim at finding a feature subset that achieve higher classification accuracies by embedding classifier characteristics into the feature selection process [9, 10].

Embedded methods are hybrid approaches using filters and wrappers. A large number of algorithms have been applied to feature selection like evolution approaches such as genetic algorithm (GA) based selection [11–13]. Wrapper and Embedded methods can efficiently obtain high classification accuracy, but the execution time is higher than Filter methods [14].

## 2.1 Features Ranking Methods

These methods assign a weight to each feature and rank the feature accordingly. Filter techniques assess the relevance of the features by looking only at the intrinsic properties of the data. In most cases a feature relevance score is calculated, and low scoring features are removed [1]. We describe several features ranking strategy that we experiment.

Fisher score (fscore) is a simple feature selection technique which measures the discrimination of two sets of real numbers [6]. Based on statistics characteristics, it is independent of the classifiers.

Given training vectors  $x_k$ ,  $k = 1, 2, \dots, m$ . the numbers of positive examples are  $n_{plus}$  and negative examples are  $n_{neg}$  respectively, then the fscore of the  $j$ th feature in Eq. (1) is defined from equation Fscore [6]

$$F(j) = \frac{(xb_j^{(+)} - xb_j)^2 + (xb_j^{(-)} - xb_j)^2}{\frac{1}{n_{plus}-1} \sum_{i=1}^{n^+} (x_{i,j}^{(+)} - xb_j^{(+)})^2 + \frac{1}{n_{neg}-1} \sum_{i=1}^{n^-} (x_{i,j}^{(-)} - xb_j^{(-)})^2} \quad (1)$$

- $xb_j$ : the average of  $j$ th feature of whole instance
- $xb_j^{+}$ : the average of  $j$ th feature of positive instance
- $xb_j^{-}$ : the average of  $j$ th feature of negative instance
- $x_{ij}^{+}$ : the  $j$ th feature of the  $i$ th positive instance
- $x_{ij}^{-}$ : the  $j$ th feature of the  $i$ th negative instance



## 2.2 Support Vector Machine Recursive Feature Elimination

Support vector machine recursive feature elimination (SVM-RFE) is an embedded FS algorithm proposed by Guyon et al. [9]. It starts with all the features, uses criteria from the coefficients in Support Vector Machines models to assess features, and recursively removes features that have small criteria recursively in a backward elimination manner. SVM-RFE is a FS method that uses SVM weights as the ranking criterion of features. It has both linear and nonlinear versions. The nonlinear SVM-RFE uses a special kernel strategy and is preferred when the optimal decision function is nonlinear [8].

## 2.3 Minimum Redundancy Maximum Relevance

The minimum Redundancy Maximum Relevance (mRMR) method aims at selecting maximally relevant and minimally redundant set of features [2]. Max Relevance is to search features with the mean value of all mutual information values between individual feature  $x_i$  and class  $c$ .

If two features highly (correlated) depending on each other and removing one of them, the class discriminative power is not affected. The minimal redundancy (Min-Redundancy) condition is added to select mutually exclusive features. The criterion combining the above two constraints is called minimal Redundancy Maximal Relevance (mRMR) [15].

To find the optimal features defined by Eq. (2), incremental search methods is used. Let assume we already have  $S_{m-1}$ , the feature set with  $m-1$  features. The task is to select the  $m$ th feature from the set  $\{X-S_{m-1}\}$ . This is done by selecting the feature that maximizes Eq. (2).

$$\max_{x_j \in S_{m-1}} [I(x_j; c)] - \frac{1}{m-1} \sum_{x_i \in S_{m-1}} I(x_j; x_i) \quad (2)$$

## 2.4 Related Work

The authors [3] indicated that while Computer aided diagnosis CADx shows promising results for classifying an abnormality into benign or malignant, the diagnostic accuracy is not very high. So, the authors proposed a new feature selection based on support vector machines (SVM) and mutual information-based feature selection method which minimizes redundancy among features and maximizes relevance to classes (mRMR). They have tested their architecture on the dataset of mass and calcification lesions found in the Digital Database of Screening

Mammography (DDSM) [16]. The results showed that the proposed scheme is competitive to other classification methods.

Maka and Kung [17] investigated various wrapper and filter techniques for reducing the feature dimension of pairwise scoring matrices and proved that these two types of selection techniques are complementary to each other. Two fusion strategies are then proposed to combine the ranking criteria of filter and wrapper methods and merge the features selected by the filter and wrapper methods. Evaluations on a subcellular localization benchmark and a microarray dataset demonstrate that feature subsets selected by the fusion methods are superior to those selected by the individual methods for a broad range of feature dimensions.

The authors [8] proposed a novel hybrid approach by correlation-based filters and Support Vector Machine—Recursive Feature Elimination (SVM-RFE) method for robust feature selection, which aims to achieve robust results by aggregating multiple feature subsets. In the first stage, they incorporate correlation based filters to identify relevant Features and Complementary Features, and generate multiple groups for robustness; in the second stage, they aggregate multiple groups with SVM-RFE into a compact feature subset. Experimental results on both UCI data sets and microarray data sets have proved the effectiveness of the proposed approach.

The authors [18] introduced multiple SVM-RFE, where the SVM was trained on multiple subsets of data and the genes were ranked using statistical analysis, and demonstrated its effectiveness in choosing genes in microarray data. From the experiments, it was found that SVM-RFE (Correlation) outperformed SVM-RFE (mRMR) in terms of classification accuracy. The authors observed that SVM-RFE (mRMR) converges faster than other methods while it does not achieve the best performance.

Tang et al. [19] proposed two-stage SVM-RFE algorithm, where initial gene subset was selected using several multiple MSVM-RFE models with different gene, and in the second stage, at each iteration, genes were selected by eliminating one gene.

The authors [20] combined mRMR and ReliefF algorithms in a two-stage strategy for gene selection. In the first stage, ReliefF method select small subset of genes, and then, mRMR method was applied to choose non redundant genes into the subset. The experimental results on seven different datasets show that the mRMR relief gene selection algorithm is very effective.

Peng et al. [21] presented a new approach for feature selection in biomedical data. The proposed approach is characterized by adding a pre-selection step based on filter to improve the effectiveness in searching the feature subset that achieves the best classification performance. Receiver operating characteristics curves (ROC) is used to characterize the performance of the individual feature and the subset of features in the classification. The experiments on biomedical datasets show that proposed method improves the performance measured by area under curve of ROC compared to sequential forward floating search (SFFS).

### 3 The Proposed Architecture

This section presents a robust feature estimation and ranking method based on ranking the features by using different criterion: fisher ratio, and mRMR. In this study the ranked features by Fisher’s ratio and maximum relevance, minimum redundancy (mRMR) are compared to make the intersection between features and keep them as final subset of optimal features.

We propose to improve robustness of feature selection through multiple cycle, by doing this, the assessment of features tends to be less sensitive to the inaccurate estimation of the statistical parameters applied on databases from UCI repository. Each criteria provides specific subset given its search abilities to obtain a solution that is complementary from the other but not optimal. The selection criteria consist of computing the common subset between filters method.

The SVM-RFE [9] is applied in the second stage to evaluate the effect in term of accuracy for the classifier. The overall feature selection and classification scheme of the study framework is shown in Fig. (1).

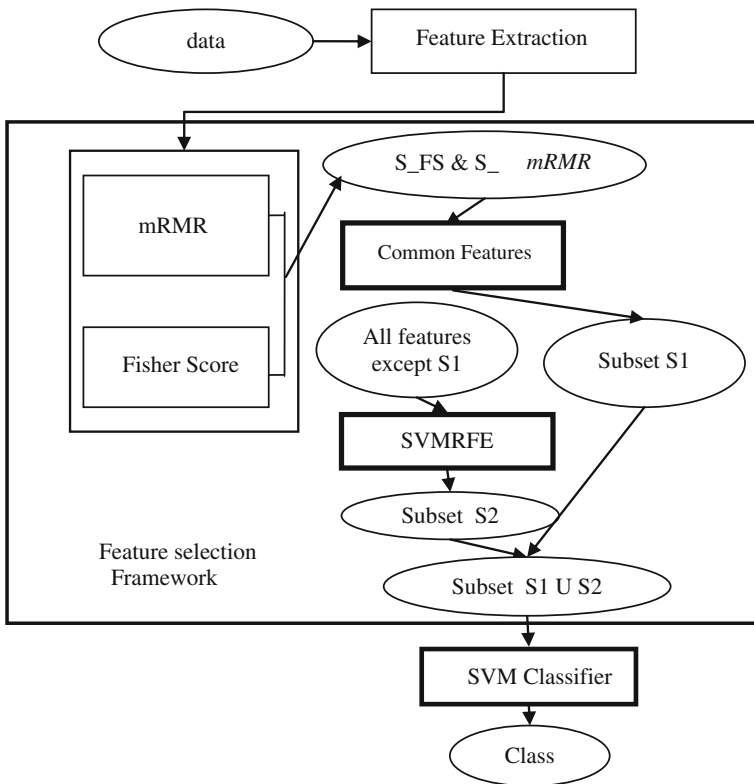


Fig. 1 Disease recognition architecture

To classify the medical data from well known database like cancer disease, diverse phases used in this work are described below:

- 1 Feature Extraction: compute the features.
- 2 Feature Selection: apply the proposed feature selection methods based on method called FS\_MRMR\_SVMRFE algorithm to choose the best subset of relevant features.
- 3 SVM Classifier: Classification method Support Vector Machines (SVM) is used to evaluate the proposed approach.

### 3.1 Feature Extraction

The first stage of disease classification schemes is the feature extraction. The number of features selected for breast cancer Wisconsin includes ten features and class label (two classes: benign-malign). Hepatitis dataset was used considering twenty features including class.

### 3.2 Feature Selection

The second stage is feature selection. The features were used from hepatitis data (twenty features including class: live-death) from UCI repository and breast cancer Wisconsin (ten features including class: malign-benign).

We propose a features selection algorithm Fisher score and Maximum relevance minimum redundancy FS\_MRMR\_SVM and evaluated on support vector machines SVM classifier. We describe the main phases below:

#### Filter Stage

Fisher's ratio is univariate filter method evaluating each feature individually, where mRMR [2] is a method based on evaluating mutual information and searching the relevant features to the target class and achieving minimal redundancy with other set of features. mRMR method provides features that have a less correlation with each other. Each filter method provides a subset of features  $S_{FS}$  from ficher score and  $S_{mRMR}$  from mRMR method. These two group of features  $S_{FS}$  and  $S_{mRMR}$  are compared to have the best common features selected.

#### Features Selection Criteria

Assume  $S_i$  and  $S_0$  denote feature subsets selected using different filter methods, respectively.

$K$  is the cardinality of  $S_i$  and  $S_0$

The final subset between these two features subsets can be measured using the first  $M$  ( $M < K$ ) equal features.

$S_i \cap S_0$  is the number of common features between  $S_i$  and  $S_0$ .

In this study,  $S_i = S\_FS$  and  $S_0 = S\_mRMR$ .

### **SVM-RFE algorithm**

SVM-RFE is a FS method that uses SVM weights as the ranking criterion of features. The previous resulted subset is used as input for SVMRFE method. It has four steps:

1. Input all features except  $S\_FS \cap S\_MRMR$ .
2. Train a Support Vector Machines on the full training set;
3. Order features using the weights of the resulting classifier;
4. Eliminate features with the smallest weight (lowest rank);
5. Repeat the process with the training set limited to the remaining features.

---

#### **Algorithm FS\_MRMR\_SVMRFE**

---

##### **Input**

All feature  $F_1, F_2, \dots, F_{max}$

##### **Output**

BestSb: Best Subset of features:  $S_{final}$

---

1. Initialize the training dataset from hepatitis and breast cancer Wisconsin.
2. Rank the features by mRMR filter method to have  $S\_mrmr$ .
3. Rank the features with fisher score which provide features scores  $S\_fscore$ , then ranked them.
4. Calculate the common features between these two methods individually.  
 $S_1 = S\_mrmr \cap S\_fscore$ .
5. Apply Support vector machine Recursive feature elimination SVMRFE to test  $F_1, F_2, \dots, F_{max}$  except  $S_1$  with SVMRFE to get the second subset  $S_2$  with classifier and remove the worst features.  
Final subset  $S_{final} = S_1 \cup S_2$ .
6. Design training strategy using a support vector machines as classifiers for the recognition of disease type.

### **3.3 SVM Classifier**

Support Vector machine is a powerful machine learning technique that uses kernel to construct linear classification boundaries in higher dimensional space [6, 22]. SVMs have a good generalization performance in various applications. Different kernels were used (RBF radial basis function, polynomial and linear).

## **4 Experimental Results**

In this section, we first describe the experimental settings, and then compare our feature selection method FS\_mRMR\_SVMRFE with three feature selection algorithms regarding the effectiveness. SVMRFE, mRMR, fisher score were applied with SVM Classifier.

SVM classifier with Matlab is used in our experiments, to evaluate the predictive accuracy on the selected feature subset with 10-fold Cross-Validation. The parameters of classifiers are set to default values. In the following, we compare several feature ranking algorithms.

#### 4.1 Databases

We have used two dataset Wisconsin Breast cancer Dataset WBCD taken from UCI machine learning repository and hepatitis dataset in our experiments.

The Wisconsin Breast Cancer Dataset [23] WDBC datasets contains 683 samples taken from needle aspirates from human breast cancer tissue. It consists of nine features, each of which is represented as integer between 1 and 10.

Hepatitis database from UCI [23] was used. It contains twenty features including class attribute. The numbers of samples are 155. The features are: Class(DIE, LIVE), Age, Sex, Steroid, Antivirals, Fatigue, Malaise, Anorexia, Liver Big, Liver Firm, Spleen, Palpable, Spiders, Ascites, Varices, Bilirubin, Alk, Phosphate, Sgot, Albumin, Protime, Histology.

### 5 Discussion

Different filters ranking methods provide different subset of features like fisher score and MRMR did. These results present benefits for choosing the complementary features that interact differently on classifier (Tables 1 and 2).

SVMRFE method provides a different subset of ranked features than fisher score like shown in Tables 3 and 4. SVMRFE method achieves better accuracy than fisher score for 11 features when fscore is better for 8 features. The results on

**Table 1** Advantage and drawbacks of feature selection methods

Feature selection methods	Advantages	Drawbacks
Filters Ranking [1]	Simple and fast	Do not account redundancy among features. Independent from the classifier
Wrappers [10]	Achieve higher classification accuracies. Apply a specific machine learning algorithm to guide the selection of features	Time consuming methods
Embedded [14]	Higher classification accuracy. Apply both classifier and filter techniques	Time consuming methods but less than wrappers

**Table 2** Works on feature selection methods

Works	Methods	Databases
[3]	Mutual information-based feature selection method	DDSM mammographic database
[8]	Hybrid approach by correlation-based filters and Support Vector Machine—Recursive Feature Elimination (SVM-RFE)	UCI and microarray data sets
[17]	Various wrapper and filter techniques for reducing the feature dimension of pairwise scoring matrices	Evaluations on a subcellular localization benchmark and a microarray dataset
[18]	Multiple SVM-RFE, where the SVM was trained on multiple subsets of data. SVM-RFE (Correlation) outperformed SVM-RFE (mRMR) in terms of classification accuracy	Gene expression based cancer classification
[19]	Two-stage SVM-RFE algorithm	Gene data
[20]	mRMR and ReliefF algorithms	Gene data
[21]	Receiver Operating characteristics curves (ROC) is used to characterize the performance of the individual feature and the subset of features in the classification	Biomedical datasets

**Table 3** Hepatitis dataset with SVMRFE method

Number of features	SVM classifier accuracy (%)	Selected features
8	75.00	5-14-9-17-7-6-10-15
11	93.75	15-18-6-9-4-16-10-3-17-8-7

**Table 4** Hepatitis dataset with Fisher score method

Number of features	Accuracy (%)	Selected features
8	87.50	12-14-17-18-13-19-11-6
11	75.00	12-14-17-18-13-19-11-6-1-15-2

WDBC indicate clearly that SVMRFE method is more accurate than fisher score like shown in Tables 5 and 6.

Additional features might be noisy. It was observed that classification accuracy decreases like shown in Table 4 with Fischer score from 8 to 11 features on Hepatitis dataset.

Tables 7 and 8 demonstrate that the accuracy on two dataset WDBC and Hepatitis is respectively better 99.89 % with 11 features and 97.81 % with 8 features than other methods (fisher score, mRMR, Svmrfe). We conclude that combining Maximum Relevance Minimum Redundancy mRMR (select the features that minimizes redundancy and maximizes relevance) and Fisher score in first stage and then compute the common features contribute in better classification accuracy.

**Table 5** Breast cancer Wisconsin dataset with Fisher score method

Number of features	SVM classifier accuracy (%)
5	97.79
6	97.06
7	97.06
8	97.79
9	98.53

**Table 6** Breast cancer Wisconsin dataset with SVMRFE method

Number of features	SVM classifier accuracy (%)
6	98.52
7	98.52
8	97.79
9	97.79

**Table 7** SVM classifier accuracy on different feature selection methods: Hepatitis dataset

Methods	#features	Accuracy%
Proposed method	11	99.89
Fisher score		75.00
mRMR		81.25
SVMRFE		93.75

**Table 8** SVM classifier accuracy on different feature selection methods: WDBC dataset

Methods	#features	Accuracy%
Proposed method	8	97.81
Fisher score		97.79
mRMR		97.05
SVMRFE		97.80

In the second stage, applying Support Vector Machine Recursive Feature Elimination SVMFE for additional feature leads to preserve the relevant features that are ignored by the first stage and keep the most relevant one. The union of subsets provided by these two stages (Table 7 with 11 features) achieves better accuracy (Table 7: Accuracy = 99.89 %) than each method applied separately.

Table 9 indicates that the result from the first stage (Fscore and mRMR) achieves with six features 95.58 % of accuracy, the performance is improved in the second stage with 97.81 %.

**Table 9** Breast cancer Wisconsin dataset with proposed method

Number of features	SVM classifier accuracy (%)	List of features
First stage = 5 intersect (Fscore and mRMR)	95.58	8-3-7-9-4-5
Second stage = 7 with SVMRFE	97.81	2-6
Final list of features	97.81	8-3-7-9-4-5-2-6



## 6 Conclusion

The Fisher score and SVMRFE algorithms provide different subsets of best features and keeping only one of them is not an appropriate approach. The proposed feature selection approach provide the final subset of features obtained by fusion of best common features from filter ranking methods and the best ranked features with SVMRFE achieves better performance than each method taken separately with the SVM classifier. The two stage feature selection scheme is more accurate for disease classification compared to the other methods.

## References

1. Saeys, Y., Inza, I., Larranaga, P.: A review of feature selection technique in bioinformatics. *J. Bioinform. Oxford university press*, 1–10 (2005)
2. Ding, C., Peng, H., Long, F., Ding, C.: Feature selection based on mutual information: criteria of max-dependency, max-relevance, and min-redundancy. *IEEE Trans. Pattern Anal. Mach. Intell.* **27**(8) (2005)
3. Yoon, S., Kim, S.: Mutual information-based SVM-RFE for diagnostic classification of digitized mammograms. *J. Pattern Recognit. Lett.* **30**, 1489–1495 (2009)
4. Mitra, S., Shankar, B.U.: Medical image analysis for cancer management in natural computing framework. *Inf. Sci.* **306**, 111–131 (2015)
5. Yang, F., Mao, K.Z.: Robust feature for microacray data based on multicriterion fusion. *IEEE/ACM trans. Comput. Biol. Bioinform.* **8**(4), 1080–1092 (2011).
6. Akay, M.F.: Support vector machines combined with feature selection for breast cancer diagnosis. *J. Expert Syst. Appl.* **36**, 3240–3247 (2009)
7. Yang, P., Bing B., Zhou, J.Y., Yang, A., Zomaya, Y.: Stability of feature selection algorithms and ensemble feature selection methods in bioinformatics, pp. 1–23 (2006).
8. Zhang, J., Hu, X., Li, P., He, W., Zhang H.Y.: A hybrid feature selection approach by correlation based filters and svm-rfe. In: *International Conference on Pattern Recognition*, 3684–3689 (2014).
9. Guyon, J., Weston, S., Barnhill, S., Vapnik, V.: Gene selection for cancer classification using support vector machines. *Mach. Learn.* **46**(1–3), 389–422 (2002)
10. Bolon Canedo, V., Sanchez Maono, N., Betanzos, A.: A review of feature selection methods on synthetic data. *J. knowl. Inform. Syst.* **34**, 483–519 (2013).
11. Jirapech Umpai T., Aitken. S.: Feature selection and classification for microarray data analysis: Evolutionary methods for identifying predictive genes. *BMC Bioinform.* **6**(1), 148 (2005)
12. Li, L., Weinberg, C.R., Darden, T.A., Pedersen, L.G.: Gene selection for sample classification based on gene expression data: study of sensitivity to choice of parameters of the ga/knn method. *Bioinform.* **17**(12), 1131–1142 (2001)
13. Umbach, D.M., Li L., Terry, P., Taylor. J. A.: Application of the ga/knn method to seldi proteomics data. *Bioinform.* **20**(10) (2004)
14. Yan, K., Zhang, D.: Feature selection and analysis on correlated gas sensor data with recursive feature elimination. *J. Sens. actuators B chem.* 353–363 (2015).
15. Piyushkumar A.M., Rajapakse, J.C.: SVM-RFE with mrmr filter for gene selection, *IEEE Trans. Nanobioscience* **9**(1) (2010)

16. Heath, M., Bowyer, K., Kopans, D., Moore, R., Kegelmeyer, W.: The digital database for screening mammography. In: Yaffe, M. (ed.), *Proceeding 5th IWDM*. Medical Physics Publishing, pp. 212–218 (2001).
17. Maka, M.W., Kung, S.Y.: Fusion of feature selection methods for pairwise scoring SVM. *Neurocomputing* **71**, 3104–3113 (2008)
18. Kai-Bo D., Rajapakse, H., Wang H., Azuaje F.: Multiple SVM-RFE for gene selection in cancer classification with expression data. *IEEE Trans. Nanobioscience* **4**(3), 228–234 (2005).
19. Tang, Y.C., Zhang Y.Q., Huang, Z.: Development of two stage SVMRFE Gene selection strategy for microarray expression data analysis. *IEEE ACM. Trans. Comput. Biol. Bioinform.* **4**(3), 365–381 (2007).
20. Zhang, Y., Ding, C., Li, T.: Gene selection algorithm by combining relief and mRMR. *BMC Genom.* **9**(2), S27 (2008)
21. Peng, Y., Wu, Z., Jiang, J.: A novel feature selection approach for biomedical data classification. *J. Biomed. Inform.* **43**, 15–23 (2010)
22. Vapnick, V.: *Statistical learning theory*, Wiley (1998)
23. <https://archive.ics.uci.edu/ml/datasets.html>

# A Formal Approach for Maintainability and Availability Assessment Using Probabilistic Model Checking

Abdelhakim Baouya, Djamel Bennouar, Otmame Ait Mohamed and Samir Ouchani

**Abstract** Availability is one of the crucial characteristics that measures the system quality and influences the users and system designers. The aim of this work is to provide an approach to improve the system availability by taking into account different system situations at design step using SysML state machine diagram. We construct a formal model of state machine in the probabilistic calculus which supports modeling of concurrency and uncertainty. In this paper, we consider a single industrial control equipment and a multiprocessing computing platform where its behavior is modeled by SysML state machine diagram and we use logical specification of maintainability and availability properties. The probabilistic model checker PRISM has been used to perform quantitative analyses of these properties.

**Keywords** SysML state machine diagram · Reliability · Availability · Maintainability

## 1 Introduction

Constraints on system design in terms of reliability, availability and maintainability are becoming more stringent. For critical systems, availability constraints are having an increasing influence on the design and maintenance cost. It is necessary today, to

---

A. Baouya (✉)  
LIMPAF Lab, CS Department, University of Blida, Blida 1, Blida, Algeria  
e-mail: baouya.abdelhakim@gmail.com

D. Bennouar  
LIMPAF Lab, CS Department, University of Bouira, Bouira, Algeria  
e-mail: dbennouar@gmail.com

O.A. Mohamed  
ECE Department, Concordia University, Montreal, Canada  
e-mail: otmane.aitmohamed@concordia.ca

S. Ouchani  
SnT Center, University of Luxembourg, Luxembourg City, Luxembourg  
e-mail: samir.ouchani@uni.lu

take efficiently these constraints into consideration during the design process to reach a compliant solution. Thus, the evaluation and the prediction of system’s behavior at early stage of design is beneficial to handle time and effort.

The concept of reliability is quantifiable and suitable to describe the behavior in time of repairable systems according to the historical statistics [10], whereas, availability can be defined as the ratio of delivered service under given conditions at a stated instant of time [4]. Maintainability can be described as the ability of the system to be restored to a specified state following a failure [4]. The reliability functions are discussed in numerous publications [18, 20, 24] and we can state that the most approaches rely on the application of *Markov processes*. However, the quantification becomes complex when the number of system states is large [10]. Recently, the automated approaches such as Model Checking [5, 7, 21, 23] are used frequently for these purposes.

The *Model checking* [13] is a formal technique used to verify systems whose behavior is unpredictable, especially stochastic in nature. The technique consists on the exploration of every possible system behavior to check automatically that the specifications are satisfied. The verification can be focused on either qualitative or quantitative properties [1]. Quantitative properties puts the constraints on a certain event, e.g. the probability of processor failure in the next 3 h is at a least 0.88, while qualitative properties assert that certain event will happen surely (i.e. Probability = 1).

In this paper, we are interested in the formal verification of probabilistic systems modeled as SysML state machine diagram. The overview of our framework is depicted in Fig. 1. It takes State machine diagrams as input and constructs a formal model of state machine in the probabilistic calculus which supports modeling of concurrency and uncertainty. After that, we encode our model in language of the PRISM symbolic probabilistic model checker [15]. Commercial tools for reliability prediction, such as Lambda Predict [26], cannot be used to estimate the performance at the required moment as they do not support reward modeling (i.e. cost). However,

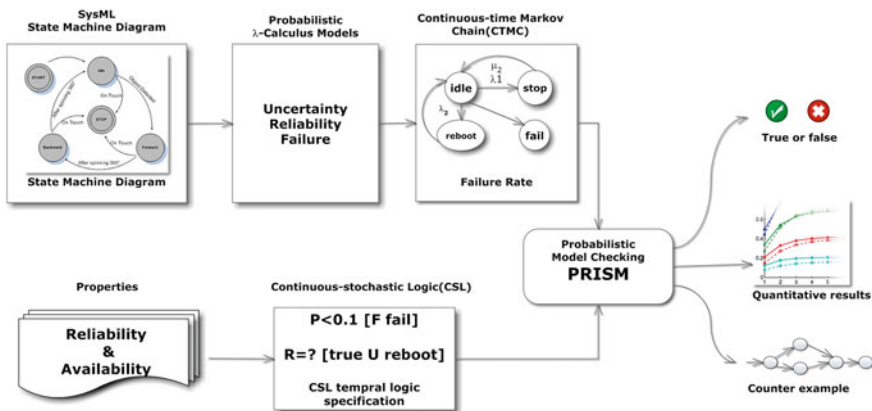


Fig. 1 A SysML State machine diagram verification approach

the probabilistic model checker PRISM overcomes this limitation. We analyze the logical properties expressed in Continuous-stochastic logic (CSL) [28] to check the system availability and maintainability.

The remainder of this paper is structured as follows: Sect. 2 discusses the related work. We recall the system life cycle states in Sect. 3. Section 4 describes SysML state machine diagram and its operational semantics. PRISM Model Checker is presented in Sect. 6. Section 7 illustrates the application of our mapping rules on case study for availability and maintainability assessment. Section 8 draws conclusions and lays out the future works.

## 2 Related Work

There are a numerous attempts to use formal methods to address the problems of design behavior prediction especially in automotive systems [6], industrial process control [10] and avionic navigation [17, 29]. Dhouibi et al. [6] presented a safety-based approach for system architecture optimization. The approach is based on Genetic Algorithm [27] for best components allocations. However the specification is not explained and the algorithm is time consuming. Huang et al. [12] proposed a verification of SysML State Machine Diagram by extending the model with MARTE [19] features to express the execution time. The tool has as input the State Machine Diagram and as output timed automata expressed in UPPAAL syntax [3]. UPPAAL uses Computational Tree Logic (CTL) properties to check if the model is satisfied with respect to liveness and safety properties. Morant et al. [20] proposed a Markov representation of availability and failure according to the statistical observations. However, the analysis did not refer to any relation between reliability and availability for safety interpretation. Nevertheless, Lu et al. [18] constructed a formal model of GNSS based positioning system directly in the probabilistic Pi-calculus that supports concurrency and uncertainty which is directly mapped to PRISM language for availability interpretation. Qiu et al. [25] used UML state chart with failure rates to evaluate the availability of systems where the approach is based on simulation method. However, the mapping rules and simulation tool are not clearly described in the paper. Liu et al. [17] used Architecture Analysis and Design Language (AADL) to describe the system architecture and used Error Model Annex (i.e. textual representation of state transitions) with the Risk-based Failure Mode Effect Analysis (RFMEA) property to express error effects. The developed plug-in extracts a set of measures for quantitative assessments. However, the authors restricted themselves to the generation of a set of failure rates only.

Compared to the existing works, our work maps a standard behavioral diagram called SysML State Machine into PRISM code. In addition, We construct a formal model of state machine in the probabilistic calculus which supports modeling of concurrency and uncertainty. Our goal is to adopt probabilistic model checking for system availability and maintainability assessment on the basis of the system reliability and the failure rate of its components. Table 1 highlights the comparison of our work with the existing approaches.

**Table 1** Comparison with the existing approaches

Paper	SysML	Approach	Formalization	Automation
[6]		Genetic algorithm		√
[12]	√	Model checking		√
[10]		Analytic		
[20]		Analytic		
[18]		Model checking	√	√
Our	√	Model checking	√	√

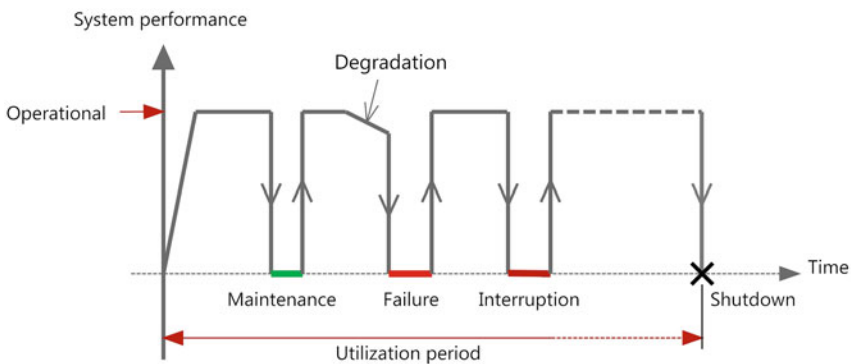
### 3 System Life-Cycle

As shown in Fig. 2, system life-cycle is a final loop that begins from execution to the shutdown and includes four states [10]; operational, failure, interruption (i.e. Accident) and maintenance. Three types of stops are considered: stop 1 after preventive maintenance, stop 2 after failure and stop 3 after an interruption:

- Stop 1 or maintenance time is the necessary time to perform the preventive maintenance represented by mean time to maintenance (MTTM).
- Stop 2 or repairing time is the time required to repair the system after breakdown represented by mean time to repair (MTTR).
- Stop 3 or preparing time is the time to restore the system to the operating state after an interruption represented by mean time to preparing (MTTP).

Availability therefore, is the probability for the system to function correctly at the required moment [16], the basic definition is:

$$Availability = \frac{Operational\ time}{Total\ utilization\ period}$$



**Fig. 2** System life-cycle [10]

In our case, availability is computed using CSL temporal logic in Sect. 7. Moreover, we adopt the following indicators cited in [10] to assess availability:

- MTBF: Mean Time Between Failures is the mean time between two consecutive failures.
- MTBM: Mean Time Between Maintenance is the mean time between two preventive maintenance.
- MTBI: Mean Time Between Interruptions (i.e. Accident) is the mean time between two interruptions.

## 4 SysML State Machine Diagram

SysML State Machine diagram (SMD) is a graph-based diagram to describe state-dependent behavior [22]. Table 2 shows the sub set of interesting artifacts used for verification in this paper and its corresponding algebraic expression and PRISM commands. A behavior starts (resp. stops) executing when its initial (resp. final) pseudo-state becomes active. We note that state behavior (i.e. do, entry and exit) are ignored in this paper. Transitions are defined by triggers and guards. The trigger (i.e. events) causes a transition from the source state when the guard is valid. In addition, the control node supports junction, choice, join, fork and terminate. A junction splits an incoming transition into multiple outgoing transitions and realizes a static conditional branch, as opposed to a choice pseudo-state which realizes a dynamic conditional branch. To illustrate how a rate value is specified, the transition leaving choice nodes are annotated with the  $\ll\textit{rate}\gg$  stereotype. We present in Definition 1, the formal definition of SysML state machine diagrams that embed the rate function.

**Definition 1** State machine diagrams is a tuple  $S = (i, \textit{fin}, \mathcal{N}, E, \textit{Rate})$ , where:

- $i$  is the initial node,
- $\textit{fin} = \{\odot, \times\}$  is the set of final nodes,
- $\mathcal{N}$  is a finite set of state machine nodes,
- $E$  is a set of events (i.e. triggers),
- $\textit{Rate}: (\{i\} \cup \mathcal{N}) \times E \times (\textit{fin} \cup \mathcal{N}) \rightarrow \mathbb{R}_{\geq 0}$  is a rate function assigning for each transition from  $(\{i\} \cup \mathcal{N})$  to  $(\textit{fin} \cup \mathcal{N})$  and  $\alpha \in E$  a positive real value  $\lambda$ .

## 5 State Machine Syntax

We formalize state machine diagrams by developing a calculus where its terms are presented in Table 2 according to the graphical notation defined in the standard. Using this calculus, a marked term is typically used to denote a reachable configuration, whereas, the unmarked term corresponds to the static structure of the diagram.

**Table 2** Formal notation of SysML state machine diagram artifacts



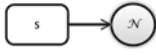
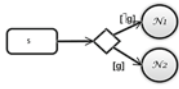

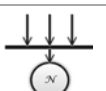
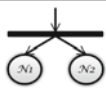
Artifacts	Formal notation	PRISM representation
	$l : i \mapsto \mathcal{N}$	$\square Initial \rightarrow (Initial' = false) \& (\mathcal{N}' = true);$
	$l : \odot$	$\square Final \rightarrow (Final' = false) \& \dots \& (\mathcal{N}'_i = true);$
	$l : s \mapsto \mathcal{N}$	$\square S \rightarrow (S' = false) \& (\mathcal{N}' = true);$
	$l : D(\lambda_1, g, \mathcal{N}_1, \lambda_2, \mathcal{N}_2)$	$\begin{aligned} [l_{g_1}] g_1 \rightarrow \lambda_1 : (l'_g = false) \& (\mathcal{N}'_1 = true); \\ [l_{g_2}] g_2 \rightarrow \lambda_2 : (l'_m = false) \& (\mathcal{N}'_2 = true); \end{aligned}$
	$l : M(x) \mapsto \mathcal{N}$	$\begin{aligned} \square l_{x_1} \rightarrow (l'_{x_1} = false) \& (M'_x = true); \\ \square l_{x_2} \rightarrow (l'_{x_2} = false) \& (M'_x = true); \\ \square M_x \rightarrow (M'_x = false) \& (\mathcal{N}' = true); \end{aligned}$
	$l : J(x) \mapsto \mathcal{N}$	$\square l_{x_1} \& l_{x_2} \rightarrow (l'_{x_1} = false) \& (l'_{x_2} = false) \& (\mathcal{N}' = true);$
	$l : F(\mathcal{N}_1, \mathcal{N}_2)$	$\square Fork \rightarrow (Fork' = false) \& (\mathcal{N}'_1 = true) \& (\mathcal{N}'_2 = true);$

Figure 3 shows the formal operational semantic based on our state machine calculus terms presented in Table 2 that are part of [2]. To support tokens we augment the “Over bar” operator with integer value  $n$  such that the  $\overline{\mathcal{N}}^n$  denotes the term  $\mathcal{N}$  marked with  $n$  tokens. Furthermore, we use a prefix label  $l$  for each node to uniquely reference it in the case of a backward flow connection. Let  $\mathcal{L}$  be a collection of labels ranged over by  $l; l_0; l_1, \dots$  and  $\mathcal{N}$  be any node (except initial) in the state machine.

$$\text{INIT } l : i \mapsto \mathcal{N} \xrightarrow{l_1} l : \bar{i} \mapsto \mathcal{N}, \text{ PRG-1 } l : \bar{i} \mapsto \mathcal{N} \xrightarrow{l_1} l : i \mapsto \overline{\mathcal{N}}$$

$$\text{FORK } l : \overline{F(\mathcal{N}_1, \mathcal{N}_2)}^n \xrightarrow{l_1} l : \overline{F(\overline{\mathcal{N}}_1, \overline{\mathcal{N}}_2)}^{n-1}, \text{ JOIN } l : \overline{\mathcal{N}} \mapsto l' : J(x, y) \xrightarrow{l_1} l : \overline{\mathcal{N}} \mapsto l' : J(\overline{x}, \overline{y})^n$$

$$\text{CHOICE } l : \overline{D(\lambda_1, g, \mathcal{N}_1, \lambda_2, \mathcal{N}_2)}^n \xrightarrow{g}_{\lambda_1} l : \overline{D(g, \overline{\mathcal{N}}_1, \mathcal{N}_2)}^{n-1}, \text{ FINAL } S[l : \odot] \xrightarrow{l} |S|$$

$$\text{JUNCTION } l' : \overline{\mathcal{N}} \mapsto M(x, g_1, \mathcal{N}_1, y, g_2, \mathcal{N}_2) \xrightarrow{l} l : \overline{\mathcal{N}} \mapsto l' : M(\overline{x}, g_1, \overline{\mathcal{N}}_1, y, g_2, \overline{\mathcal{N}}_2)^n$$

**Fig. 3** A symbolic semantic of State Machine Calculus



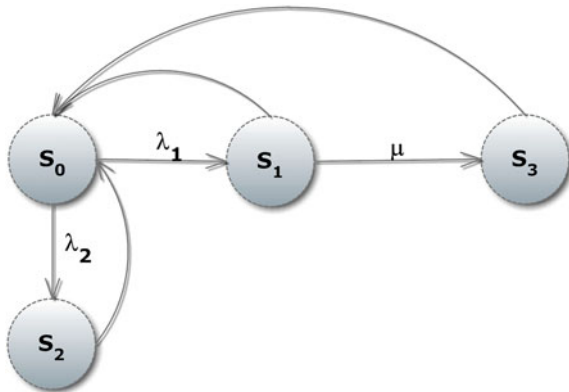
## 6 The PRISM Model Checker

In this paper, we use PRISM probabilistic model checker [14]. It supports the analysis type of probabilistic models: Discrete-time Markov chains (DTMC), Continuous-time Markov chains (CTMC), Markov decision process (MDP). Moreover, PRISM allows us to verify properties specified in PCTL [9] and CSL [28] temporal logic.

In this paper, we focus on Continuous-Time Markov chains (CTMCs) in reliability and availability analysis, such that [11, 15]. A CTMC involves a set of states  $S$  and a transition rate matrix  $\mathbf{R}: S \times S \rightarrow \mathbb{R}_{\geq 0}$ . The delay before which a transition between states  $s$  and  $s'$  is specified by the rate  $\mathbf{R}(s, s')$ . The probability that a transition between state  $s$  and  $s'$  might take place within time  $t$  is given by  $1 - e^{-\mathbf{R}(s,s') \times t}$  which matches the SysML state machine diagram semantics (Sect. 4). We define each transition from  $s$  to  $s'$  in PRISM as one command as shown in Fig. 6. The global state of model is derived from the state of individual value of command variables. The guard  $s0 = \text{true}$  indicates that command is only executed when variable  $s0$  is true. The update  $(s1' = \text{true}) \ \& \ (s0' = \text{false})$  and their associated rate indicate that the value of  $s0$  will change to false and  $s1$  will change to true with rate “ $\lambda_1$ ”. In CTMC, when multiple possible transitions are available in a state, a race condition occurs [13] and this can arise in several ways. Firstly, within a module, multiple transitions can be specified either as several different updates in a command, or as multiple commands with overlapping guards.

Lets assume that we have a system for satellite error detection capability. The Markov model of such a system as shown in Fig. 4, can be build with four states ( $s_0$ : Operational,  $s_1$ : Fault detected,  $s_2$ : Interruption detected,  $s_3$ : Satellite replacement and Launch) representing the satellite status. The failure rates  $\lambda_1, \lambda_2$  are constant between states where  $\mu = 1/24$ , 24h is the time to decide to build a new satellite (i.e. Mean Time To Repair). This system can be described using PRISM modeling language as shown in Fig. 6.

**Fig. 4** A simple Markov chain to illustrate the failure occurrence



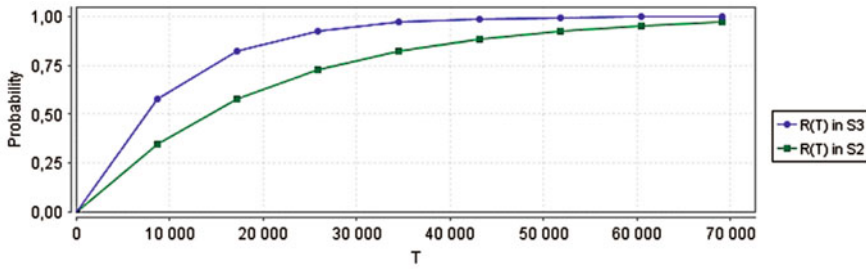


Fig. 5 Reliability versus time

Fig. 6 Sample PRISM code

```

module satellite
s0 :bool init true;
s1 :bool init false;
s2 :bool init false;
s3 :bool init false;
[] (s0=true) → lambda_1:(s1'=true) & (s0'=false);
[] (s1=true) → mu:(s3'=true)&(s1'=false);
[] (s0=true) → lambda_2: (s0'=false) &(s2'=true);
endmodule
    
```

In order to perform model-checking, a property should be specified in Continuous stochastic logic (CSL). For example, CSL allows the expression of logical states such as “what is the expected reward cumulated up to time-instant  $t$  for a computer to reboot”  $R_{\Rightarrow}[C^{\leq t}]$ , where “reboot” labels the reward construct in PRISM or “what is the probability of an error occurring within  $T$  time steps”:  $P_{<0.1}[F \leq 10(s3 = true)]$ ; the property is true in a state  $s3$  of the Markov chain if the set of paths that start from  $s0$  and reach the state  $s3$  in the first 10 times units has a probability of at least 0.1.

In our study, we use rewards (i.e. state Cost) to calculate the expected time ‘ $T$ ’ for maintenance with respect to the CSL property. PRISM can be augmented with rewards: real values associated with states and transitions of the model [14]. For example, the cost of visiting the state “ $s2 = true$ ” is equal to 1. Rewards are associated with models using the rewards construct:

**rewards** “maintainability”

$S2 = true: 1;$

**endrewards**

For the Markov chain in Fig. 4, if  $\lambda_1 = 0.0001$  and  $\lambda_2 = 0.00005$ , then the reliability function of that Markov model can be generated using PRISM as displayed in Fig. 5. The reliability is obtained by checking the model against the property: “the probability that a satellite will need to be replaced by a new one due to complete failure in 8 years” and expressed using CSL as  $P = ?[F^{\leq T} s3]; T = 0:70656:8640$  (Figs. 6 and 7).

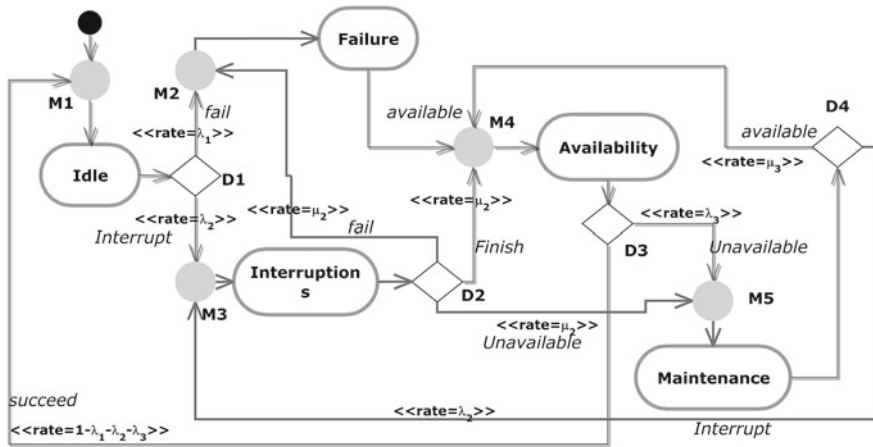


Fig. 7 A failure model and maintainability plan [10]

## 7 Case Study for Availability Assessment

### 7.1 Case Study 1: Industrial Process Control

In the following, we present a case study [10] (Fig. 7) describing an industrial control equipment consisting of printing system which is a complex line including 11 machines which are: an uncurlor, a debtor, 4 printing units, a wipe-catcher system, a dryer, a cooler, a paper passage an folding machine. From the designer’s point of view, the high degree of automation machines makes it possible to have a reduced human intervention on the machine utilization with availability equal to 100 %. The essential role of users is to supervise the working of the machine, except the beginning settings of impression and charging row material. However, the observations at user site show that system is rarely in nominal mode of operation. It is available for about 60 % of its use time. We have observed some events as failures, interruptions, preventive maintenances. Taking into account the production type (process shop), it is very important to note that if any machine of the printing system is stopped, all production will stop. So, the company applied a preventive maintenance. Three types of stop are observed: (1) Stops caused by the preventive maintenance which is the most happening and it is represented by state “maintenance”, (2) Stops caused by failure and it is represented by state “Failure”, in spite of preventive maintenance, we observed some stops caused by failure due to raw material and consumable types (ink, solvent, etc.) used in the process, (3) Stops caused by interruptions (i.e. Accidents), in particularly, at the system setting up and it is represented by state “Interruption”. To assure production continuity user intervenes some times on operating system to replace a failing component which is an undesirable behavior (Figs. 8 and 9).

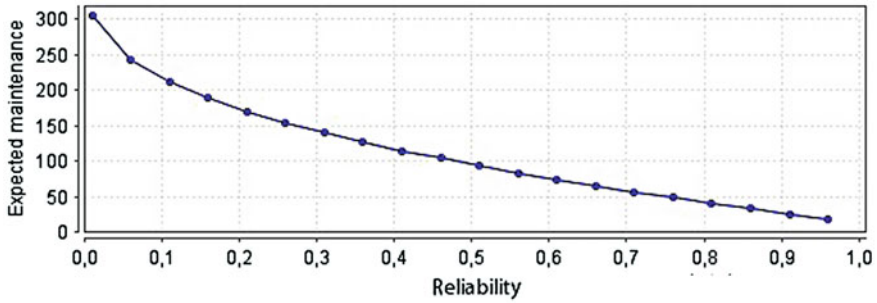


Fig. 8 Maintenance versus reliability

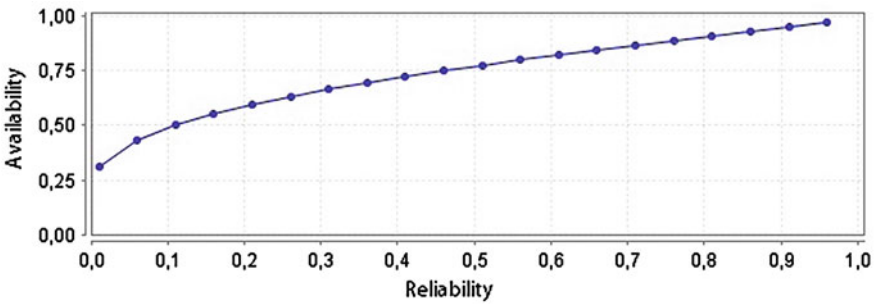


Fig. 9 Availability versus reliability

Table 3 Parameters for the CTMC model and analyses—case study 1

R	$\frac{R}{\lambda_1} = MTBF$	$\lambda_3 = \frac{1}{MTBM}$	$\lambda_2 = \frac{1}{MTBA}$	$\mu_1 = \frac{1}{MTR}$	$\mu_3 = \frac{1}{MTM}$	$\mu_2 = \frac{1}{MTP}$
90 %	3600 s	40 %	5 %	90 %	90 %	90 %

For system analysis, operations related to failures, maintenances, interruptions (i.e. Accidents), repairing and preparing were collected and presented in Table 3. we use R to express the reliability of the designed system. If the system fails, we say that the system moves from normal state (i.e. Idle) to failure state. Taking into account system life cycle aspects, the indicators required to assess availability and maintainability at design stage are described in Sect. 3.

We assume that the time delay is a random variable selected from an exponential distribution, which is an assumption used in PRISM. according to the system reliability theory, the reliability of a system from  $R(t)$  can be defined as

$$R(t) = Pr\{T > t\} = e^{-\lambda t} \tag{1}$$

and, then we can obtain

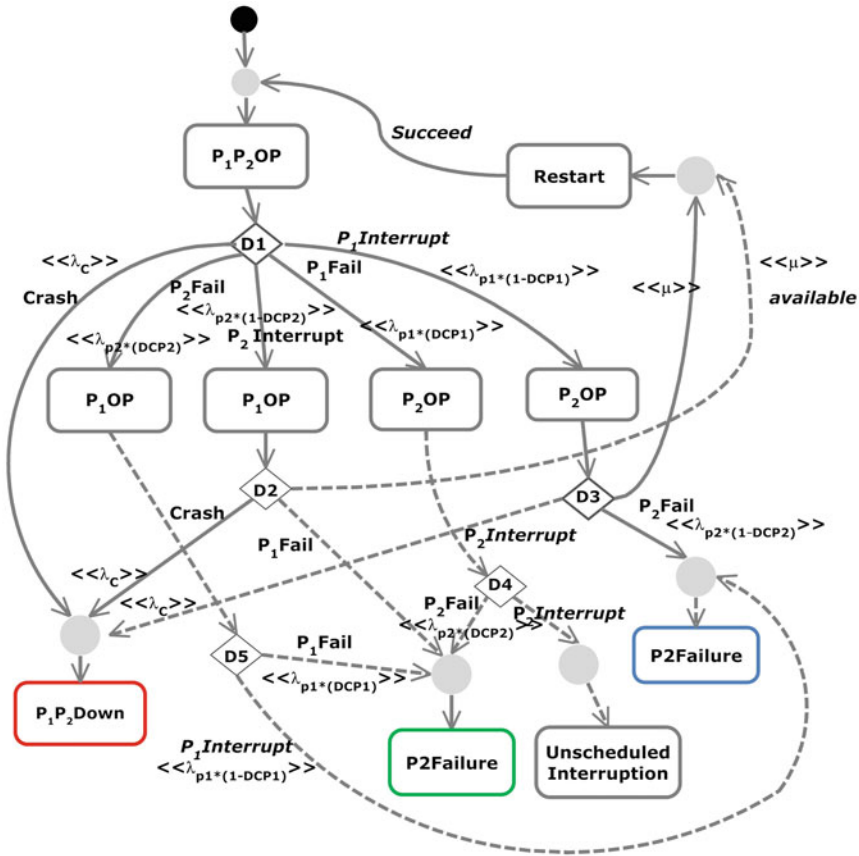


Fig. 10 A failure model of computing platform

$$\lambda(t) = \frac{-\ln R(t)}{MTBF} \tag{2}$$

Failures typically occur at some constant failure rate  $\lambda$ , failure probability depends on the rate  $\lambda$  and the exposure time  $t$ . Typically failure rate are carefully derived from substantiated historical data [10].

PRISM provides support for automated analysis of quantitative properties. In case of our system two properties are analyzed for (1) maintainability and (2) availability assessment:

1. The system maintenance times when the reliability ranges from 0.01 to 0.99 in 3600 s:  $R\{maintenance\}_{= ?}[C \leq T]; T = 3600, R = 0.01 : 0.99 : 0.01$ ;
2. The availability of system in 3600 s when the reliability ranges from 0.01 to 0.99:  $R\{availability\}_{= ?}[C \leq T]/T; T = 3600, R = 0.01 : 0.99 : 0.01$ ;

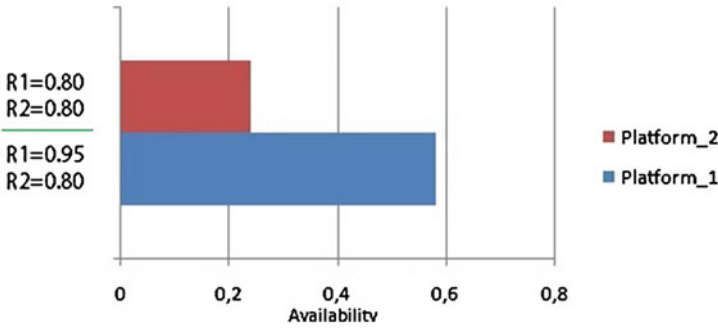


Fig. 11 Availability versus platform reliability

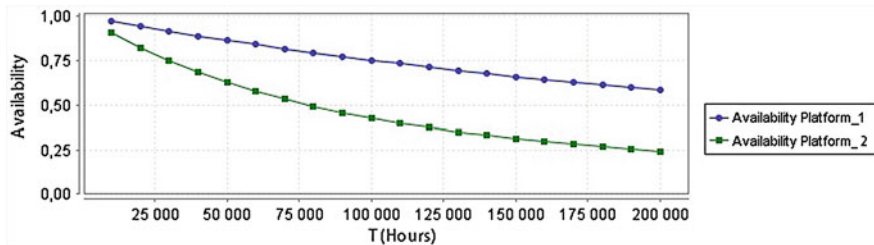


Fig. 12 Availability versus time

As shown in Fig. 11, when the reliability of of the dual core is 0.95 in *platform*<sub>1</sub> the availability is equal to 0.528 however, for the *platform*<sub>2</sub> when reliability is equal to 0.80 the availability is very low and equal to 0.247. As shown in Fig. 12, if the time increases the availability decreases from 0.97 to 0.58 for the first platform and decreases from 0.9 to 0.24 for the second platform. So, it is obvious that the availability decreases in time due to the processors performance degradation but it is clear that the first platform offers more performance than the second one due to the high reliability. For high availability, designer could assume the reliability  $\geq 95\%$ . Nevertheless, the verification of the first property is sufficient to attest that the architecture of the first platform offers more performance than the second one.

### 7.2 Case Study 2: Computing Platform

In this case study we expect a better architectural platform based on availability assessment. The platform consists on two parallel processors P1 and P2. Two kind of configuration platform are checked where the firsts one; the processor P1 is dual-core and the second architecture; the processor is single core. The case study is well detailed in [8] but in our paper it is modeled using SysML. We try to summarize the failure observations data in Table 4 to enrich our state machine diagram in Fig. 10

**Table 4** Parameters for the CTMC model and analyses—case study 2

Platform	$R_{P1}$	$R_{P2}$	$DC_{p1}$ (%)	$DC_{p2}$ (%)	$\lambda_{crash}$	$\mu_{repair}$
1	0.95	0.80	99	60	$200 \times 10^{-9}$	1/24
2	0.80	0.80	99	60	$100 \times 10^{-9}$	1/24

where  $\mu_{repair}$  is a repair rate and  $\lambda_{p1}, \lambda_{p2}$  is a failure rate of the first and second processor calculated from the reliability of both processors and  $DC_{p1}, DC_{p2}$  are diagnostic coverage of the first and second processors. We assume that the MTBF of the processors is 24 years. In addition, red state refers to the crash of two processors, green state is a state when processor 1 and 2 fails, blue state is a state when interruption occurs at P1 and P2 fails.

For best platform configurations, two properties are analyzed for availability assessment:

1. The system availability when the reliability of the dual core is 0.95 in *platform*<sub>1</sub> and 0.80 in *platform*<sub>2</sub> at 200000 h:  $R\{availability\}_{=?}[C \leq T]/T; T = 200000;$
2. The availability of system at different instants T when the reliability of the dual core is 0.95 in *platform*<sub>1</sub> and 0.80 such as  $R\{availability\}_{=?}[C \leq T]/T; T = 1 : 200000 : 10000;$

As shown in Fig. 11, when the reliability of of the dual core is 0.95 in *platform*<sub>1</sub> the availability is equal to 0.528 however, for the *platform*<sub>2</sub> when reliability is equal to 0.80 the availability is very low and equal to 0.247. As shown in Fig. 12, if the time increases the availability decreases from 0.97 to 0.58 for the first platform and decreases from 0.9 to 0.24 for the second platform. So, it is obvious that the availability decreases in time due to the processors performance degradation but it is clear that the first platform offers more performance than the second one due to the high reliability. For high availability, designer could assume the reliability  $\geq 95\%$ . Nevertheless, the verification of the first property is sufficient to attest that the architecture of the first platform offers more performance than the second one.

## 8 Conclusion

In this paper, we presented a formal approach for maintainability and availability assessment of probabilistic systems. PRISM language requires considerable expertise, and engineers do not have the necessary level of training to master its use. For this purpose, we propose a mapping mechanism of the SysML state machine into the input language of the probabilistic model checker PRISM. Moreover, we proposed a calculus dedicated to this diagram that captures precisely their underlying semantics.

For quantitative assessment, we have shown the effectiveness of our approach by applying it on a case study where availability and maintainability are evaluated using

CSL properties. The results are close to [10] and more accurate since the assessments are correlated to reliability. The presented work can be extended in the following two directions. First, we will look for an approximation of other kind of distributions in probabilistic model since our approach is based on exponentiation distribution. Second, we plan to document more interruptions and failure states for a precise interpretation.

**Acknowledgments** This research was performed as part of the LIMPAF/CNEPRU/C00L07UN10 0120110008 project supported by the Algerian Ministry of Higher Education and Scientific Research and the LIMPAF Lab at the University of Bouira, Algeria.

## References

1. Baier, C., Katoen, J.P.: Principles of Model Checking (Representation and Mind Series). The MIT Press (2008)
2. Baouya, A., Bennouar, D., Ait Mohamed, O., Ouchani, S.: On the probabilistic verification of time constrained sysml state machines. In: Fujita, H., Guizzi, G. (eds.) Intelligent Software Methodologies, Tools and Techniques, Communications in Computer and Information Science, vol. 532, pp. 425–441. Springer International Publishing (2015)
3. Behrmann, G., David, A., Larsen, K.G.: A tutorial on uppaal. In: Formal Methods for the Design of Real-Time Systems, pp. 200–236 (2004)
4. Birolini, A.: Reliability engineering: theory and practice. Basic Concepts, Quality and Reliability (RAMS) Assurance of Complex Equipment and Systems, pp. 1–24. Springer, Berlin (2014)
5. Calinescu, R., Ghezzi, C., Johnson, K., Pezze, M., Rafiq, Y., Tamburrelli, G.: Formal verification with confidence intervals to establish quality of service properties of software systems. *IEEE Trans. Reliab.* **99**, 1–19 (2015)
6. Dhouibi, M., Saintis, L., Barreau, M., Perquis, J.M.: Safety driven optimization approach for automotive systems. In: Reliability and Maintainability Symposium (RAMS), 2015 Annual, pp. 1–7 (2015)
7. Franco, J., Barbosa, R., Zenha-Rela, M.: Reliability analysis of software architecture evolution. In: 2013 Sixth Latin-American Symposium on Dependable Computing (LADC), pp. 11–20 (2013)
8. Ghadhab, M., Kuntz, M., D.K., Fetzer, C.: Formal techniques for safety-critical systems. In: Fourth International Workshop, FTSCS 2015, Paris, France, November 6 and 7, 2015. Springer International Publishing (2016)
9. Hahn, E.M., Han, T., Zhang, L.: Synthesis for PCTL in parametric Markov decision processes. In: Proceedings of 3rd NASA Formal Methods Symposium (NFM'11). LNCS, vol. 6617. Springer (2011)
10. Houssin, R., Coulibaly, A.: Safety-based availability assessment at design stage. *Comput. Ind. Eng.* **70**, 107–115 (2014)
11. Hoque, K., Ait Mohamed, O., Savaria, Y., Thibeault, C.: Early analysis of soft error effects for aerospace applications using probabilistic model checking. In: Artho, C., Ölveczky, P.C. (eds.) Formal Techniques for Safety-Critical Systems, Communications in Computer and Information Science, vol. 419, pp. 54–70. Springer International Publishing (2014)
12. Huang, X., Sun, Q., Li, J., Pan, M., Zhang, T.: An mde-based approach to the verification of sysml state machine diagram. In: Proceedings of the Fourth Asia-Pacific Symposium on Internetware. *Internetware'12*, pp. 9:1–9:7. ACM, New York (2012)



13. Kwiatkowska, M., Norman, G., Parker, D.: Stochastic model checking. In: Bernardo, M., Hillston, J. (eds.) *Formal Methods for the Design of Computer, Communication and Software Systems: Performance Evaluation (SFM'07)*. LNCS (Tutorial Volume), vol. 4486, pp. 220–270. Springer (2007)
14. Kwiatkowska, M.Z., Norman, G., Parker, D.: PRISM 4.0: verification of probabilistic real-time systems. In: *Computer Aided Verification—23rd International Conference, CAV 2011, Snowbird, UT, USA, July 14–20, 2011*. Proceedings, pp. 585–591 (2011)
15. Kwiatkowska, M., Norman, G., Parker, D.: Prism: Probabilistic model checking for performance and reliability analysis. *SIGMETRICS Perform. Eval. Rev.* **36**(4), 40–45 (2009)
16. Lazzaroni, M., Cristaldi, L., Peretto, L., Rinaldi, P., Catelani, M.: *Reliability engineering: basic concepts and applications in ICT. Repairable Systems and Availability*, pp. 85–92. Springer, Berlin (2011)
17. Liu, Y., Shen, G., Huang, Z., Yang, Z.: Quantitative risk analysis of safety-critical embedded systems. *Softw. Qual. J.* 1–25 (2016)
18. Lu, Y., Peng, Z., Miller, A.A., Zhao, T., Johnson, C.W.: How reliable is satellite navigation for aviation? Checking availability properties with probabilistic verification. *Reliab. Eng. Syst. Saf.* **144**, 95–116 (2015)
19. Mallet, F., de Simone, R.: MARTE: a profile for RT/E systems modeling, analysis and simulation. In: *Proceedings of the 1st International Conference on Simulation Tools and Techniques for Communications, Networks and Systems and Workshops, SimuTools 2008, Marseille, France, March 3–7, 2008*, p. 43 (2008)
20. Morant, A., Gustafson, A., Söderholm, P.: Safety and availability evaluation of railway signalling systems. In: Kumar, U., Ahmadi, A., Verma, A.K., Varde, P. (eds.) *Current Trends in Reliability, Availability, Maintainability and Safety, Lecture Notes in Mechanical Engineering*, pp. 303–316. Springer International Publishing (2016)
21. Norman, G., Parker, D.: Quantitative verification: Formal guarantees for timeliness, reliability and performance. Technical Report. The London Mathematical Society and the Smith Institute (2014)
22. O.M. Group (ed.): *OMG Systems Modeling Language (Object Management Group SysML)* (2012)
23. Ouchani, S., Ait Mohamed, O., Debbabi, M.: A property-based abstraction framework for sysml activity diagrams. *Knowl. Based Syst.* **56**, 328–343 (2014)
24. Peng, Z., Lu, Y., Miller, A., Johnson, C., Zhao, T.: A probabilistic model checking approach to analysing reliability, availability, and maintainability of a single satellite system. In: *Modelling Symposium (EMS), 2013 European*, pp. 611–616 (2013)
25. Qiu, S., Sallak, M., Schön, W., Cherfi-Boulanger, Z.: Availability assessment of railway signalling systems with uncertainty analysis using statecharts. *Simul. Model. Pract. Theory* **47**, 1–18 (2014)
26. Reliasoft: Lambda Predict. <http://www.reliasoft.com/predict/>
27. Sivanandam, S.N., Deepa, S.N.: *Introduction to Genetic Algorithms*, 1st edn. Springer Publishing Company (2010) (Incorporated)
28. Song, L., Zhang, L., Godskesen, J.: Bisimulations and logical characterizations on continuous-time markov decision processes. In: McMillan, K., Rival, X. (eds.) *Verification, Model Checking, and Abstract Interpretation. Lecture Notes in Computer Science*, vol. 8318, pp. 98–117. Springer, Berlin (2014)
29. Tian, Y., Wan, L., hung Chen, C., Yang, Y.: Safety assessment method of performance-based navigation airspace planning. *J. Traffic Transp. Eng. (English Edition)* **2**(5), 338–345 (2015)

# A Locally Sequential Globally Asynchronous Net from Maximality-Based Labelled Transition System

Adel Benamira and Djamel-Eddine Saidouni

**Abstract** Given a maximality-based labelled transition system, in this paper we show that such system can be decomposed and considered as distributed components, where each component is a sequential behaviour. In a distributed context, the synchronisation between components is interpreted as an asynchronous interaction. Hence, sequential maximality-based labelled transition systems are represented as locally sequential globally asynchronous nets.

**Keywords** Maximality semantics · Bisimulation relation · Distributed systems · Petri nets · LSGA nets

## 1 Introduction

In [6, 7], distributed systems have been defined as a system which consists of sequential components that reside on different locations. These components evolve concurrently. The interactions between components are asynchronous communications.

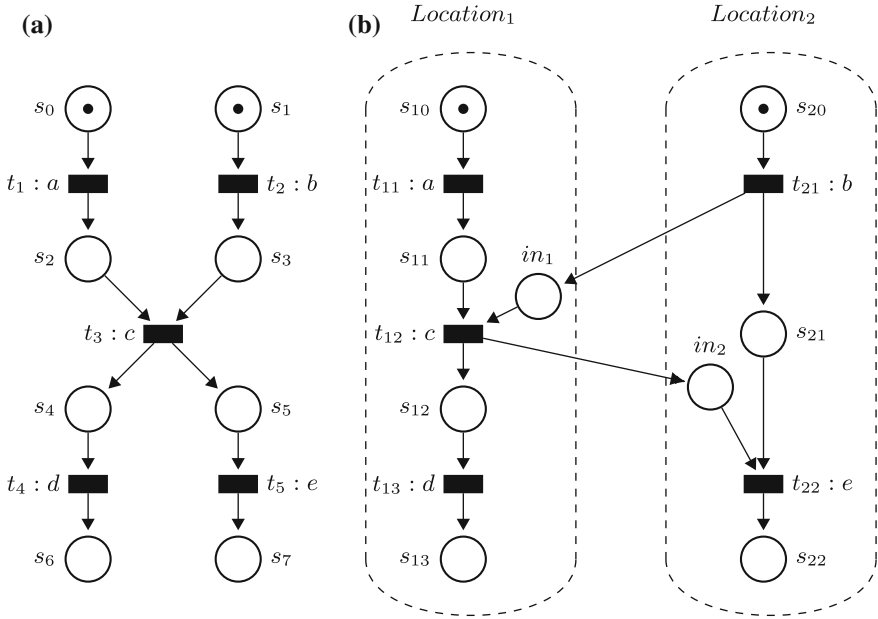
Nowadays formal methods are frequently used in different areas during the development of concurrent applications. Their use allows the verification of application properties before their implementation. In general verification processes are based on centralized algorithms. However these applications may be implemented on a distributed system where the synchronization between the different components are implemented as asynchronous communication. Hence the following questions have been emerged: which specifications may be implemented on a distributed system ?

---

A. Benamira (✉) · D.-E. Saidouni  
MISC Laboratory, Abdelhamid Mehri University, 25000 Constantine, Algeria  
e-mail: benamira.adel@univ-guelma.dz

D.-E. Saidouni  
e-mail: djamel.saidouni@univ-constantine2.dz

A. Benamira  
Computer Science Department, University of 08 May 45, 24000 Guelma, Algeria



**Fig. 1** LSGA net of Petri net. **a** Petri net  $N$ . **b** LSGA net of  $N$

and what is the suitable equivalence relation to compare the behaviour of a centralised applications with their distributed implementations?

In the Petri nets framework, Glabbeek et al. [6, 7] gave a precise characterisation of distributable nets and their definition by corresponding class of Petri nets, called LSGA nets (Locally Sequential Globally Asynchronous nets). The ST-bisimulation relation has been proved the suitable equivalence relation between the Petri net specification and their LSGA nets [5, 11, 12].

Figure 1 gives an example of a Petri net with one among its distributed implementations.

Remark that the proposed result is closed to Petri nets model, the use of another specification model requires the definition of a new approach (see Fig. 2) for the generation of distributed implementations (LSGA) from a given specifications. To generalize the result to any input specification model we define a distributed implementation from a semantics<sup>1</sup> model rather than a specification model.

The ST-semantics is originally defined in [11] over Petri nets. In this semantics, non atomic actions are split into starts and ends sub actions. In the literature, the ST-semantics has been applied to process algebras [1, 8]. Another concurrency semantics model, named Maximality-based Labeled Transition System (MLTS), has been defined and used for expressing the semantics of process algebras and P/T Petri nets

<sup>1</sup>Which compatible to the ST-idea, indeed the validation of a distributed implementation is based on the ST-bisimulation.

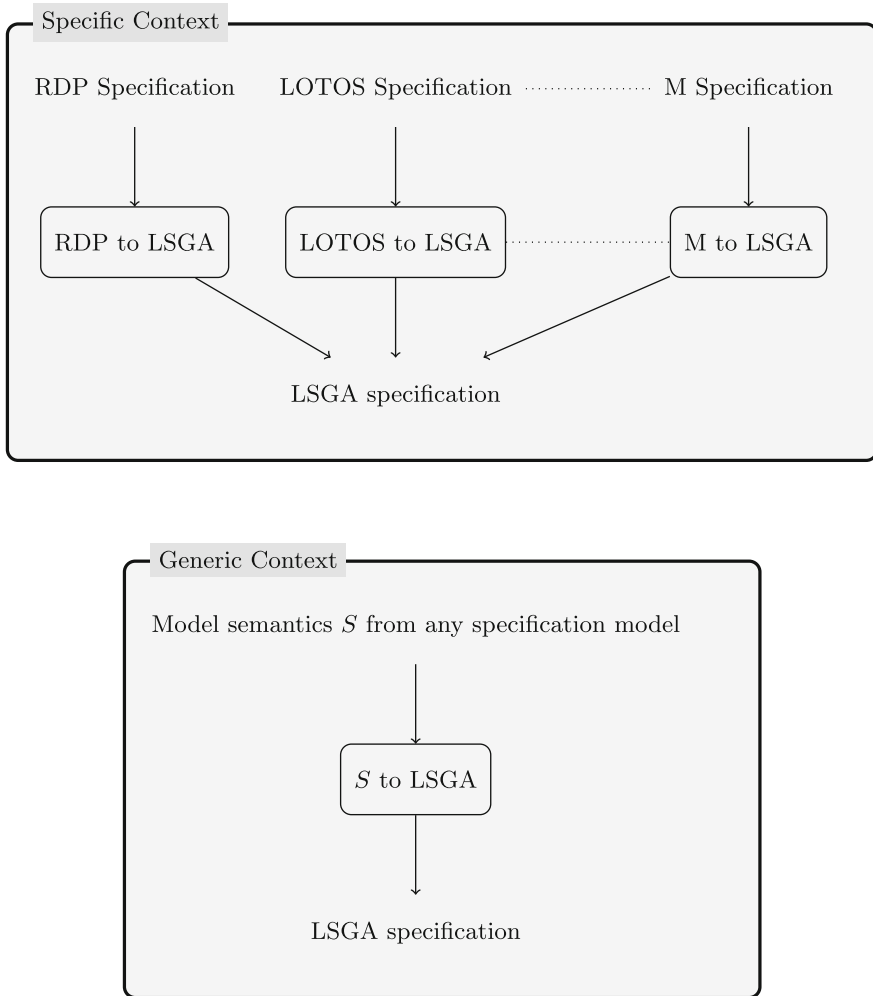
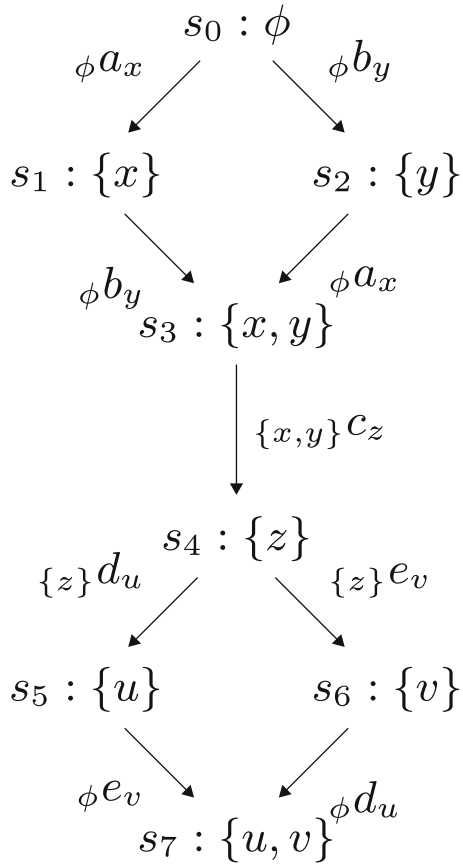


Fig. 2 Specific and generic generation of LSGA specification

with the hypothesis that actions are not necessarily atomic [2–4, 9, 10], i.e. actions are abstractions of finite processes and may elapse in time. The main interest of maximality-based labelled transition system model is that it can be implemented and used for verifying correctness properties without splitting actions into starts and ends sub actions. In this paper, we describe how a MLTS may be seen as a distributed components (sub-MLTS) where synchronizations between components are asynchronous as for LSGA.

Consider the Petri net of Fig. 1a. By applying the approach of [9], the corresponding maximality-based labelled transition system of this Petri net is given by Fig. 3.

Fig. 3 A MLTS



At first, from [4] we can recall that a maximality-based labelled transition system is given by a graph labelled on both states and transitions. Each state is labelled by a set of event names. Each event name identifies the start of execution of an action (eventually under execution) which occurred before this state. This action is said to be potentially under execution in this state. A transition between two states  $s_i$  and  $s_j$  is labelled by a 3-uple  $(M, a, x)$  (denoted  ${}_M a_x$ ) where  $x$  is the event name identifying the start of execution of the action  $a$  and  $M$  denotes the set of event names representing some causes of the action  $a$ . Elements of  $M$  belong to state  $s_i$ . Occurrence of this transition terminates actions identified by  $M$ , thus, the set of event names corresponding to state  $s_j$  is that of  $s_i$  from which we subtract the set  $M$  and add the event name  $x$ . Formal definition of a maximality-based labelled transition system will be given in Sect. 2.2.

In the initial state (state  $s_0$ ) of the maximality-based transition system of Fig. 3, no action is running, from where the association of the empty set with this state. From state  $s_0$ , actions  $a$  and  $b$  can start their execution independently, their starts are respectively identified by event names  $x$  and  $y$ .  $a$  and  $b$  can be launched in any order.

The set  $\{x\}$  (resp.  $\{y\}$ ) in state  $s_1$  (resp.  $s_2$ ) stipulates that the action  $a$  (resp.  $b$ ) are potentially under execution in this state. The set  $\{x, y\}$  in  $s_3$  shows that actions  $a$  and  $b$  can be executed simultaneously.

Note that when the system is in state  $s_1$ , while the action  $a$  has not been terminated yet, the only evolution concerns the start of  $b$ . However, when  $a$  and  $b$  terminate, we can start the action  $c$  caused by  $a$  and  $b$  since the action  $c$  which is dependent from the end of  $a$  and  $b$ . When  $c$  terminates, we can start the action  $d$  or  $e$ . Resulting states are respectively  $s_5$  and  $s_6$ . We can observe that from state  $s_5$  (resp.  $s_6$ ), the start of  $e$  (resp.  $d$ ) is always possible. The set  $\{u, v\}$  in  $s_7$  shows that actions  $d$  and  $e$  can be executed simultaneously.

We proceed by defining basic notions of LSGA nets and MLTSs in Sect. 2. In Sect. 3, we show how to decompose a MLTS in set of sequential components such that their interaction defines the initial MLTS, from which we have a direct transformation to LSGA net. This paper is ended by some conclusions of this work.

## 2 Preliminaries

### 2.1 Distributed Systems

From [6, 7], a distributed system is defined as follow:

- A distributed system consists of components residing on different locations.
- Components work concurrently.
- Components only allow sequential behaviour.
- Interactions between components are only possible by explicit communications.
- Communication between components is time consuming and asynchronous.

Asynchronous communication is the only interaction mechanism in a distributed system for exchanging signals or information.

- The sending of a message happens always strictly before its receipt (there is a causal relation between sending and receiving a message).
- A sending component sends without regarding the state of the receiver; in particular there is no need to synchronise with a receiving component. After sending the sender continues its behaviour independently of receipt of the message.

In the next, the formal definition of distributed systems in terms of Petri nets [6, 7] is introduced with given the precise characterisation of distributed Petri net.

**Definition 1** A (labelled, marked) Petri net is a tuple  $N = (S, T, F, I, L)$  where:

- $S$  and  $T$  are disjoint sets (of places and transitions),
- $F : (S \times T \cup T \times S) \rightarrow \mathbb{N}$  (the flow relation including arc weights),
- $I : S \rightarrow \mathbb{N}$  (the initial marking), and
- $L : T \rightarrow A$ , for  $A$  a set of actions, the labelling function.

**Definition 2** A multiset over a set  $S$  is a function  $M : S \rightarrow \mathbb{N}$ , i.e.  $M \in \mathbb{N}^S$ . For multisets  $M$  and  $N$  over  $S$  write  $M \leq N$  if  $M(s) \leq N(s)$  for all  $s \in S$ .  $M + N \in \mathbb{N}^S$  is the multiset with  $(M + N)(s) = M(s) + N(s)$ , and  $M - N$  is the function given by  $(M - N)(s) = M(s) - N(s)$  (it is not always a multiset). The function  $0 : S \rightarrow \mathbb{N}$  given by  $0(s) = 0$  for all  $s \in S$  is the empty multiset. A multiset  $M \in \mathbb{N}^S$  with  $M(s) \leq 1$  for all  $s \in S$  is identified with the set  $\{s \in S \mid M(s) = 1\}$ . A multiset  $M$  over  $S$  is finite if  $\{s \in S \mid M(s) > 1\}$  is finite. Let  $\mathcal{M}(S)$  denote the collection of finite multisets over  $S$ .

**Definition 3** For a finite multiset  $U : T \rightarrow \mathbb{N}$  of transitions in a Petri net, let  $\bullet U, U^\bullet : S \rightarrow \mathbb{N}$  be the multisets of input and output places of  $U$ , given by  $\bullet U(s) = \sum_{t \in T} F(s, t) \cdot U(t)$  and  $U^\bullet(s) = \sum_{t \in T} U(t) \cdot F(t, s)$  for all  $s \in S$ .

$U$  is enabled under a marking  $M$  if  $\bullet U \leq M$ . In that case  $U$  can fire under  $M$ , yielding the marking  $M' = M - \bullet U + U^\bullet$ , written  $M \xrightarrow{U} M'$  or  $M[U]M'$ .

**Definition 4** The concurrency relation  $\sim \subseteq T^2$  is given by  $t \sim u \Leftrightarrow \exists M \in [M_0], M[\{t\}][\{u\}]$  such that  $[\ ]$  is a conflict relation.  $N$  is a structural conflict net iff for all  $t, u \in T$  with  $t \sim u$  we have  $\bullet t \cap^\bullet u = \emptyset$ .

For example, the net of Fig. 4 [6, 7], has not a structural conflict net because  $[\ ] = \{(t_1, t_2); (t_2, t_3)\}$ . In the other hand, the net of Fig. 1a is it ( $[\ ] = \emptyset$ ).

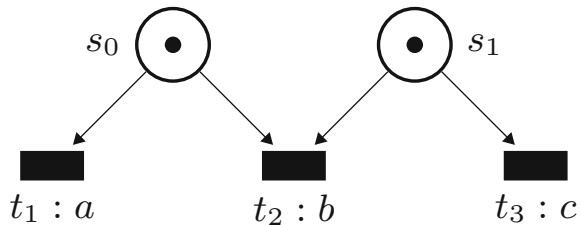
A distributed Petri net is a Petri net in which a transition and all its input places reside on the same location and location actions can only occur sequentially. The function  $D : S \cup T \rightarrow Loc$  ( $Loc$  a set of locations) is defined to associate localities to the elements of a net.

The system of Fig. 5 is a distributed Petri net with  $Loc = \{1, 2\}$  and  $D = \{(s_1, 1), (t_1, 1), (s_3, 1), (s_4, 1), (t_3, 1), (s_6, 1), (s_2, 2), (t_2, 2), (s_5, 2), (s_7, 2), (t_4, 2), (s_8, 2)\}$ .

**Definition 5** A Petri net  $N = (S, T, F, I, L)$  is distributed iff there exists a distribution  $D$  such that:

1.  $\forall s \in S, t \in T. s \in^\bullet t \Rightarrow D(t) = D(s)$ ,
2.  $\forall t, u \in T. t \sim u \Rightarrow D(t) \neq D(u)$ .

**Fig. 4**  $N$  has not a structural conflict



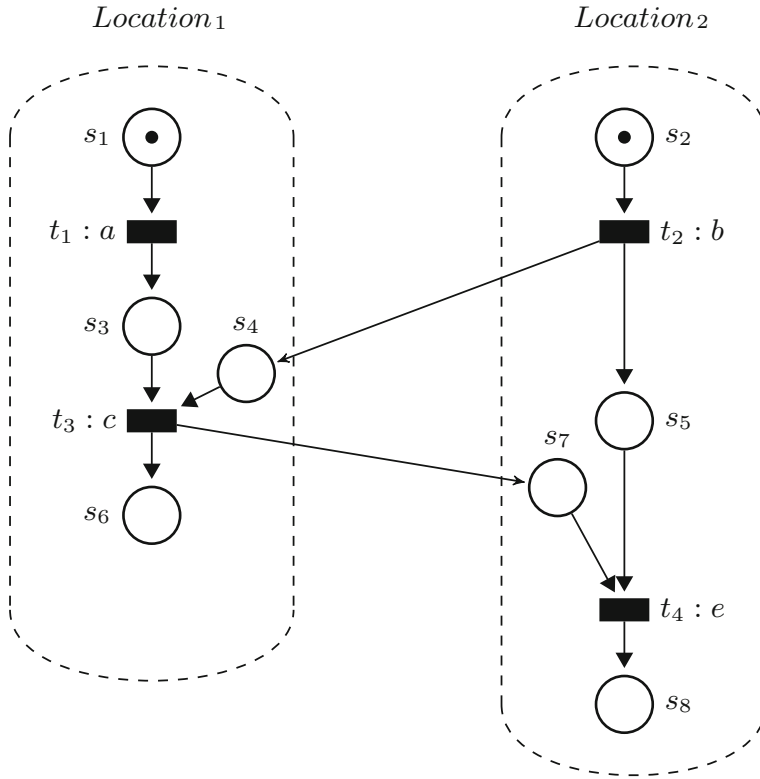


Fig. 5 Distributed Petri net

**Proposition 1** Every distributed Petri net is a structural conflict net.

**Definition 6** Let  $N = (S, T, F, M_0, L)$  be a net,  $I, O \subseteq S, I \cap O = \emptyset$  and  $O^* = \emptyset$ .

1.  $(N, I, O)$  is a component with interface  $(I, O)$ .
2.  $(N, I, O)$  is a sequential component with interface  $(I, O)$  iff  $\exists Q \subseteq S \setminus (I \cup O)$  with  $\forall t \in T. |^*t \upharpoonright Q| = 1 \wedge |t^* \upharpoonright Q| = 1$  and  $|M_0 \upharpoonright Q| = 1$ .  $A \upharpoonright Y$  denotes the signed multiset over  $Y$  defined by  $(A \upharpoonright Y)(x) = A(x)$  for all  $x \in Y$ .

$C = (N, I, O)$  can be regarded as a component of distributed system equipped with a mailbox  $I$  and an address  $O$  outside  $C$ , the first is introduced to receive messages and the second to send messages.

**Definition 7** Let  $\mathfrak{K}$  be an index set.

Let  $((S_k, T_k, F_k, M_{0k}, L_k), I_k, O_k)$  with  $k \in \mathfrak{K}$  be components with interface such that  $(S_k \cup T_k) \cap (S_l \cup T_l) = (I_k \cup O_k) \cap (I_l \cup O_l)$  for all  $k, l \in \mathfrak{K}$  with  $k \neq l$  and  $I_k \cap I_l = \emptyset$  for all  $k, l \in \mathfrak{K}$  with  $k \neq l$ . Then the asynchronous parallel of these components is defined by



$$\|_{k \in \mathfrak{K}} ((S_k, T_k, F_k, M_{0K}, L_k), I_k, O_k) = ((S, T, F, M_0, L), I, O)$$

with  $S = \cup_{k \in \mathfrak{K}} S_k$ ,  $T = \cup_{k \in \mathfrak{K}} T_k$ ,  $F = \cup_{k \in \mathfrak{K}} F_k$ ,  $M_0 = \cup_{k \in \mathfrak{K}} M_{0k}$ ,  $L = \cup_{k \in \mathfrak{K}} L_k$ ,  $I = \cup_{k \in \mathfrak{K}} I_k$  and  $O = \cup_{k \in \mathfrak{K}} O_k \cup_{k \in \mathfrak{K}} I_k$ .

**Definition 8** A Petri net  $N$  is an LSGA net iff there exists an index set  $\mathfrak{K}$  and sequential components with interface  $C_k$ ,  $k \in \mathfrak{K}$ , such that  $(N, I, O) = \|_{i \in \mathfrak{K}} C_k$  for some  $I$  and  $O$ .

We can see that the net of Fig. 5 as an LSGA net with two sequential components  $C_1$  and  $C_2$  such that  $C_1 = (N_1, \{s_4\}, \{s_7\})$  and  $C_2 = (N_2, \{s_7\}, \{s_4\})$  with:

- $N_1 = (S_1, T_1, MS_1, LT_1)$  such that  $S_1 = \{s_1, s_3, s_4, s_6, s_7\}$  and  $T_1 = \{t_1, t_3\}$ .
- $N_2 = (S_2, T_2, MS_2, LT_2)$  such that  $S_2 = \{s_2, s_4, s_5, s_7, s_8\}$  and  $T_2 = \{t_2, t_4\}$ .

From [7], every LSGA net is distributed net and every LSGA net is a structural conflict net.

## 2.2 Maximality-Based Labeled Transition Systems

A maximality-based labelled transition system is given by a graph labelled on both states and transitions. Each state is labelled by a set of event names. Each event name identifies the start of execution of an action (eventually under execution) which occurred before this state. This action is said to be potentially under execution in this state. A transition between two states  $s_i$  and  $s_j$  is labelled by a 3-uple  $(M, a, x)$  (denoted  ${}_M a_x$ ) where  $x$  is the event name identifying the start of execution of the action  $a$  and  $M$  denotes the set of event names representing some causes of the action  $a$ . Elements of  $M$  belong to state  $s_i$ . Occurrence of this transition terminates actions identified by  $M$ , thus, the set of event names corresponding to state  $s_j$  is that of  $s_i$  from which we subtract the set  $M$  and add the event name  $x$ .

**Definition 9** Let  $\mathcal{M}$  be a countable set of event names, a maximality-based labeled transition system of support  $\mathcal{M}$  is a tuple  $(\Omega, \lambda, \mu, \xi, \psi)$  with:

- (a) •  $\Omega = (S, T, \alpha, \beta, s_0)$  is a transition system such that:
- $S$  is the set of states in which the system can be found, this set can be finite or infinite.
  - $T$  is the set of transitions indicating state switch that the system can achieve, this set can be finite or infinite.
  - $\alpha$  and  $\beta$  are two applications of  $T$  in  $S$  such that for all transition  $t$  we have:  $\alpha(t)$  is the origin of the transition and  $\beta(t)$  its goal.
  - $s_0$  is the initial state of the transition system  $\Omega$ .
- $(\Omega, \lambda)$  is a transition system labeled by the function  $\lambda$  on an alphabet  $Act$  called support of  $(\Omega, \lambda)$ . In the other words  $\lambda : T \rightarrow Act$ .

- $\psi : S \rightarrow 2^{\mathcal{M}}$  is a function which associates to each state the finite set of maximal event names present in this state.<sup>2</sup>
  - $\mu : T \rightarrow 2^{\mathcal{M}}$  is a function which associates to each transition the finite set of event names corresponding to actions that have already begun their execution and the end of their executions enables this transition.
  - $\xi : T \rightarrow \mathcal{M}$  is a function which associates to each transition the event name identifying its occurrence.
- (b) such that  $\psi(s_0) = \phi$  and for all transition  $t$ ,  $\mu(t) \subseteq \psi(\alpha(t))$ ,  $\xi(t) \notin \psi(\alpha(t)) - \mu(t)$  and  $\psi(\beta(t)) = (\psi(\alpha(t)) - \mu(t)) \cup \xi(t)$

In what follows, we use the following assumptions:

- In this present paper we suppose the uniqueness of event name.
- Let  $mlts = (\Omega, \lambda, \mu, \xi, \psi)$  a maximality-based labeled transition system such that  $\Omega = \langle S, T, \alpha, \beta, s_0 \rangle$ .  $t \in T$  is a transition for which  $\alpha(t) = s$ ,  $\beta(t) = s'$ ,  $\lambda(t) = a$ ,  $\mu(t) = E$  and  $\xi(t) = x$ . The transition  $t$  will be noted  $s \xrightarrow{E^a_x} s'$ .
- The set of Maximality-based labelled transition systems is noted  $\mathfrak{MLT}\mathfrak{S}$ .

### 3 LSGA Net from MLTS

In this section, we assume a given  $mlts = (\Omega, \lambda, \mu, \xi, \psi)$  to be a maximality-based labelled transition system over  $\mathcal{M}$  such that  $\Omega = \langle S, T, \alpha, \beta, s_0 \rangle$ .

Firstly, we define a partition of  $\mathcal{M}$  such that the only interaction between their elements is the synchronous interaction and each element represents a sequential behaviour.<sup>3</sup> In the other words, we decompose  $mlts$  into a set of sequential MLTSs so that their parallel composition is a MLTS that is the initial MLTS.

Secondly, for each sequential MLTS we define a component net with interface. The asynchronous parallel composition of the all component nets, which associated to the initial MLTS, defines a LSGA net.

#### 3.1 Generation of Sequential MLTSs Set

In the following, we define two fundamental relations with which the  $\mathcal{M}$  is structured in the way that the sequential behaviour is clearly deduced from global behaviour.

##### Definition 10

- The direct causality relation  $\leq \subseteq \mathcal{M}^2$  is given by  $x \leq y$  if and only if  $\exists s \xrightarrow{E^a_y} s'$  such that  $x \in E$ .
- the independence relation  $\parallel \subseteq \mathcal{M}^2$  is given by  $x \parallel y$  if and only if  $\exists s \in S$  such that  $x, y \in \psi(s)$ .

<sup>2</sup> $2^{\mathcal{M}}$  denotes the part sets of  $\mathcal{M}$ .

<sup>3</sup>Which equivalent to the notion of a sequential component of distributed system.

We note that the relation  $\leq$  is not transitive: let  $s \xrightarrow{E_1 a_x} s_1 \cdots \xrightarrow{E_p a_y} s_p \cdots \xrightarrow{E_n a_z} s_n$ . The assertion  $(x \in E_p) \wedge (x \leq y) \wedge (x, y \in E_n) \wedge (y \leq z)$  does never satisfied indeed  $x \notin \psi(s_p)$  (see Definition 9(b)), hence  $x \leq y \wedge y \leq z \not\Rightarrow x \leq z$ .

The conflict relation  $[\ ] \subseteq \mathcal{M}^2$  is given by  $x[\ ]y$  if and only if  $x \not\leq y$  and  $y \not\leq x$  and  $x \not\parallel y$ , in the other words, the conflict has been deduced from basic relations  $\leq$  and  $\parallel$ . We tell that  $(\mathcal{M}, \leq, \parallel)$  is a set of events  $\mathcal{M}$  which is structured by  $\leq$  and  $\parallel$ .

$mlts$  is a structural conflict if and only if  $\nexists x, y \in \mathcal{M} : x[\ ]y$ . Throughout the rest of this section, we restrict<sup>4</sup> our study to structural conflict MLTS.

Next, we define a set of concepts with which we characterise the structure  $(\mathcal{M}, \leq, \parallel)$ .

Let  $x \in \mathcal{M}$ , event  $x$  is a synchronous point if and only if:

- $\exists t : s \xrightarrow{E a_x} s' \in T$  such that  $|E| \geq 2$  or
- $|\{s \mid \forall t : s' \xrightarrow{E a_y} s \in T \wedge x \in E\}| \geq 2$ .

Let  $\mathbb{S} : \mathcal{M} \longrightarrow 2^{\mathcal{M}}$ , the notation  $\mathbb{S}_{\mathcal{M}}$  is the set of all synchronous and branch-out points in  $\mathcal{M}$ .

In the system of Fig. 3, the event  $z$  is both synchronous and branch-out point, the event  $z$  is a synchronous point indeed the action  $c$  is dependent to the end of  $a$  and  $b$ , and it is a branch-out point as the end of  $c$  causes the execution of  $d$  or  $e$ .

Let  $\sigma \subseteq \mathcal{M}$  such that  $x_1 \leq x_2 \leq \cdots \leq x_n$ ,  $\sigma$  is a sequence if and only if  $\sigma \cap \mathbb{S}_{\mathcal{M}} = \emptyset$ . Let  $\sigma_1 = \{x_{11}, x_{12}, \dots, x_{1n}\}$  and  $\sigma_2 = \{x_{21}, x_{22}, \dots, x_{2m}\}$  two not empty sequences, the order  $\sigma_1 \leq \sigma_2$  is defined if and only if  $x_{1n} \leq x_{21}$ .

The sequence  $\sigma$  is a full sequence if and only if  $\exists y \notin \mathbb{S}_{\mathcal{M}} \wedge \exists x \in \sigma$  such that  $x \leq y$  or  $y \leq x$  then  $y \in \sigma$ . Let  $\mathbb{F} : \mathcal{M} \longrightarrow 2^{\mathcal{M} \times \mathcal{M}}$ , the notation  $\mathbb{F}_{\mathcal{M}}$  is the set of all full sequences in  $\mathcal{M}$ .

Let  $\sigma_1 = \{x_{11}, x_{12}, \dots, x_{1n}\}$  and  $\sigma_2 = \{x_{21}, x_{22}, \dots, x_{2m}\}$  be two not empty full sequences, the order  $\sigma_1 \leq_{\mathbb{S}} \sigma_2$  is defined if and only if  $\exists x \in \mathbb{S}_{\mathcal{M}} : x_{1n} \leq x \leq x_{2m}$ , the set  $(\mathbb{F}_{\mathcal{M}}, \leq_{\mathbb{S}})$  is a partial order. The relation  $\sigma_1 \parallel \sigma_2$  is introduced if and only if  $x_{11} \parallel x_{21}$ .

The next lemma says that  $\mathcal{M}$  is well structured w.r.t definition of full sequences.

**Lemma 1** *The full sequences over  $\mathcal{M}$  have the following proprieties.*

1. For each not empty full sequences  $\sigma_1, \sigma_2 \in \mathbb{F}_{\mathcal{M}}$ :

- (a)  $\sigma_1 \parallel \sigma_2 \Rightarrow \forall x \in \sigma_1, \forall y \in \sigma_2 : x \parallel y$ .
- (b)  $\sigma_1 \leq_{\mathbb{S}} \sigma_2 \vee \sigma_2 \leq_{\mathbb{S}} \sigma_1 \vee \sigma_1 \parallel \sigma_2$ .
- (c)  $(\sigma_1 \leq \{x\} \wedge \sigma_1 \leq \{y\}) \Rightarrow (x = y)$ .
- (d)  $(\{x\} \leq \sigma_1 \wedge \{y\} \leq \sigma_1) \Rightarrow (x = y)$ .

2. For each not empty full sequences  $\sigma_1, \sigma_2, \sigma_3 \in \mathbb{F}_{\mathcal{M}}$ :

- (a)  $(\sigma_1 \leq_{\mathbb{S}} \sigma_2 \wedge \sigma_3 \leq_{\mathbb{S}} \sigma_2) \Rightarrow \exists x \in \mathbb{S}_{\mathcal{M}}$  such that  $\sigma_1 \leq \{x\} \leq \sigma_2 \wedge \sigma_3 \leq \{x\} \leq \sigma_2$ .

<sup>4</sup>From the fact that every LSGA net is a structural conflict net.

(b)  $(\sigma_1 \leq_{\mathbb{S}} \sigma_2 \wedge \sigma_1 \leq_{\mathbb{S}} \sigma_3) \Rightarrow \exists x \in \mathbb{S}_{\mathcal{M}}$  such that  $\sigma_1 \leq \{x\} \leq \sigma_2 \wedge \sigma_1 \leq \{x\} \leq \sigma_3$ .

*Proof* Let  $\sigma_1 = \{x_{11}, x_{12}, \dots, x_{1n}\}$  and  $\sigma_2 = \{x_{21}, x_{22}, \dots, x_{2m}\}$ .

- For Property 1(a): we proceed by absurd. If  $\exists u \in \sigma_1$  and  $\exists v \in \sigma_2$  such that  $u \leq v$  we have a contradiction. Let  $x_{11} \leq x_{12} \leq \dots x_{1i} \leq u$  with  $(i \leq n)$  and  $u \leq v$  we have  $x_{11} \leq x_{12} \leq \dots x_{1i} \leq v$ . So we have  $x_{21} \leq v$  and  $x_{11} \leq v$ , in other words,  $v$  is a synchronous event, which contradicts the definition of a full sequence  $\sigma_2$ . Similar if  $v \leq u$ , we have  $u$  as a synchronous event.
- For Property 1(b): from the fact that we have only one case from  $x_{11} \leq x_{21}, x_{21} \leq x_{11}$  and  $x_{11} \parallel x_{21}$ , and by definition of  $\leq$  and  $\parallel$ , we have one from  $\sigma_1 \leq_{\mathbb{S}} \sigma_2, \sigma_2 \leq_{\mathbb{S}} \sigma_1$  and  $\sigma_1 \parallel \sigma_2$ .
- For Property 1(c): by absurd,  $\exists x, y \in \mathbb{S}_{\mathcal{M}} : x \neq y$  such that  $\sigma_1 \leq \{x\}$  and  $\sigma_1 \leq \{y\}$  hence  $x_{1n} \leq \{x\}$  and  $x_{1n} \leq \{y\}$ . So  $x_{1n}$  is a branch-out point, in the other words, we have a contradiction to the definition of a full sequence  $\sigma_1$ .
- Proof of Property 1(d) is similar to proof of Property 1(c).
- For Property 2(a): holds from Property 1(c) and definition of  $\mathbb{F}_{\mathcal{M}}$ .
- For Property 2(b): holds from Property 1(d) and definition of  $\mathbb{F}_{\mathcal{M}}$ .

In the next, we present, in the first, how generate a maximality-based labeled transition system from a given full sequence. In the second, the synchronous parallel operator of maximality-based labeled transition systems is defined.

**Definition 11** Let  $\sigma = \{x_1, x_2, \dots, x_n\}$  sequence in  $\mathcal{M}$  such that  $x_1 \leq x_2 \leq \dots \leq x_n$ . The construction  $\mathcal{G}(\sigma) = (\Omega_{\sigma}, \lambda_{\sigma}, \mu_{\sigma}, \xi_{\sigma}, \psi_{\sigma})$  is a maximality-based labeled transition system such that  $\Omega_{\sigma} = \langle S_{\sigma}, T_{\sigma}, \alpha_{\sigma}, \beta_{\sigma}, s_{\sigma}^0 \rangle$  such that:

- $s_{\sigma}^0 \xrightarrow{\phi^{a_{x_1}}} s_1 \in T_{\sigma}$  which, in the *mlts* of the origin, the beginning of execution of  $a \in Act$  is associated to event  $x_1$ .
- $\forall i \in 2 \dots n : s_{i-1} \xrightarrow{\{x_{i-1}\}^{a_{x_i}}} s_i \in T_{\sigma}$  which, in the *mlts* of the origin, the beginning of execution of  $a \in Act$  is associated to event  $x_i$ .

**Definition 12** Let  $mlts_1 = (\Omega_1, \lambda_1, \mu_1, \xi_1, \psi_1)$  and  $mlts_2 = (\Omega_2, \lambda_2, \mu_2, \xi_2, \psi_2)$  be two maximality-based labeled transition systems such that  $\Omega_1 = \langle S_1, T_1, \alpha_1, \beta_1, s_1^0 \rangle$  and  $\Omega_2 = \langle S_2, T_2, \alpha_2, \beta_2, s_2^0 \rangle$ . The synchronous parallel of  $mlts_1$  and  $mlts_2$  over  $L \subseteq \mathcal{M}$  is defined by  $mlts_1 \parallel [L] \parallel mlts_2 = (\Omega, \lambda, \mu, \xi, \psi)$  such that  $\Omega = \langle S, T, \alpha, \beta, s_0 \rangle$  with:

1.  $s_0 = (s_1^0, s_2^0)$ .
2.  $S = S_1 \times S_2$ .
3.  $\psi(S) = \psi(S_1) \cup \psi(S_2)$ .
4.  $\forall s \xrightarrow{E^{a_x}} s' \in T_1$  such that  $x \notin L \Rightarrow \forall s'' \in S_2 : (s, s'') \xrightarrow{E^{a_x}} (s', s'') \in T$ .
5.  $\forall s \xrightarrow{E^{a_x}} s' \in T_2$  such that  $x \notin L \Rightarrow \forall s'' \in S_1 : (s'', s) \xrightarrow{E^{a_x}} (s'', s') \in T$ .
6.  $\forall s_1 \xrightarrow{E_1^{a_x}} s'_1 \in T_1$  and  $\forall s_2 \xrightarrow{E_2^{a_x}} s'_2 \in T_2$  such that  $x \in L \Rightarrow (s_1, s_2) \xrightarrow{E_1 \cup E_2^{a_x}} (s'_1, s'_2) \in T$ .

**Lemma 2** *The synchronous parallel operator have the following proprieties.*

1. For each  $\sigma_1, \sigma_2 \in \mathbb{F}_{\mathcal{M}}$  such that  $\sigma_1 \parallel \sigma_2$ :
  - (a)  $mlts' = \mathcal{G}(\sigma_1) \parallel \mathcal{G}(\sigma_2)$  such that  $\mathbb{F}_{\mathcal{M}'} = \{\sigma_1, \sigma_2\}$  and  $\mathbb{S}_{\mathcal{M}'} = \phi$ .
  - (b) if  $\sigma_1 \leq \{x\} \wedge \sigma_2 \leq \{x\}$  then  $mlts' = \mathcal{G}(\sigma_1 \leq \{x\}) \parallel \mathcal{G}(\sigma_2 \leq \{x\})$  such that  $\mathbb{F}_{\mathcal{M}'} = \{\sigma_1, \sigma_2\}$  and  $\mathbb{S}_{\mathcal{M}'} = \{x\}$ .
  - (c) if  $\sigma_1 \leq \{x\} \wedge \sigma_2 \leq \{y\}$  then  $mlts' = \mathcal{G}(\sigma_1 \leq \{x\}) \parallel \mathcal{G}(\sigma_2 \leq \{y\})$  such that  $\mathbb{F}_{\mathcal{M}'} = \{\sigma_1, \sigma_2\}$  and  $\mathbb{S}_{\mathcal{M}'} = \{x, y\}$ .
2. For each  $\sigma_1, \sigma_2, \sigma_3 \in \mathbb{F}_{\mathcal{M}}$ :
  - (a) if  $\sigma_1 \leq \sigma_2 \wedge \sigma_3 \leq \sigma_2$  which  $\sigma_1 \leq \{x\} \leq \sigma_2 \wedge \sigma_3 \leq \{x\} \leq \sigma_2$  then  $mlts' = \mathcal{G}(\sigma_1 \leq \{x\}) \parallel \mathcal{G}(\{x\} \leq \sigma_2) \parallel \mathcal{G}(\sigma_3 \leq \{x\})$  such that  $\mathbb{F}_{\mathcal{M}'} = \{\sigma_1, \sigma_2, \sigma_3\}$  and  $\mathbb{S}_{\mathcal{M}'} = \{x\}$ .
  - (b) if  $\sigma_1 \leq \sigma_2 \wedge \sigma_1 \leq \sigma_3$  which  $\sigma_1 \leq \{x\} \leq \sigma_2 \wedge \sigma_1 \leq \{x\} \leq \sigma_3$  then  $mlts' = \mathcal{G}(\sigma_1 \leq \{x\}) \parallel \mathcal{G}(\{x\} \leq \sigma_2) \parallel \mathcal{G}(\{x\} \leq \sigma_3)$  such that  $\mathbb{F}_{\mathcal{M}'} = \{\sigma_1, \sigma_2, \sigma_3\}$  and  $\mathbb{S}_{\mathcal{M}'} = \{x\}$ .
3. For each  $C_1 = \sigma_0 \leq \{x_1\} \leq \sigma_1 \leq \{x_2\} \dots \leq \{x_n\} \leq \sigma_n$  and  $C_2 = \sigma'_0 \leq \{y_1\} \leq \sigma'_1 \leq \{y_2\} \dots \leq \{y_m\} \leq \sigma'_m$ ,  $mlts' = \mathcal{G}(C_1) \parallel \mathcal{G}(C_2)$  such that  $\mathbb{F}_{\mathcal{M}'} = \{\sigma_1 \dots \sigma_n, \sigma'_0 \dots \sigma'_m\}$  and  $\mathbb{S}_{\mathcal{M}'} = \{x_1 \dots x_n, y_0 \dots y_m\}$ .

It is straightforward to prove Lemma 2 by Definitions 11 and 12.

Lemma 2 means that the synchronous parallel operator is an identity function over  $\mathbb{F}_{\mathcal{M}} \times \mathbb{F}_{\mathcal{M}} \times \mathbb{S}_{\mathcal{M}}$ . Consequently, the synchronous parallel operator of all paths of  $(\mathbb{F}_{\mathcal{M}}, \leq_{\mathbb{S}})$  is the initial MLTS. Therefore, we can take each path with their synchronous points as sequential component. Hence,  $mlts$  has been decomposed into a set of sequential MLTSs so that their parallel composition is the initial MLTS.

In the following, we give a formal definition of a decomposition.

**Definition 13** Let  $Y = \{\sigma_0, \sigma_1, \dots, \sigma_n\}$  be a path in  $(\mathbb{F}_{\mathcal{M}}, \leq_{\mathbb{S}})$  and  $S = \{s_0, s_1, \dots, s_{n-1}\}$  be a subset of  $\mathbb{S}_{\mathcal{M}}$  such that  $C = \sigma_0 \leq s_0 \leq \sigma_1 \leq s_1 \dots \leq s_{n-1} \leq \sigma_n$ . The sequence  $C$  is an element of  $\mathbb{C}(\mathcal{M})$  if and only if:

$$\forall C' \in \mathbb{C}(\mathcal{M}) : C' \cap C \subseteq \mathbb{S}_{\mathcal{M}}.$$

An element of  $\mathbb{C}(\mathcal{M})$  is an alternative sequence of full sequence and elements of  $\mathbb{S}_{\mathcal{M}}$ .

For example, given  $mlts$  of Fig. 3 with  $\mathbb{F}_{\mathcal{M}} = \{\{x\}, \{y\}, \{u\}, \{v\}\}$  and  $\mathbb{S}_{\mathcal{M}} = \{z\}$ . We have a multi-possible decomposition of  $mlts$ :

$$\mathbb{C}(\mathcal{M}) = \{\{x, z, u\}, \{y, z, v\}\} \text{ or } \mathbb{C}(\mathcal{M}) = \{\{x, z, v\}, \{y, z, u\}\}.$$

$$\mathcal{G}(\{x, z, u\}) \parallel \mathcal{G}(\{y, z, v\}) = mlts = \mathcal{G}(\{x, z, v\}) \parallel \mathcal{G}(\{y, z, u\})$$

**Theorem 1** *Let  $mlts = (\Omega, \lambda, \mu, \xi, \psi)$  to be a maximality-based labeled transition system such that  $\Omega = \langle S, T, \alpha, \beta, s_0 \rangle$  and let  $(\mathcal{M}, \leq, \parallel)$  associated to  $mlts$ .*

$$mlts = SPC(\mathcal{M})$$

With  $SPC(\mathcal{M}) = \mathcal{G}(C_1) \parallel [\mathbb{S}_{\mathcal{M}}] \parallel \mathcal{G}(C_2) \parallel [\mathbb{S}_{\mathcal{M}}] \parallel \mathcal{G}(C_3) \dots \mathcal{G}(C_{n-1}) \parallel [\mathbb{S}_{\mathcal{M}}] \parallel \mathcal{G}(C_n)$  which  $C_i \in \mathbb{C}(\mathcal{M})$ ,  $SPC$  is a synchronous parallel composition of all elements of  $\mathbb{C}(\mathcal{M})$ .

*Proof* Holds by the fact that the structure of  $\mathcal{M}$  is preserved by the synchronous parallel operator  $\parallel [\dots]$  (see Lemma 2).

### 3.2 Generation of LSGA

From the definition of  $\mathbb{C}(\mathcal{M})$ , we can have a distribution of  $\mathcal{M}$  in different localities  $D$  such that for each  $C_1, C_2 \in \mathbb{C}_{\mathcal{M}}$  and for each events  $x$  and  $y$  of  $C_1$  and for each event  $z$  in  $C_2 : D(x) = D(y) \neq D(z)$ .<sup>5</sup> In the other words, we can transform each  $C \in \mathbb{C}_{\mathcal{M}}$  to a component net with interface, thereafter we have a LSGA net.

To transform the synchronous to asynchronous interaction between  $C_1, C_2 \in \mathbb{C}_{\mathcal{M}}$  such that  $C_1 \cap C_2 = S \neq \phi$  we must redefine the sequences  $C_1, C_2$  as follow  $\forall s \in S \implies (s \in C_1 \wedge s \notin C_2) \vee (s \notin C_1 \wedge s \in C_2)$ .

In the following, we give a formal definition of the transformation of the synchronous to asynchronous interaction.

**Definition 14** Let  $\mathbb{A}_{\mathcal{M}}$  be a set of the asynchronous components generated from  $\mathbb{C}_{\mathcal{M}}$ . We can define  $\mathbb{A}_{\mathcal{M}}$  as follow:

- $\forall \mathcal{A}_1, \mathcal{A}_2 \in \mathbb{A}_{\mathcal{M}} \implies \mathcal{A}_1 \cap \mathcal{A}_2 = \phi$  and
- $\forall C_1, C_2 \in \mathbb{C}_{\mathcal{M}}$  such that  $C_1 \cap C_2 = S \neq \phi$ , we have  $\mathcal{A}_1 = (C_1 \setminus S) \cup S_1$  and  $\mathcal{A}_2 = (C_2 \setminus S) \cup S_2$  such that  $S = S_1 \cup S_2$ .

**Definition 15** Let  $C \in \mathbb{A}(\mathcal{M})$  which  $C = c_0 \leq c_1 \leq c_2 \leq \dots \leq c_n$ . Let  $\mathbf{Cio}(C) = (N, I, O)$  be a component net with interface such that  $N = (S, T, F, M_0, L)$  be a Petri net and:

- For each  $c_j \in \mathbb{F}_{\mathcal{M}}$  which  $c_j = x_{j1} \leq x_{j2} \leq \dots \leq x_{jm}$ :
  - $x_{ji} \in T$  with  $i \in \{1 \dots m\}$ .
  - $s_{ji} \in S$  with  $i \in \{0 \dots m\}$ .
  - $F(x_{ji}, s_{ji}) = 1 \wedge F(s_{j(i-1)}, x_{ji}) = 1$  with  $i \in \{1 \dots m\}$ .
- For each synchronous point  $c_j \in \mathbb{S}_{\mathcal{M}}$  which  $c_j = \{x\}$ :
  - $x \in T$ ,
  - $i_{jk} \in I$  with  $k \in \{0 \dots |Left(x)| - 1\}$  such that  $Left(x) = \{y | \forall y \in \mathcal{M} \cdot y \geq x\}$ ,
  - $o_{jk} \in O$  with  $k \in \{1 \dots |right(x)| - 1\}$  such that  $right(x) = \{y | \forall y \in \mathcal{M} \cdot x \geq y\}$ ,
  - $F(s_{(j-1)p}, x) = 1$  such that  $p = |c_{j-1}| + 1$  and  $\forall i_{jk} \in I : F(i_{jk}, x) = 1$
  - $F(x, s_{(j+1)p}) = 1$  such that  $p = |c_{j+1}| + 1$  and  $\forall o_{jk} \in O : F(x, o_{jk}) = 1$ .
- $s_{00} = M_0$ .

<sup>5</sup>From the fact that for each  $C_1, C_2 \in \mathbb{C}_{\mathcal{M}}$  and for each event  $x$  of  $C_1$  and event  $y$  in  $C_2$  such that  $x, y \notin \mathbb{S}_{\mathcal{M}} \cdot x \parallel y$ .

**Definition 16** The asynchronous parallel composition of all element  $C_i \in \mathbb{A}(\mathcal{M})$  is a LSGA i.e.  $\mathcal{Lsga}(\mathcal{M}) = \parallel_{i \in \mathbb{N}} \mathbf{Cio}(C_i)$  for all  $C_i \in \mathbb{A}(\mathcal{M})$ .

By Definition 16 and Theorem 1 it follows:

**Lemma 3** *Let  $mlts$  to be a maximality-based labeled transition system over  $\mathcal{M}$ . Let  $mlts'$  to be a corresponding maximality-based labeled transition system of  $\mathcal{Lsga}(\mathcal{M})$ :  $mlts = mlts'$ .*

## 4 Conclusions

In this paper, we define a distributed implementation from a semantics model rather than a specification model. We proposed an approach for decomposing a given MLTS to a set of sequential MLTSs related only by synchronous interactions. This decomposition has twofold objectives: Firstly, the behaviour of this decomposition and the initial MLTS are identical; Secondly, the interaction between sequential MLTSs can be seen as an asynchronous interaction. In other words, our decomposition produces a distributed system compatible to the definition of R.V. Glabbeek U. Goltz and J.W. Schicke-Uffmann. For proving this compatibility, we introduced the definition of a component net with interface from a sequential MLTS.

## References

1. Aceto, L., Hennessy, M.: Adding action refinement to a finite process algebra. In: Automata, Languages and Programming, 18th International Colloquium, ICALP91, Madrid, Spain, July 8–12, 1991, Proceedings, pp. 506–519 (1991)
2. Benamira, A., Saïdouni, D.: Maximality-based labeled transition systems normal form. In: Modeling Approaches and Algorithms for Advanced Computer Applications, Studies in Computational Intelligence, vol. 488, pp. 337–346. Springer (2013)
3. Bouneb, M., Saïdouni, D., Ilić, J.: A reduced maximality labeled transition system generation for recursive petri nets. *Formal Asp. Comput.* **27**(5–6), 951–973 (2015). <http://dx.doi.org/10.1007/s00165-015-0341-3>
4. Courtiat, J.P., Saïdouni, D.E.: Relating maximality-based semantics to action refinement in process algebras. In: FORTE, pp. 293–308 (1994)
5. Glabbeek, R.J.V.: The refinement theorem for ST-bisimulation semantics. In: Proceedings IFIP TC2 Working Conference on Programming Concepts and Methods, Sea of Gallilee, Israel, April 1990, pp. 27–52. North-Holland (1990)
6. Glabbeek, R.J.V., Goltz, U., Schicke, J.: On synchronous and asynchronous interaction in distributed systems. In: Mathematical Foundations of Computer Science, 33rd International Symposium, MFCS 2008, Torun, Poland, August 25–29, Proceedings. LNCS, vol. 5162, pp. 16–35. Springer (2008)
7. Glabbeek, R.J.V., Goltz, U., Schicke-Uffmann, J.: On characterising distributability. *Log. Methods Comput. Sci.* **9**(3) (2013). [http://dx.doi.org/10.2168/LMCS-9\(3:17\)2013](http://dx.doi.org/10.2168/LMCS-9(3:17)2013)
8. Hennessy, M.: Concurrent testing of processes (extended abstract). In: CONCUR '92, Third International Conference on Concurrency Theory, Stony Brook, NY, USA, August 24–27, 1992, Proceedings, pp. 94–107 (1992). <http://dx.doi.org/10.1007/BFb0084785>

9. Saïdouni, D.E., Belala, N., Bouneb, M.: Aggregation of transitions in marking graph generation based on maximality semantics for Petri nets. In: VECoS'2008, University of Leeds, UK. eWiC Series, The British Computer Society (BCS) (July, 2–3rd 2008). ISSN: 1477-9358
10. Saïdouni, D.E., Belala, N., Bouneb, M.: Maximality-based structural operational semantics for Petri nets. In: Proceedings of INTELLIGENT SYSTEMS AND AUTOMATION:(CISA'09), Tunisia. vol. 1107, pp. 269–274. American Institute of Physics (2009). ISBN: 978-0-7354-0642-1
11. van Glabbeek, R.J., Vaandrager, F.W.: Petri net models for algebraic theories of concurrency. In: PARLE, Parallel Architectures and Languages Europe, Volume II: Parallel Languages, Eindhoven, The Netherlands, June 15–19, 1987, Proceedings, pp. 224–242 (1987)
12. Vogler, W.: Bisimulation and action refinement. In: STACS 91, 8th Annual Symposium on Theoretical Aspects of Computer Science, Hamburg, Germany, February 14–16, 1991, Proceedings, pp. 309–321 (1991). <http://dx.doi.org/10.1007/BFb0020808>



# A Pairwise Approach for Model Merging

Mohammed Boubakir and Allaoua Chaoui

**Abstract** There are several software engineering activities that require merging a set of models to produce a single one. In practice, models are often merged in a pairwise way, without considering the order in which models are combined. In this case, the quality of the results is not always guaranteed as it depends on the order of merging. The approach presented in this paper aims to improve the results, by considering the order of merging. It involves an iterative process, which is repeated until merging all models. In each iteration, we first compare the set of input models to measure the similarity degree of each pair of them. Then we combine a subset of these pairs of models, such that the sum of their similarity degrees is maximal.

**Keywords** Model merging · Model comparison · Maximum weight matching · Combining a set of models · Compare · Match · Merge

## 1 Introduction

Model merging is considered to be an important task in diverse software engineering practices, especially with the increase adoption of MDE (Model-Driven Engineering) in software engineering. For example, it can be used in the ontology research field to build a global ontology from a set of local ones [1]. Model merging is also used in Software Product Line Engineering (SPLE) [2] to migrate a set of similar product variants into a software product line (SPL). In literature, model merging is generally implemented through three operators: *compare*, *match* and

---

M. Boubakir (✉) · A. Chaoui  
MISC Laboratory, Faculty of NTIC,  
Department of Computer Science and Its Applications,  
University Constantine 2-Abdelhamid Mehri, Constantine, Algeria  
e-mail: boubakirmohamed@yahoo.fr

A. Chaoui  
e-mail: a\_chaoui2001@yahoo.com

*merge* [3]. The first and the second operator detect relationships between models, while the third one gives a way to combine them in a single model [4].

Many approaches have been proposed to address the problem of model merging. For example, [5, 6] address the comparison of UML models, [4] proposes a solution for matching and merging Statecharts models, [7] studies the problem of detecting many-to-many matches in diagrams, [8] proposes to merging a set of models by treating simultaneously all input models. The vast majority of these approach focuses only on the case of two models. Only a few of them [8] provides a solution to deal with many (more then two) models. However, several software development activities require combining many models together. This includes for example model versioning [9], and Software Product Lines [3, 10, 11].

In practice, model merging is often performed in a pairwise way, i.e., the set of input models are merged progressively, by combining only two models at a time, without any consideration of the order in which models are combined. This way of model merging does not provide any guarantee on the result quality, because this later depends on the order of merging [8].

In this context, we present in this paper a pairwise approach for model merging, which aims to improve the quality of the results, by considering the order of combining the set of input models. Our main idea is to combine, as much as possible, the most similar pairs of models. The set of input models are merged iteratively by repeating the following steps: We firstly compare input models in order to assign a similarity degree for each pair of them. Then we combine a subset of these pairs of models such that the sum of their similarity degrees is maximal. We implemented, and evaluated the proposed approach by applying it on two UML class diagrams.

The remainder of this paper is structured as follows: Sect. 2 presents work related to our approach. A motivating example is presented in Sect. 3. Section 4 gives background on model merging. We present our approach in Sect. 5, and we evaluate it in Sect. 6. Finally, we conclude the paper and give an outlook on our future work in Sect. 7.

## 2 Related Work

In the literature, there are several works that address the problem of model merging. The majority of this work focuses on merging two input models. Some other works focus on model comparison. Complete surveys on model comparison can be found in [12, 13].

The authors of [14] address the problem of detecting differences between subsequent releases of a given object oriented software. First, they propose to model the problem using a bipartite graph, where vertices represent classes of the two releases, and edges are weighted by the similarity degrees between classes.

Kelter et al. propose in [5] an approach for comparing UML models represented in XMI format. Xing and Stroulia focus also on UML diagrams. They present

UMLDiff [6], an algorithm for detecting the differences between UML class diagrams of subsequent versions of object-oriented software. The approach called MADMatch [7] addresses the problem of detecting many-to-many matches in diagrams. This problem is abstracted as a graph matching problem, and solved using tabu search. In [4], Nejati et al. propose an approach for merging Statecharts models basing on a heuristic operator for finding matches between models.

In contrast to the previous work, Rubin and Chechik [8] propose an approach for merging together many (two or more) input models, focusing on the matching problem. The authors formulated this problem as a weighted set packing problem, which is known as a NP-hard problem, and proposed a heuristic algorithm which simultaneously treats all input models. Our work is similar to this later as we aim to address the problem of merging many models. However, we perform the merging in a completely different way. We don't consider simultaneously all input models, but we propose merging them in a progressive and pairwise way. In this context, we exploit the various existing approaches and tools, by tacking into account the order of merging.

### 3 Motivating Example

As motivating example, we consider the three UML models of Fig. 1, inspired from [8]. The first model ( $M_1$ ) contains a single element<sup>1</sup> (the *University* class), which contains two properties (the attributes *name* and *webAddress*). The second model ( $M_2$ ) contains two elements: the *School* class, which contains two properties (the attributes *name* and *address*), and the *Student* class, which contains also two properties (the attributes *name* and *age*). Finally, the third model ( $M_3$ ) contains a single element (the *Student* class), which contains three elements (the attributes *name*, *surname*, and *age*). Each element has an identifier (the number that appears in parentheses at the bottom right of the element in Fig. 1). Each line connecting a pair of elements is labeled by the similarity degree between these two elements. We describe in the following section how to calculate this similarity degree.

Figure 2 illustrates four different results of merging the three models of Fig. 1. For example, the first model ( $RM_1$ ) contains two elements (1, 2) and (3, 4), which are obtained, respectively, by combining the element 1 with the element 2, and the element 3 with the element 4, while the second one ( $RM_2$ ) is the result of combining the element 1 with the element 3, and the element 2 with the element 4. The properties highlighted in bold and blue color represent the shared properties, i.e., the properties that belong both to the two original elements. As shown in Fig. 2. It is obvious that the first merge is better then the second one, as it allows combining

---

<sup>1</sup>Similarly to [8], we represent a model as a set of elements, where each element contains a set of properties. For the example of Fig. 1, the elements are the UML classes, and the properties are the names and the attributes of these classes.

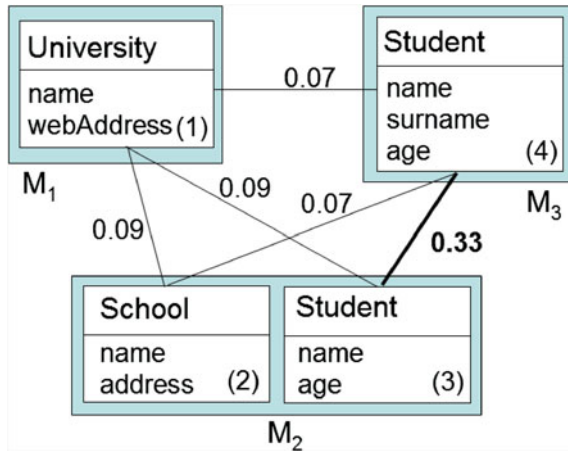


Fig. 1 Example of UML models

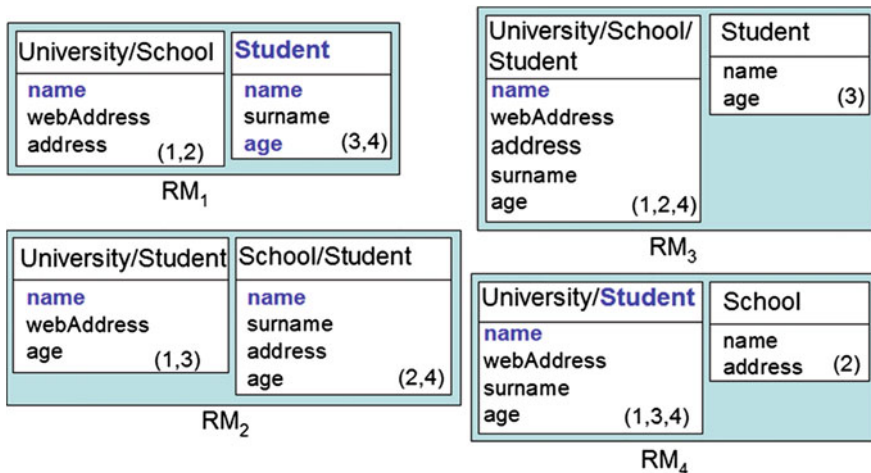


Fig. 2 Example of the result of merging a set of models

the elements, which are the most similar to each other. For example, it combines the elements 3 and 4, which have three shared properties (*Student*, *name*, and *age*), and only one unshared property (*surname*). We present in the next section how to measure the quality of a merge by giving it a weight. The higher this weight is, the higher the quality of the merge will be. In our case, the merges producing the four models  $RM_1$ ,  $RM_2$ ,  $RM_3$ , and  $RM_4$  are respectively assigned the following weights: 0.42, 0.16, 0.13, and 0.31. The first merge is the best because it has the largest weight.

As we can see, there are many ways to merge a set of models. For example, here are some ways to merge the three models of Fig. 1:

1. First,  $M_1$  and  $M_2$  are merged by combining the elements 1 and 2 to produce a model containing the elements (1, 2) and 3. The result is then merged with  $M_3$  by combining the two elements 3 and 4 to produce the model  $RM_1$ .
2. First,  $M_1$  and  $M_2$  are merged by combining the elements 1 and 3 to produce a model containing the elements (1, 3) and 2. The result is then merged with  $M_3$  by combining the two elements 2 and 4 to produce the model  $RM_2$ .
3. First,  $M_1$  and  $M_3$  are merged by combining the elements 1 and 4 to produce a model containing the elements (1, 4). The result is then merged with  $M_2$  by combining the two elements (1, 4) and 3 to produce the model  $RM_4$ .

This example shows that the quality of the result produced by a merge depends on two factors: (1) the order in which the input model are merged (merging the models  $M_1$ ,  $M_2$ , and  $M_3$  according to the order  $M_1$ ,  $M_2$ ,  $M_3$  is different to merging them according to the order:  $M_1$ ,  $M_3$ ,  $M_2$ ), and (2) the manner of matching the elements of a pair of models (Merging  $M_1$  and  $M_2$  by combining the element 1 with the element 2 is different to merging them by combining the element 1 with the element 3). Before presenting in detail our approach, and present how we address the two previous factors, we will present in the next section some concepts of model merging.

## 4 Background on Model Merging

In this section, we present some basic concepts of model merging, which are necessary for implementing our approach. We firstly give a definition to the concept of model merging, in the case of two models, and present its three basic steps: *compare*, *match*, and *merge*. This definition assumes that a model is represented as a set of elements. Merging a set of  $n$  ( $n \geq 2$ ) models requires to manipulate the concept of tuple, in addition to the concept of pair of elements manipulated in the case of only two models. So, in the second time, we give a definition to the concept of tuple, and present how to assign a similarity degree to a given tuple by comparing its elements. Finally, we define the concept of *tuple match* as a way of structuring the elements of a set of models in tuples.

### 4.1 Definition of Model Merging

Model merging aims to combine a set of models in a single one. It is defined in [3] as a process consisting of three steps, which are respectively, performed using the following operators: *compare*, *match*, and *merge*. The first and the second one are heuristic based operators.

**Compare.** This operator allows measuring the similarity between the model elements. It assigns a similarity degree (a number between 0 and 1) for each pair of elements.

**Match.** This operator is applicable on two different models and their similarity degrees. It allows to decide for each two elements denoted by  $e_1$  and  $e_2$ , whether they are considered to be similar, i.e., they represent the same element, where  $e_1$  and  $e_2$  belong respectively to the first and the second model.

**Merge.** This operator is applicable on a pair of models and their matched elements, and produces a single model, where the elements are defined as follow: (1) we copy each unmatched element in the resulting model, (2) we combine each pair of matched elements, than we add the result to the resulting model.

## 4.2 Tuple

Giving a set of models  $M = \{M_1, M_2, \dots, M_n\}$ , and the set of all its elements denoted by  $E_M$ , and defined as follow:

$$E_M = \bigcup_{i=1..n} E_i \quad (1)$$

where  $E_i$  represents the elements of the model  $M_i$ . We define a tuple [8] denoted by  $t$  as a non empty subset of  $E_M$ . This means that a tuple must contains at least one element. It is said to be valid if it does not contain two elements belonging to the same model. More formally:

$$\forall (e_1, e_2) \in t, \forall M_i \in M, (e_1, e_2) \in M_i^2 \rightarrow e_1 \neq e_2 \quad (2)$$

For example, the set of elements  $\{1, 2\}$ , and  $\{1, 2, 4\}$  of Fig. 1 are considered as valid tuples respectively denoted by  $(1, 2)$  and  $(1, 2, 4)$ . However, the set  $\{1, 2, 3\}$  cannot be considered as a valid tuple because it contains two elements, 2 and 3, that belong to the same model  $M_2$ .

## 4.3 Similarity Degree of Tuples

A similarity degree (a number in  $[0..1]$ ) is assigned to a given tuple using a function denoted by  $S$ . This function assigns 0 for each invalid tuple and for each tuple containing only one element. In our work, we adopt the formula (3) [8] to measure the similarity degree of a given tuple denoted by  $t$ . This formula assumes that a model element is represented as a set of properties. In the case of our example, elements are classes, and properties are class names and attributes. In addition, when comparing the elements of a giving tuple, the property representing the name (for example, the property *University* in the element 1 of Fig. 1) is handled as any other properties.

$$S(t) = \frac{\sum_{2 \leq j \leq m} j^2 \times d_j}{n^2 \times |\pi(t)|} \tag{3}$$

where  $m$  represents the number of the elements of  $t$ ,  $n$  represents the total number of models,  $d_j$  represents the distribution of properties (the number of properties that appear in  $j$  elements of the tuple  $t$ ), and  $\pi(t)$  represents the set of distinct properties of all elements of the tuple  $t$ . For example, when comparing the elements of the tuple (1,3,4) of Fig. 1, we have:  $m = 3$  (the tuple contains three elements: 1, 3, and 4),  $n = 3$  (we have 3 models),  $d_2 = 2$  (there are two properties that appear twice in (1,3,4): *Student* and *age* appear both in the element 3 and 4),  $d_3 = 1$  (there is one property, *name*, that appears thrice in (1, 3, 4)),  $\pi((1, 3, 4)) = \{University, name, webAddress, Student, age, surname\}$ , so  $|\pi(1, 3, 4)| = 6$ , and finally, we have:

$$S(1, 3, 4) = \frac{2^2 \times 2 + 3^2 \times 1}{3^2 \times 6} = \frac{17}{54} = 0.31$$

### 4.4 Tuple Match

We define a *tuple match* denoted by  $H$  (or a *match*, for simplicity), on a set of models as a set of tuples, satisfying the following properties [8]:

- (a) All tuples of  $H$  are valid.
- (b) All tuples of  $H$  are disjoint,  $\forall (t_1, t_2) \in H^2, t_1 \cap t_2 = \emptyset$ .
- (c) The set  $H$  is maximal, i.e., if we add any additional tuple in it, the previous properties will be violated.

For example, the tuple (1, 2) and (3, 4) of Fig. 1 can be considered as a *match* denoted ((1, 2), (3, 4)). However, the tuple (1, 4) cannot be considered as a *match* because it can be augmented by the tuple (2) or (3).

For each *match* denoted by  $H$ , we assign a similarity degree denoted by  $S_h$  and calculated as follow [8]:

$$S_h(H) = \sum_{t \in H} S(t) \tag{4}$$

where  $S$  is the function that returns the similarity degree of a given tuple.

Table 1 shows all possible *matches* of the three models of Fig. 1 and their similarity degrees.

**Table 1** Example of match and their similarity degrees

Match number	1	2	3	4
Match	((1,2), (3,4))	((1,3), (2,4))	((1,2,4), (3))	((1,3,4), (2))
Similarity degree	0.42	0.16	0.13	0.31

Each *match* corresponds to a possibility of merge. For example, Fig. 2 shows the four possibilities of merging the models of Fig. 1 using the four *matches* presented in Table 1 (the *match* number  $i$  in Table 1 corresponds to the model  $RM_i$  of Fig. 2). The quality of a merge is measured using a weight, which is equal to the similarity degree of the corresponding *match*. The merge is considered to be good if it has a large value of weight. For example, the weight value of the merge producing the model  $RM_1$  is equals to 0.42. It is the best merge because it has the largest value of weight.

## 5 Our Approach

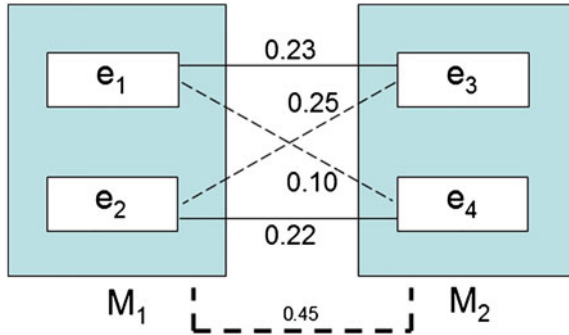
### 5.1 Overview

We present here our approach for merging a set of models. The main idea of this approach consists of merging, as much as possible, the most similar pairs of models. i.e., we try the maximum to combine each model with the most similar to it. To this end, we firstly compare each pair of models in order to define a similarity degree between them, and to identify the optimal match between their elements. Then, we try to merge the most similar pairs of models. We continue this process until obtaining a single model. Our approach is implemented as an algorithm, which we present in more detail in the reminder of this section. But before that, we present our implementation of the three model merging operators: *compare*, *match*, and *merge*.

### 5.2 Compare

The first step towards merging a set of models consists of comparing these models in order to measuring the similarity between them. We describe here how to compare a pair of models. First, we compare each pair of elements denoted by  $(e_i, e_j)$ , where  $e_i$  and  $e_j$  belong respectively to the first and the second model. This assigns a similarity degree to  $(e_i, e_j)$  using the formula (3). The result of the comparison is than represented using a bipartite weighted graph with two disjoint sets of vertices (the two partitions of the graph), containing respectively the elements of the first model and those of the second one (each vertex represents an element). The edge connecting each two elements is labeled by the similarity degree between them. Figure 3 gives an example of comparison result between the elements of two models denoted by  $M_1$  and  $M_2$ . The comparison between these two models produces two matches denoted by  $mt_1$  and  $mt_2$ , where  $mt_1 = ((e_1, e_3), (e_2, e_4))$ , and  $mt_2 = ((e_1, e_4), (e_2, e_3))$ , and where  $S_h(mt_1) = 0.45$  and  $S_h(mt_2) = 0.35$ .  $S_h(mt_1)$  and  $S_h(mt_2)$  represent respectively the similarity degree of  $mt_1$  and  $mt_2$ . They are calculated using the formula (4).





**Fig. 3** Example of comparison result between the elements of two models (The *dashed line* connecting the two models is labeled by the similarity degree between them)

### 5.3 Match

Basing on the result of the previous step, we identify the best match between the elements of the two input models, and we assign a similarity degree to this pair of models. This later is equal to the similarity degree of the best *match*. For example, the similarity degree of the two models of Fig. 3 is equal to 0.45, which represents the similarity degree of the best match (*mt1*). It is obvious that the problem of finding the best match can be modeled as the maximum weight matching in bipartite graphs. This later can be solved in polynomial time using the Hungarian method [15].

### 5.4 Merge

Giving a pair of models and the result of the *match* operator, we combine the two input models to obtain only one model, where the elements are the result of combining matched pairs of elements (the elements considered to be similar by the *match* operator), and the unmatched elements (the elements which are considered, by the *match* operator, to be not similar to any other element).

### 5.5 Model Merging Algorithm

We present here different steps of our model merging algorithm (see Algorithm 1). This later receives as input a set of models denoted by  $M$ , and uses three variables:  $G$ ,  $P$ , and  $m$ .  $G$  is a set of 3-uplets, where the first and the second term of each 3-uplet represent two models. The third term represents the similarity degree

between these models.  $P$  is a set of pairs of models.  $m$  is a model. The algorithm involves three main steps, which are repeated until merging all models (until  $M$  contains a single model).

```

Algorithm 1
1: Input: M
2: Var: G, P, m
3: Output: M
4: begin
5: while |M|>1 do
6:   G := ∅
7:   for all (Mi, Mj) ∈ M2 do
8:     compareAndMatch(Mi, Mj)
9:     G := G ∪ {(Mi, Mj, simDeg(Mi, Mj))}
10:  end for
11: P := maxWeightMatch(G)
12: for all (Mi, Mj) ∈ P do
13:   m := merge(Mi, Mj, optimalMatch(Mi, Mj))
14:   M = M \ {Mi, Mj}
15:   M = M ∪ {m}
16: end for
17: end while
end.

```

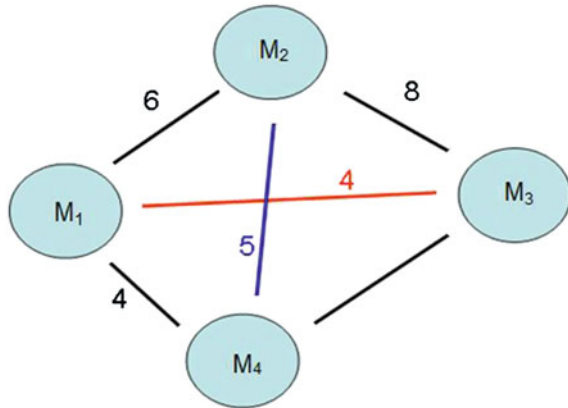
In the first step (lines 7–10), we use the *compareAndMatch()* procedure to compare each pair of models basing on our *compare* and *match* operators described above. This produces for each pair of models a similarity degree and the optimal match between their elements. The similarity degree between each pair of models is returned by the *simDeg()* function, and arranged in  $G$  (line 9). The similarity degrees between all pairs of models are represented by a complete weighted graph, where each vertex represents a model and each edge weight represents the similarity degree between two models. Figure 4 gives an example of the result of comparing four models denoted respectively by  $M_1$ ,  $M_2$ ,  $M_3$  and  $M_4$ .

In order to combine as possible the most similar pairs of models, we merge  $m$  pairs of models, such that the sum of their similarity degrees is maximal, where  $m = n/2$  and  $n$  is the number of models.<sup>2</sup> This problem is modeled as a *maximum weight matching* in general graph where weights represent similarity degrees between models. The *maximum weight matching* problem consists of finding a matching that has maximum weight. A matching in a graph is a subset of its edges

---

<sup>2</sup>If  $n$  is impair, then  $m = (n - 1)/2$ .

**Fig. 4** Example of comparison result between a set of models



such that no two edges in this matching are incident to the same vertex. The weight of a matching is equal to the sum of the weights of its edges. We propose to solve this problem using the implementation of the Edmond’s algorithm [16] proposed by Gabow [17]. For example, it is possible to merging the elements of Fig. 4 according to the following three ways:

- (a) Merging  $M_1$  with  $M_2$  and  $M_3$  with  $M_4$ . The sum of the similarity degree is equals to 13 (6 + 7).
- (b) Merging  $M_1$  with  $M_3$  and  $M_2$  with  $M_4$ . The sum of the similarity degree is equals to 9 (4 + 5).
- (c) Merging  $M_1$  with  $M_4$  and  $M_2$  with  $M_3$ . The sum of the similarity degree is equals to 12 (4 + 8).

We choose the first way because it corresponds to the largest value of the sum of the similarity degrees. This produces two models, which will be merged in the next iteration of the algorithm.

So, in the second step of the algorithm (line 11), we identify a subset of pairs of models with a maximum sum of similarity degrees, using the *maxWeightMatch()* function, which is based on Gabow’s implementation of the Edmond’s algorithm. The result is arranged in  $P$ .

Finally, in the third step (lines 12–16): we use our merge operator (line 13) to combine each pair of models ( $M_i, M_j$ ) from  $P$  basing on the optimal match (calculated in line 8 by the *compareAndMactch()* procedure), which is returned by the *optimalMatch()* function. Then we replace ( $M_i, M_j$ ) in  $M$  by the resulting model (line 14 and 15).

## 6 Evaluation

In this section, we assess the feasibility of our approach. To this end, we first calculate its complexity. Then, we evaluate it on two case studies.

## 6.1 Complexity

Let  $n$  and  $k$  be, respectively the number of input models, and the size (number of elements) of the largest model. The Hungarian Method has time complexity  $O(a^3)$ , where  $a$  is the number of vertices in the larger one of the two graphs. The implementation of the Edmond's algorithm that we used has time complexity  $O(b^3)$ , where  $b$  is the number of vertices in the graph. In each iteration, our algorithm compares  $n*(n - 1)/2$  pairs of models using the Hungarian algorithm, and identifies pairs of models with the maximum sum of similarity degrees, using a single call to the Edmond's algorithm. After each iteration, the number of models is divided by 2. Therefore, the time complexity of our algorithm is polynomial both in  $n$  and  $k$ , and it is bonded by  $O(\log_2(n) * (n^2 * k^3 + n^3))$ .

## 6.2 Empirical Evaluation

In order to evaluate our approach, we first implemented it in Java and compared it with three other algorithms denoted by *algo1*, *algo2*, *algo3*. The first algorithm merges input models in a random order. The second algorithm, first sorts the list of input models in descending order by their size (number of elements), then combines them. The third algorithm, sorts the list in an ascending order. We performed the evaluation using two case studies: Hospital and Warehouse [8]. The first consists of a set of 8 different variants of Hospital system, with 221 classes in all models. The second one consists of a set of 16 different variants of Warehouse system, with 388 classes in all models. Both the two systems are modeled using UML class diagrams.<sup>3</sup>

We consider that an algorithm is better if it produces a model with a height value of weight. So, we applied each algorithm to each of the two case studies, and we measured the weight of the resulting models. To perform the comparison, we calculated the percentage of the improvement (degradation) that our algorithm provided compared by the other algorithms, for each case study.

Table 2 summarized the results. The first three columns give the results obtained by *algo1*, *algo2*, and *algo3*. Column 4 and column 5 give respectively the results obtained by our approach, and the percentage of the improvement (degradation) that it provided compared by the best of the other algorithms. The percentage value is preceded by the minus sign (–), in the case of degradation.

The result produced by our approach in the Hospital case, has a weight value of 4.56, if we compare this value with 3.17 produced by *algo1*, we find that our algorithm improves by 7.8 % the result obtained by *algo1*. Similarly, if we compare our approach with *algo2*, we find that it improves the result by 43.84 %. However, our approach does not outperform *algo3*, and presents a degradation of only

---

<sup>3</sup>These models are available at <http://www.cs.toronto.edu/~mjulia/NwM>.

**Table 2** Results of the evaluation

	algo1	algo2	algo3	Our approach	Improvement/Degradation (%)
Hospital	4.23	3.17	<b>4.58</b>	4.56	-0.43
Warehouse	0.89	0.97	0.93	<b>1.23</b>	26.80

0.43 %. In the case of Warehouse, our approach outperforms all other algorithms, with significant improvement. It improves the results produced by *algo1*, *alog2*, and *algo3*, respectively, by 38.2 %, 26.80 %, and 32.25 %.

Comparing our approach with the best of the three other algorithms, it presents a negligible degradation (0.43 %), with the first case study, and a considerable improvement (26.80 %) in the second one.

## 7 Conclusion and Future Work

Model merging, which consists of combining a set of models to obtain a single one, is an important step in a number of software engineering activities. When merging a set of models, the quality of the results is influenced by the order in which these models are combined.

In this paper, we presented an approach for model merging, which proposes to consider the order of combining the set of input models, in order to improve the quality of the results. The proposed approach consists of repeating the following steps until merging all models: First, models are compared, and each pair of them is assigned a similarity degree. Then, pairs of models with a maximum sum of similarity degrees are merged. We implemented, and evaluated the proposed approach by applying it on two case studies, and the experiments show that it is promising. In the near future, we plan to apply our approach on more large case studies, and consider other types of models other than UML class diagrams.

## References

1. Sabetzadeh, M., Nejati, S., Easterbrook, S., Chechik, M.: A relationship-driven framework for model merging. In: Proceedings of the Workshop on Modeling in Software Engineering. 29th International Conference on Software Engineering, Minneapolis (2007)
2. Pohl, K., Böckle, G., Van der Linden, F.J.: Software Product Line Engineering: Foundations, Principles and Techniques. Springer, New York (2005)
3. Rubin, J., Chechik, M.: Combining related products into product lines. In: FASE'12, pp. 285–300. Springer (2012)
4. Nejati, S., Sabetzadeh, M., Chechik, M., Easterbrook, S., Zave, P.: Matching and merging of statecharts specifications. In: ICSE 2007, pp. 54–64, IEEE (2007)
5. Kelter, U., Wehren, J., Niere, J.: A generic difference algorithm for UML models. *Softw. Eng.* **64**, 105–116 (2005)

6. Xing, Z., Stroulia, E.: UMLDiff: an algorithm for object-oriented design differencing. In: ASE, pp. 54–65. ACM (2005)
7. Kpodjedo, S., Ricca, F., Galinier, P., Antoniol, G., Guéhéneuc, Y.-G.: MADMatch: Many-to-many Approximate Diagram Matching for Design Comparison. IEEE TSE (2013)
8. Rubin, J., Chechik, M.: N-way model merging. In: ESEC/FSE, pp. 301–311. ACM (2013)
9. Altmanninger, K., Seidl, M., Wimmer, M.: A survey on model versioning approaches. Int. J. Web Inf. Syst. **5**, 271–304 (2009)
10. Zhang, X., Haugen, O., Moller-Pedersen, B.: Model comparison to synthesize a model-driven software product line. In: SPLC, pp. 90–99. IEEE (2011)
11. Martinez, J., Ziadi, T., Bissyandé, T., Klein, J., Le Traon, Y.: Bottom-up adoption of software product lines—a generic and extensible approach. In: SPLC 2015, pp. 101–110. ACM (2015)
12. Stephan, M., Cordy, J.R.: A survey of model comparison approaches and applications. In: 1st International Conference on Model-Driven Engineering and Software Development, pp. 265–277. INSTICC Press (2013)
13. Kolovos, D.S., Di Ruscio, D., Pierantonio, A., Paige, R.F.: Different models for model matching: an analysis of approaches to support model differencing. In: Proceedings of the 2009 ICSE Workshop on Comparison and Versioning of Software Models, CVSM 2009, pp. 1–6. IEEE Computer Society, Washington, DC (2009)
14. Antoniol, G., Canfora, G., Casazza, G., De Lucia, A.: Maintaining traceability links during object-oriented software evolution. Softw.-Pract. Exp. **31**, 331–355 (2001)
15. Kuhn, H.W.: The Hungarian method for the assignment problem. Naval Res. Logistics Q. **2**, 83–97 (1955)
16. Edmonds, J.: Maximum matching and a polyhedron with 0,1-vertices. J. Res. Nat. Bureau Stan. Sect. B **69**, 125–130 (1965)
17. Gabow, H.N.: An efficient implementation of Edmonds’ algorithm for maximum matching on graphs. J. ACM (JACM) **23**, 221–234 (1976)

# Author Index

## A

Abrishambaf, R., 177  
Allaoua, Chaoui, 187  
Amine, Abdelmalek, 77  
Atmani, Baghdad, 137  
Azizi, Nabiha, 281

## B

Babahenini, Mohamed Chaouki, 153  
Bachir, Abdelmalik, 261  
Baouya, Abdelhakim, 295  
Batouche, Mohamed, 217  
Benamira, Adel, 311  
Bennouar, Djamal, 295  
Benyettou, M., 177  
Bilami, Azeddine, 249  
Bouarara, Hadj Ahmed, 77  
Boubakir, Mohammed, 327  
Boucheham, Bachir, 123  
Boudia, Mohamed Amine, 77  
Boudraa, B., 165  
Boudraa, M., 165  
Bougueroua, Salah, 123  
Boukhalfa, Kamel, 233  
Bouzoubia, Samira, 91

## C

Cabral, J., 177  
Chaib, Aouatef, 187  
Chaoui, Allaoua, 327  
Chikhi, Salim, 91

## D

Djafri, Khaoula, 67  
Djellali, Hayet, 281

## F

Faraoun, Kamel Mohamed, 3

## G

Gheraibia, Youcef, 67  
Guerrache, Fares, 19

## H

Haddadou, Hamid, 19  
Hamou, Reda Mohamed, 77  
Hannache, Oussama, 217

## I

Imen, Boussebough, 187

## K

Khellat-Kihel, S., 177  
Krimou, Habiba, 67

## L

Layeb, Abdesslem, 91, 107

## M

Makhlouf, Sid Ahmed, 201  
Mansoul, Abdelhak, 137  
Medjram, Sofiane, 153  
Meghraoui, D., 165  
Menad, Hanane, 77  
Mendil, Boubekeur, 49  
Merazi-Meksen, T., 165  
Mohamed, Otmame Ait, 295  
Monteiro, J.L., 177  
Moussaoui, Abdelouahab, 31

## O

Ouchani, Samir, 295

## R

Rahmani, Amine, 77  
Rahmani, Mohamed Elhadi, 77

**S**

Sahraoui, Somia, [249](#)  
Saidouni, Djamel-Eddine, [311](#)  
Semar-Bitah, Kahina, [233](#)  
Souyah, Amina, [3](#)

**T**

Taleb-Ahmed, Abdelmalik, [153](#)  
Tighzert, Lyes, [49](#)

**Y**

Yagoubi, Belabbas, [201](#)  
Yamina, Mohamed Ben Ali, [153](#)

**Z**

Zendaoui, Zakaria, [107](#)  
Zine, Nacira Ghoualmi, [281](#)  
Zouaoui, Hakima, [31](#)  
Zouaoui, Samia, [261](#)